THERMODYNAMIC PROPERTIES OF THE METHANE-ETHYLENE SYSTEM

by

JUN WUNG LEE

MARCH, 1976

A thesis submitted for the Degree of

DOCTOR of PHILOSOPHY in the FACULTY of ENGINEERING

in the UNIVERSITY of LONDON

and for the DIPLOMA of IMPERIAL COLLEGE

Department of Chemical Engineering and Chemical Technology
Imperial College of Science and Technology
London

ABSTRACT

An apparatus of Burnett-type was used for the determination of accurate compressibility factors of ethylene and three methane-ethylene mixtures using a multiple expansion technique.

Results were obtained in the temperature range 243 - 297°K, upto 41 bar pressure for ethylene, and 223 - 299°K, upto 86 bar pressure for the mixtures.

The experimental measurements were fitted, using a non-linear least-squares curve fitting technique, to (i) the virial equation for each individual isotherm and (ii) a modified Benedict-Webb-Rubin equation which allowed all isotherms to be treated simultaneously.

The compressibility factors, Z, which were determined from the 10-coefficient modified B-W-R equation, are believed to be accurate to ±0.0003 for ethylene and agree with a maximum difference of 0.0005 at 0°C and 0.001 at 25°C (extrapolated) with those of Michels and co-workers.[1] There are no reliable data for ethylene available below 0°C.[2]

The accuracy of the Z values for the mixtures is estimated at less than 0.0005 and they agree reasonably well with those of Edmister and co-workers[3] where the temperature ranges overlap.

The results for ethylene were compared with those predicted by the principle of corresponding states, extended to allow for non-spherical molecules in terms of shape factors,[4] using methane as reference substance. The value for the acentric factor of 0.085 found from vapour pressure measurements was found to adequately represent the P-V-T data. The root-mean-square deviation of predicted Z from the experimental values was

$0.24 \cdot 10^{-2}$.

For the mixtures the extended principle was again employed together with the so-called 'van der Waals rule', proposed by Rowlinson,[5] for calculating the parameters of the hypothetical equivalent single fluid. The geometric mean correction factor, ζ_{ij}, for the potential energies of CH_4-C_2H_4 was found te be 0.975 (additivity of molecular diameters was found to be adequate) and when this factor was used, the over-all RMS deviation of predicted Z values from the experimental ones was $0.48 \cdot 10^{-2}$.

References to This Abstract

(1) Michels, A., and Geldermans, M., Physica,'s Grav., 9, 967 (1942).

(2) Angus, S., 'Ethylene,1972', (IUPAC), Butterworths, (1974).

(3) McMath, H.G. and Edmister, W.C., A.I.Ch.E.J., 15, 370, (1969), and Lee, R.C. and Edmister, W.C., A.I.Ch.E.J., 16, 1047 (1970).

(4) Leach, J.W., Chappelear, P.S. and Leland, T.W., A.I.Ch.E.J., 14, No.4, 568 (1968).

(5) Leland, T.W., Rowlinson, J.S. and Sather, G.A., Trans. Faraday Soc., 64, 1447 (1968).

CONTENTS

ABSTRACT 2
TABLES OF CONTENTS 4
ACKNOWLEDGEMENTS 8

Chapter 1 Introduction 9
1-1 General 9
1-2 Prediction of Thermodynamic Properties 13
1-3 Equations of State 15
1-4 Other Thermodynamic Properties 20
1-5 Measurement of the Compressibility Factors 23

Chapter 2 Experiment 27
2-1 Introduction 27
2-2 The Low Temperature System 31
2-2-1 Introduction 31
2-2-2 The Pressure Vessel 33
2-2-3 The Radiation Shield 35
2-2-4 The Inlet Tubes 37
2-2-5 The Outer Jacket 40
2-2-6 The Cryostat 41
2-2-7 Low Temperature System Wires 42
2-3 The Expansion Vessel 43
2-4 The Vacuum System 46
2-5 The Gas Storage System 48
2-6 Temperature Control Systems 50
2-6-1 Introduction 50
2-6-2 The Temperature Control of the Pressure Vessel 51
2-6-3 The Temperature Control of the Radiation Shield 55
2-7 Temperature Measurement 59
2-7-1 Introduction 59
2-7-2 Resistance Measurement by an A.C. Double Bridge 61

2-7-3 Resistance Measurement by a Potentiometer 62
2-8 Pressure Measurement 64
2-8-1 Introduction 64
2-8-2 Pressur Measurement with an Oil Piston Gauge 66
(a) Oil Piston Gauge 68
(i) The Acceleration due to Gravitation 70
(ii) The Mass of the Balancing Weights 70
(iii) The Buoyancy Effects and Other Corrections 73
(iv) Hydraulic Head of Oil 75
(b) The Differential Pressure Cell 77
2-8-3 The Gas-Operated Piston Gauge 79
2-8-4 The Atmospheric Pressure 82
2-8-5 The Precision Pressure Gauge 83
(a) Introduction 83
(b) Modification to the PPG 87
(c) The Calibration of the PPG Null-Shift with Pressure 90
(d) The Sensitivity of the PPG 93
2-9 The Pressure Gradients due to Gravitation 99
2-10 Calibration of Volumes and Pressure Distortion of the Vessels 101
2-11 Errors in Pressure Measurement 105
2-12 Experiment 107
2-13 Preparation of Gas Mixtures and Gas Analysis 110

Chapter 3 Treatment of Experimental Data and Discussion 113
3-1 Introduction 113
3-2 The Method of Data Reduction 115
3-2-1 The Graphical Method of Data Reduction 116
3-2-2 The Analytical Method of Data Reduction 118

3-3 The Non-Linear Least-Squares Procedure 123

3-3-1 The Non-Linear Least-Squares Procedure for the Virial Equation 126

3-3-2 The Non-Linear Least-Squares Procedure for the Bender Equation 133

3-4 Treatment of Experimental Data for the Non-Isothermal Burnett Apparatus 136

3-4-1 Calculation of the Residual from the Virial Equation 138

3-4-2 Calculation of the Residual from the Bender Equation 141

3-5 The Computation and the Results 142

3-5-1 Introduction 142

3-5-2 Description of Computer Program 144

3-5-3 The Results 148

3-5-4 The Interactional Second Virial Coefficients of Methane-Ethylene System 152

3-6 Discussion 199

3-6-1 Introduction 199

3-6-2 Comparison of the Compressibility Factors 201

3-6-3 The Compressibility Factors of Mixture 3 202

3-6-4 The Compressibility Factors of Other Mixtures 213

3-6-5 The Compressibility Factors of Ethylene 214

3-6-6 Errors in the Compressibility Factors 216

3-6-7 The Volume of the Pressure Vessel 218

3-6-8 Compressibility Factors of Other Workers 220

(i) Ethylene 220

(ii) Ethylene-Methane Mixtures 223

Chapter 4 Prediction of Compressibility Factors 236
4-1 Introduction 236
4-2 The Theoretical Basis of the Principle of Corresponding States 238
4-3 The Principle of Corresponding States 243
4-4 Departure from the Principle of Corresponding States; The Compressibility Factors of Ethylene 248
4-5 The Extension of the Principle of Corresponding States; The Compressibility Factors of Methane-Ethylene Mixtures 261
4-6 The Application of the Principle of Corresponding States to the Second Virial Coefficients 286

REFERENCES 293

ACKNOWLEDGEMENTS

I wish to thank my supervisor, Dr. Graham Saville, for his patient advice and untiring assistance in both experimental and theoretical aspects of this project. I am also greatly indebted to Dr. Saville for his kindness and encouragement, without which this work would not have been possible.

My thanks are also due to the staffs of the departmental analytical service laboratory and the glass workshop for their willing help and the goods stores for their efficient supply of all the materials.

I am grateful to the British Council for their financial support and valuable guidance in many aspects of my life as a foreign student.

I would like to dedicate this work to my parents, my wife and my daughter for their unchanging love and devotion.

CHAPTER ONE

INTRODUCTION

1-1 General

Ever since the discovery of ethylene by, among others, the Dutch chemists, at the end of 18'th century the importance of ethylene in the field of chemistry as one of the basic chemical compounds has been ever increasing. The physical and chemical properties of ethylene, however, were not clearly understood until the end of the 19'th century when organic chemistry was established as one branch of science and distinguished from what is now known as inorganic chemistry. The development of organic chemistry along with other fields of science brought a better understanding of the chemical properties of organic compounds as a whole, and especially of those basic hydrocarbons such as methane and ethylene. Unlike methane, which is abundant in nature as the main constituent of natural gas, ethylene has to be manufactured artificially from other organic materials such as ethane, propane, alcohol etc. Nevertheless its importance was firmly established early in the 20'th century because of the versatility of its chemical reactions with other compounds due primarily to its unsaturated double bond.

The use of ethylene on a tonnage scale as a raw material in synthetic organic chemistry dates from about 1933 when the process of polymerisation of ethylene into polyethylene was discovered in the Winnington Laboratories of ICI Ltd. by Gibson and Fawcett.[79] The discovery of the conversion of

ethylene under high pressure into a solid thermoplastic polymer was an event of outstanding significance in the development of the petrochemical industry.

During and after World War II the demand for ethylene increased sharply and thus the methods of menufacturing ethylene were converted from non-petroleum processes, which employed methods such as dehydration of ethyl alcohol or more expensively, hydrogenation of acetylene, into petrochemical processes in which ethylene is manufactured from light hydrocarbons such as ethane, propane or from naphtha by catalytic cracking. The main constituents of the 'cracked' gas are hydrogen, methane, ethylene, ethane and higher hydrocarbons (both paraffins and olefins upto about C_4 depending on the raw material used). However whatever is used as a raw material, methane always appears as the main impurity in the gas mixture. Methane content too varies according to the raw material used and when, as an example, propane is used as a raw material, methane content in the cracked gas is about 30% (mole per cent) whereas about 28% methane is present as an impurity when naphtha is used.

Thus the basic problem in the ethylene manufacturing industry is, apart from catalytic cracking of the raw material, ethylene recovery from the cracked gas, i.e. removal of the impurities, notably methane, from the mixture. The separation of methane from the gas mixture, or, demethanisation as is called, is therefore one of the more important parts of an ethylene plant and very careful attention has always to be paid to its design, since about 15% of the total capital cost and 30 - 40% of the total energy needed are consumed in this part of the plant.(79)

Fortunately the critical temperature of methane (190°K) is very much lower than that of the other constituents in the cracked gas -ethane (306°K), propane (370°K) ethylene (282°K) and propylene (365°K)- and for this reason methane together with the small amount of hydrogen present (less than 15 mole %) is separated by condensation of ethylene etc. at about 35 bar and 170 - 180°K. The column in which this condensation takes place requires refrigeration and this is usually supplied by conventional vapour compression refrigerators using ethylene or propylene, depending on the temperature involved, as the working fluid. These are chosen, rather than, say the fluorinated hydrocarbons, since they are readily available from the product streams of the plant.

Of course, the 'demethaniser' forms only one part of the plant and in a complete plant there are other separation stages as well. Thus 'optimum' design is usually established on the basis of systems analysis and will involve economic as well as engineering factors. However, such designs must be based largely on thermodynamic considerations and there is clearly a need for precise thermodynamic data, particularly on the rather complex mixtures involved. Unfortunately it is impracticable, in a reasonable length of time, to make experimental measurements on multicomponent mixtures covering the whole of the composition range and one is forced to derive multicomponent properties from a knowledge of the constituent binaries. (The way in which this is done is considered below.) From the point of view of demethanisation part of the plant, the binary which is dominant is that of methane-ethylene.

Despite the facts mentioned above, actual volumetric measurement data for ethylene and for its mixture with methane are quite rare in the literature mainly due, it is believed, to the difficulties associated with accurate pressure measurement in a low temperature system.

In the case of ethylene the work of Michels et al,[14,15,16] published more than two decades ago, is still regarded as the most reliable data. Although there are some other sources of data published (see Chapter 3), in most cases, however, the data are believed to be less accurate than what was originally claimed. For this reason both Angus[17] and Miller[79] have presented P-V-T data according to Michels work almost exclusively in their extensive compilations 'IUPAC ETHYLENE Table' and 'Ethylene and Its Industrial Derivatives' respectively.

The experimental range of Michels work, however, extends only from $0^{o}C$ upwards, and for this reason the region below $0^{o}C$ in the IUPAC table is left blank. (see Fig 3-7).

Volumetric data for the methane-ethylene system are even rarer and only two papers are believed to have been published[18,19] and then only for two isotherms below $0^{o}C$.

In this thesis we report the results of experimental P-V-T measurements on ethylene in the temperature range 243 - $297^{o}K$ upto 41 bar pressure and for the methane-ethylene system in the temperature range 223 - $299^{o}K$ and at pressures of upto 86 bar (the maximum pressure depending on the composition of the mixture concerned). Thus extending our knowledge of the thermodynamic properties to that appropriate to the design of ethylene separation plant.

1-2 Prediction of Thermodynamic Properties

One of the most important subjects in the field of thermodynamics is the prediction or estimation of thermodynamic properties, since it has never been possible for experimentalists to supply all of the accurate data which chemical engineers require in designing chemical plant.

Modern design procedures are usually computer aided, although a fully computer designed process plant is still some time off, and clearly there is a need here for a reliable computerised method for estimating the necessary thermodynamic data, usually for multicomponent mixtures. Thus in the design of the demethaniser of an ethylene plant a programme to provide liquid vapour equilibria plus the associated enthalpies of a mixtures containing the substances listed in the previous section will be needed.

The principle of corresponding states has a long history in meeting these demands, and because of its theoretical basis in statistical thermodynamics this method is considered to be preferable to the empirical ones. The principle is based on the conformality of the intermolecular potential curves of different substances. This restricts its applicability to non-polar, spherical molecules, but in addition, until a theory of mixing is incorporated, the principle cannot be applied to mixtures.

The deviation from the principle of corresponding states in the case of a pure substance is in most cases due to the non-spherical shape of the molecule, since the potential energy between the molecules is function not only of the distance

but also the relative orientations of the molecules. (We are not considering the polar molecules here.) Departures from the principle, however, can be allowed for quantitatively, by introducing 'shape factors' and these in turn can be correlated with so called Pitzer's acentric factor.[39] Leland and co-workers have expressed these shape factors as slowly varying functions of reduced properties and the acentric factor.[40,53]

In the case of mixtures, by far the most successful theory in the recent years has been the result of amalgamating a 'one-fluid model' with the principle of corresponding states. In the simplest form of the theory, the mixture is replaced by a hypothetical simple fluid whose intermolecular potential energy is assumed to be conformal with the pure substances which form the mixture. The method is also called the 'pseudo critical method' since it is often expressed in terms of critical parameters.

The extension to include non-conformal (but non polar) substances has been carried out by Rowlinson[68,69] who used the so called 'van der Waals rule' for calculating the parameters of the hypothetical simple fuild, and it is this form of the theory that is used in this work.

The van der Waals formulation for the parameters of the simple fluid involves the interaction parameters for unlike molecular interactions. Since we cannot learn anything about these from measurements on pure substances the unlike interaction parameters must be obtained from measurements on mixtures. We therefore determine these parameters for the methane-ethylene system from our P-V-T results.

Since the principle of corresponding states is applicable

to both liquid and vapour, and therefore to the determination of liquid-vapour equilibrium, we use the parameters thus derived to investigate the accuracy with which the latter can be estimated.

1-3 Equations of State

A large amount of thermodynamic data can be most conveniently handled and utilized in the form of an equation of state. An equation of state is an equation which relates pressure volume and temperature, the simplest of which is that of a perfect gas,

$$PV = RT \qquad (1\text{-}3\text{-}1)$$

where V is molar volume and R is the gas constant. The equation of state (1-3-1) has a long history and dates back to the work of Boyle and Charles in the 17'th and 18'th centuries when the foundations of what we now know as the perfect gas laws were laid down.(2)

Real gases depart from perfect gas behaviour because of the finite size of the molecules and forces between them. The compressibility factor, Z, was therefore defined by

$$Z = PV/RT \qquad (1\text{-}3\text{-}2)$$

Z is a function of temperature and pressure (or density) and is a convenient measure of the non-ideality of a gas because it is dimensionless. As the pressure tends to zero then the gas becomes more ideal and hence Z approaches the value of unity.

Many equations of state, both theoretical and empirical,

have been proposed to express quantitatively the variation of the compressibility factor with pressure and temperature. The first practical equation of state to improve upon the ideal gas law, Eq.(1-3-1), is that of van der Waals,

$$(P + a/v^2)(v - b) = RT \qquad (1\text{-}3\text{-}3)$$

where a and b are positive constants which are characteristic of the particular gas. The terms a/v^2 and b are pressure and volume correction terms respectively, which arise from the non-ideality of a real gas, and thus this equation can be regarded as a semi-empirical equation.(81)

A modification of Eq.(1-3-3) but more useful from a practical point of view is that of Redlich and Kwong,(42)

$$P = \frac{RT}{v - b} - a/(T^{\frac{1}{2}}v(v + b)) \qquad (1\text{-}3\text{-}4)$$

Eq.(1-3-4) like van der Waals equation has only two parameters and hence it is easy to use over wide ranges of conditions but does not give high accuracy, especially near the critical point.(44)

One of the most practically successful equations of state is the empirical equation of Benedict-Webb-Rubin, which has 8 arbitrary parameters to be determined from experimental P-V-T data;

$$P = \frac{RT}{V} + \frac{B_oRT - A_o - C_o/T^2}{V^2} + \frac{bRT - a}{V^3} + \frac{a\alpha}{V^6} +$$

$$\frac{c}{V^3T^2}\left(1 + \frac{\gamma}{V^2}\right)e^{-\gamma/V^2} \qquad (1\text{-}3\text{-}5)$$

where A_o, B_o, C_o, a, b, c, α and γ are constants.

The advantage of Eq.(1-3-5) is its ability to give high accuracy (about 0.5%) for whole fluid region (including the liquid phase) upto 1.8 times the critical density. However this equation is very complex compared with Eq.(1-3-3) and (1-3-4), and it is laborious and time-comsuming to solve such an equation.

For this reason, despite its high accuracy, it has rarely been used until recently in the field of engineering. The difficulties, however, have been overcome by the use of computing machines which allow one to solve quite complex equations of state without much difficulty. In general the most accurate equations are also the most complex, thus various equations with more parameters have been proposed. Nevertheless all these modern equations of state are modified forms of the B-W-R equation and like it, are empirical.

In 1963 Strobridge proposed a 16-coefficient equation whose parameters for nitrogen from 63 to 300°K upto about 200 bar were determined by a least-squares curve fit.(45)

In 1970 Bender(30) modified and further extended it to a 20-coefficient equation which can be expressed as

$$P = \rho T\left\{R + B\rho + C\rho^2 + D\rho^3 + E\rho^4 + F\rho^5 + (G + H\rho^2)\rho^2 \exp(-a_{20}\rho^2)\right\} \qquad (1\text{-}3\text{-}6)$$

where B, C, · · H are expressed as functions of temperature containing a total of 19 coefficients. The 20 coefficients in Eq.(1-3-6) were determined for nitrogen, argon, oxygen,(29) carbon dioxide and methane(30) for the whole fluid region from experimental P-V-T data. (see Eq. 3-3-2, section 3-3).

In 1973 Stewart and Jacobsen(46) increased the number of parameters to 33 and determined the parameters for nitrogen and oxygen by means of a least-squares curve fitting technique.

The same equation was used by McCarty[47] in 1974 and the parameters for methane were published.

These equations with many parameters were needed not so much to improve the accuracy of the P-V-T fit as to ensure equality of the fugacity of the coexisting liquid and gaseous phases and thereby reproduce the saturation line. Not all of the parameters (e.g. 20 in Bender equation) are therefore necessary in representing a restricted range of the P-V-T surface. Thus in representing the P-V-T measurements made in this work where the experimental range covered only the gas phase with maximum reduced density of $0.3\rho_c$, an equation of state such as Eq.(1-3-6) can be simplified by reducing the number of terms in both density and temperature, and also by neglecting the exponential term which is so-called the correction term for the liquid region. The optimum number of the parameters can only be determined empirically from the experimental P-V-T data and this will be discussed in greater detail in Chapter 3.

Apart from the empirical equations of state described above another important equation is the virial equation of state which is an expansion of Z as an infinite series in powers of density;

$$Z = PV/RT = 1 + B\rho + C\rho^2 + D\rho^3 + \cdots \qquad (1\text{-}3\text{-}7)$$

Although an equation of state of this type, but in truncated form, was first suggested as an empirical representation of PVT data its significance lies in its relationship with the intermolecular potential forces which cause the non-ideality of a real gas.[82]

Statistical mechanical considerations show that the second

virial coefficient, B, is a function of the interaction between pairs of molecules, as described in Chapter 4, the third virial coefficient, C, is a function of the interaction between three molecules, and so on. The second virial coefficient is one of the few macroscopic properties which can provide quantitative information on the intermolecular forces between a pair of molecules.

For mixtures the second virial coefficient is given by[82]

$$B_{mix} = \sum_{i}^{n}\sum_{j}^{n} x_i x_j B_{ij} \qquad (1\text{-}3\text{-}8)$$

where x_i and x_j are the mole fractions of i'th and j'th components respectively, and B_{ii} and B_{jj} are the second virial coefficients of pure substnaces i and j respectively. B_{ij} $(i \neq j)$ is the interactional second virial coefficient which is directly related to the interaction between molecule i and molecule j.

Similarly,

$$C_{mix} = \sum_{i}^{n}\sum_{j}^{n}\sum_{k}^{n} x_i x_j x_k C_{ijk} \qquad (1\text{-}3\text{-}9)$$

where C_{ijk} is related to the interaction between the three unlike molecules i, j and k.

Thus by measurement of the compressibility factors and hence second and third virial coefficients of mixtures, it is possible to obtain information on the intermolecular forces between unlike molecules.

Although a power series in density such as the virial equation can be used to represent simultaneously both liquid and gas phases it has not been particularly successful in the past, hence the use of an exponential terms in the B-W-R and succeeding equations, nor if it were so used would the

coefficients so obtained be virial coefficients in the statistical sense for it is believed that the statistical mechanical virial equation does not converge at high densities.

From a practical point of view there is an important difference between Eq.(1-3-6) and Eq.(1-3-7) in that in Eq.(1-3-6) the compressibility factor is expressed in terms of density as well as temperature, while in Eq.(1-3-7) the compressibility factor is expressed in terms only of density. It follows that the coefficients of the virial equation being functions of temperature can be fitted to P-V-T data only for a given isotherm, whereas those of Bender equation can be fitted simultaneously to any given set of isotherms. This makes Eq.(1-3-6) particularly valuable when handling experimental P-V-T results which contain only a limited number of data points on each isotherm.

In this work both Eq.(1-3-6) and (1-3-7) are used and the compressibility factors thus produced from these equations are compared and discussed in Chapter 3.

1-4 Other Thermodynamic Properties

An equation of state based on accurate PVT measurements is important not only in interpolation of the data and calculation of the compressibility factor but also, of course, in connection with the calculation of other thermodynamic properties. The changes in thermodynamic properties of a gas over ranges of temperature and pressure can be calculated from the particular equation of state chosen by manipulating the so-called fundamental equations and the Maxwell relations. That is, we have four

fundamental equations,

$$dU = TdS - PdV \tag{1-4-1}$$

$$dH = TdS + VdP \tag{1-4-2}$$

$$dA = -SdT - PdV \tag{1-4-3}$$

$$dG = -SdT + VdP \tag{1-4-4}$$

and we have Maxwell relations

$$\left(\frac{\partial T}{\partial V}\right)_S = -\left(\frac{\partial P}{\partial S}\right)_V \tag{1-4-5}$$

$$\left(\frac{\partial T}{\partial P}\right)_S = \left(\frac{\partial V}{\partial S}\right)_P \tag{1-4-6}$$

$$\left(\frac{\partial S}{\partial V}\right)_T = \left(\frac{\partial P}{\partial T}\right)_V \tag{1-4-7}$$

$$\left(\frac{\partial S}{\partial P}\right)_T = -\left(\frac{\partial V}{\partial T}\right)_P \tag{1-4-8}$$

Thus one can calculate, for example, the enthalpy, H, of a gas at temperature T_1 and pressure P_1 from the above equations (1-4-1) to (1-4-8). That is, by dividing Eq.(1-4-2) by dP, keeping T constant,

$$\left(\frac{\partial H}{\partial P}\right)_T = T\left(\frac{\partial S}{\partial P}\right)_T + V \tag{1-4-9}$$

From the Maxwell equation (1-4-8) we have

$$\left(\frac{\partial H}{\partial P}\right)_T = -T\left(\frac{\partial V}{\partial T}\right)_P + V \tag{1-4-10}$$

Therefore the partial derivative $\left(\frac{\partial H}{\partial P}\right)_T$ can be calculated from an equation of state of the form

$$f(P,V,T) = 0 \tag{1-4-11}$$

The total derivative of ehthalpy, dH, with respect to T and P can be expressed as,

$$dH = \left(\frac{\partial H}{\partial T}\right)_P dT + \left(\frac{\partial H}{\partial P}\right)_T dP \qquad (1\text{-}4\text{-}12)$$

Since

$$C_P = \left(\frac{\partial H}{\partial T}\right)_P \qquad (1\text{-}4\text{-}13)$$

and from Eq.(1-3-10),

$$dH = C_P dT + \left\{ V - T\left(\frac{\partial V}{\partial T}\right)_P \right\} dP \qquad (1\text{-}4\text{-}14)$$

Hnece by integrating Eq.(1-4-14) in two stages

(i) from T_o to T_1 at constant P_o

(ii) from P_o to P_1 at constant T_1

we have

$$H - H_o = \int_{T_o}^{T_1} C_P dT + \int_{P_o}^{P_1} \left\{ V - T\left(\frac{\partial V}{\partial T}\right)_P \right\} dP \qquad (1\text{-}4\text{-}15)$$

Similarly

$$S - S_o = \int_{T_o}^{T_1} \frac{C_P}{T} dT - \int_{P_o}^{P_1} \left(\frac{\partial V}{\partial T}\right)_P dP \qquad (1\text{-}4\text{-}16)$$

where H_o and S_o are arbitrary values at some chosen standard state, (P_o, T_o), such as at 1 atm., 0^oC. Other thermodynamic properties such as fugacity (or chemical potential), C_p and C_v can be evaluated similarly.

Thus from a knowledge of C_{p_o} and from the equation of state, $H - H_o$ can be calculated. Of course some accuracy is lost in the differentiation and integration and thus high precision is required in the equation of state and hence in the P-V-T measurements, if the procedure is to be successful.

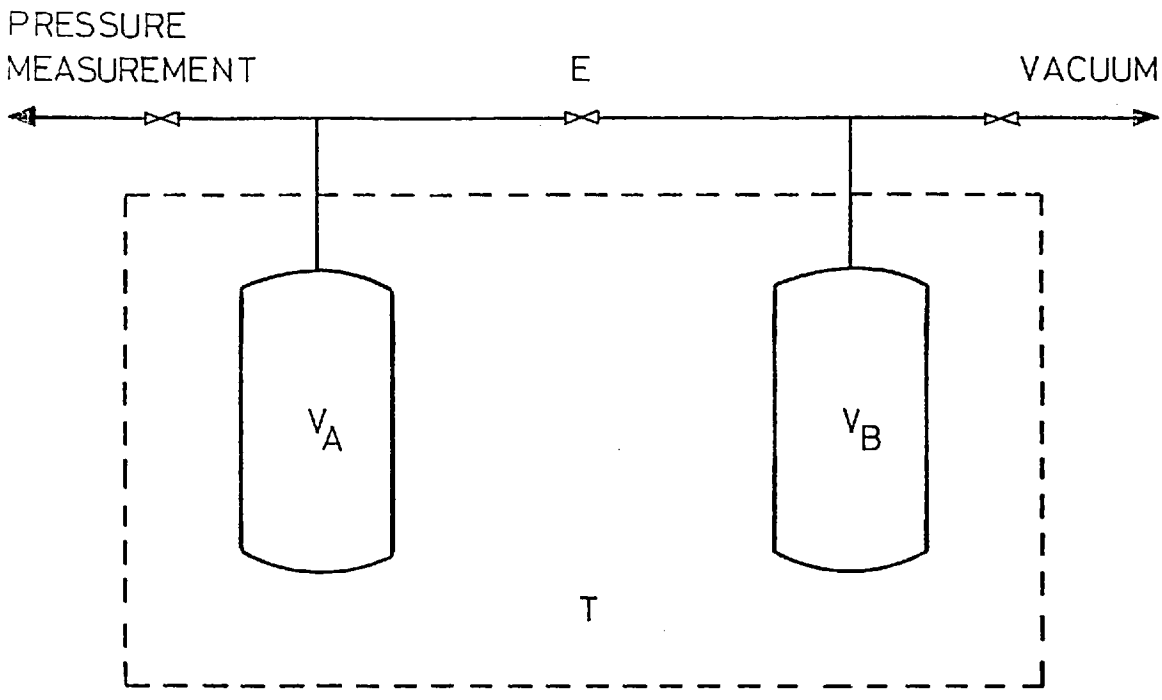


FIG 1-1 BURNETT EXPANSION APPARATUS (SCHEMATIC)

1-5 Measurement of the Compressibility Factor

The compressibility factor given by Eq.(1-3-2) can be directly determined from an equation of state chosen using experimental P-V-T data. In virtually all methods, the gas under investigation is contained in a well defined volume and the pressure and temperature are measured. The general principles of P-V-T measurement were summarised by Saville[2] and Mason and Spurling[82] compiled all papers published between 1920 to 1967 which report P-V-T measurements.

In 1936 Burnett[22] introduced a multiple expansion method which avoids the need for accurate volume determination, direct mass or normal volume measurements, absolute temperature measurement, and the use of mercury as a confining fluid.

A typical Burnett multiple-expansion apparatus is shown schematically in Fig 1-1.

Initially the unknown quantity of gas is confined at a fairly high pressure in V_A, with the expansion valve E closed, and its pressure is measured. The gas is then allowed to expand into V_B, and the pressure is again measured after temperature equilibrium is achieved. Valve E is then closed again and V_B evacuated. This process is continued until the lowest measurable pressure is attained. The sequence of pressures, P_o, P_1, P_2, $\cdots P_j$, $\cdots P_n$ constitute the basic data of a Burnett 'RUN'.

Material balance is taken before and after each expansion, i.e. the number of moles of gas, n_o, in V_A prior to the first expansion is given by

$$n_o = P_o V_A/(RTZ_o) \qquad (1\text{-}5\text{-}1)$$

where Z_o is the compressibility factor at pressure P_o.
After the first expansion,

$$n_o = P_1(V_A + V_B)/(RTZ_1) \qquad (1\text{-}5\text{-}2)$$

Hence by equating Eq.(1-5-1) and (1-5-2)

$$P_o/P_1 = N(Z_o/Z_1) \qquad (1\text{-}5\text{-}3)$$

where

$$N = (V_A + V_B)/V_A \qquad (1\text{-}5\text{-}4)$$

N is called the 'cell constant' or 'apparatus constant'.
After the second expansion

$$P_1/P_2 = N(Z_1/Z_2) \qquad (1\text{-}5\text{-}5)$$

and after j'th expansion,

$$P_{j-1}/P_j = N(Z_{j-1}/Z_j) \qquad (1\text{-}5\text{-}6)$$

From Eq.(1-5-3) and Eq.(1-5-5),

$$P_2N^2 = (P_o/Z_o)\cdot Z_2 \qquad (1\text{-}5\text{-}7)$$

and generally

$$P_jN^j = (P_o/Z_o)\cdot Z_j \qquad (1\text{-}5\text{-}8)$$

Eq.(1-5-8) shows that, in order to obtain Z_j at a given pressure P_j, N and (P_o/Z_O) must be known. Determination of these values can be accomplished from either a graphical or analytical method of data treatment. These procedures are described in Chapter 3.

The Burnett method requires good temperature control and precise pressure measurements. The methods of controlling temperature and measurements of pressure and temperature are described in Chapter 2.

As no accurate measurements of volume, mass of gas, or absolute temperature are necessary, the method is particularly suited to the determination of precise values of Z at low density and low pressure, where other methods may lack the necessary precision at low pressures, at very high temperatures where the accurate measurement of absolute temperature is difficult. However, as compressibility factors are not measured directly in a Burnett apparatus, their accuracy may be affected not only by experimental errors in measurement but also by such factors as the magnitude of N and hence the number of expansions in a RUN, and the method of data treatment employed.

When both vessel V_A and V_B in Fig 1-1 are kept at a same temperature T (usually called an 'isothermal' Burnett apparatus), temperature control of two vessels at low temperature becomes difficult, and furthermore leakage problems can occur with expansion valves. For these reasons a 'non-isothermal' Burnett apparatus may be employed, as in this work, in which volume V_A is at the experimental temperature, T_A, while volume V_B is at a temperature T_B which is easily maintained constant, such as 0^oC. The Valves are also at temperature T_B. In this case the material balance before and after j'th expansion is given by (ignoring the dead space between the two vessels),

$$P_{j-1}V_A/T_A(Z_A)_{j-1} = P_jV_A/T_A(Z_A)_j + P_jV_B/T_B(Z_B)_j \qquad (1\text{-}5\text{-}9)$$

The dead-space between the vessels presents a severe problem since there also exists a temperature gradient. Thus in order to calculate an accurate material balance the volume and the local temperatures must be known. To reduce the errors which can occur in this part the volume of the dead-space must be as small as possible.

In computation of the results from a 'non-isothermal' experiment we clearly need also the equation of state at temperature T_B so as to calculate Z_B. This can come from other sources or from an experiment at $T_A = T_B$. The way in which this is dealt with is described in Chapter 3.

CHAPTER TWO

EXPERIMENT

2-1 Introduction

Determination of compressibility factors of gases and gas mixtures by Burnett method involves a series of expansions of the gas under investigation from one vessel(here called the low temperature system or piezometer) to another(the expansion vessel). Before and after each expansion pressure and temperature are measured.

Accurate measurement of pressure, which is needed in the Burnett procedure, can be achieved only when the temperature of the gas is maintained at a certain value with minimum fluctuations. Thus the non-isothermal Burnett apparatus requires, basically,

i) low temperature system

ii) expansion vessel

iii) temperature control system

iv) temperature measurement system

v) pressure measurement system

vi) vacuum system.

The schematic diagram of the experimental apparatus is shown in Fig 2-1.

In order to get accurate results from the Burnett Apparatus a high vacuum system is prerequisite, for after each measurement the material inside the expansion vessel should be evacuated thoroughly. Moreover temperature control of pressure vessel is possible only when a good vacuum is maintained between the pressure vessel and outer jacket.

throughout this work the expansion vessel was in a ice-bath at $0^{o}C$ and the pressure vessel was at the experimental

temperature. Both vessels were double-walled so that the pressure of the inner volume could be equalized to that of outer volume by filling both sides with gas at the same pressure. This reduced changes in the experimental volume due to elastic distortion of the vessels concerned. The gases in the inner and outer volumes were kept separate by the Precision Pressure Gauge (P.P.G.) which was a spiral quartz Burdon tube. The outer volume was then connected to the pressure measurement system so that the dead space of actual experimental volume could be minimized.

Although it was desirable to keep exactly the same pressure on each side of the spiral tube, practically this was difficult especially at high pressure. Moreover the null position of the P.P.G. itself shifted with pressure (section 2-8-5). Thus the P.P.G. null was calibrated against pressure change for each individual gas so that the null position could be found at a given pressure, and the P.P.G. sensitivity was calibrated against pressure difference between inside and outside the spiral tube so that accurate pressure difference could be calculated. These P.P.G. calibrations will be discussed extensively in section 2-8-5 (c) and (d), since this part could lead the largest possible error in measuring the pressure. The temperature was measured by means of a platinum resistance thermometer. The resistance of the thermometer was measured either by an A.C. Precision Double Bridge (runs 17, 18, 19 and 20) or by a potentiometer with a suspension galvanometer (all other runs).

The pressure between 20 bar and 100 bar were measured by means of an oil piston gauge and between 20 bar down to about 3 bar were measured by means of a gas piston gauge.

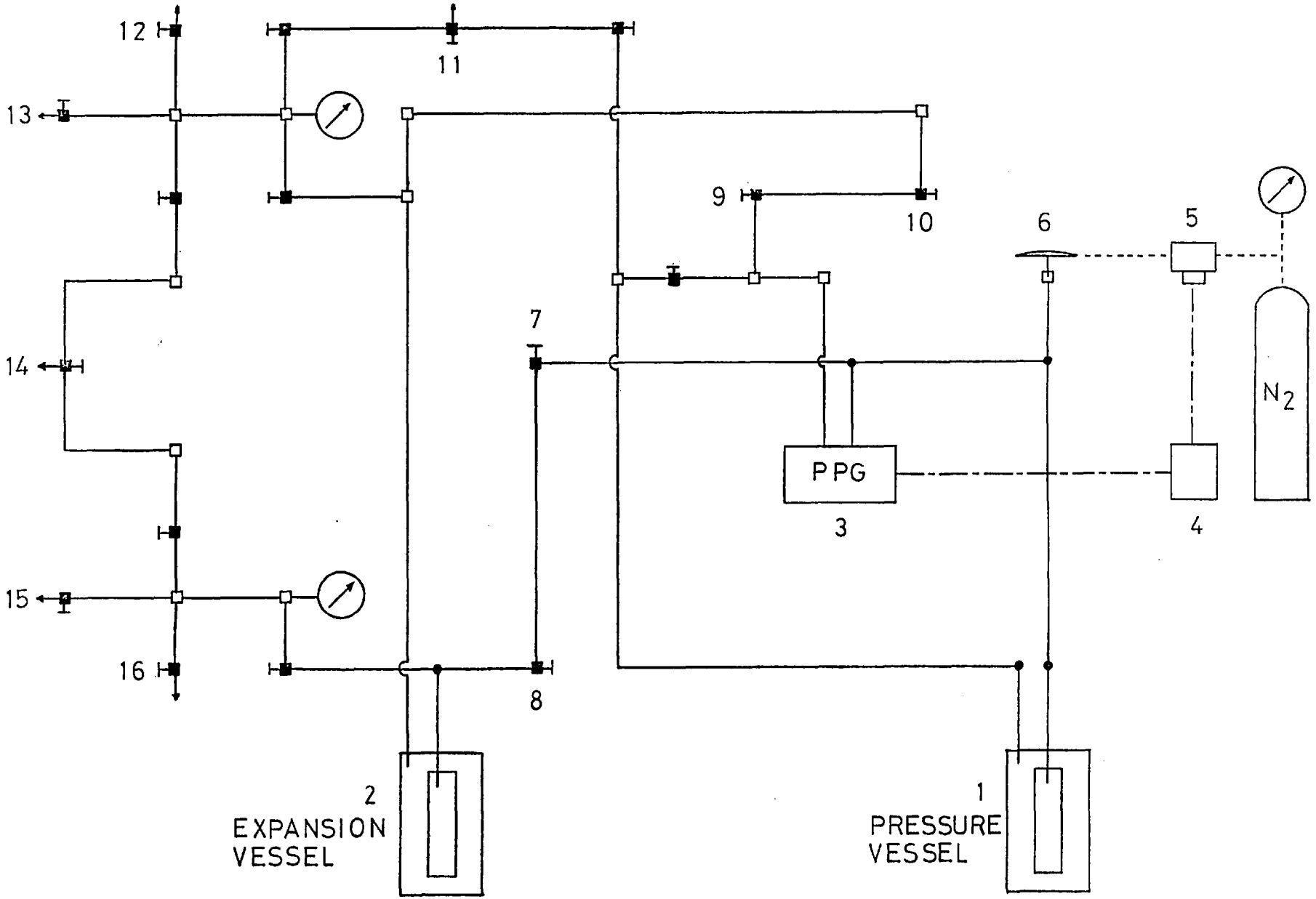


FIG 2-1 THE BURNETT APPARATUS (SEE NEXT PAGE)

FIG 2-1 (CONTINUED)

———	S/S TUBING
.....	CU TUBING
-—-—	ELECTRIC WIRE
	VALVE
□	S/S AMINCO JOINT
•	SWAGELOK COUPLING

1		PRESSURE VESSEL	SEC. 2-2	FIG. 2-2, 2-3 & 2-4
2		ICE BATH VESSEL	SEC. 2-3	FIG. 2-6
3		PPG	SEC. 2-8-5	FIG. 2-20
4		AUTO TRIGGER	SEC. 2-8-5	FIG. 2-22
5		SOLENOID VALVE	〃	〃
6		PNEUMATIC VALVE	〃	〃
8	10	INNER & OUTER VOLUME EXPANSION VALVES		
7	9	〃	FINE CONTROL VALVES	
11		TO PRESSURE MEASUREMENT		FIG. 2-16
12	16	TO VACUUM	SEC. 2-4	FIG 2-7
13	14	TO GAS STORAGE	SEC. 2-5	FIG 2-8
15		VENT		

The whole apparatus was housed in a polyethylene cabinet, in which the temperature was controlled at a few degrees above ambient room temperature by means of a toluene regulator with a proportionating head in conjunction with two pairs of 200 watt electric bulbs. The air inside the cabinet was circulated by two 10-inch fans. The cabinet temperature remained constant with less than 0.1°C fluctuation during daytime.

One experimental run normally took 2-4 days depending on the first pressure, the experimental temperature and the species of gases.

2-2 The Low-Temperature System

2-2-1 Introduction

As shown in Fig 2-2 the low temperature system consists of the pressure vessel, the radiation shield, the inlet tubing and outer-jacket. The double-walled pressure vessel is suspended within a copper radiation shield which is again suspended inside a brass outer-jacket. The space between the pressure vessel and the outer jacket was evacuated thoroughly (lower than 10^{-5} torr) in order to eliminate the heat transfer by conduction and convection.

Ten platinum resistance thermometers, which were connected in series and housed in the pressure vessel wall, were used as a part of an automatic temperature control system which regulated the power supply to the heater circuits wound outside the pressure vessel, thus maintaining its temperature at a constant value.

The pressure vessel was surrounded by a constant temperature environment(radiation shield) whose temperature was controlled

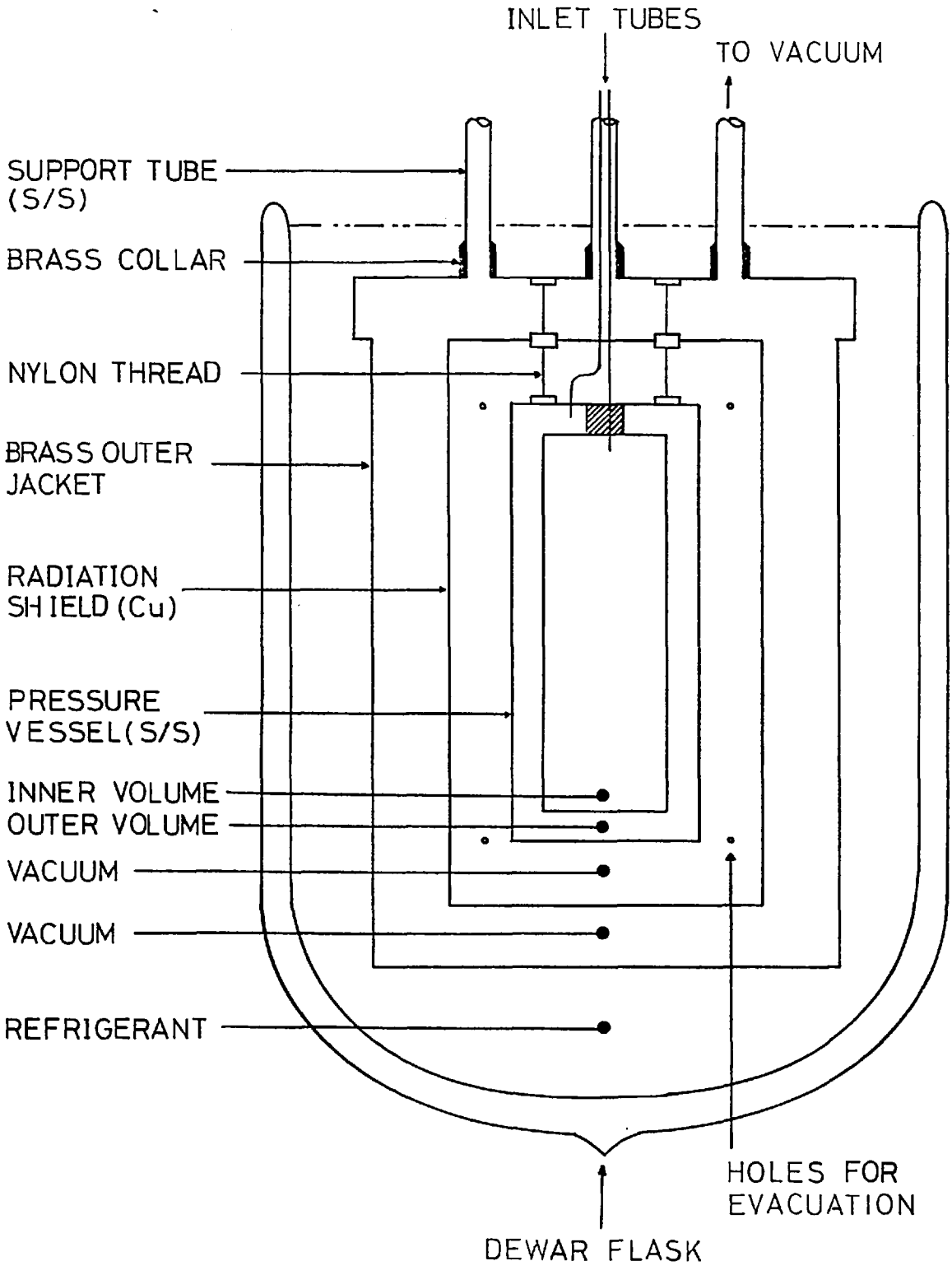


FIG 2-2 LOW TEMPERATURE SYSTEM

at about 1°C below that of pressure vessel.

The low temperature system was thus designed such that the heat loss from the pressure vessel was small and radiative, giving close temperature control and small temperature gradients within the vessel.

2-2-2 The Pressure Vessel

The double walled pressure vessel was made of EN58J stainless steel. The inner vessel with 0.125 inch wall thickness contained the gas under investigation and the outervessel with 1 inch wall thickness was filled at a same pressure as that of inner vessel with same gas. The inside surface of the inner vessel was polished to reduce adsorption of the gas and it was assembled by electron beam welding (by courtesy of Vickers Ltd.) to avoid any damage to the polished surface.

10 holes of 0.125 inch diameter were drilled around the outer wall to house temperature controlling platinum resistance thermometers. As shown in Fig 2-3, the vessel was provided with a central well which contained the platinum resistance thermometer for the temperature measurement. Two heaters (32 swg manganin), each of which consisted of three sub-heaters connected in parallel, were non-inductively wound along the length of the outer wall. The heaters were electrically insulated from the pressure vessel by a layer of nylon material which was streched over the vessel and then painted with Formvar (a solution of polyvinyl formal in chloroform).

A copper-constantan thermocouple was soldered to the pressure vessel at its mid-point to regulate the radiation shield temperature(Fig 2-11). The electrical circuits of the

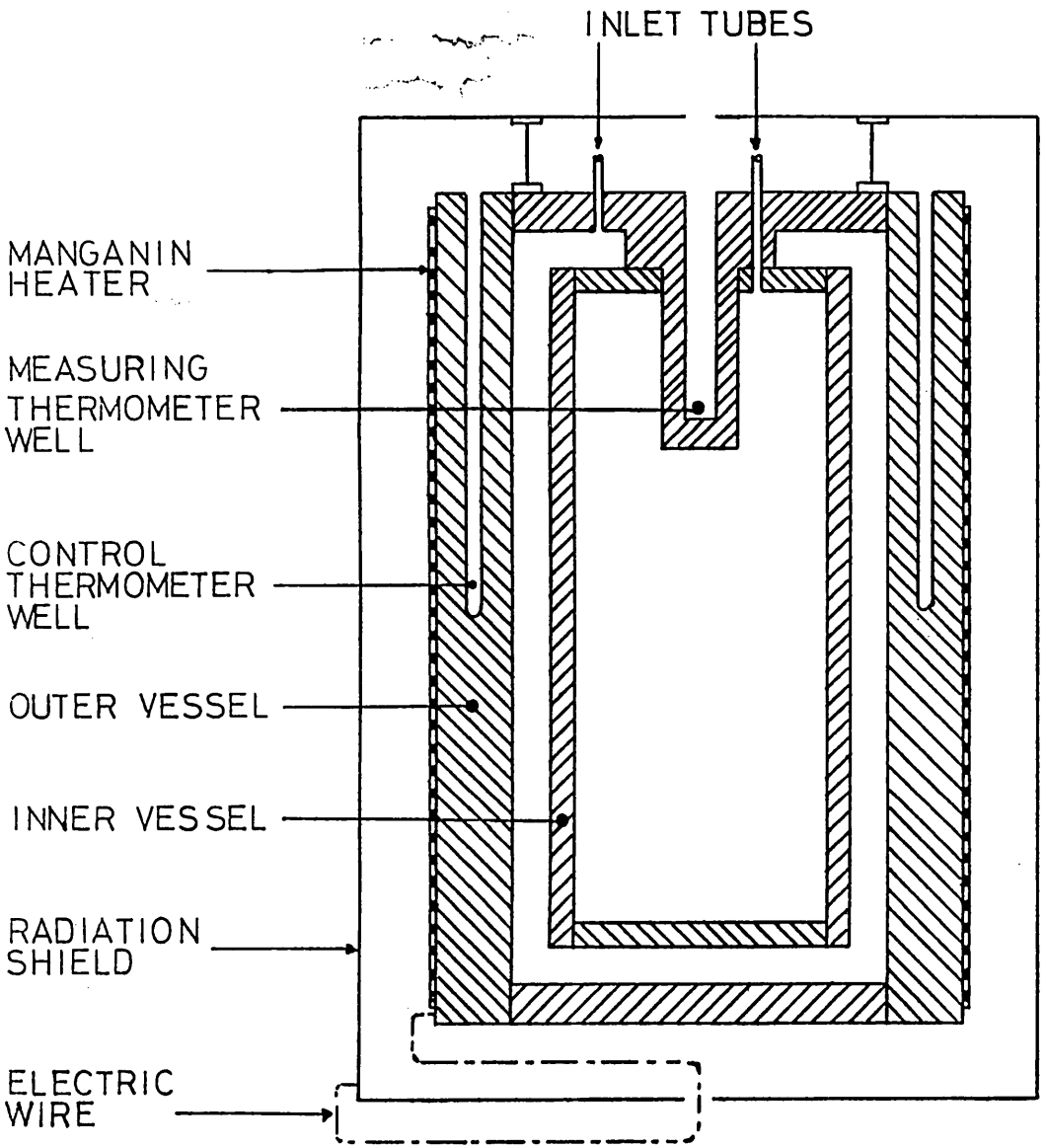


FIG 2-3 PRESSURE VESSEL

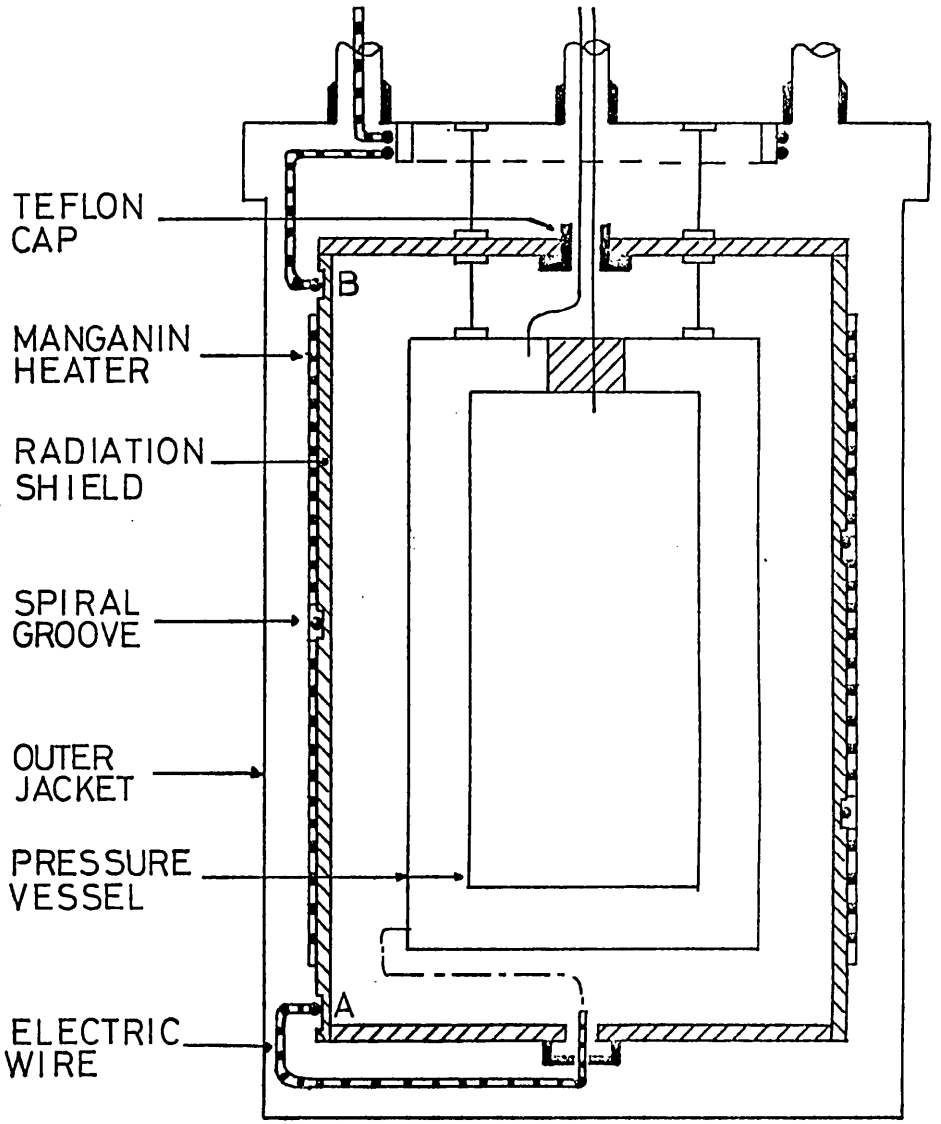


FIG 2-4 RADIATION SHIELD

pressure vessel will be described in section 2-6.

2-2-3 The Radiation Shield

As the name implies, the radiation shield served to prevent direct heat transfer by radiation between the pressure vessel and outer brass jacket.

The temperature control of the pressure vessel, therefore, largely depended on the environment provided by the radiation shield, the temperature of which should differ from that of the pressure vessel by a small constant amount. Cylinderically shaped radiation shield was made of copper, 0.125 inch thickness, and consisted of three parts, i.e. side cylinder, top and bottom end plates, both end plates were fixed to its side cylinder by means of screws. Each of end plates had a hole at its center to lead gas inlet tubes (top) and electrical leads from the pressure vessel (bottom). Both end plates consisted of two copper plates between which a manganin heater was sandwiched and insulated by mica.

Outside the cylinder there were two spiral grooves from top down to bottom to embed two silicon-rubber cables, one housed all the heater wires and the other housed the thermocouple and thermometer wires.

The idea of these spiral grooves was that by having longer wires from point B,colder (Fig 2-4), to point A, the temperature of the wires at B would be closer to that of radiation shield, and hence the heat transfer by conduction through the metal wires could be prevented. Three thermocouples were soldered on top, side and bottom parts of the shield to monitor the temperature differences between side and both end plates (Fig 2-11). The temperature differences were

adjusted by means of rheostats in the heater circuits as shown in Fig 2-12 and 2-13.

Spare wires were included in both cables in the grooves mentioned above to prevent re-wiring of the radiation shield heaters in case of breakage or shorting in the wires. Nylon stocking material was used to cover the outside of the cylinder and was painted with formvar. This cover not only held the two cables in the grooves but served as an insulant onto which six parallel heaters were wound non-inductively. Extra insulation was provided over a 2 cm wide band at each end of the cylinder where the soldered connections were to be made.

All the wires from the pressure vessel, led through the hole at the center of the bottom plate, together with the wires from the radiation shield itself were aligned in two rows onto the doubly insulated end ring of the cylinder and fixed by means of formvar except for the uncovered end tips of the wire which were bent perpendicularly to the cylinder surface in order to make marking and soldering of individual wire easy.

These wire tips were soldered to appropriate wires of the cables in the groove, and covered with nylon material and twice painted with formvar. The wires from the groove on top of the cylinder plus those from inlet tubes (point B, Fig 2-4) were similarly marked, soldered and insulated. Wires for heaters, thermocouples and thermometers were separated and sheathed in three silicone-rubber sleevings, which were led out of the low temperature system through two pipes of the outer jacket.

The hole at the top plate were sealed by a teflon cap with two 1/16 inch dia. holes through which the inlet tubes

passed. The other hole at the bottom end was sealed by a thin copper plate by means of three screws. This measure was necessary to prevent direct heat losses from the pressure vessel through these holes by radiation.

The radiation shield was suspended from four hooks screwed into the underside of the outer jacket by means of several strands of nylon dental floss which served as both thermal and electrical insulant. The pressure vessel was suspended similarly from the top plate of the radiation shield.

The interior of the radiation shield was covered with thin silver foil to reduce radiation heat loss from the pressure vessel.

Temperature control of the radiation shield together with all the electric circuits involved will be discussed in section 2-6-3 in detail.

2-2-4 Inlet Tubes

As shown in Fig 2-5 inlet tube system consisted of two stainless steel pipes (0.063 in. o.d., 0.043 in. i.d.), 11 Cu-constantan thermocouples and two heaters. These tubes were the intermediate part between the pressure vessel, which was at experimental temperature, and outside environment. Unlike the pressure vessel the inlet tubes were not protected from the radiation heat loss. Thus without a proper heating device, the gas inside this part could inadvertently condense. Further, temperature control and measurement were important, as computation of the results required a knowledge of the amount of material in the inlet tubes.

For these reasons, the two tubes were wrapped with a

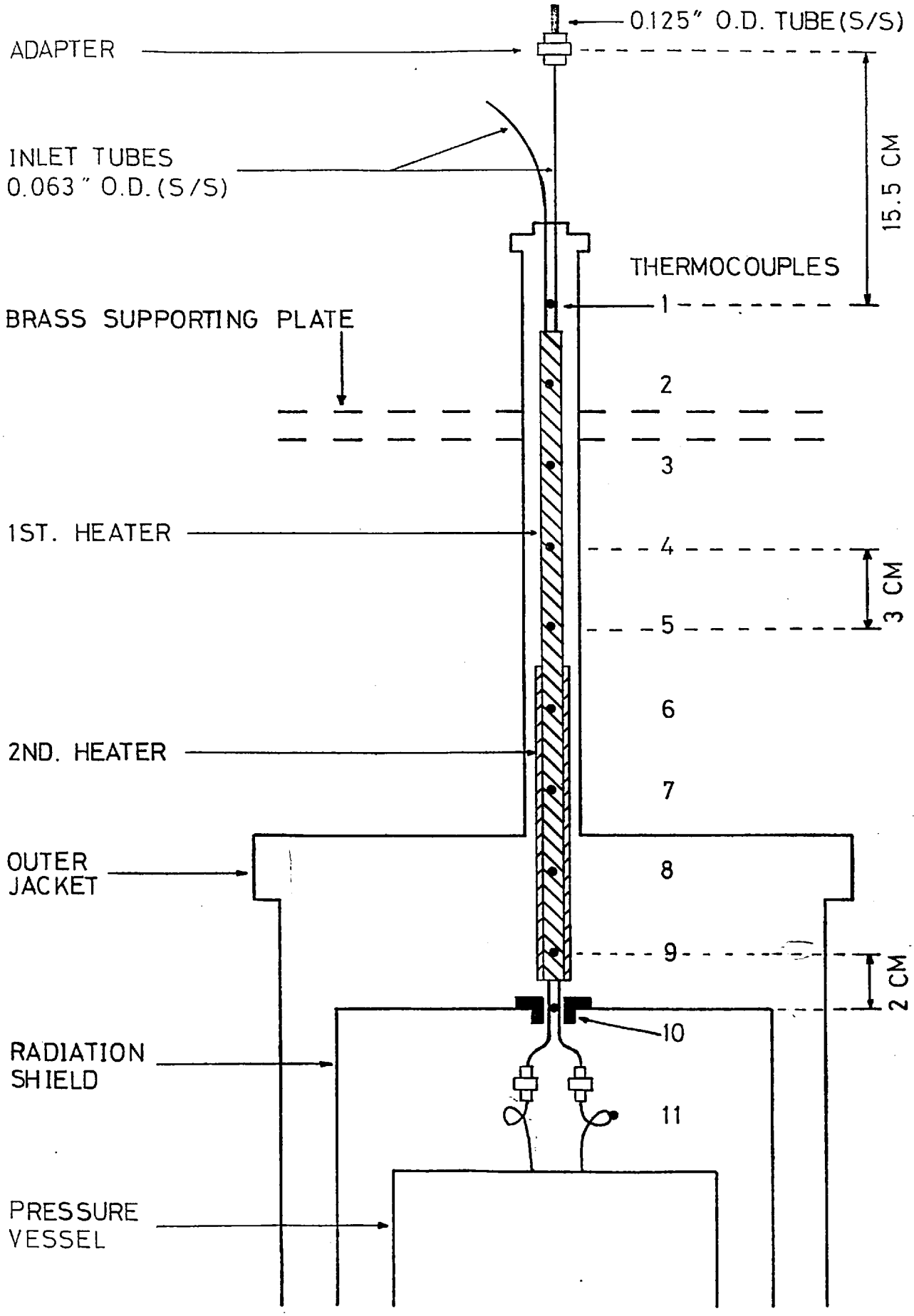


FIG 2-5 INLET TUBES & THERMOCOUPLE POSITIONS

thin sheet of air mail paper and painted with Formvar. Along the wrapped tube 11 thermocouples were attached by means of Formvar paint. Two 32 swg manganin heaters were then wound non-inductively on top, one covered whole length (except the part from the radiation shield to the pressure vessel) and the other was wound on the bottom half of the first heater, where the temperature was the lowest along the tube (Fig 2-5).

The inlet tubes were connected to the pressure vessel by means of 'Swagelok' couplings. Between these couplings and the pressure vessel the tubes were coiled (9 cm) to reduce the temperature gradient between the inlet tubes and the pressure vessel. The inlet tubes passed through at the central support tube of the outer jacket and came out to atmosphere through two tiny holes in a brass adaptor and were sealed by means of soft-soldering. The heater and thermocouple wires were sheathed separately in two silicone-rubber sleevings and soldered at point B (Fig 2-4) to appropriate wires which led out of the low temperature system.

The number of thermocouples provided, 11, was strictly more than were needed to determine the temperature gradient to the required accuracy. However, this did allow experimentation to continue when, as in this work, 3 thermocouples developed faults.

The inner volume of the inlet tube was measured by using mercury. A tube of known length was filled with mercury and weighed. Then the specific volume (cc/cm of tube) was calculated from the mercury density.[3] After several measurements at different temperatures the inner volume per cm was found to be 0.00954 cc.

2-2-5 The Outer Jacket

The outer jacket was made of brass and supported by four stainless-steel tubes which were thin-walled to reduce heat transfer from outside to the refrigerant.

At bottom of each support tube, a brass collor had been hard-soldered on and this brass collar was then soft-soldered to the brass jacket. Each of the four supports then passed through four corresponding collars provided on a 0.25 in. brass support plate which was fixed on a framework of 'Handy-Angle.

The lead out wires were sheathed in silicone-rubber sleeving (about 1 meter long) and wound several times around a ring which was screwed and soft-soldered to the underside of the top of the jacket. This measure was to reduce the temperature of the wires to nearer that of the radiation shield, thus reducing the disturbing effect on the temperature control of the radiation shield.

The central support tube contained the inlet-tubes, the second contained all the heater wires, the third contained all the wires from the platinum thermometers and the thermo-couples, and the fourth support was directly connected to the vacuum system. This fourth support did not contain any electric wires, because possible condensation of mercury from the two diffusion pumps would cause electrical short circuits.

The cable passed through a black-waxed B29 brass cone/glass socket joint at the top of the support tubes. Each group of wires were led out to the atmosphere through black-waxed B29 cone/socket seals.

The seal was made by baring the wires, embedding them into the black wax of the socket and inserting the waxed

cone stopper with a gentle heat. The wires, which were now in the atmosphere, were soldered to 16 swg pins, of the same metal, mounted in a perspex disc on each stopper cone.

The inside surface of the jacket was covered with thin aluminum foil to reduce radiation heat transfer between the refrigerant and the radiation shield.

The jacket cylinder was soldered to its lid by using low melting point (115°C) indium/tin solder to avoid damage to any part of electric circuits in the radiation shield and also to avoid melting the other soldered part of the jacket (i.e. the soldered connection between the support tubes and the outer jacket).

2-2-6 The Cryostat

The outer jacket was immersed in a cooling fluid contained in a large silvered Dewar flask with a viewing strip, through which the level of the refrigerant was observed. The outer surface of the Dewar was wound with self-adhesive tape in case of explosion of the double walled Dewar due to thermal stress.

The refrigerant used depended on the temperature range under investigation. During testing and practicing, measurements were made of nitrogen gas with liquid N_2 as refrigerant. When experimenting with ethylene and ethylene-methane mixtures, solid carbon dioxide/ethanol mixture was used as refrigerant (-80°C) due to the higher critical point of ethylene and its mixtures than those of pure N_2 and CH_4.

For some of the runs above 0°C, cooling at about -10°C from a small refrigeration unit was used. In this case a 0.25 in. soft copper tube was coiled around the outer

jacket and connected to the refrigerator (Grant LC 10 Circulator), in which ethanol was used as cooling medium. With proper insulation (polyurethane) the temperature of ethanol inside the Dewar was kept at -5°C with ±0.5°C fluctuations.

2-2-7 Low Temperature System Wires

Wires for low temperature system were chosen such that the temperature control and measurement systems were least disturbed electrically due to change of temperature of the wires. Low temperature system wires can be categorized as following.

a) Thermocouples: 40 swg copper and 36 swg manganin were used. The sizes of wires were not changed throughout the system to the measuring instrument, except at the pin blocks (section 2-2-4). The ice-point junctions were soldered by using low emf solder and housed in thin glass tubes which were immersed in distilled water-ice mixture in a small dewar flack.

b) Heaters: All heaters were wound non-inductively with 32 swg manganin wire. Inside the spiral groove of the radiation shield 32 swg copper wire was used because there would be no temperature fluctuations in the radiation shield wall, and the resistance would be constant.

c) Platinum resistance thermometer: There were 11 platinum resistance thermometers in the pressure vessel, one for temperature measurement (calibrated) and the other 10 for temperature control of the pressure vessel. The lead out wire was 32 swg copper in the spiral groove.

d) Inside the support tubes: These tubes were in contact

with the refrigerant, and the variations in the level of liquid could cause changes in the resistance of the wires leading to errors in temperature measurement and control. Thus both the thermometer and heater leads were of manganin, whose thermal coefficient of electrical resistance is much smaller than that of copper. 32 swg manganin was used for heaters and 28 swg manganin for the thermometers. The platinum resistance thermometer wires had to have a low resistance and 28 swg was the largest diameter that could be handled in wiring the system, especially at the black-waxed cone-socket sealing through which all the leads passed out to the atmosphere.

e) Outside the system: From the pin-blocks at the top of the support tubes there were no restrictions on the size of wires and hence, 18 swg copper wire was used for both thermometers and heaters. Three groups of heaters, thermometer and thermocouple wire were sheathed in p.v.c. sleevings respectively and passed through three separate 1/2 in.-copper tube from above the pin-blocks to various controlling and measuring instruments.

Spare leads were provided for all electrical circuits both inside and outside the system to avoid unnecessary labor in case of breakage of electrical leads.

2-3 The Expansion Vessel

The expansion vessel (also called the ice-bath vessel) was made of EN58J stainless steel and like the low temperature pressure vessel, was double-walled and hence pressure compensated to reduce volume changes in the inner vessel with pressure.

The inside surface of the inner volume was polished to reduce adsorption and assembled by precision argon-arc welding to avoid any damage to the polished surface.

The basic difference between the expansion vessel and the piezometer was that the inner member of the expansion vessel was interchangable as shown in Fig 2-6.

Originally four different inner vessels were provided and the volumes were approximately 514.9, 385.7, 281.3 and 183.8 cc respectively.

Changing from one value for the volume of the expansion vessel to another alters the value of the Burnett apparatus constant N (see Chapter 3) and thereby influences the accuracy of the results.[4,5]

In this work the optimum vessel was the smallest (183.8 cc) and it was used throughout. This choice was primarily determined by the low vapour pressure of ethylene at 0°C (40.9 bar), for, when the temperature was below the critical point at any part of the apparatus the pressure had to be limited to about 85% of the vapour pressure to avoid possible condensation of the gas. For pure ethylene the expansion vessel temperature (0°C) is well below the critical temperature of 9.5 C. The first pressure in the piezometer was, therefore, restricted such that after one expansion the pressure should not exceed 34.7 bar. Thus to obtain an adequate number of expansions during the experiment, the smallest expansion vessel was needed.

As shown in Fig 2-6, on top of the inner vessel a round stainless disc was welded, through which an inlet tube of 0.063 in. o.d., 0.043 in. i.d. was passed. Beside the inlet

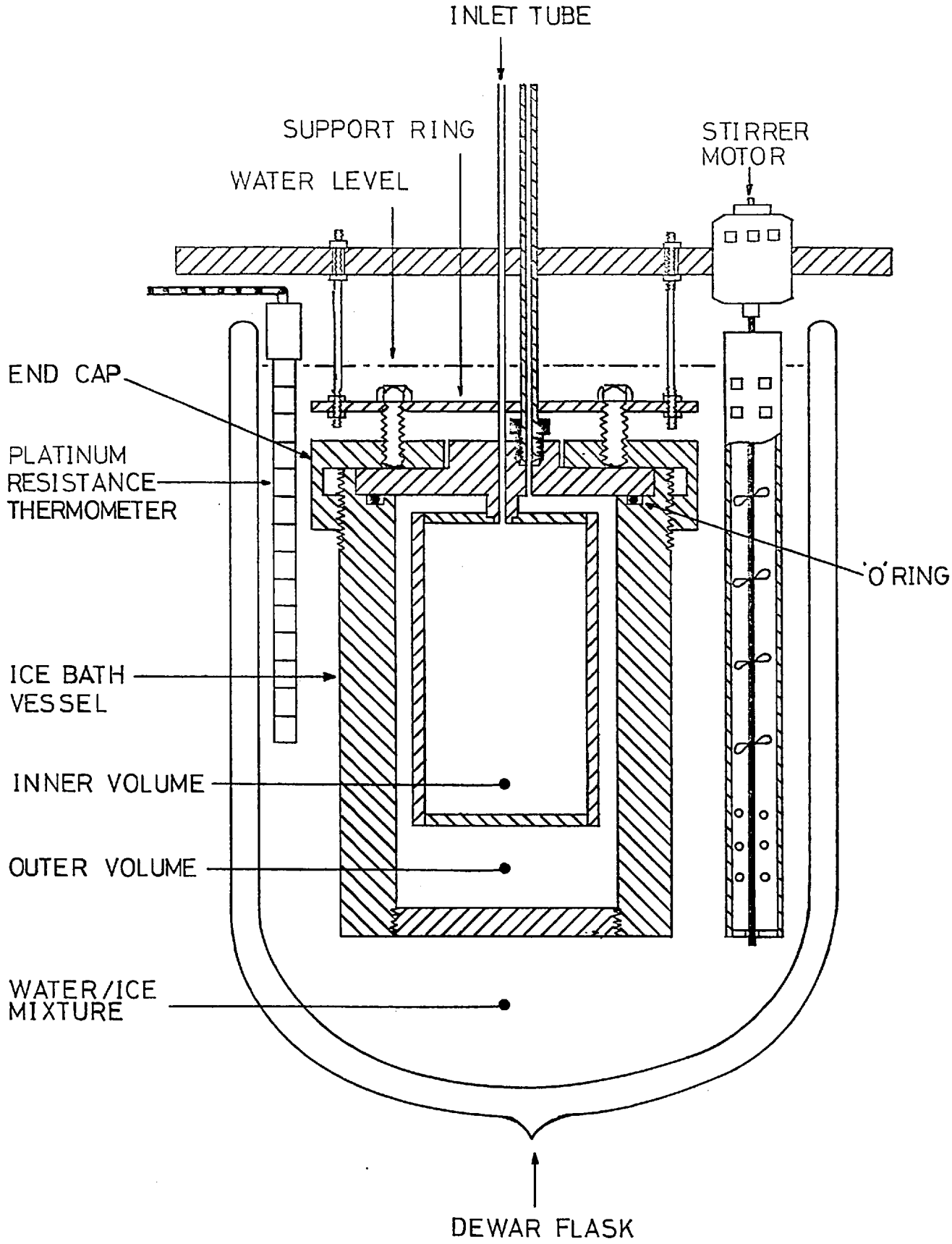


FIG 2-6 EXPANSION VESSEL SYSTEM

tube an Aminco connection thread was machined to provide any entry for the gas used to fill the outer annular space. The outer volume was sealed from the atmosphere by means of a rubber 'O' ring in the groove on the outer cylinder onto which the disc of the inner vessel was placed. The disc was held by means of the end-cap of the outer jacket and eight 3/8 in. stainless steel bolts which screwed through the end cap to provide uniform loading. The bolts were tightened to give a leak-proof seal at the 'O' ring. The bolts also passed through a steel ring which was connected by means of four 3/8 in. diameter steel rods to the framework of the apparatus and thus served to support the whole vessel.

The vessel was immersed in a mixture of distilled water and finely crushed ice in a large Dewar flask. The water was circulated by means of a six-bladed stirer inside a plastic tube with holes through which water flowed upward.

A platinum resistance thermometer was provided to check the temperature stability of the circulating water around the expansion vessel.

2-4 The Vacuum System

A schematic diagram of the vacuum system is shown in Fig 2-7. As shown in the diagram two separate vacuum systems were provided with appropriate interconnecting taps.

Under normal conditions one system was for evacuating the outer jacket, and the other for the expansion vessel. The two systems were, however, interconnected in such a way that, one system would be used in both purposes in case of failure of the other.

A rotary pump was connected to a mercury diffusion

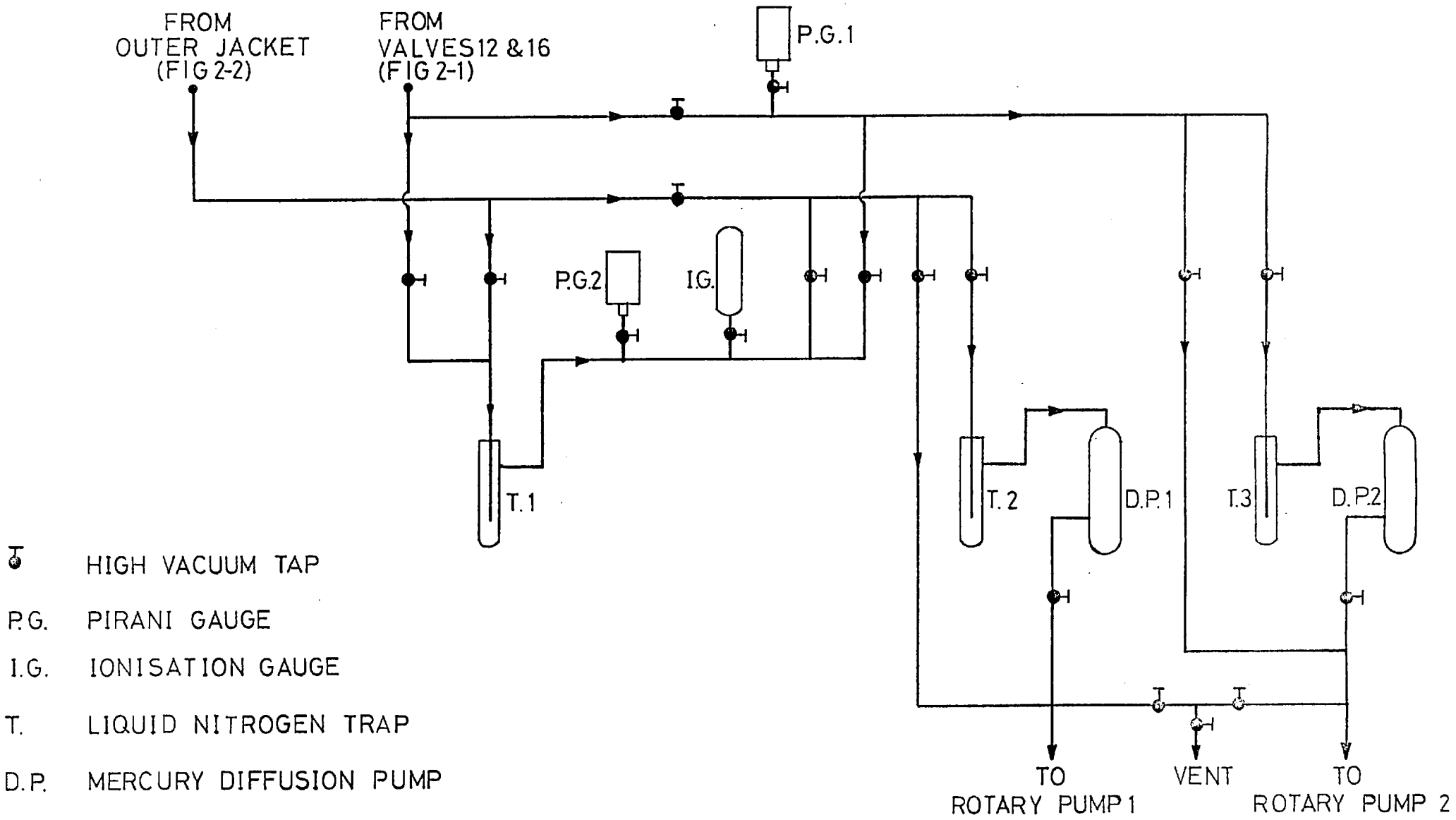


FIG 2-7 VACUUM SYSTEM

pump with two liquid nitrogen traps between which a Pirani and an ionisation gauge heads were provided.

The vacuum inside the outer-jacket was kept below 10^{-5} torr on ionisation gauge throughout this work. Evacuation of the expansion vessel to less than 10^{-4} torr on the ionisation gauge took normally less than one hour. However, the vessel was evacuated for more than one hour, since the pressure inside vessel could be higher than that of indicated value on the gauge because of small diameter of the inlet tube of the expansion vessel.

2-5 The Gas Storage System

The gas storage system was provided as an economy measure. Since the compensating gas was the same as the experimental gas, it was possible to collect the gas in a storage pressure vessel and to use it again.

The schematic diagram of the system was shown in Fig 2-8. As shown in the diagram the gas vented from the expansion vessel was collected in the storage vessel with a pressure switch. The pressure switch was adjusted such that, when the pressure inside the vessel exceeded 150 atm., the pressure switch closes the solenoid valve circuit and hence energized the valve which, in turn, opened the pneumatic valve by means of N_2 gas. The solenoid valve circuit was open when the pressure reached about 80 atm. and hence shut the pneumatic valve again.

The inside volume of stainless-steel vessel was about 1.5 liter. The vessel was sealed by means of a silver-plated metal 'O' ring, seated in the groove on top of the vessel. An end plate was placed on the 'O' ring and pressed by means of an end cap with eight-3/8 in. stainless steel

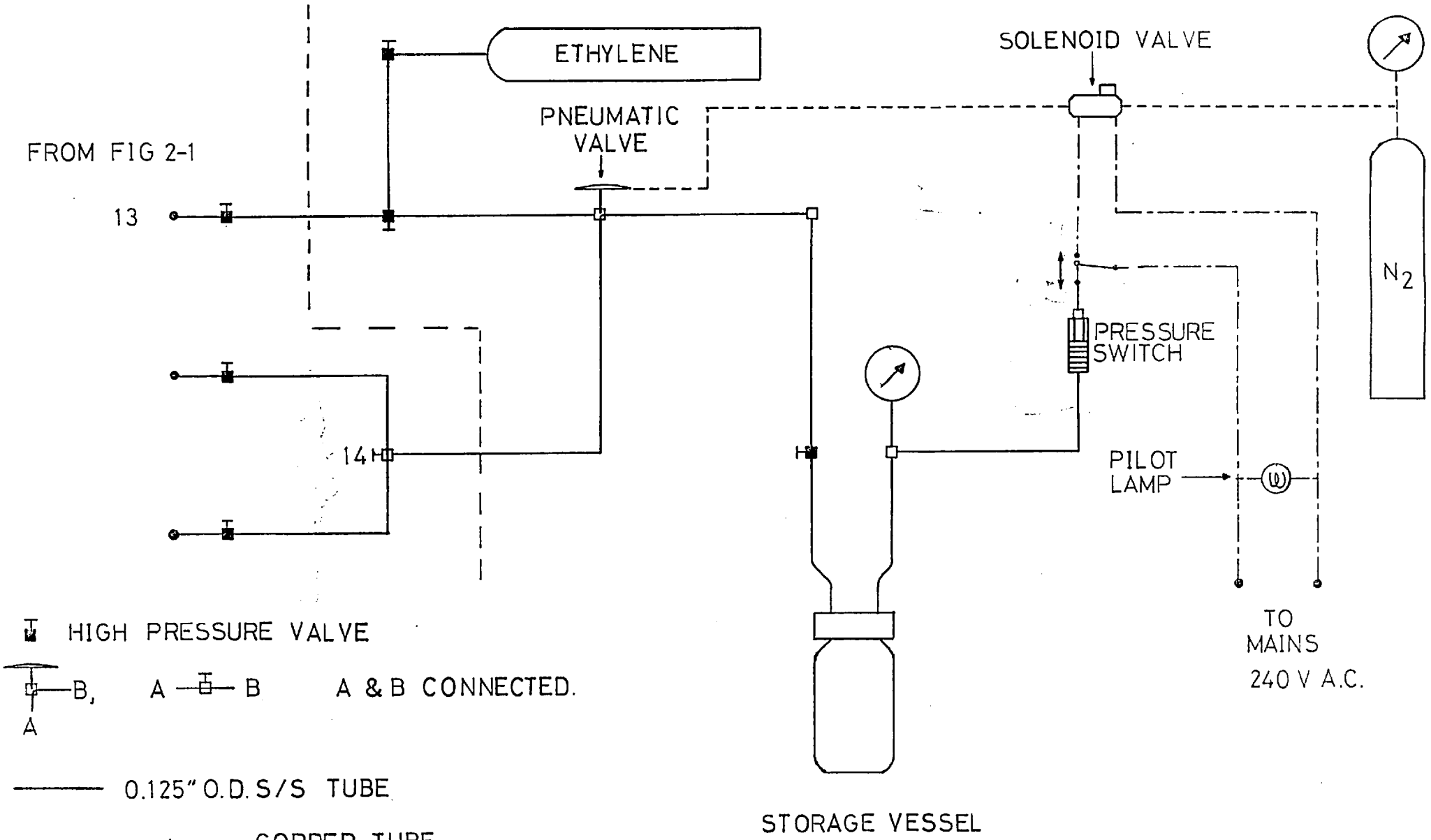


FIG 2-8 GAS STORAGE SYSTEM

bolts.

The vessel was held in a handy-angle framework outside the polyethylene cabinet. When ethylene was used, the vessel was immersed in a large Dewar-flask with a solid CO_2/ethanol mixture to collect more ethylene by condensation.

2-6 Temperature Control Systems

2-6-1 Introduction.

Two independent temperature control systems were provided for the low temperature system, i.e. one for the pressure vessel and the other for the radiation shield.

As shown in Fig. 2-9 the principle idea of temperature

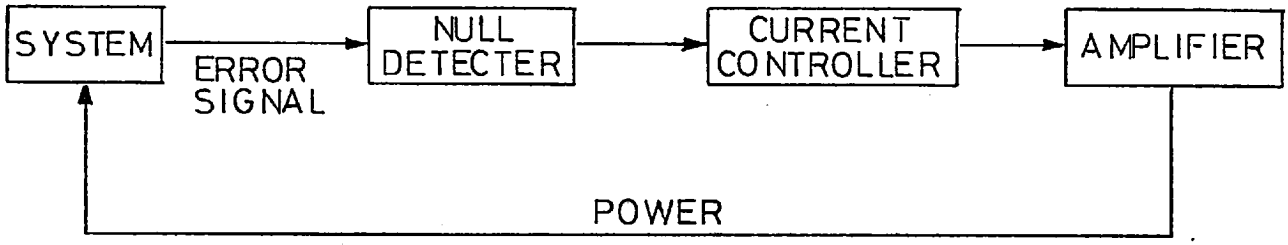


FIG 2-9

control of the pressure vessel was that 10 platinum resistance thermometers, which were connected in series and housed in vertical wells drilled around the outer wall of the pressure vessel, comprised one arm of a Wheatstone bridge, the off-balance signal from the bridge formed an input to an electrical control system in which the unbalance signal was detected, amplified and supplied to the heaters around the pressure vessel.

In the case of the radiation shield, the unbalance signal came from thermocouples soldered on the surfaces of the radiation shield and the pressure vessel.

The e.m.f. from the thermocouple was compared with a micro-volt source set such that, at the control point, the temperature of the radiation shield was kept at lower temperature than that of the pressure vessel.

The radiation shield needed a larger power supply unit than the pressure vessel because of the large temperature difference between the shield and the brass outer-jacket.

2-6-2 The Temperature Control Of The Pressure Vessel

Ten platinum thermometers (De Gaussa type P5), each of nominal 100 ohm at 0°C, were housed in ten equally spaced vertical wells around the outer wall of the pressure vessel. Each thermometer had silver extension leads which were connected in series, thus giving 1000 ohm at 0°C and a temperature coefficient of resistance of about 4 ohm/ C.

As shown in Fig 2-10, a compensation lead was provided in the variable resistance arm of the bridge (R_3).

The ratio arms R_1 and R_2 were set to 1000 ohm, which was close to that of R_4. The variable resistance R_3 consisted of five decade boxes, giving maximum resistance of 10,000 ohm with a minimum increment of 0.1 ohm, thus the R_3 could be preset to the nearest 0.1 ohm, corresponding to 0.025°C.

When the resistance (R_4) of the platinum thermometer was exactly same as that of the pre-set variable resistance,

i.e. $R_1 = R_2$ (pre-set)

$R_3 = R_4$ or $R_1/R_2 = R_3/R_4$ (2-6-1)

the bridge was balanced.

When $R_3 \neq R_4$ or the bridge was off-balance the resistance of the thermometer changed to $R_4 + dR_4$, and hence voltage across A and B (Fig. 2-10) existed. This output voltage

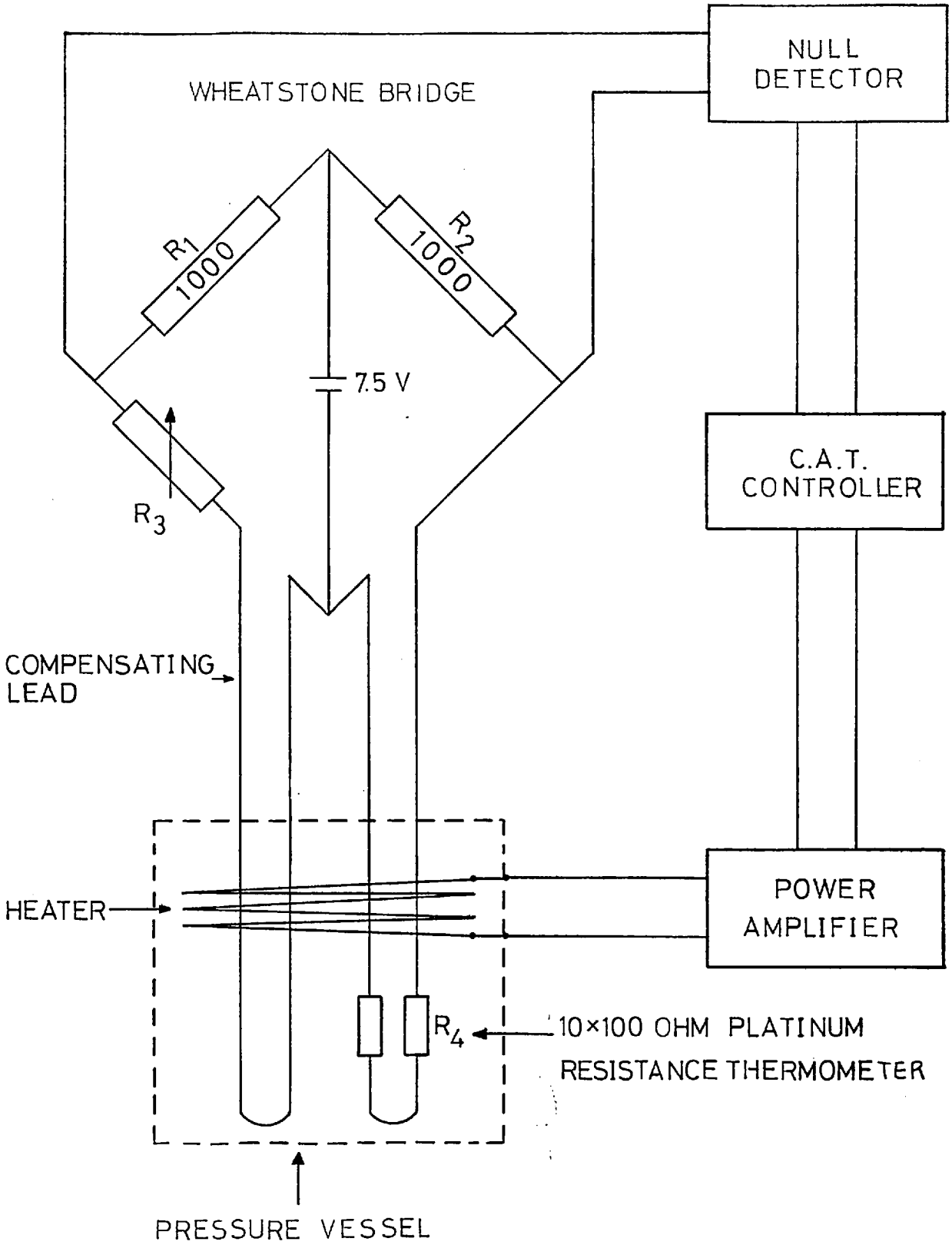


FIG 2-10 PRESSURE VESSEL TEMPERATURE CONTROL CIRCUIT

forms the input signal to the control circuit.

The output sensitivity of the bridge may be calculated from

$$\Delta V = \frac{1000 \cdot V \cdot dR_4}{(1000 + R_4)^2} \qquad (2\text{-}6\text{-}2)$$

where dR_4 is the unbalance resistance.

Three 2.5 V-battery (Alkaline Batteries, Model Alkad), connected in series, were used for the bridge circuit. At $0^{\circ}C$, $0.001^{\circ}C$ change in temperature caused 0.004 ohm change in resistance of the thermometer and hence from eq(2-6-2) gave 7.5 microvolts output voltage across A and B. This output voltage formed an error signal to an electronic D.C. Null Detector (Leeds and Northrup, model 9834-2). This instrument was a high-gain, low-noise operational amplifier, giving an output voltage of from -0.5 to +0.5 volts, displayed on a front panel.

The output from the null detector was controlled and further amplified by a Current-Adjusting-Type Control Unit (Leeds and Northrup, Series 60), which gave from 0 to 5 mA output. This instrument had three-action control; a proportional, integral and rate control.

Thus the voltage output from the current controller could be described as

$$V_{OUT} = A \cdot V_{IN} + B \cdot \int V_{in}\, dt + C \cdot \frac{dV_{in}}{dt} \qquad (2\text{-}6\text{-}3)$$

where A, B, C = constants

V_{in} = input voltage from the null detector to the current controller.

V_{out} = output voltage from the controller.

The proportional control functioned in rapid response

to the input error signal and amplified the input voltage to $A \cdot V_{in}$ volts.

The integral control provided an extra restoring output to maintain the control point at the correct set position at which the error signal was zero. The rate control supplied a further restoring signal in proportion to the rate of change of temperature. The output from the control unit was finally amplified by a power Supply-Amplifier (Hewlett-Packard, model 6823a), which gave a maximum output power of 10 watts at 20 volts D.C. and 0.5 amp. The output from the Supply-Amplifier formed the power supply to the heaters wound outside the pressure vessel. It could be also used manually as a direct power supplier independent of the current controller, and was used in this way when rapid heating was needed. Two 80-ohm-heater, each consisting of three sub-heaters connected in parallel, were wound alternately on the pressure vessel and connected in parallel, thus giving an over-all resistance of 40 ohm, consistent with the Power Supply-Amplifier rating. (10 watts, 20 volts).

Further, in case of failure in one of the two 80-ohm heaters the other could be used although at half power, without rewiring the heater circuits of the pressure vessel.

When the temperature was under control the fluctuation of the Null Detector was normally ± 0.2 division/hour, which corresponded to $\pm 0.001^{\circ}$C/hour change in temperature. However the temperature was constant within 0.0005°C (0.1 div. on the null detector) when actual measurement was taken, this normally taking less than half an hour.

Before expansion the system was set to manual and the pressure vessel was heated rapidly because of rapid temperature

drop was taking place due to the Joule effect while expansion. After regaining the original temperature by manual heating, the system was again set to 'auto'. It took normally 1/2 to one hour to reach a stable temperature under Automatic Control.

2-6-3 Temperature Control of The Radiation Shield.

Temperature control of the radiation shield was, in principle, same as that of the pressure vessel except for the method of producing the error signal.

As shown in Fig. 2-11, the thermocouple between the pressure vessel and the radiation shield together with the micro-volt source produced the error signal. The micro-volt source was connected to the thermocouple in series, thus the combined e.m.f. was the input to the Null Detector. The source was made of a mercury-cadmium cell and 1 mega-ohm resistor. Between the cell and the 1 mega-ohm resistor several terminals were provided between which various small resistors were connected in series, thus giving various e.m.f.'s ranging from 50 to 250 micro volt (equivalent to 1.5-7.5°C).

By choosing appropriate terminals the radiation shield temperature could be pre-set from 1.5 to 7.5°C below that of the pressure vessel.

Both the Null Detector and the Current-Adjusting Controller were of the same types as those of the pressure vessel control system. The power Sypply-Amplifier having a maximum output of 50 watts at 1 amp., supplied the power to the radiation shield and the inlet tube heaters. Four 600-ohm-heaters were wound along the side of the radiation shield and connected in parallel thus giving 150 ohm resistance.

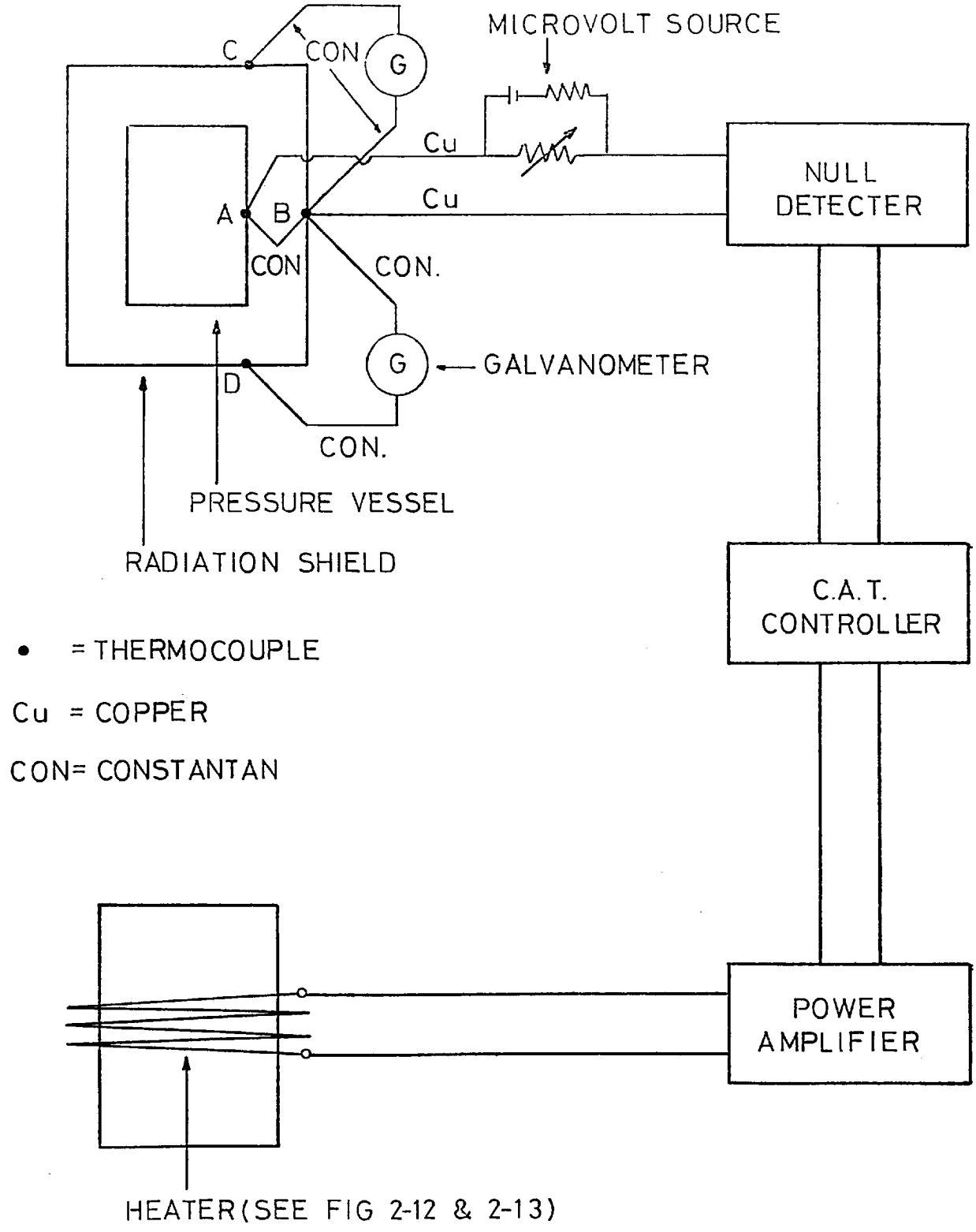


FIG 2-11 RADIATION SHIELD TEMPERATURE CONTROL SYSTEM

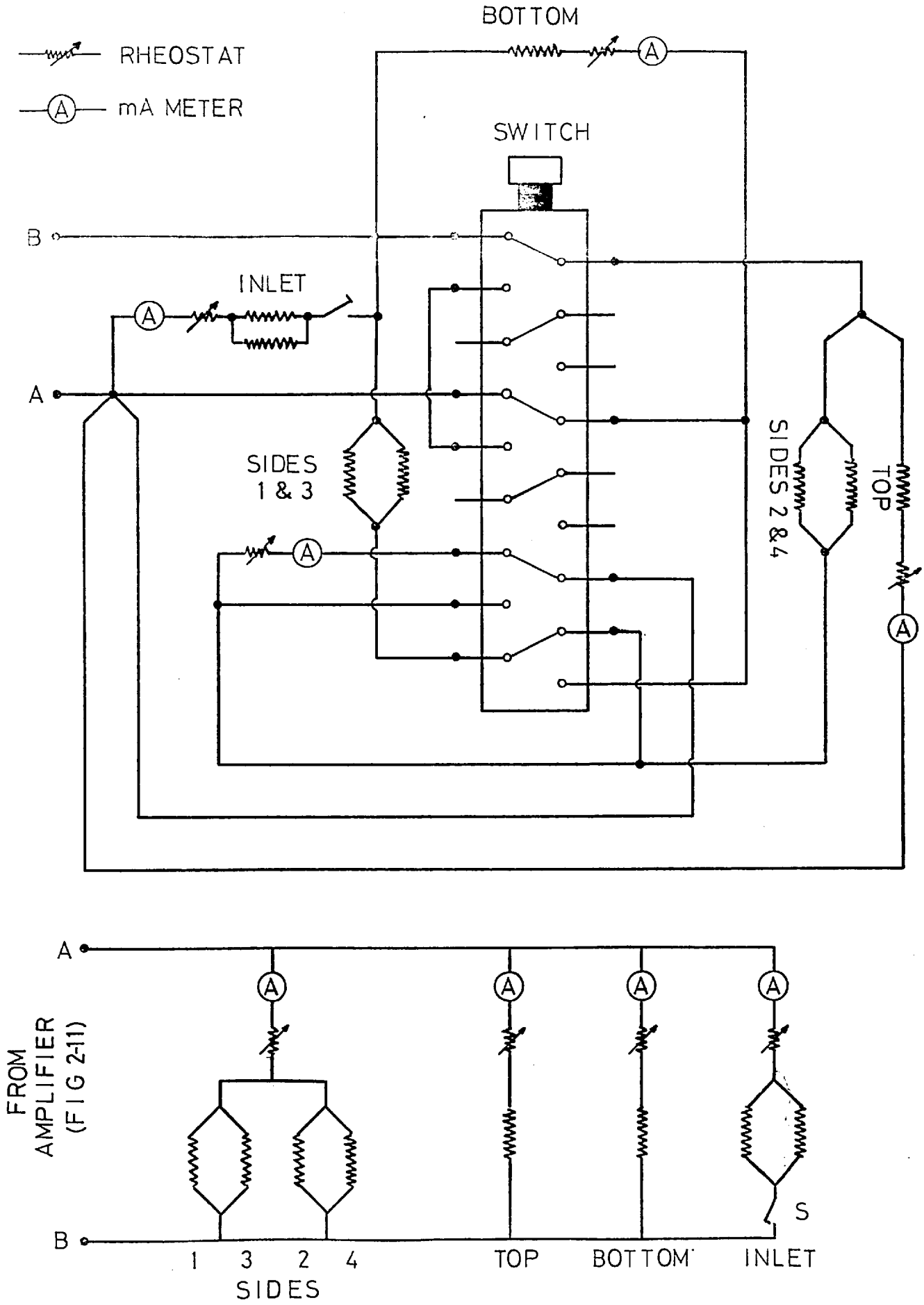


FIG 2-12 RADIATION SHIELD HEATERS (PARALLEL)

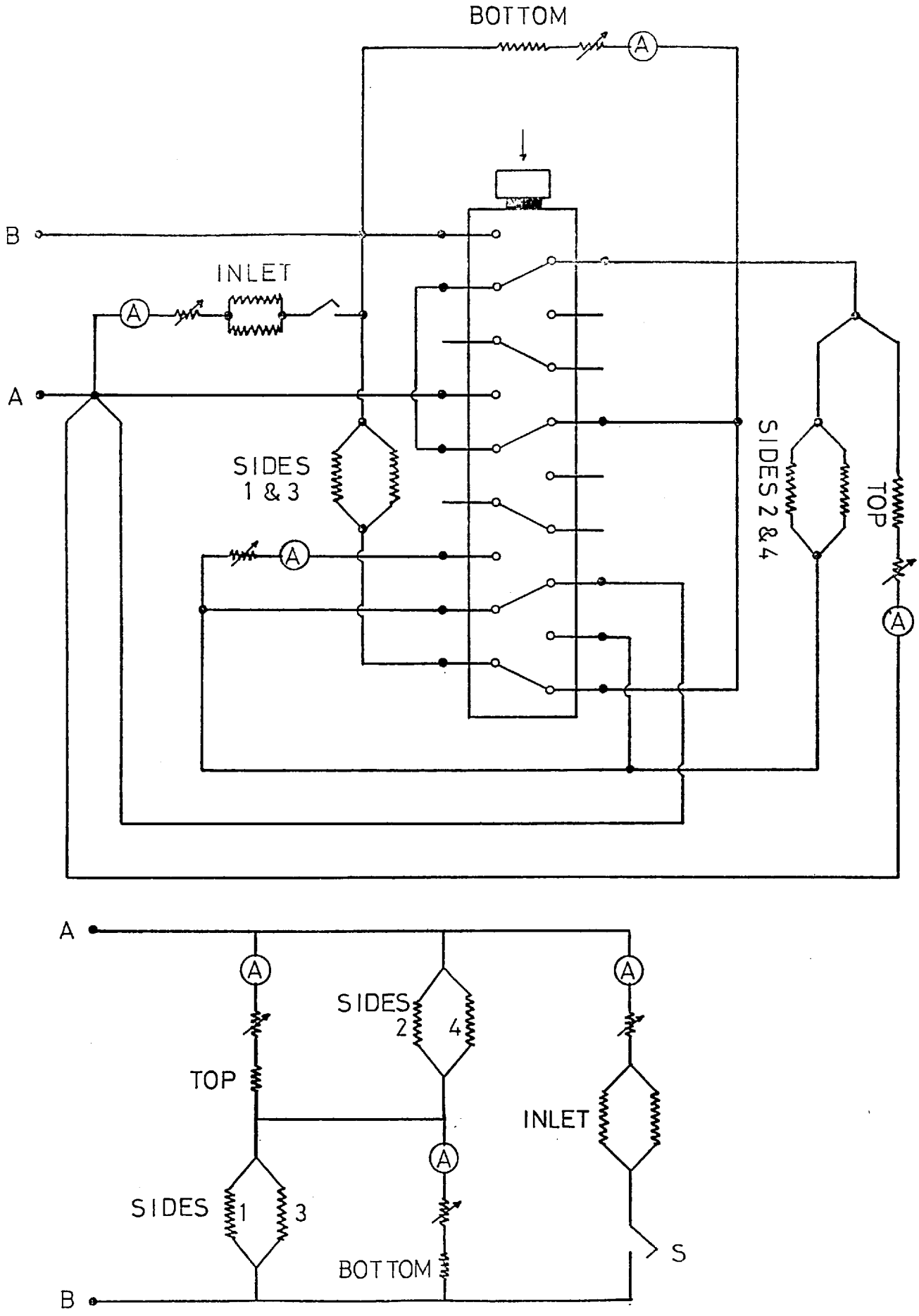


FIG 2-13 RADIATION SHIELD HEATERS (SERIES)

The top and bottom plates each had one 45-ohm heater. Two thermocouples between side wall and both end plates (B-C and B-D, Fig 2-11) were provided to monitor the temperature differences, whose e.m.f.'s were indicated by means of two 10-ohm suspension galvanometers. By manual adjustment of the three rheostats (Fig 2-12) all three parts could be maintained at the same temperature.

The heater circuits were connected to a change-over switch thus the radiation shield could be heated either by a parallel or a series heater circuit. Both circuits in series and parallel together with the change-over switch were shown in Fig 2-12 and 2-13.

The inlet tube heater (90 ohm) was also connected in parallel to the other heater circuits with an on-off switch which was provided to prevent overheating at the top of the inlet tubes if rapid heating of the radiation shield was required before filling the gas. The radiation shield temperature was controlled to within $0.1^{\circ}C$, corresponding to $\pm$ 0.3 microvolts in the output of the differential thermocouple (A-B).

With a solid-CO_2/ethanol mixture as refrigerant, the maximum practical experimental temperature was near $300^{\circ}K$ since at about $300^{\circ}K$ the heating level of the radiation shield was nearly 1 amp and temperature control was becoming difficult.

2-7 Temperature measurement

2-7-1 Introduction

The temperature of the pressure vessel was measured by means of a platinum resistance thermometer (Tinsley type

5187L, No. 193958). It was of the type of having a helium-filled outer platinum sheath and both resistance and potential leads, with a nominal resistance of 25 ohm at 0°C.

It was calibrated at the National Physical Laboratory with respect to the International Practical Temperature Scale of 1948.

The temperature was given by the Callender van Dusen equation,

$$t = \frac{R_t - R_o}{\alpha R_o} + \delta\left(\frac{t}{100} - 1\right)\left(\frac{t}{100}\right) + \beta\left(\frac{t}{100} - 1\right)\left(\frac{t}{100}\right)^3 \qquad (2\text{-}7\text{-}1)$$

where t = temperature in degree C (IPTS 1948)

R_t = resistance of the thermometer at t°C

R_o = resistance of the thermometer at 0°C

The constants of the equation (2-7-1) were calibrated as,

R_o = 24.8370 ohm

α = 0.00392617

β = 0 for $t > 0°C$

β = 0.1096 for $t < 0°C$

δ = 1.4936

The differences between IPTS 48 scale and the IPTS 68 scale were given by Hust.[6] These differences in the range 150 - 325°K were fitted to a polynomial in temperature and the resultant equation was used to change the measured values to the IPTS 68 scale. The maximum difference between the scales in this range was 0.04°K.

Eq (2-7-1) was solved by means of Newton-Raphson iteration method using first approximation of $t = (R_t - R_o)/\alpha R_o$ in a computer program (section 3-5).

The resistance of the thermometer was measured by

means of

i) an A.C. Precision Double Bridge for runs 17, 18 19 and 20

ii) a Potentiometer with two Automatic Current Controllers for the rest of the runs.

2-7-2 Resistance Measurement by an A.C. Double Bridge

The instrument was an A.C. Precision Double Bridge (Automatic Systems Laboratories Ltd., model H8). The ratio arms of the bridge were balanced by means of a 'quadrature' control and an 'in-phase' control. In principle the A.C. bridge compared the resistance of a standard resistor with that of thermometer and displayed the value of the ratio (r) on the front panel by adjusting eight decade switches.

$$r = R_t / (R_t + R_s) \qquad (2\text{-}7\text{-}2)$$

where R_t = resistance of thermometer

R_s = Resistance of a standard resistor

The standard resistor used was of nominal 50 ohm resistance (Tinsley type 1659, No. 175884). The resistance of the standard resistor at temperature $t^{o}C$ was given by

$$R_s = 50.0008 + (t_s - 20) \cdot 10^{-5} \quad \text{ohms} \qquad (2\text{-}7\text{-}3)$$

Coaxial wire was used to avoid electrical noise and all the connections were made by means of low-noise plug with gold plated pins, to which the leads were soldered using low e.m.f. solder.

The bridge was equipped with a changeover switch which could change the positions of the ratio arms, thus giving a check on the accuracy of the banance position. Difference between the 'normal' and 'check' positions were usually

equivalent to about 0.001°C. The bridge sensitivity was equivalent to 0.0005°C. The over-all accuracy of the absolute temperature measurement was estimated as ± 0.005°K.

2-7-3 Resistance Measurement by a Potentiometer

Except for runs 17, 18, 19 and 20 thermometer resistance was measured by means of a Thermo-electric Free Potentiometer (Diesselhorst Pattern, Tinsley Type 3589 R/AUTO) together with two Automatic Current Controllers (Tinsley, Type 5750).

Unlike the A.C. Double Bridge the potentiometer displayed the voltages across a 10 ohm standard resistor (Tinsley, Type 3504 B) and the platinum thermometer by adjusting five decade switches on the front panel. As shown in Fig 2-14 two Automatic Current Controllers (Tinsley, Type 5750) were used; one for the potentiometer current the other for the thermometer and the standard resistor.

The resistance of the standard resistor of nominal 10 ohm at 20°C was given by

$$\rho_S = 10 + (20 - t) \cdot 7.45 \cdot 10^{-6} \qquad (2\text{-}7\text{-}4)$$

where t = temperature of the resistor °C.

The auto-current controller was to give a stable current (stability, 2 parts in 10^6) with a range of 10 to 50 mA. The voltage across the standard resistor and thermometer were adjusted by means of a 50 ohm suspension galvanometer (Tinsley, Type 4500), having a sensitivity of 500 mm of deflection per micro amp. Two thermometers and the standard resistor were connected in series, having about 3 mA of constant current from the current controller and connected to the galvanometer by means of a Thermometer Selection

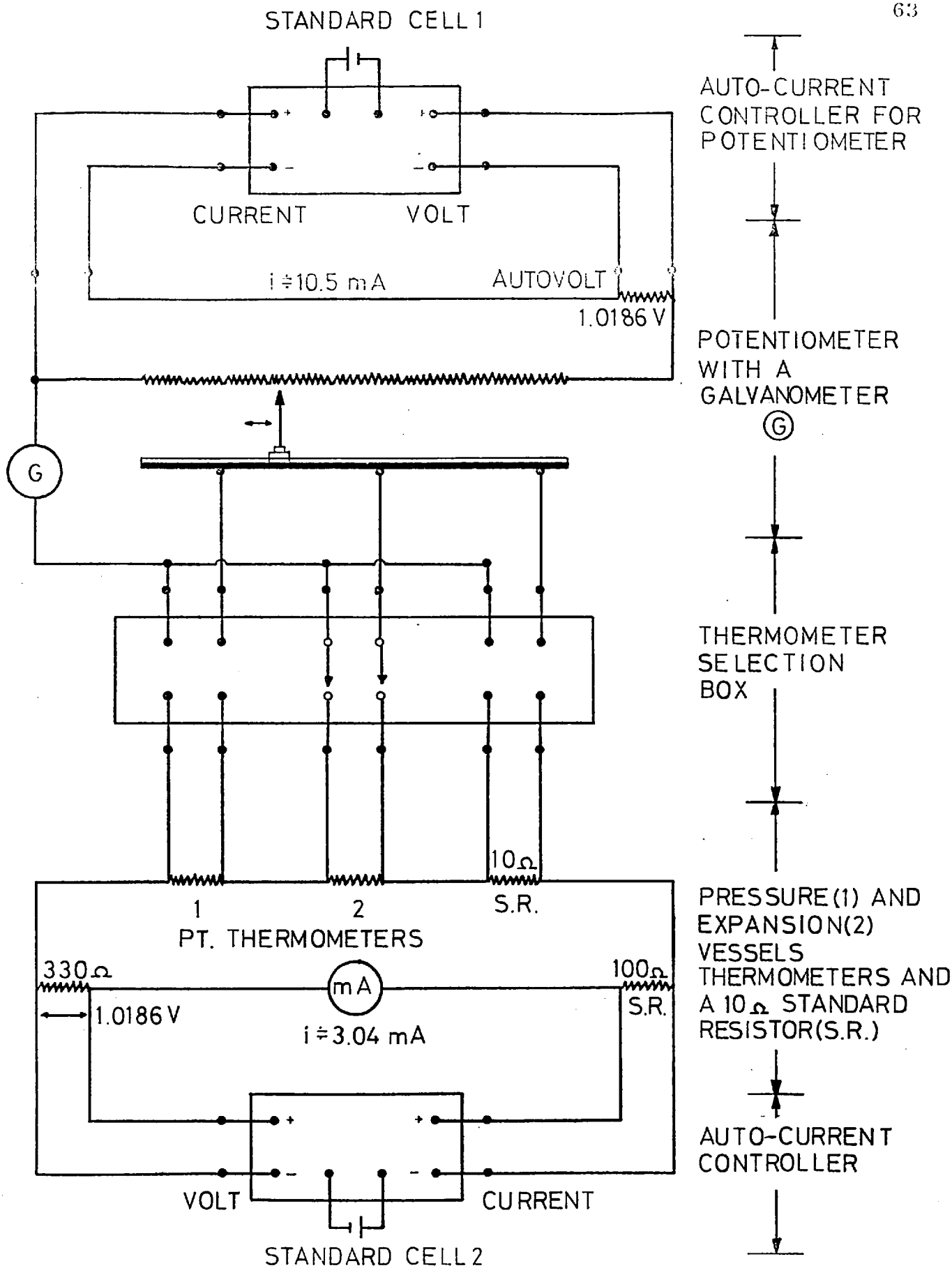


FIG 2-14 TEMPERATURE MEASUREMENT POTENTIOMETER CIRCUIT

Box (Cambridge Instrument). (Fig 2-14)

Having about 3mA current across the thermometer the maximum error of 0.75 micro volt ($75\ mV \cdot 10^{-5}$) corresponded to about 0.5 mm deflection on the 50 ohm galvanometer. which corresponded to less than $0.005^{o}C$

The overall absolute error in temperature measurement was estimated as less than $\pm\ 0.01^{o}C$.

2-8 Pressure Measurement

2-8-1 Introduction

The pressure of the gas in the outer volume of the pressure vessel was measured by means of either an oil-piston gauge or a gas operated piston gauge depending on the magnitude of the pressure. A Precision Pressure Gauge (P.P.G.) was then used to measure the pressure difference between inner and outer volumes of the pressure vessel and hence calculated the pressure within the experimental system. Since it was necessary to allow for the pressure generated by the various 'gas heads' it was convenient to divide the apparatus into several parts and to number them for computational purposes, and throughout this work these numbers refer to the particular part of the apparatus shown Fig. 2-15.

In the computations the reference pressure was taken, for convenience, as the value at the position of the top-most thermocouple in the inlet tubes (Fig 2-5).

As mentioned earlier, without careful calibration, the P.P.G. could lead to a large error in pressure measurement, because of its null position shift with pressure. The calibration of the P.P.G. is discussed in section 2-8-5.

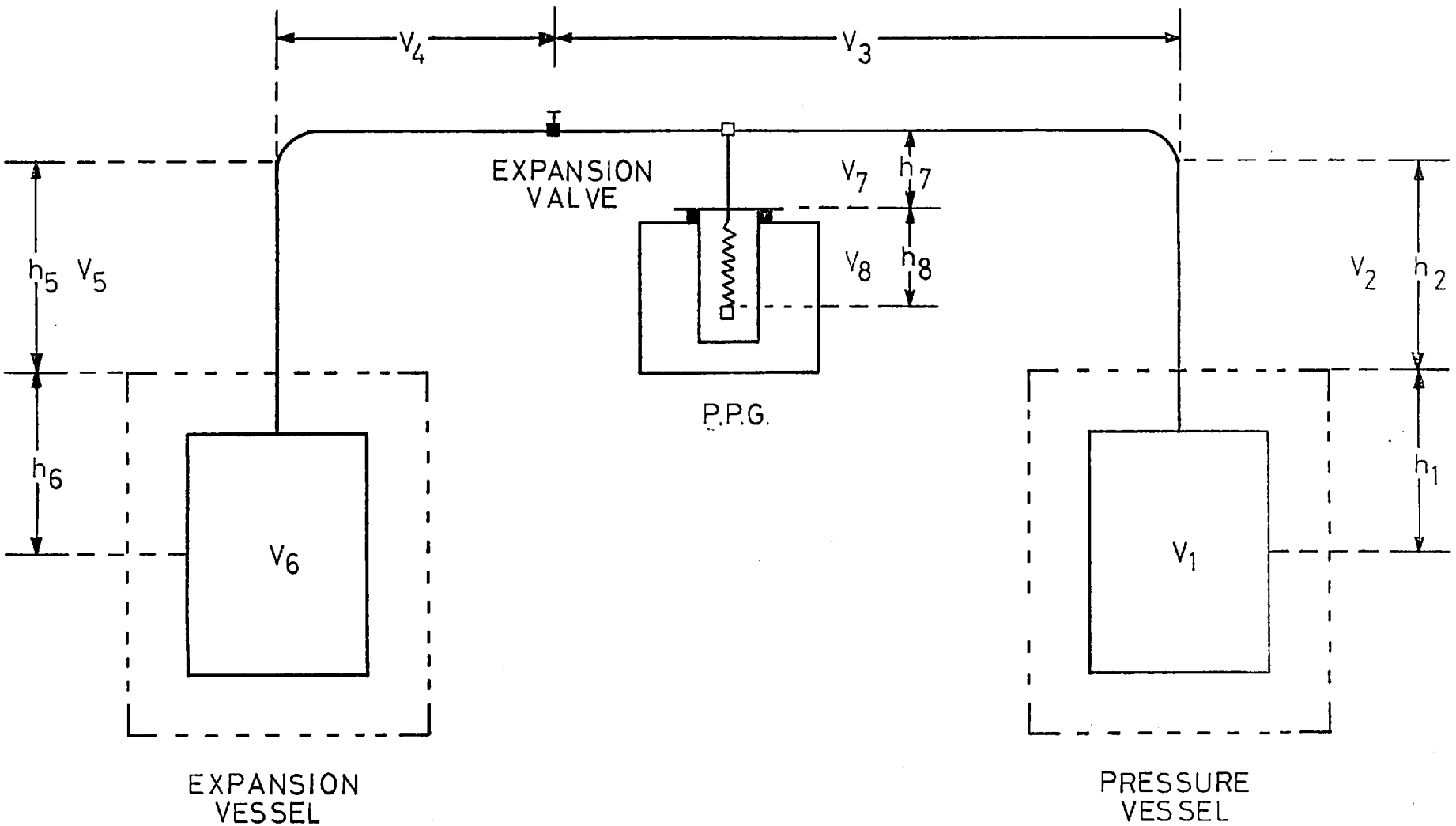


FIG 2-15 APPARATUS VOLUME AND PRESSURE-HEADS

A Differential Pressure Cell (D.P.C.) was used to separate the oil from the gas being investigated. Below 20 bars pressure measurement with the oil-piston gauge became difficult due to friction between the piston and the cylinder. Thus, in this range the pressure was measured by means of a gas operated piston gauge. The gas piston gauge was calibrated against the oil piston gauge where their ranges overlapped and a calibration equation of the form

$$P = a + bm \qquad (2\text{-}8\text{-}1)$$

was used to calculate the gas piston pressure. The minimum measurable pressure with this gas piston gauge was about 2.5 bar, below which the friction increased considerably and measurement was again difficult.

In the following sections,

i) pressure measurement with piston gauges

ii) pressure correction in the P.P.G.

iii) pressure correction due to gravitational effect

will be discussed.

A computer programme was written for calculating the pressures in the various parts of the apparatus and the results were represented in bar (10^6dyne/cm^2) throughout this work.

2-8-2 Pressure Measurement with an Oil Piston-Gauge

The pressure is defined as

$$P = \frac{F}{A} = \frac{m \cdot g}{A} \qquad (2\text{-}8\text{-}2)$$

where m = mass

g = acceleration due to gravity

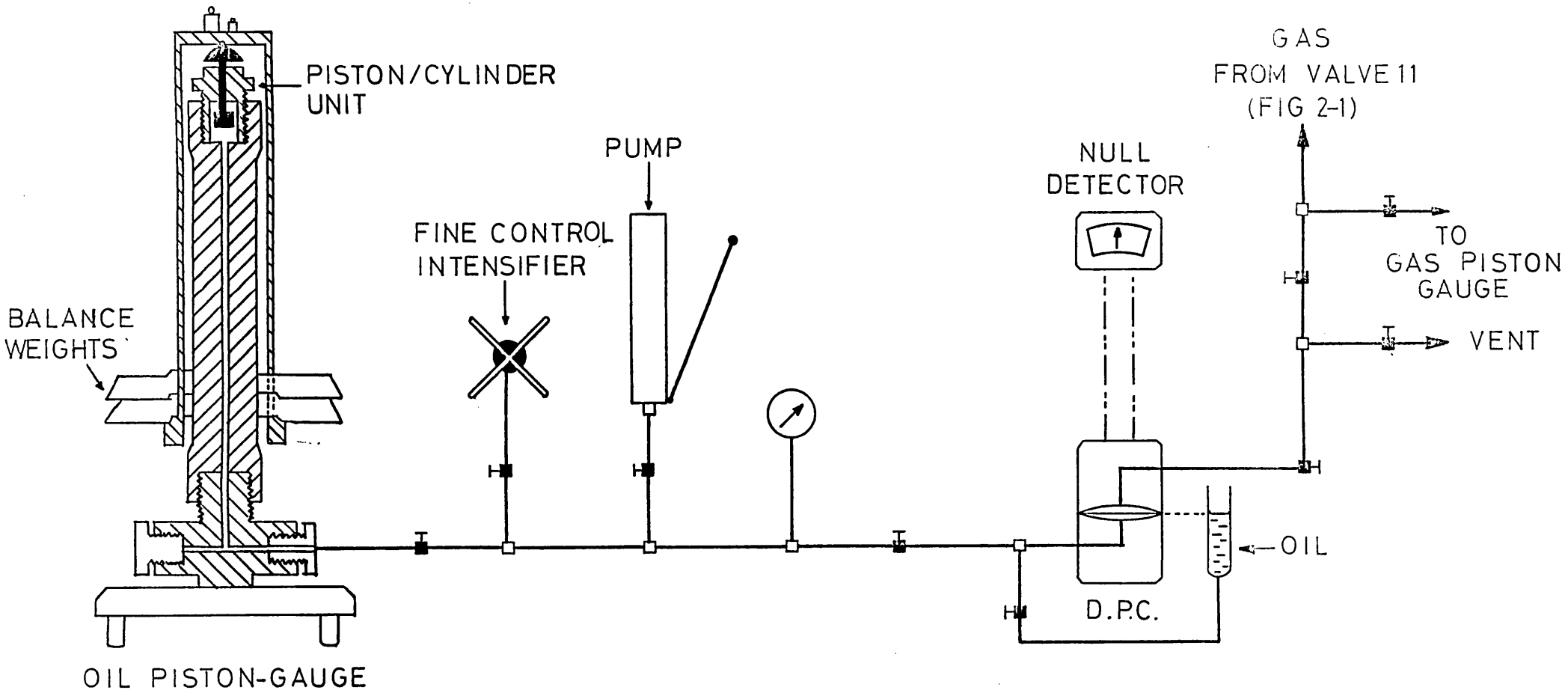


FIG 2-16 PRESSURE MEASUREMENT SYSTEM (OIL)

A = area upon which the force exerts.

Thus accurate measurement of pressure depends on the values of m, g and A, and efforts were made to get these values as precisely as possible.

The schematic diagram of pressure measurement for oil system is shown in Fig 2-16.

(a) Oil Piston-Gauge

The gauge used was Budenberg oil piston gauge with a piston-cylinder unit, No. K231, having 0.125 in.^{2} nominal piston area. The characteristics of this piston gauge were described in detail by Bett,[7] who calibrated it against a standard mercury column. The piston/cylinder unit (Fig 2-17) was submitted to the National Physical Laboratory for calibration of the effective area of the piston against a primary standard piston-gauge.

The calibrated effective area at P bar and 20^{o}C was given by

$$A_p = A_o (1 + bP) \qquad (2\text{-}8\text{-}3)$$

where A_p = piston area at P bar and 20^{o}C in cm^2.

$A_o = 0.806424 \pm 0.000013$ cm^2.

$b = 4.0 \cdot 10^{-7}$ bar^{-1}

The effective area at temperature t was given by

$$A = A_p \{1 + 2\alpha (t - 20)\} \qquad (2.8.4)$$

whree A = piston area at P bar and t^{o}C

$\alpha = 11.5 \cdot 10^{-6}$ ^{o}C^{-1}

The oil used during the calibration was a mixture of Shell 'Diala-B' and Shell 'Talpa-30' in the ratio of 3:2.

The same mixture was used in this work.

The excess of pressure of the oil over atmospheric pressure was counter-balanced by means of balancing disc weights which were supported on a stainless-steel carriers. This carrier rested on a stainless-steel ball bearing on top of the piston-cap. The pressure was taken when the piston was suspended in the middle of the movable length of the piston and rotated freely at the rate of 35 - 40 r.p.m. Since the disc weights only went up in steps of about 0.15 bar, additional analytical weights were used to balance to the nearest 0.01 gm. Thus total mass (m) was the sum of the mass of the disc weight, the extra weights, the carrier, the ball bearing and the piston.

Apart from the gravitational force there existed some other forces, i.e. the upward force due to buoyancy in air and oil, and down ward force dwo to surface tension.

The total force in eq(2-8-2) was, therefore, given by

$$F = M \cdot g - F_a - F_o + F_s \qquad (2\text{-}8\text{-}5)$$

where M = total counter balancing mass

g = acceleration due to gravitation

F_a = upward force due to buoyancy in air

F_o = upward force due to buoyancy in oil

F_s = downward force due to surface tension at the oil meniscus at the top of the piston

Thus the pressure at the oil piston gauge was calculated by dividing this force F (eq 2.8.5) by the effective area of the piston A (eq 2-8-4).

(i) The Acceleration due to gravitation

The absolute values of the acceleration due to gravity was determined at the National Physical Laboratory.[8]

$$g = 981.182 \text{ cm/sec}^2 \qquad (2\text{-}8\text{-}6\text{-}a)$$

The value was also determined at the Department of Geophysics, Imperial College in 1971 by using a comparative gravimeter. The value was given as

$$g = 981.202 \text{ cm/sec}^2 \quad \pm 0.006 \text{ cm/sec}^2 \qquad (2\text{-}8\text{-}6\text{-}b)$$

This value was used for this work.

(ii) The Mass of the Balancing Weights.

The balancing disc weights were calibrated with a 10 kg balance (Stanton Instrument) against rhodium-plated brass analytical weights.

Prior to weighing the disc weights, the analytical weights were calibrated against a standard weight. This standard was a chromium-plated brass and calibrated at the National Physical Laboratory in 1951, and the calibrated value was 6653.759 gm to the nearest 0.001 gm. This value was assumed to be correct, since the mass had been carefully preserved and used only a few times. A combination of analytical weights of 6653.76 gm was balanced against the standard mass and balanced again with the nominal weight on the other side of the balance. The geometric mean of the two readings was determined as 6653.7635 gm, giving less than 0.0036 gm of error in nominal weight of 6653.76 gm, and thus no corrections to these values were necessary. The balancing of the disc weights was carried out by means of substitutional method. Before balancing each weight the mid-

point and the sensitivity of the balance was determined by the method of oscillation and found to be 0.002 gm/division.

The buoyancy effect in air for the balancing analytical weights was considered in calculating true mass of the objects being weighed, thus

$$M = M_b \left\{ 1 + \rho \left(\frac{1}{d} - \frac{1}{d_b} \right) \right\} \qquad (2\text{-}8\text{-}7)$$

where M = true mass

M_b = nominal mass of the analytical weights

d = density of the object being weighed

d_b = density of the brass analytical weights

ρ = density of air.

The densities of the materials concerned were given by

cast iron	7.10	$gm \cdot cm^{-3}$
steel	7.83	"
S/S	7.90	"
brass	8.40	"

The value for the oil-blacked cast iron disc was that determined by Bett,[7] and the density of air was taken from tables of ambient air density given by Kaye and Laby.(9)

The true masses of the disc weights, the piston, the carrier and the ball bearing are given in Table 2-1.

Several weights were re-weighed a few days later and they were found to be reproducible to within 0.005 gm. The buoyancy effect amounted to about 0.15 gm for the largest weight and the error in this correction was estimated less than 0.005 gm.

TABLE 2-1

Masses of Piston-Gauge Disc Weights, Carrier and Piston

Weight Number	Mass (gm.)
18	6668.41
19	6669.29
20	6669.40
21	6669.54
22	6670.28
23	6669.97
24	6668.86
25	6669.27
60	2666.51
61	2666.48
62	2666.50
64	1333.05
65	1333.06
66	666.21
67	666.52
69 (steel)	266.70
71 (")	266.73
141 (")	266.50
72 (")	133.34
73 (")	133.19

Piston Unit (steel)	45.17
Carrier (s. steel)	1130.86
Ball (s. steel)	2.04

Thus the maximum probable error in the measurement of the weights was estimated as less than 0.01 gm.

(iii) The Buoyancy Effects and Other Corrections.

There were two kinds of buoyancy effects in the piston/cylinder unit, i.e. one in air above level A (Fig 2-17) and the other in oil between levels A and B. The upward force due to buoyancy in air is given by

$$F_a = \sum \frac{m_i g}{d_i} \rho \qquad (2\text{-}8\text{-}8)$$

where d_i = density of individual mass above level A

ρ = density of air

The mass of the piston and the piston cap above level B was estimated from the total mass and the dimensions. The tables of ambient air density(9) in the ranges of 25 - 32°C and 730 -780 mm Hg atmospheric pressure were represented for computational purposes by the following equation,

$$\rho = \{1.180 - 0.0045\,(t-27) + 0.0016\,(h-767)\} \times 10^3 \qquad (2\text{-}8\text{-}9)$$

where ρ = the air density, $gm \cdot cm^{-3}$

t = temperature, °C

h = atmospheric pressure, mm Hg.

The error in the value of disc weight density was estimated as less than 1.5% and the error in the calculation of air density by eq 2-8-9 was estimated as less than 0.5%, thus giving total 2% error in the calculation of the air buoyancy, which corresponded to an error of 4 parts in 10^6 in pressure.

The buoyancy effect in oil is given by

$$f_o = g \cdot V_{ab} \cdot \rho_o \qquad (2\text{-}8\text{-}10)$$

where f_o = upward force due to oil buoyancy between levels A and B

V_{ab} = the volume of the piston between A and B

ρ_o = density of the oil

Since the reference level was chosen at B when it was calibrated at the National Physical Laboratory a downward force due to the hydraulic head of the oil between A and B was taken account into the calculation of f_o, i.e.

$$f_o = g \cdot \rho_o \cdot V_{AB} - g \cdot \rho_o \cdot A \cdot h_{AB} = g \cdot \rho_o \{ (V_{Ac} + V_{cB}) - A \cdot h_{AB} \}$$

$$= g \cdot \rho_o \{ V_{cB} + A (h_{Ac} - h_{AB}) \} \qquad (2\text{-}8\text{-}11)$$

where A = cross-sectional area of the piston

ρ_o = the oil density

V_{cb} = the volume of the part of the piston between C and B, and estimated as 0.947 cm^3 from its dimension.

$h_{ac} - h_{ab}$ = 0.992 cm, also estimated from the dimension.

The Eq.(2-8-11) was used in the computation of the oil buoyancy and the maximum error due to uncertainty in V_{cb}(± 0.015 cm^3) was estimated as 0.0013 N which corresponded to $1.6 \cdot 10^{-4}$ bar in pressure.

Finally the effect of surface tension was estimated by the National Physical Laboratory at the time of the calibration.

$F_s = 0.0096$ N (2-8-12)

Thus total downward force was computed from Eq.(2-8-5). giving the pressure at level B (Fig 2-17).

(iv) Hydraulic Head of Oil

In the oil piston-gauge system the oil was separated from the gas by the diaphragm of the Differential Pressure Cell (D.P.C.). The gas pressure was nulled at this level by an electronic null detector. Thus the calculated pressure at level B in Fig 2-17 was different from the gas pressure by the hydraulic head of oil between level B and the diaphragm

Hence

$$\Delta P = g \cdot \rho_p \cdot h \qquad (2\text{-}8\text{-}13)$$

where ρ_p = the density of the oil at pressure P

h = the height from the diaphragm and level B.

The diaphragm position was marked (by the manufacturer) on the outside of the D.P.C. and the distance between level A and the diaphragm, $h + h_{ab}$, was measured by means of an accurate cathetometer.

The mean of several measurements was,

$h + h_{ab} = 34.46$ cm or $h = 30.744$ cm (2-8-14)

The maximum error in h was due to the uncertainty in the exact diaphragm position and was estimated as 0.05 cm.

The density of the oil at atmospheric pressure was measured by Roe[1] and given in Table 2-2.

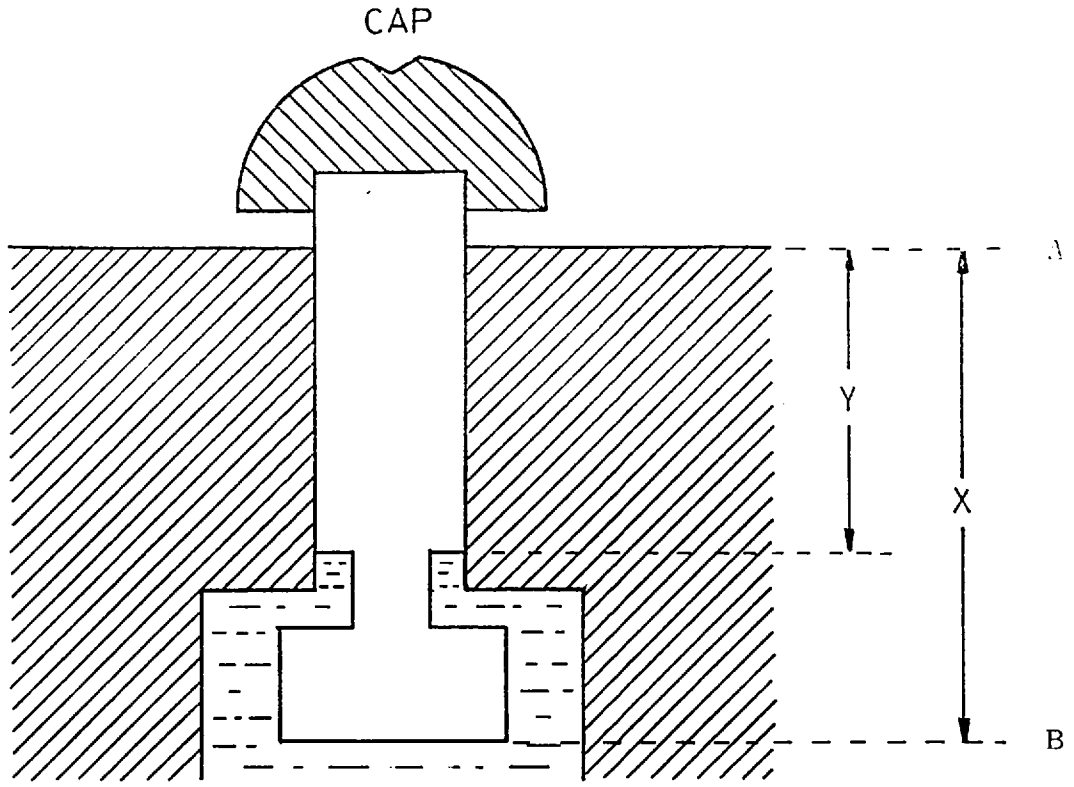


FIG 2-17 PISTON/CYLINDER UNIT

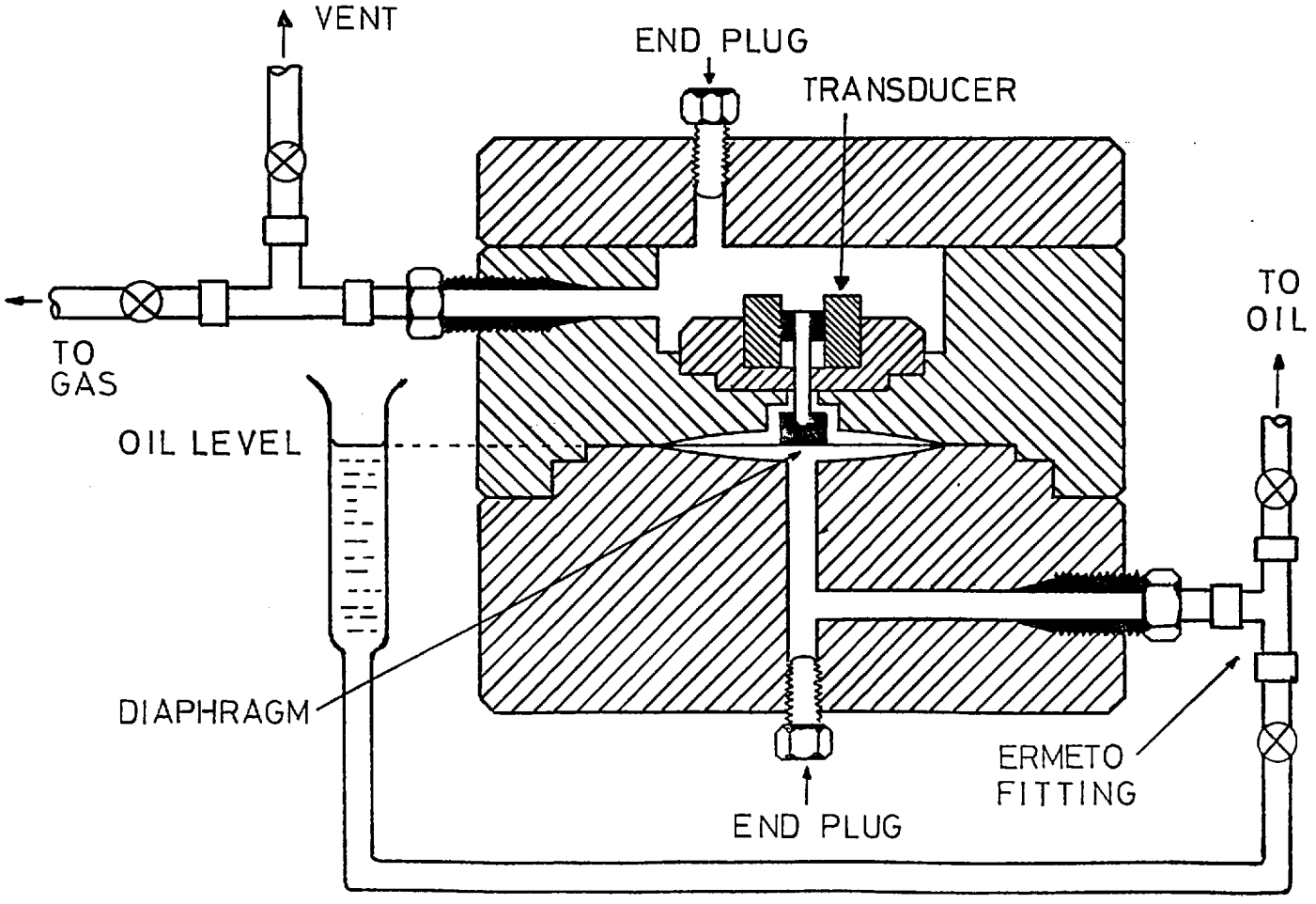


FIG 2-18 DIFFERENTIAL PRESSURE CELL

TABLE 2-2

Density of 3:2 Mixture of "Diala B" and Talpa 30 Oil

Temperature (^{o}C)	Density gm/cm^3 at 1 atm.
20.0 (N.P.L.)	0.8840
25.1	0.8792
26.6	0.8779
27.5	0.8772
28.6	0.8765
29.8	0.8757
32.0	0.8744

The density change with pressure was calculated by the equation,

$$\rho_P = \rho_o (1 + \beta P) \qquad (2\text{-}8\text{-}15)$$

where ρ_P = oil density at pressure P

β = compressibility of the oil, $9 \cdot 10^{-5}$ bar^{-1}

The compressibility (β) was calculated from the measured values for mineral oils of similar constitution to the mixture used.[10] This leads to a total maximum possible error in ρ_P of 0.0015 gm/cm^3 at 100 bar or 0.2%. Combined with the error in h, the maximum possible error in ΔP was about 0.35% of ΔP at 100 bar, or 0.0001 bar.

(b) The Differential Pressure Cell

The Differential Pressure Cell (RUSKA) together with an electronic Null Indicator served to separate the oil from the gas and to equalise the pressures of the two media.

As shown in Fig 2-18, the D.P.C. consisted of two pressure chambers separated by a thin diaphragm. A difference in pressure in the two chambers caused a deflection of the diaphragm and a resultant signal to the electronic circuit. The signal was obtained as the output of a differential transformer whose movable core was attached to the diaphragm. It was amplified and displayed on a Null Indicator which had a maximum sensitivity of 0.0003 bar pressure difference for full scale deflection. The null position itself was subject to change with pressure[2] and was calibrated by the maker,

$$\Delta P = P \cdot 2 \cdot 10^{-6} \text{ bar} \qquad (2\text{-}8\text{-}16)$$

This value was not very much different from that found by Roe[1] ($P \cdot 2 \cdot 10^{-6}$) and Eq.(2-8-16) was, therefore, used to estimate the null shift with pressure. The upper chamber of the D.P.C. was filled with gas and had much larger volume than the lower chamber which was filled with oil.

Before pressurising both chambers, the upper chamber was open to air, and the lower chamber was open to the oil level indicator (Fig 2-18) outside the D.P.C., thus giving null position on the detector by adjusting the oil level to the mark of the diaphragm position.

When operating the D.P.C. care was taken to make sure that the pressure in the upper chamber (gas) did not greatly exceed that in the lower chamber, because this could cause a permanent null shift of the D.P.C.

2-8-3 The Gas-Operated Piston Gauge

Pressure below 20 bar was measured by means of a Gas-Operated Piston Gauge (Budenberg) having nominal piston area of 0.125 in^2.

As shown in Fig 2-19, the piston/cylinder unit was lubricated by oil, which separated the gas from the air outside the piston/cylinder unit.

This gauge was calibrated against the mass on the piston carrier by using the oil piston gauge in the range of 7.5 - 30 bar. Nitrogen gas was monitored to both piston-gauges from the expansion vessel. The gas pressure was measured by the oil piston gauge and the mass on the gas piston carrier was recorded. It was found that the relationship between P and mass on the carrier was very linear between 10 - 38 bars and was represented as

$$P = a + b \cdot m \qquad (2\text{-}8\text{-}17)$$

where m = mass on the carrier of the gas piston gauge

P = pressure in bar

a, b = constants.

The constants a and b in Eq.(2-8-17) were determined by means of a least-squares curve fit, and found to be,

$a = 0.68840$ bar

$b = 0.00121615$ $bar \cdot gm^{-1}$

The mean value of the pressure differences between the oil piston pressure and the one calculated from the Eq.(2-8-17) was estimated as less than $2 \cdot 10^{-4}$ bar.

With reference to Fig 2-19, a plastic self-adhesive marker was attached to the outside of the cylinder in order to keep constant floating height of the piston when pressure was measured. This measure was necessary to avoid the variation of buoyancy effect of the piston in oil. The leakage of the lubricating oil (3-in-1 oil) through the clearance between the piston and cylinder caused variation of the oil level in the cylinder, hence a change in buoyancy. Therefore oil was refilled through the filler plug (Fig 2-19) after each measurement. A box of 12 weights was supplied for the gas-piston gauge and the mass of each individual weight was calibrated in the same way as those of the oil piston gauge (section 2-8-2, ii). The masses of the 12 disc-weights were given in Table 2-3.

TABLE 2-3

Masses of Gas-Operated Piston-Gauge Weight

Weight No.	Material	Mass, gm.
1	steel	5670.97
2	"	5671.00
3	"	5670.94
4	"	2835.58
5	"	2835.54
6	"	2268.21
7	"	1134.05
8	"	1134.02
9	"	567.20
10	"	283.48
11	S/S	113.46
12	"	113.45

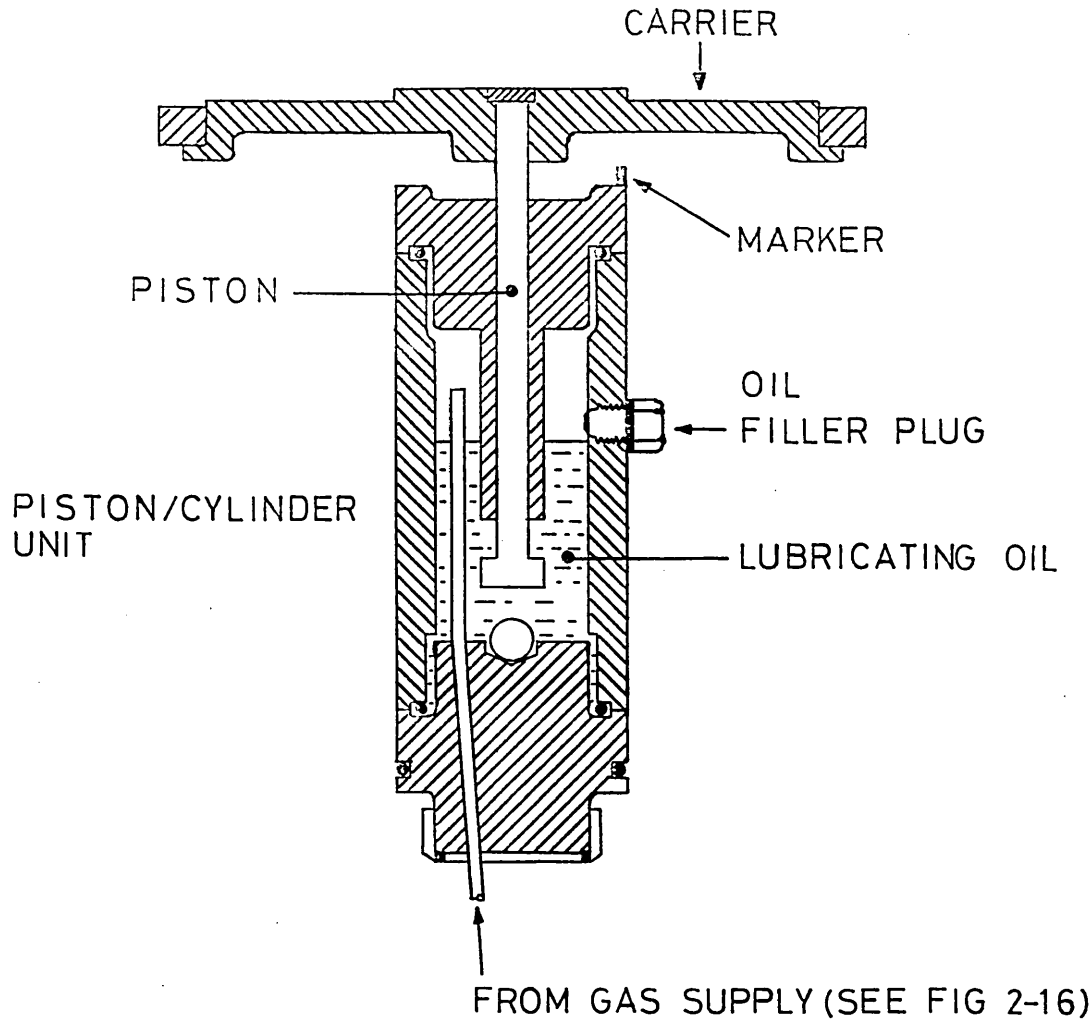


FIG 2–19 GAS PISTON GAUGE

A temperature change caused variations in the piston area and also in buoyancy, and these effects had to be taken acount into Eq.(2-8-17), thus giving,

$$P = \frac{a\left\{1 - \frac{(\rho - \rho_o)}{d_c}\right\} + bm\left\{1 - \frac{\rho - \rho_o}{d_w}\right\}}{1 + 2.3 \cdot 10^{-5}\,(t - t_o)} \qquad (2\text{-}8\text{-}18)$$

where ρ_o = air density at the time of calibration, 0.001197 gm/cc

t_o = temperature at the time of calibration, 26.5°C

ρ = air density at t°C, computed from Eq.(2-8-9).

d_c = average density of the carrier and piston, 4.0 gm/cc

d_w = average density of the weights, 7.8 gm/cc

The sensitivity of the gas-piston gauge was about 10^{-4} bar, having reproducibility of about $2 \cdot 10^{-4}$ bar. These were checked by using P.P.G. When pressure was measured the carrier was rotated freely at about 20 - 35 revolutions per minute, the direction of rotation being immaterial.

2-8-4 The Atmospheric Pressure

Atmospheric pressure was measured by means of a standard Fortin Barometer having 13 mm bore diameter. The pressure was then calculated by the equation,

$$P_{atm} = \rho_t g h + \Delta P \qquad (2\text{-}8\text{-}19)$$

where g = acceleration due to gravitation, 981.202 $cm \cdot sec^{-2}$

ρ_t = density of the mercury in the barometer at barometer temperature $t^{\circ}C$, $gm \cdot cm^{-3}$

h = barometer reading, cm

ΔP = atmospheric pressure difference between the barometer and the apparatus.

Mercury density, ρ_t, was calculated by the equation,

$$\rho_t = \frac{\rho_{t_0}}{\{1 + \beta(t - t_0)\}} \qquad (2\text{-}8\text{-}20)$$

where ρ_{t_0} = 13.54588 $gm \cdot cm^{-3}$, mercury density at $20^{\circ}C$ and 1 atm. taken from the table given by Bigg.[11]

β = $1.8159 \cdot 10^{-4}$ $^{\circ}C^{-1}$, volume thermal expansion coefficient of mercury.

The reading of the mercury column, h, was corrected for capillary depression, according to values given by Bould and Vickers,[12] and for the scale expansion of the brass tube of the barometer.

Thus

$$h = \frac{h' + \Delta h}{(1 + \alpha \Delta t)} \qquad (2\text{-}8\text{-}21)$$

where h' = reading from the barometer, cm.

h = capillary depression of mercury, cm.

$\alpha = 1.84 \cdot 10^{-5}\ ^{o}C^{-1}$, linear thermal expansion coefficient of brass

t = t - 20 ^{o}C, the brass scale was calibrated at 20 ^{o}C.

t = barometer temperature.

The maximum possible intrinsic error in reading h' was estimated as 0.02 cm, or $2.6 \cdot 10^{-4}$ bar.

2-8-5 The Precision Pressure Gauge

(a) Introduction

In order to reduce the 'dead space' between the pressure vessel and expansion vessel, a quartz spiral Bourdon tube was used as a null manometer which separated the experimental gas from the reference gas, whose pressure was measured by the piston gauges as described in the previous sections.

During pressure measurement of the reference gas, there was inevitably a pressure difference between the experimental gas and the reference gas although it was kept as small as possible.

Thus the quartz spiral Buordon tube was used not only as a nulling device but as a means of measuring the small pressure difference between the two sides (i.e. by using the mechanical device provided for measuring the angle of rotation of a light beam reflected from a mirror on the quartz spiral). The main advantage of using the quartz spiral tube as a null manometer was the almost absolute constant volume of the quartz tube (volume changes by less than one part in 10^{10} at about 100 bar),

As shown in Fig 2-20, the quartz Bourdon tube consisted of a several turn helicoil, 7 cm long and 1 cm in diameter, made from a quartz tube of about 2 mm diameter and of the order of 0.1 mm wall thickness. One end of the coil had a rigid mounting and the other end was suspended torsionally between two quartz fibres to reduce effect due to vibration. A mirror was attached at the free end.

The characteristics of this type of null manometer was summarised by Saville.(2)

The instrument used in this work was a Precision Pressure Gauge (P.P.G.), made by Texas Instruments, Model 145 with a Type 4 Stainless-Steel Capsule, rated at a maximum pressure difference of 8.5 bar at total pressure up to 136 bar.

The principle of the P.P.G. was that a light beam from a source passed through a sapphire window of the capsule and was reflected from the mirror attached to the quartz spiral. The image was focused onto two silicon photocells. When the image was divided equally between the two photocells the output from each cell was equal and opposed and no current flowed through the ammeter on the front panel of the P.P.G.

A pressure difference between the two parts caused a distortion of the spiral tube and hence change in the position of the mirror. This in turn changed the position of the focus on the photocells, which gave rise to a deflection on the ammeter accordingly.

The optical system, including photocells, was mounted on a worm-gear turntable that rotated about a central vertical axis. A digital counter was operated through a system of gearing from the turntable, giving a reading of 300.000 for the full-scale 100^{o} rotation. When the operational mode of the P.P.G. was changed from 'METER' to 'SERVO', the output from the photocells formed a signal to an electrical motor which automatically drove the turntable until the light beam focused evenly on the two main photocells. Supplementary photocells provided the restoring signal for the servo-system when the light-beam moved 'off' the central photocells. The capsule was maintained at a constant temperature of $45^{o}C$ by means of heaters wound around the outside of the capsule.

The two ports were nulled at atmospheric pressure by opening the two ports to the atmosphere and rotating manually the turntable until no electric current flowed through the ammeter.

It was found that the null position of the P.P.G. depended on the total pressure and also on the particular gas in the capsule. This null-shift, however, could be characterised as follows.

(i) The shift was nearly proportional to the total pressure.

(ii) At constant pressure, the null position was almost constant.

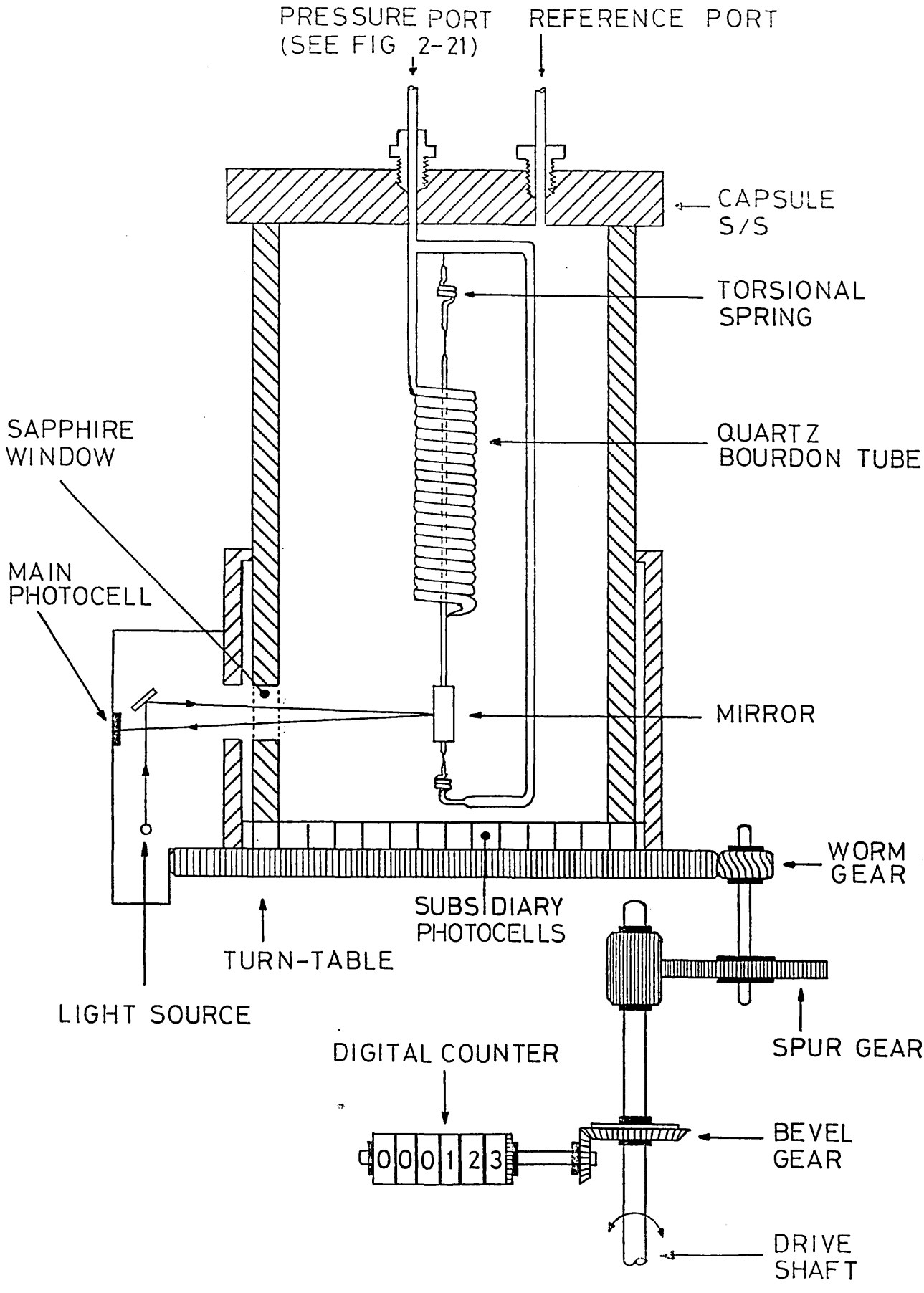


FIG 2-20 PRECISION PRESSURE GAUGE

(iii) The magnitude of the shift depended on the particular gas in the capsule.

This last phenomenon was due to the variation of the refractive index of the gas in the capsule with pressure change.(1)

It was also found that the digital counter reading was not proportional to the pressure difference but showed a periodic deviation from the linear relationship. This fact was due to mechanical imperfection of the gears in the P.P.G. Thus two different calibrations were made, i.e.

(i) the calibration of null shift with pressure change,

(ii) the calibration of the P.P.G. sensitivity with pressure difference between the two ports.

The P.P.G. was also modified in two ways, i.e.

(i) automatic safety device for the quartz spiral in the event of an excessive pressure difference across the tube (8.5 bar),

(ii) the modification of the original pressure port of the capsule in order to reduce the 'dead space' volume.

(b) Modifications to the P.P.G.

The original pressure port of the capsule was modified in order to reduce the dead space at the entrance of the capsule. As shown in Fig 2-21, a stainless steel tube (0.125 in. o.d., 0.03 in. i.d.) was hard-soldered through the center of the brass filler which was then machined to seat the entrance of the port above the quartz spiral.

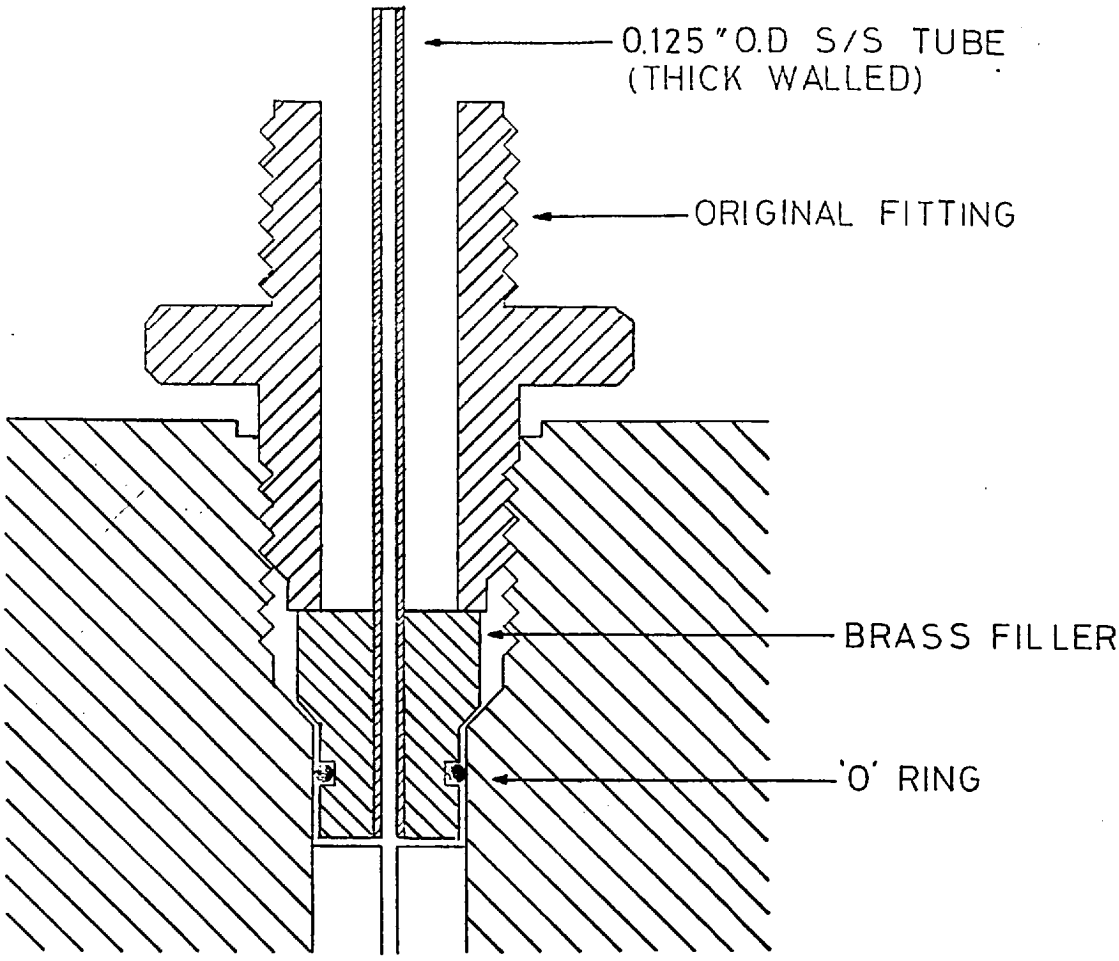


FIG 2-21 P.P.G. MODIFICATION TO ENTRANCE OF PRESSURE PORT

A rubber 'O' ring, which seated in a groove at lower part of the brass filler, sealed the pressure port from the atmosphere. The brass filler was held in place by the original fitting which screwed onto the brass filler.

This modification reduced the entrance volume from 2 cm^3 to less than 0.1 cm^3.

Another modification to the P.P.G. was to protect the quartz spiral from breakage due to excessive distortion of the spiral (i.e. excessive pressure difference across the quartz spiral).

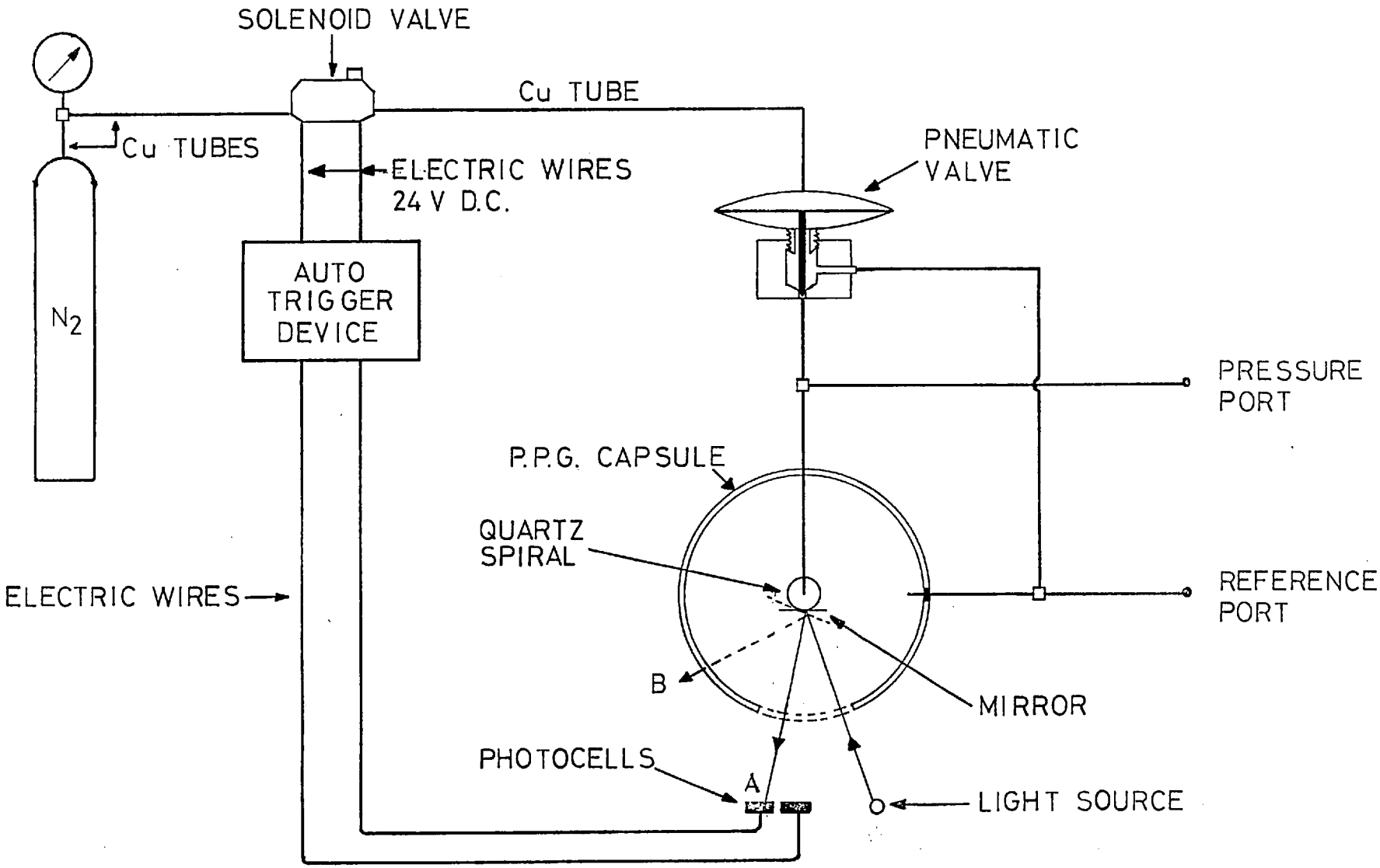


FIG 2-22 P.P.G. SAFETY DEVICE

As shown in Fig 2-22 pressure port and reference port were connected to a gas operated pneumatic valve (Autoclave Engineers). The pneumatic valve was controlled by means of a 24 volt D.C., 3-way solenoid valve (ASCO.). When the solenoid valve was energised, N_2 gas (50 - 60 psig) was passed through the solenoid to the upper chamber of the pneumatic needle valve, and subsequently the two ports were separated.

A switching device, which controlled the solenoid valve, was designed and constructed by the Electronics Workshop.

The principle of the automatic safety device was that when the reflected light beam from the mirror was on either side of the photocells, position A in Fig 2-22, the current from the photocell formed a signal to the automatic switch which amplified the signal and energised the 24 volt D.C. solenoid. If, on the other hand, the reflected beam fell outside the photocell (i.e. the spiral rotated beyond the limit of the rated angle), position B in Fig 2-22, the automatic switch received no signal and hence cut off the current to the solenoid valve. This caused depressurisation of the N_2 gas in the pneumatic valve chamber (valve opened).

(c) The Calibration of The P.P.G. Null Shift with Pressure

The P.P.G. null position change with pressure was due to the variation of the refractive index of gas in the reference port of the P.P.G. capsule.[1]

As will be shown in the next section the sensitivity of the P.P.G. depended on the angular position of the turntable. Thus after nulling the P.P.G. at atmospheric pressure by

'setting' the digital counter at '000.000' this position was 'locked permanently'.

The null shift with pressure was almost linear for N_2 and CH_4, but in the case of C_2H_4 and its mixtures with CH_4 it showed smooth curves.

Before calibration the pneumatic valve (Fig. 2-22) was open and gas was filled upto about 100 bar. Pressures were measured at an interval of 3.5 bar and the corresponding null values were recorded. The null shift with pressure for the experimental gases in this work is shown in Fig 2-23.

The relationships, null v. pressure, were determined by means of a least-squares polynomial curve fit,

$$\text{null} - 1000 = C_1 + C_2 \cdot P + C_3 \cdot P^2 \qquad (2\text{-}8\text{-}22)$$

where C_i = constant

P = absolute pressure, bar

Because of the variation of curvature (Fig 2-23) the pressure range calibrated was divided into two parts, (i.e. higher pressure part and lower pressure part) and the constants in equation (2-8-22) were determined accordingly and given in Table 2-4.

TABLE 2-4

GAS	PRESSURE (bar)	C_1	C_2	C_3
C_2H_4	3.1 - 26.8	-.338694	-.024110	$-.168468 \cdot 10^{-3}$
	26.8 - 47.6	-.477550	-.013618	$-.369572 \cdot 10^{-3}$
MIX1	3.2 - 50.8	-.335402	-.017166	$-.514425 \cdot 10^{-4}$
	50.8 - 98.5	-.354011	-.016683	$-.552990 \cdot 10^{-4}$
MIX2	3.5 - 50.7	-.043741	-.020025	$-.676438 \cdot 10^{-4}$
	50.7 -103.4	-.083842	-.016769	$-.116941 \cdot 10^{-3}$
MIX3	3.3 - 53.3	-.145473	-.019253	$-.154133 \cdot 10^{-3}$
	53.3 - 94.8	-.536285	-.002735	$-.324677 \cdot 10^{-3}$

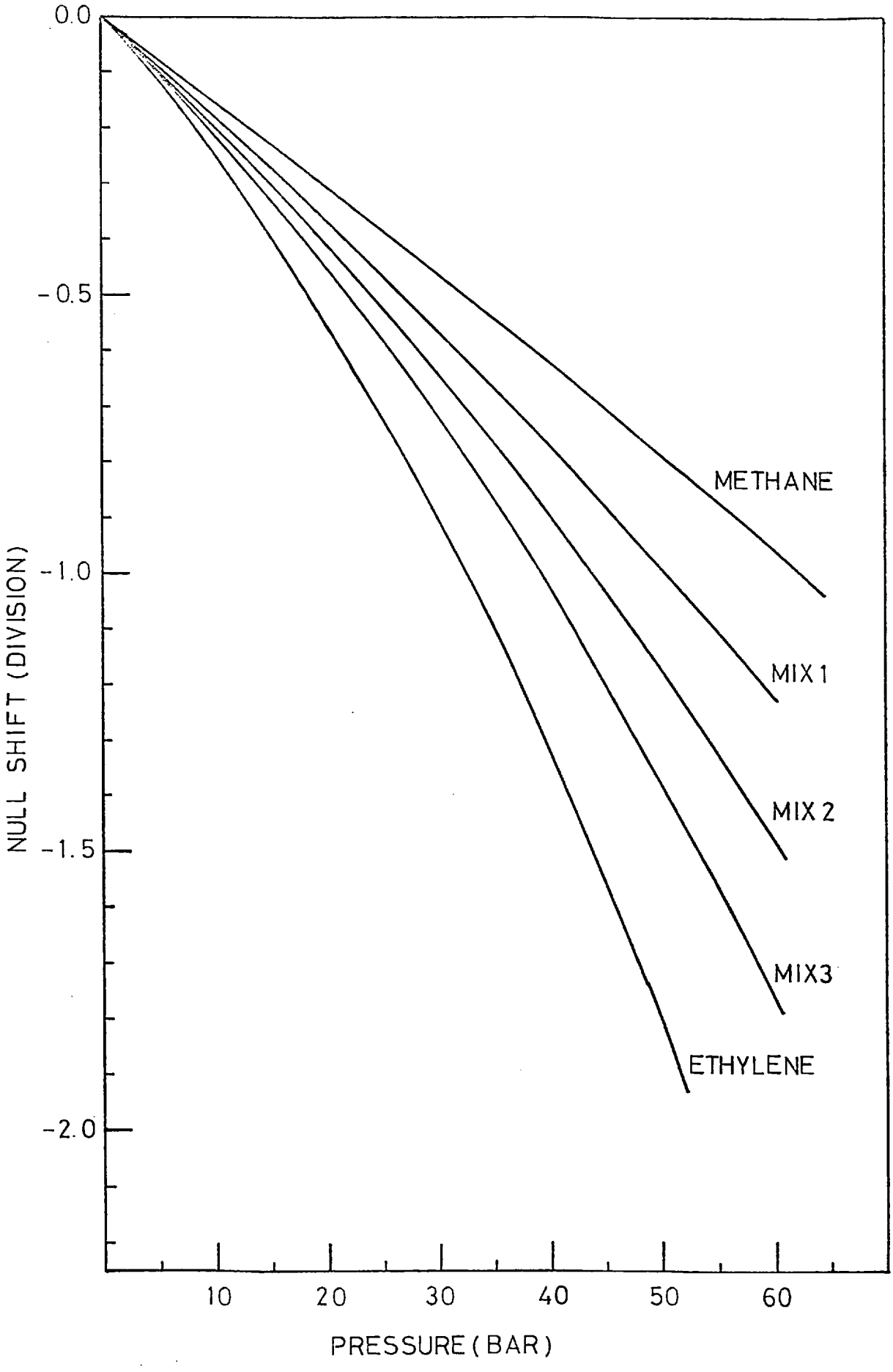


FIG 2-23 P.P.G. NULL SHIFT WITH PRESSURE CHANGE

The mean differences between the calculated P.P.G. reading from Eq.(2-8-22) and the true value were less than 000.001 division (about 10^{-4} bar) for ethylene and 000.002 for the mixtures.

(d) The Sensitivity of the P.P.G.

The P.P.G. was used not only as a nulling device but as an instrument to estimate the small pressure difference across the quartz spiral.

The pressure difference could be calculated, in principle, from the digital counter reading by multiplying by an appropriate factor.

However, apart from the P.P.G. null-shift with pressure, the sensitivity itself was found to be a function of the angular position of the turntable due to the worm gear eccentricity which transmitted the angular orientation of the turntable to the digital counter reading. Hence it was necessary to calibrate the sensitivity within a range of null-shift of the P.P.G. From the relative values of null-shift of nitrogen (999.000) and CH_4 (998.500), it was decided to calibrate within a range of $\pm$005.000 divisions which corresponded to $\pm$0.5 bar.

A U-tube mercury manometer (10 mm i.d.) was used to measure the heights of the mercury columns by means of a precision cathetometer (The Precision Tool and Instrument Co.), the accuracy of which was less than $\pm$0.005 cm ($6.6 \cdot 10^{-5}$ bar).

After setting null at atmospheric pressure by opening both ports to the atmosphere the reference port was connected to one side of the manometer and the other side of the

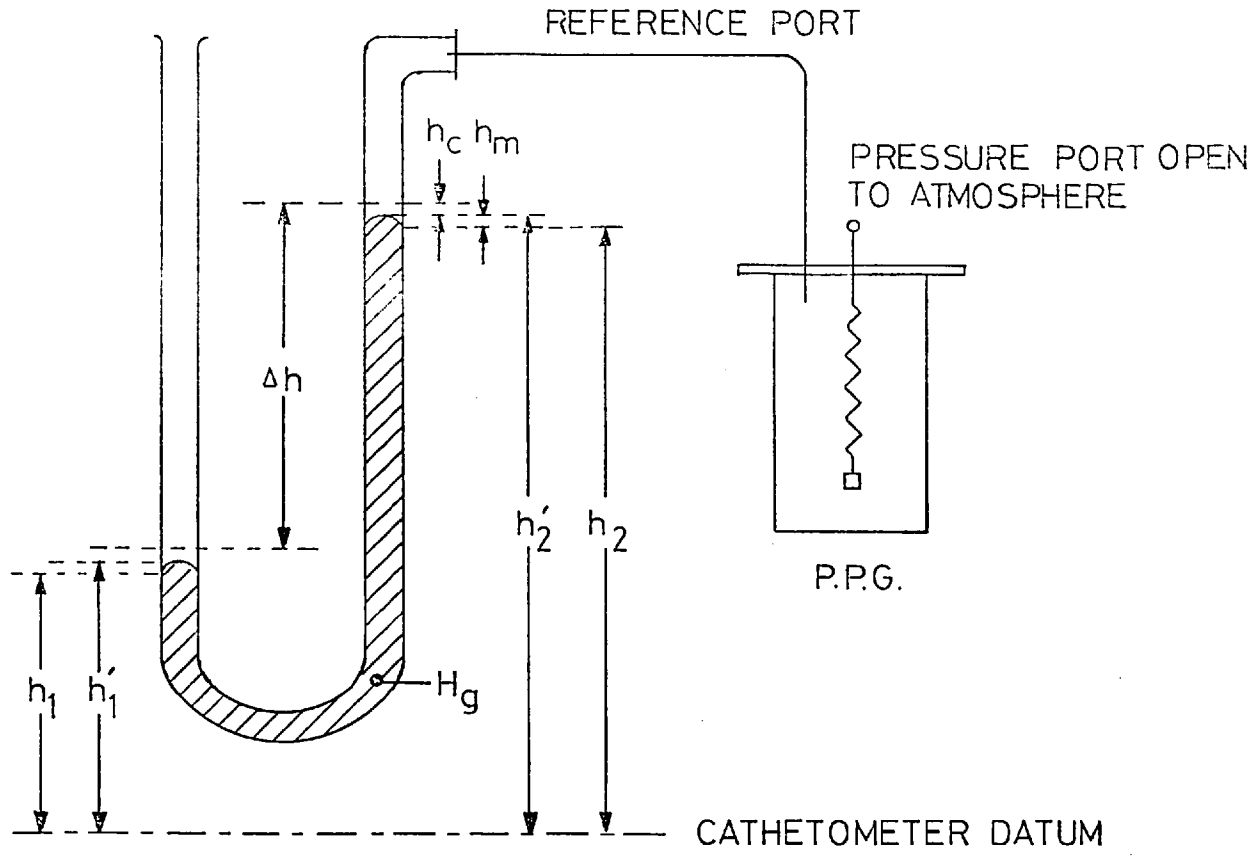


FIG 2-24 P.P.G. SENSITIVITY CALIBRATION

manometer was open to the atmosphere. The two ports of the P.P.G. was separated by the pneumatic valve (Fig 2-22) and the reference port was pressurised with N_2 gas at about 0.5 bar. With reference to Fig 2-24 the pressure difference across the quartz spiral was corresponding to the height difference

$$\Delta h = (h_2 + h_{m2} + h_{c2}) - (h_1 + h_{m1} + h_{c1}) \qquad (2\text{-}8\text{-}23)$$

where h_{m1}, h_{m2} = meniscus heights

h_{c1}, h_{c2} = capillary depression.

The capillary depression (h_c) was taken from a table given by Gould and Vickers,[12] in which the capillary depression was

related to the surface tension of mercury used and the meniscus heights (h_m). After each measurement of h_1, h_1', h_2, and h_2', the reference port pressure was reduced with an interval of about 2 cm difference in Δh, and when the pressure port pressure was higher than that of reference port, the pressure drop was made by evacuating the reference port, thus Δh was measured from +44.198 cm (0.587 bar) to -43.416 cm (-0.576 bar) with an interval of about 2 cm.

The pressure difference was then calculated by the equation,

$$\Delta P = \rho_t \cdot g \cdot \Delta h \cdot 10^{-6} \qquad (2\text{-}8\text{-}24)$$

where g = 981.202 $cm \cdot sec^{-2}$

ρ_t = density of the mercury at temperature t^oC, $gm \cdot cm^{-3}$

ΔP = reference port pressure - pressure port pressure, bar.

The density of the mercury at temperature t^oC was taken from the table given by Bigg.[11]

The pressure difference was then plotted against corresponding P.P.G. reading, $G_{exp.}$, and is shown in Fig 2-25. Though the relationship between ΔP and $G_{exp.}$ seemed to be linear from Fig 2-25, this is due to small scale of the graph and as will be shown in Fig 2-26, there was a certain periodicity about this straight line.

A linear equation of Fig 2-25 was determined by means of a least-squares polynomial curve fitting,

$$G_{cal.} = a + b \cdot \Delta P \qquad (2\text{-}8\text{-}25)$$

where $G_{cal.}$ = calculated gauge reading as a function of ΔP

a = 1000.0014136

b = -9.16312726

ΔP= pressure difference, bar.

The difference between $G_{exp.}$ (observed) and $G_{cal.}$ (Eq 2-8-25) was then plotted against ΔP (Fig 2-26-a) and a periodical deviation of ΔG was shown clearly in this graph.

The maxima of ΔG in Fig 2-26 occurred approximately at an interval of 0.3 bar of ΔP which corresponded to one full turn of the worm gear between the turntable and the digital counter (see Fig. 2-20) in the P.P.G.

In order to express this periodic deviation mathematically, a smooth line, which passed the maxima of ΔG in Fig 2-25, was drawn (Fig 2-26-a) and the deviation of ΔG from this 'tangential' curve, $\Delta G'$, was plotted against ΔP (Fig 2-26-b).

This procedure was repeated until the geometry of each cycle in Fig 2-26-b was identical so that when a Sine curve was superimposed on this periodic curve ($\Delta G'$ v. ΔP) the deviation in $\Delta G'$ was less than 0.002.

The Sine curve equation was determined from Fig 2-25-b and was given by

$$\Delta G' = 0.0069 \sin\left\{\frac{2\pi}{0.33}(\Delta P + 0.02)\right\} - 0.0069 \qquad (2\text{-}8\text{-}27)$$

and

$$\Delta P = \frac{(G_{cal.} - A)}{B} \cong \frac{G_{exp.} - A}{B} \qquad (2\text{-}8\text{-}28)$$

where A, B = constants (Eq. 2-8-25)

A correction function $G_{cor.}$ was determined in connection with Eq.(2-8-27) such that ΔP could be represented as a polynomial function of $G_{cor.}$

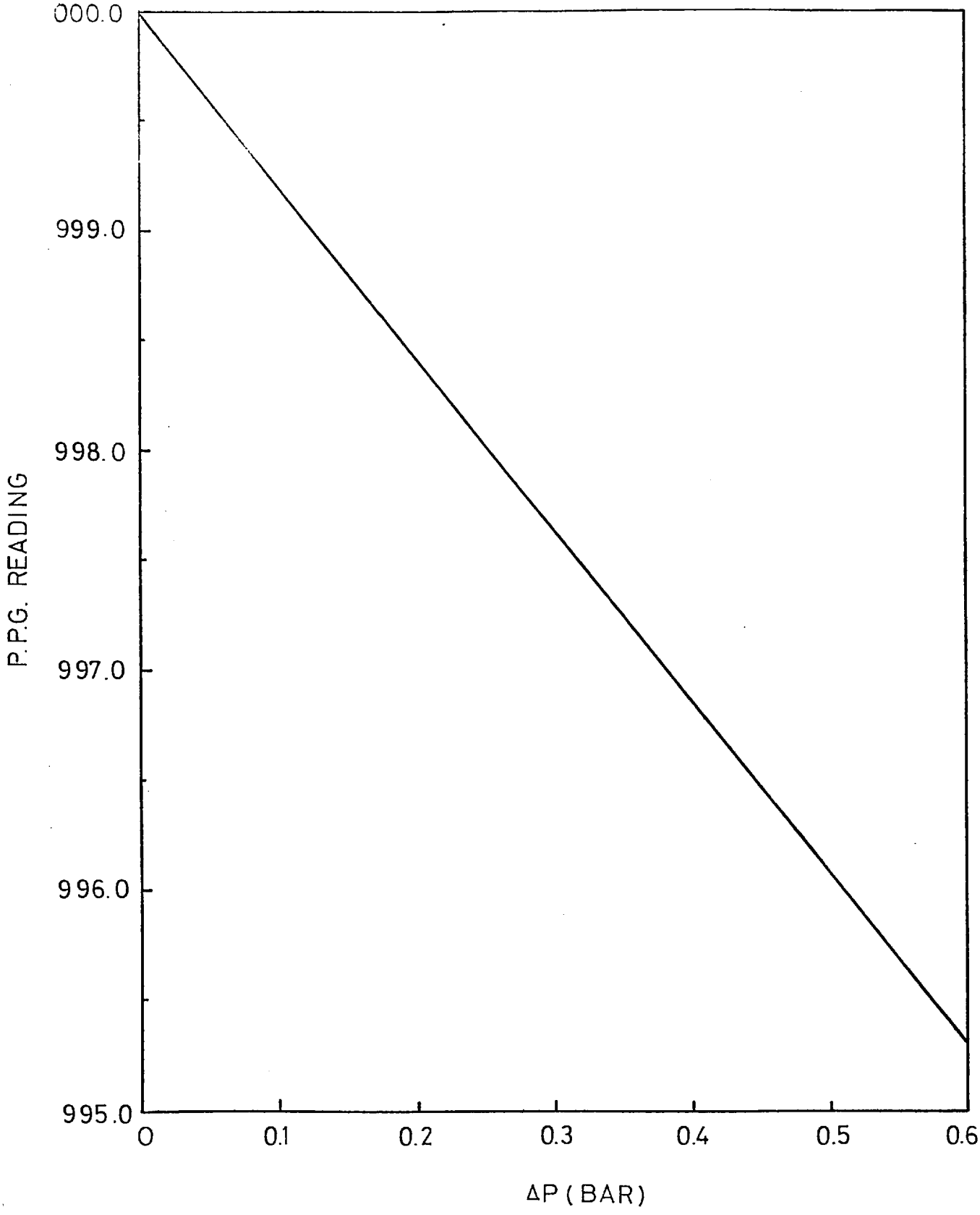


FIG 2-25 P.P.G. READING VS. ΔP

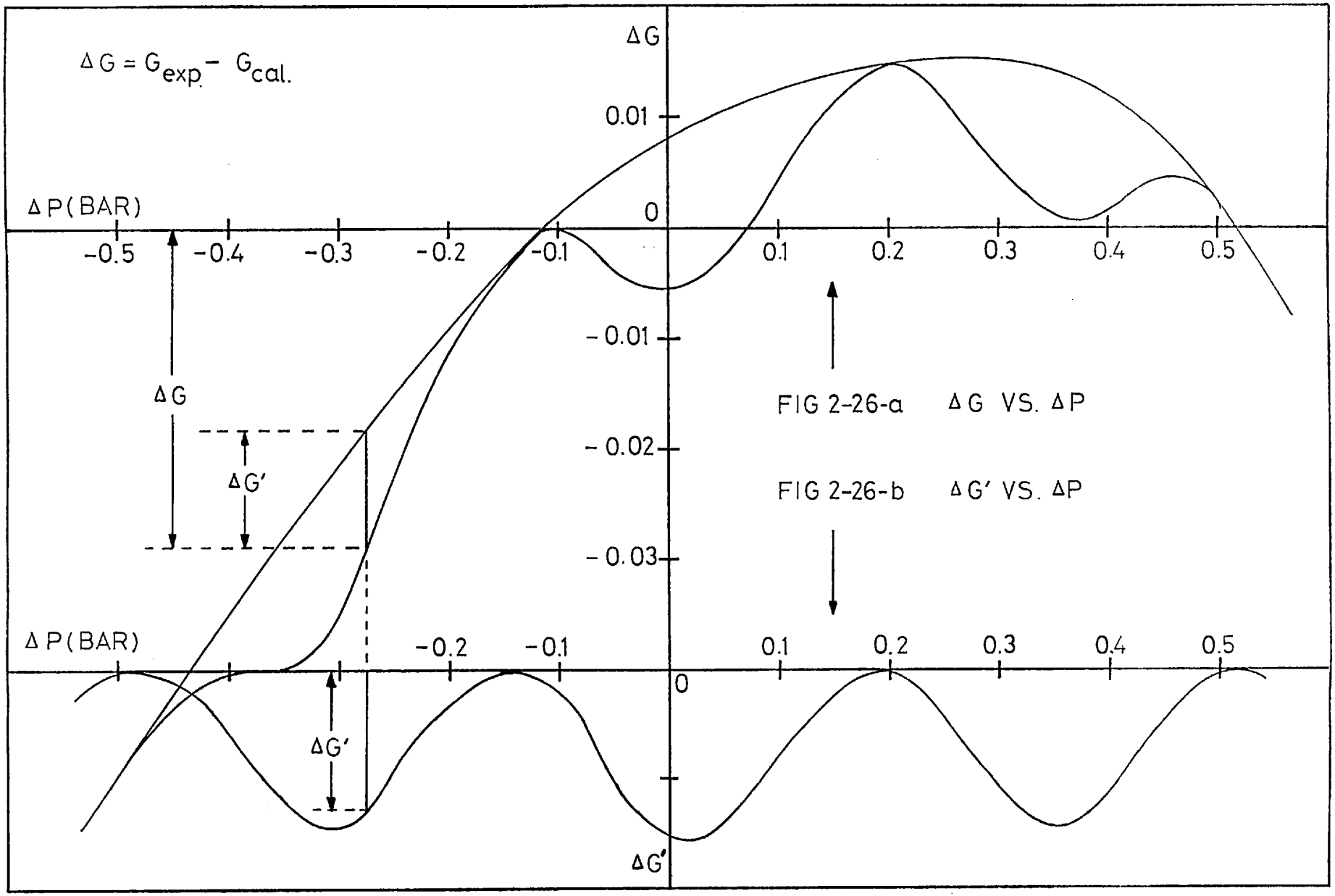


FIG 2-26 PERIODICITY OF P.P.G. SENSITIVITY

i.e.

$$P = C_1 + C_2 \cdot G_{cor.} + C_3 \cdot G_{cor.}^2 + \cdot \cdot \cdot \qquad (2\text{-}8\text{-}29)$$

where

$$G_{cor} = (G_{exp.} - 1000) - 0.0069 \sin\{2.094 (G_{exp.} - 999.487)\} \qquad (2\text{-}8\text{-}30)$$

The constants in Eq.(2-8-29) were determined by means of a least-squares polynomial curve fitting,

$C_1 = .1810659$

$C_2 = -.1099359$

$C_3 = -.1424411 \cdot 10^{-3}$

$C_4 = .8847937 \cdot 10^{-5}$

$C_5 = -.1278373 \cdot 10^{-5}$

The pressure difference across the quartz spiral were then "calculated" from the P.P.G. reading by using Eq.(2-8-29) and (2-8-30), and the differences between observed and calculated ΔP (Eq 2-8-29) were normally less than 10^{-4} bar which corresponded to the smallest division (000.001) in the digital counter.

2-9 The Pressure Gradients Due To Gravitation

The gas system of the apparatus was divided into several parts for computational purposes, and shown in Fig 2-15. As shown in the figure there were present various pressure 'heads' due to vertical height difference. The reference level was taken to be that of the top thermocouple in the inlet tubes.

The pressure gradient due to gravitation between two point separated by a vertical distance dl, in a gas column

at temperature T is given by,

$$dP = \rho g \, dh \qquad (2\text{-}9\text{-}1)$$

or

$$dP = g \frac{P \cdot M}{Z T R} \, dl \qquad (2\text{-}9\text{-}2)$$

Except for those parts where temperature gradient was present (e.g. V_2, V_{3B} and V_5), temperature and compressibility factor could be regarded as constants to a good approximation, thus

$$\Delta P = g \frac{PM}{ZTR} \, \Delta l \qquad (2\text{-}9\text{-}3)$$

Equation (2-9-3) was used to calculate the pressure gradients for all of the heights except for h_2, h_{3B} and h_5. For those parts where temperature gradients existed, linearity in T and Z was assumed between two points (T_1, Z_1) and (T_2, Z_2), then temperature and compressibility factor at height l from point 1 could be given by,

$$T = T_1 + (T_2 - T_1) \cdot l/h \qquad (2\text{-}9\text{-}4)$$

$$Z = Z_1 + (Z_2 - Z_1) \cdot l/h \qquad (2\text{-}9\text{-}5)$$

where h = distance between 1 and 2

By substituting Eq.(2-9-4) and (2-9-5) into Eq.(2-9-2),

$$dP = \frac{g P M \, dl}{\left\{T_1 + (T_2 - T_1)\frac{l}{h}\right\}\left\{Z_1 + (Z_2 - Z_1)\frac{l}{h}\right\} R} \qquad (2\text{-}9\text{-}6)$$

By integrating Eq.(2-9-6)

$$\int_{P_1}^{P_1+\Delta P} \frac{dP}{P} = \frac{gM}{P} \int_0^h \frac{dl}{\{T_1 + (T_2 - T_1)\frac{l}{h}\}\{Z_1 + (Z_2 - Z_1)\frac{l}{h}\}} \qquad (2\text{-}9\text{-}7)$$

Hence

$$\ln \frac{P_1 + \Delta P}{P_1} = \frac{gMh}{R} \cdot \frac{1}{T_2 Z_1 - T_1 Z_2} \ln \frac{T_2 Z_1}{T_1 Z_2} \qquad (2\text{-}9\text{-}8)$$

By series expansion of left hand side of Eq.(2-9-8),

$$\ln \frac{P_1 + \Delta P}{P_1} \approx \frac{\Delta P}{P_1} \qquad (P_1 \gg \Delta P) \qquad (2\text{-}9\text{-}9)$$

Hence pressure gradient along a gas column, where temperature gradient was present, could be given by,

$$\Delta P = \frac{gMh P_1}{R(T_2 Z_1 - T_1 Z_2)} \ln \frac{T_2 Z_1}{T_1 Z_2} \qquad (2\text{-}9\text{-}10)$$

Eq.(2-9-10) was used for calculating pressure gradients between each pair of thermocouples of the inlet tubes. Since ΔP in Eq.(2-9-10) was small compared to P, the error introduced by Eq.(2-9-10) was negligible.

2-10 Calibration of Volumes and Pressure Distortion of The Vessels

In order to calculate the amount of gas, the system was divided into eight sections (Fig 2-15) and each volume was calibrated accurately except for V_1 and V_6 which were actual experimental volumes and whose ratio V_1/V_6 was estimated with accuracy in the treatment of Burnett data.

For this reason V_1 and V_6 were estimated from the

measured dimensions of the vessels and the values used as first approximations in the computer programme were,

$V_1 = 377.2\ cm^3$ at 0^oC (2-10-1)

$V_2 = 183.7\ cm^3$ at 0^oC (2-10-2)

Except for V_1 and V_6, all other volumes were dead spaces. Between these vessels the connections were made in such a way that the 'dead space' volume was kept as small as possible: i.e.

(i) Inside the 0.25 in. tubing (0.07 in. i.d.) which was connected to the expansion valves by an Aminco-type fitting; 0.063 in. o.d. stainless-steel rods were inserted to reduce the internal volumes of 0.25 in. tube and that of valves.

(ii) Short lengths of the 0.25 in. tubing described in (i) were connected to 0.125 in. o.d., 0.027 in. i.d. stainless tube by 'Swagelok' couplings.

(iii) The entrance to the pressure port of the P.P.G. capsule was modified. (see section 2-8-5, Fig 2-22).

(iv) The 0.063 in steel rods were used wherever necessary.

The inlet tube volume per 1 cm length was calibrated by using mercury described in section 2-2-4.

$volume/cm = 0.00954\ cm^3/cm$ (2-10-3)

The other dead space volumes were calibrated by Roe[1] using a gas burette in conjunction with the P.P.G. as a pressure measurement instrument.

The results were,

$V_3 = 1.972\ cm^3$

$V_4 = 0.882$ "

$V_5 = 0.026$ "

$V_{3A} = 0.592$ "

$V_{3B} = 0.107$ "

The estimated maximum possible error was $0.0015\ cm^3$. The volumes of all pressure vessels are subject to change with pressure, i.e. pressure distortion. The pressure distortion of an infinitely long thick-walled cylinder, in which the vessel is not constrained by the ends in a radial direction, is given by,(13)

$$\frac{dV}{V} = \frac{1}{E(r_o^2 - r_i^2)}\left[P_i\{3(1-2\nu)r_i^2 + 2(1+\nu)r_o^2\} - (5-4\nu)r_o^2 P_o \right] \qquad (2\text{-}10\text{-}4)$$

where dV = volume increment due to pressure

V = volume at zero pressure

r_i, r_o = internal and external radii of the vessel

P_i, P_o = internal and external pressures

ν = Poisson's ratio

E = Young's modulus of elasticity

For real pressure vessels Eq.(2-10-4) is an approximation, since end-effects are present.

When $P_i = P_o$, however, equation (2-10-4) reduced to

$$\frac{dV}{V} = -\frac{3(1-2\nu)}{E} P_i = -kP_i \qquad (2\text{-}10\text{-}5)$$

and this equation is 'exact' and independent of the 'shape'

of the pressure vessel.

Thus pressure compensation to the outside of V_1 and V_6 not only reduces the magnitude of the pressure distortion but enables it to be calculated accurately.

For the pressure vessel and expansion vessel (EN58J S/S)

$E = 1.954$ bar at $20^{\circ}C$

$\nu = 0.255$ at $20^{\circ}C$

Hence,

$$(dV/V) = -0.7626 \cdot 10^{-6} \cdot P \qquad (P \text{ in bar}) \qquad (2\text{-}106)$$

For all the other dead spaces including inlet tubes the external pressure was very small compared with the internal pressure and equation (2-10-4) reduces to

$$\frac{dV}{V} = \frac{P_i}{E(r_o^2 - r_i^2)} \left\{ 3(1-2\nu) r_i^2 + 2(1+\nu) r_o^2 \right\} \qquad (2\text{-}10\text{-}7)$$

Eq.(2-10-7) was used to calculate the pressure distortion of all dead spaces and the results were,

(i) for inlet tubes;

$$dV/V = 1.51 \cdot 10^{-6} \cdot P \qquad (2\text{-}10\text{-}8)$$

(ii) for the narrow-bore 0.0625 in. o.d. tubing,

$$dV/V = 1.38 \cdot 10^{-6} \cdot P \qquad (2\text{-}10\text{-}9)$$

Eq.(2-10-9) was also used to calculate the pressure distortion of all other 'dead spaces'.

The effect of temperature on the pressure vessel volume is small compared with that of pressure distortion and the errors introduced by using Eq.(2-9-10) in calculating other

dead space volume distortion was believed to be negligible compared with the uncertainty of compressibilities in that part.

2-11 Errors in Pressure Measurement

Errors in pressure measurement can be categorized in three basic types,

(i) Systematic errors proportional to the pressure (type 1).

(ii) Systematic errors independent of pressure (type 2).

(iii) Random erros (type 3).

Because the accuracy in calculating the compressibility factors from the Burnett procedure depends largely on the successive pressure ratio (P_n/P_{n+1}) instead of individual absolute pressure, type 1 errors are much less important than those of type 2 and type 3 errors.

(a) Type 1 errors

The largest source of this type of error was the uncertainty in the calibrated effective area of the oil piston gauge (2 parts in 10^5). Others were from the uncertainties in the acceleration due to gravitation, in the masses of the disc weight, in the calculating buoyancy effects and uncertainties in various heights of the apparatus. These errors were estimated as less than 2 parts in 10^5.

In the case of the gas piston gauge, however, the errors due to the calibrated equation (2-8-17) was estimated as 5 parts in 10^5 at lowest pressure and reduced to 2 parts in 10^6 at about 100 bar.

Thus maximum probable type 1 error was estimated as about

9 parts in 10^5, although probable errors would be less than this.

(b) Type 2 errors.

The systematic errors independent of pressure were difficult to estimate. This type of errors were due to the intrinsic error in the scale of the barometer (0.02 cm, $3 \cdot 10^{-4}$ bar), the P.P.G. null-drift ($2 \cdot 10^{-4}$ bar) and the errors in the correction for the hydraulic head of oil (10^{-4} bar at 100 bar pressure). Thus total type 2 errors in pressure measurement was estimated as a maximum of about $5 \cdot 10^{-4}$ bar.

(c) Type 3 errors.

There were many sources of this type error (random) such as;

(i) temperature fluctuation in control system (5 parts in 10^6)

(ii) uncertainties in floating position both in the oil and gas piston gauges ($\pm 2 \cdot 10^{-4}$ bar, max.)

(iii) D.P.C. null shift ($3 \cdot 10^{-4}$ bar).

(iv) P.P.G. null shift calibration error (10^{-4} bar).

(v) P.P.G. sensitivity calibration ($2 \cdot 10^{-4}$ bar max.).

(vi) errors in barometer reading ($3 \cdot 10^{-4}$ bar max.).

The maximum random erros in pressure measurement was, therefore, estimated as about 10^{-3} bar.

Apart from these errors there was one systematic error that could not be determined; i.e. the error due to the

extrapolation of gas piston-gauge pressure below the calibrated pressure. It is believed to be only significant at pressures below about 3 bar.

2-12 Experiment

An experimental 'RUN' of the Burnett apparatus consisted of several expansions of the experimental gas from the pressure vessel to the expansion vessel. The pressure vessel was kept at experimental temperature while the expansion vessel was at $0^{o}C$ throughout this work.

Before starting a Burnett run following preparatory procedure was taken, i.e.;

(i) Cabinet temperature was controlled by the toluene regulator a few degrees higher than ambient temperature outside.

(ii) The ice bath was remade with freshly crushed ice and distilled water. The pressure vessel refrigerant was kept at a constant level at all times.

(iii) The gas system was flushed with experimental gas and then evacuated.

(iv) The pressure vessel was then cooled/heated to a few degree below the experimental temperature. When a rapid cooling was necessary small amount of helium gas was introduced in the brass jacket as a heat transfer medium. When experimental gas was in the system, however, helium was not used to avoid any condensation of gas in the inlet tubes due to over-cooling.

(v) Once the temperature of the pressure vessel reached the desired value (and that of the radiation shield accordingly), the apparatus was ready for filling the gas. Before filling with gas, the expansion vessel was isolated from the pressure vessel. With the pneumatic valve opened, the gas was introduced slowly into the pressure vessel (both inner and outer volumes). The vessel temperature rose by the amount which corresponded to heat capacity of the gas in the vessel.

(vi) Having the gas in it the temperature of the vessel was controlled and both automatic current controllers were set to 'AUTO'.

(vii) The D.P.C. was nulled with both chambers (upper and lower) open to atmosphere and then the upper chamber was flushed with experimental gas to remove air. After having sufficient weights on the piston guage, both chambers of D.P.C. were pressurised.

(viii) The pressure port was then separated from the reference port (P.P.G.) by means of the pneumatic valve, and the D.P.C. was connected to the reference port.

Thus the apparatus was ready for measurement.

Reference gas pressure was adjusted such that the pressure difference across quartz spiral was as small as possible. This reference pressure was then balanced by the piston gauges.

When the piston floated at exact position and the D.P.C. was at its null position with full sensitivity (in case

of oil piston gauge) following were then recorded;

(i) Weight numbers on the piston carrier together with extra weights.

(ii) The voltages across the standard resistance and the platinum resistance thermometer by means of the potentiometer.

(iii) The P.P.G. reading.

(iv) The piston temperature.

(v) Cabinet temperature.

(vi) Inlet tube thermocouple e.m.f.'s.

(vii) Barometric height.

(viii) Barometer temperature.

After these measurements the expansion vessel was isolated from the vacuum system and the ice bath temperature was checked by means of the platinum thermometer provided in the ice bath dewar.

Before expansion the inlet tubes, pressure vessel and radiation shield were heated manually, since during expansion, temperature fell sharply due to Joule's effect.

The fine control valves, which were placed between the pressure vessel and the main expansion valves were half turn opened.

The flows of the gases from both volumes of the pressure vessel were controlled by the fine control valves in such a way that pressure difference across the spiral guage was kept as small as possible during the expansion.

The temperature equilibrium in both vessels were regained after one to two hours depending on the temperature and pressure

of the experimental gas. The expansion valves were shut and the measurement was repeated while the gas in the expansion vessel was vent and evacuated.

This procedure was continued until the pressure reached to the lowest measureable value (about 3 bar).

One 'RUN' consisted of normally 6 to 9 expansion (2 - 4 days) depending on particular kind of gas under study and its temperature and pressure.

2-13 Preparation of Gas Mixtures and Gas Analysis

Pure ethylene used in this work was supplied by The British Oxygen Co. Ltd., Special Gases Division. Its purity is believed to be more than 99.85 mol% (analysed by the suppliers) with 0.1% methane as impurities. The analysis also shows very small amount of other impurities such as hydrogen (20 VPM), acetylene (10VPM) carbon monoxide (20 VPM) etc., but they are expected to have a negligible effect on the results of this work.

Pure methane used for making mixtures was Matheson ultra-high-purity (99.99%). The analysis, provided by the sypppliers, shows that the impurities are ethane (0.0038%), nitrogen (0.0016%) and traces of propane, oxygen and carbon dioxide. Both gases were analysed by the analytical service laboratory of this department by using a mass spectrometer. The results confirmed the purity of ethylene to be not less than 99.9% and that of methane 99.99%.

Three different compositions of methane-ethylene mixtures were prepared by using a gas compressor to fill a gas cylinder with the required amount of each gas.

Nominal compositions of these mixtures were 75%, 50% and 25% methane and, for convenience, they were named as mixture 1, mixture 2 and mixture 3 respectively.

In order to analyse these mixtures accurately a standard sample of a gas mixture was prepared and the composition of this standard sample was calculated to the nearest $\pm 0.015\%$ by weighing. That is, ethylene and methane were blended and compressed in a stainless-steel pressure vessel, the volume of the vessel was approximately 1000 cc and the maximum rating was 1800 psia. The vessel was thoroughly evacuated and weighed before methane was introduced upto about 54 bar and ethylene was mixed to this gas upto 110 bar.

The sample vessel was weighed before and after filling the gases by means of the 10-kg Stanton balance (see section 2-8-2). The amount of each gas in the vessel was found to be

CH_4 = 39.516 gm

C_2H_4=201.018 gm

and thus giving the standard composition of,

CH_4 = 25.583 mol %

C_2H_4= 74.417 mol %

The uncertainties in the reproducibility of the balance (5 mg), errors in the nominal weights (less than 5 mg) and errors in reading the scale (less than 5 mg) could lead to the maximum probable error of $\pm 0.015\%$.

The gas mixtures 1, 2 and 3 were analysed using a gas-chromatograph (PYE Model 104) by comparing the ratio of the methane-ethylene peak area against that of the standard sample.

Using argon as a carrier gas (25 ml/min.) through a silica column (60-80 mesh, 50°C), methane was separated first (retention time = 1 min. 10 sec.) and the ethylene peak appeared 5 sec. later (2 min. 45 sec.). The output voltage from the detector (Katharometer) was recorded on a DVM 'magnetic tape casette logger' provided by the departmental analytical laboratory with an interval of 1 second. The peak areas were then calculated by Simpson's rule by means of PDP 11/10 computer. Thus the compositions of the three gas mixtures were determined by comparing the ratios of the peak-areas to that of standard sample.

The measurement was repeated 4 - 5 times for each gas sample and the mean value was taken as the composition of each gas.

The area ratio of the standard sample (2.00665) was reproducible to $\pm$0.002 and that of mixture 3 (2.1504), for example, was $\pm$0.004; thus leading to possible errors of $\pm$0.02% and 0.04% respectively in the results. Thus combining with the errors from the standard sample weight (0.015%), the maximum probable error was estimated as less than 0.1%.

The results are;

mixture 1:	69.55 mol	% methane	30.45 mol	% ethylene
mixture 2:	45.18	"	54.82	"
mixture 3:	24.19	"	75.81	"

CHAPTER THREE

TREATMENT OF EXPERIMENTAL DATA AND DISCUSSIONS

3-1 Introduction

The estimation of compressibility factor from the Burnett apparatus data (P and T) is possible either graphically or analytically. Burnett introduced a graphical method in 1933[22] to obtain Z from the 'isothermal apparatus' (i.e. both pressure and expansion vessels were at the same temperature). Unlike an analytical method the graphical method needs no assumed equation of state, thus the compressibility can be obtained from the experimental pressure and temperature without using a computing machine. This method, however, involved extrapolations at zero pressure and, as will be shown in section 3-2, a small error in this extrapolation can lead a large error in the value of Z.

The alternative approach is to use an analytical method of data reduction. This requires an adequate equation of state whose coefficients can be determined by means of a non-linear regression analysis.

In this work the compressibility factor was determined by the analytical method, using two different equations, i.e.,

(i) the truncated virial eauation of state (see Eq. 3-3-1),

(ii) the modified Bender equations (Eq. 3-3-2 and 3-3-3).

In the case of the virial equation the calculation was based on each 'isothermal' run, since the virial coefficients B, C, etc. are functions of temperature only. Thus the coefficients are determined at the experimental temperature

from the series of pressures P_o, P_1, $\cdots$ P_n. The infinite series of the virial equation was truncated at the third virial coefficient because of the limited number of expansions in one run due to low vapour pressure of ethylene and its mixtures. Although it is desirable to know accurate values of the virial coefficients which can be directly related to the molecular forces the infinite power series does not converge at high density, thus the equation itself is useful only in the dilute or at most the moderately dense gas.[28,50] For this reason the truncated virial equation is regarded as an inadequate equation of state at high pressure. The Bender equation was therefore chosen as an alternative, for with 20 coefficients it was found to represent reasonably well the whole fluid region for several other substances, namely, argon, oxygen[29] carbon dioxide and methane.[30] The equation was modified by reducing the number of the coefficients, since this work dealt only with gas phase in which region not all the 20 coefficients of the original Bender equation were considered to be necessary (see section 3-6-3).

It is important to note that in fitting modified Bender equations (Eq. 3-3-2 and 3-3-3) all data points, i.e. for all temperatures, are treated simultaneously.

Thus in the following sections the general description of least-squares method will be followed by the two different treatments of the data. The results are listed in tables (3-1) to (3-5) and in the last section of this chapter they are compared and discussed from the point of view of least-squares principle. The best compressibility factors chosen were then compared with those of other workers wherever possible.

3-2 The Method of Data Reduction

In order to simplify the description of the methods of data treatment the 'isothermal' Burnett apparatus will first be considered, in which case both pressure and expansion vessels are at the same experimental temperature, T. It is assumed also that the volumes are independent of pressure. The treatment of the non-isothermal Burnett apparatus will be considered in section (3-4).

From a sequence of pressures in a experimental run,

$$P_o,\ P_1,\ P_2,\ \cdots\ P_n \qquad (3\text{-}2\text{-}1)$$

one can derive the two basic equations from which the corresponding compressibility factors,

$$Z_o,\ Z_1,\ Z_2,\ \cdots\ Z_n \qquad (3\text{-}2\text{-}2)$$

are to be determined.

The two equations are,

$$\frac{P_{j-1}}{P_j} = N\frac{Z_{j-1}}{Z_j} \qquad (3\text{-}2\text{-}3)$$

and

$$P_j N^j = \left(\frac{P_o}{Z_o}\right) Z_j \qquad (3\text{-}2\text{-}4)$$

where $N = (V_A + V_B)/V_A$, the apparatus (or cell) constant

(P_o/Z_o) = the run constant.

In order to determine the compressibility factor, Z_j, at pressure, P_j, from equation (3-2-4), the apparatus constant, N, and the run constant, P_o/Z_o, must be known.

There are essentially two different methods of data reduction, namely the graphical method and the analytical method.

Although the graphical method was not adopted in this work the basic idea of this method will be introduced briefly so that the advantages and the disadvantages of the two methods can be compared.

3-2-1 The Graphical Method of Data Reduction

In the original graphical method proposed by Burnett[22] the apparatus constant, N, was determined from equation (3-2-3) by extrapolation of the plot of P_{j-1}/P_j against P_j.
It may be seen from Eq.(3-2-3) that as,

$$P_j \to 0, \qquad Z_j \to 1$$

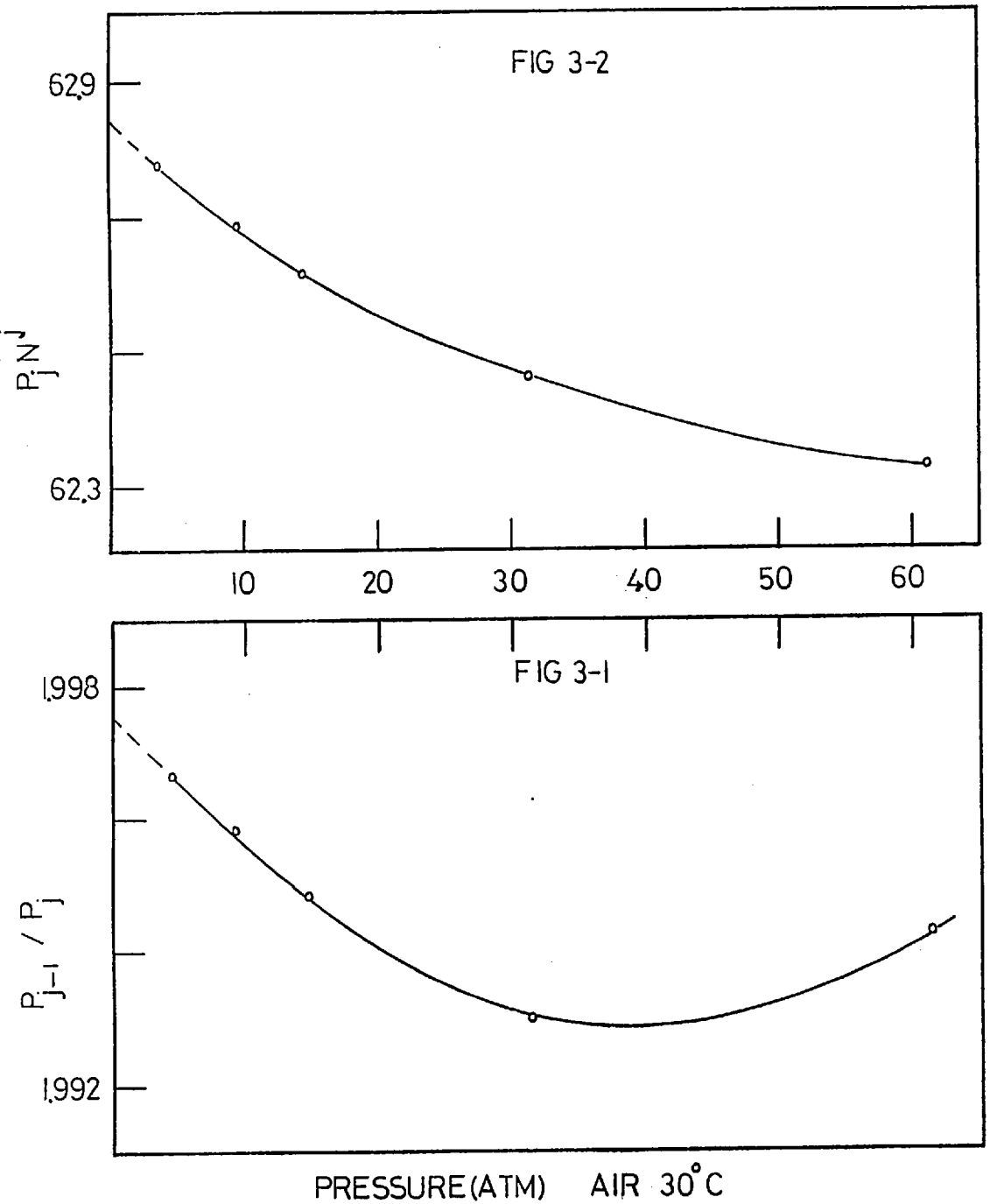
Hence from Eq.(3-2-3)

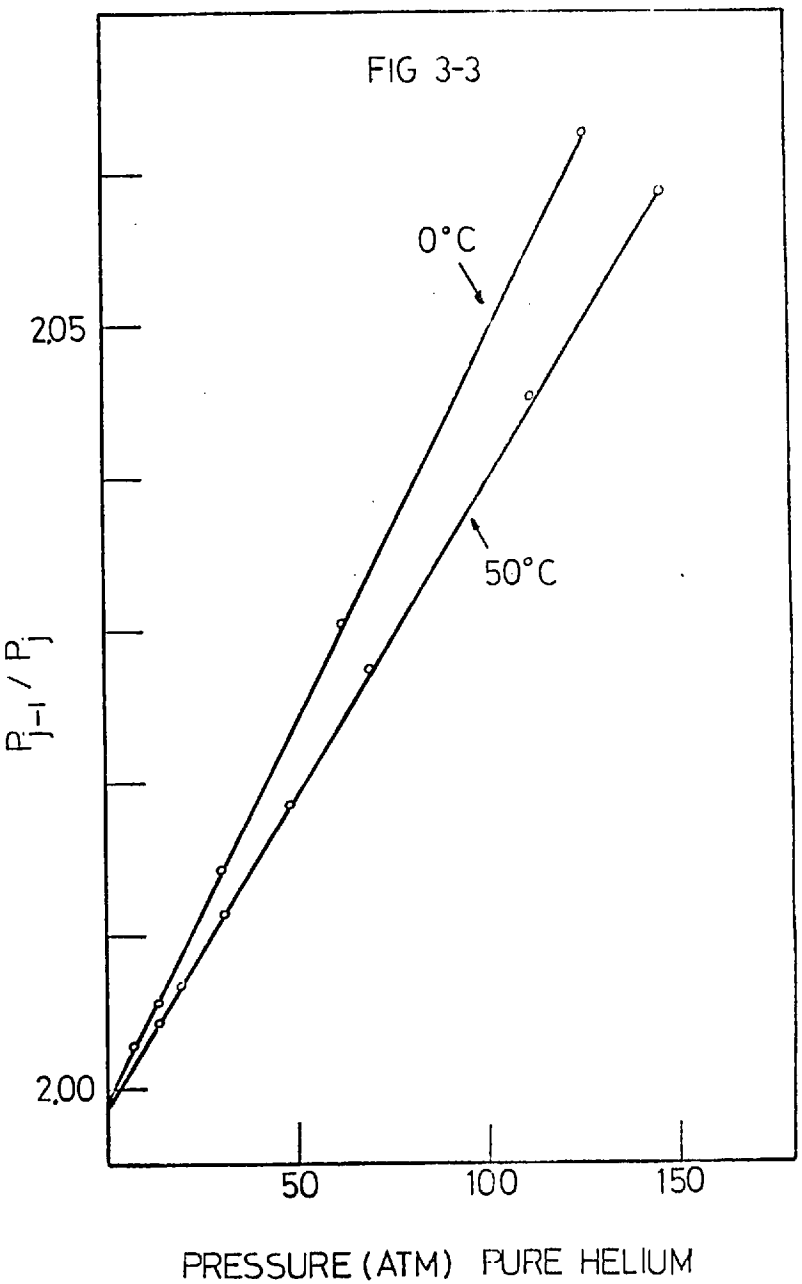
$$\lim_{P_j \to 0} \frac{P_{j-1}}{P_j} = \lim_{Z_j \to 1} N \frac{Z_{j-1}}{Z_j} = N \qquad (3\text{-}2\text{-}5)$$

The run constant is then determined by another extrapolation of the plot of $P_j N^j$ against P_j. From Eq.(3-2-4) it may be seen that as P_j approaches zero $P_j N^j$ approaches P_o/Z_o, i.e.,

$$\lim_{P_j \to 0} P_j N^j = \lim_{Z_j \to 1} \left(\frac{P_o}{Z_o}\right) Z_j = \frac{P_o}{Z_o} \qquad (3\text{-}2\text{-}6)$$

Thus from Eq.(3-2-4) one can calculate the compressibility factor Z_j at pressure P_j. The extrapolations of equations (3-2-5) and (3-2-6) are shown schematically in Fig (3-1) and (3-2) as an example for air at 30^oC, extracted from the Burnett's original paper. In Fig (3-3) the extrapolation of pressure ratio against pressure is shown for Helium at 0^oC and 50^oC.


FIG 3-2
62.9
62.3
$P_j N^j$
10
20
30
40
50
60
FIG 3-1
1.998
1.992
P_{j-1} / P_j
PRESSURE (ATM) AIR 30°C


FIG 3-3
0°C
50°C
2.05
2.00
P_{j-1} / P_j
50
100
150
PRESSURE (ATM) PURE HELIUM

As N appears to the j'th power in Eq.(3-2-1) small errors in N accumulate and lead to large errors in the compressibility factors. As shown in Fig (3-1) the first approximation of N does not give the accurate value required unless the gas under study is near-ideal. An improvement due to Canfield[31] involves the adjustment of N, within the error of the first extrapolation, to give final values of Z_j such that Z_j has the correct limiting behaviour at low density, i.e. Z_{j-1}/ρ_j is linear with ρ_j at low density.

The comparison of Fig (3-1) and Fig (3-3) suggests that N can be obtained accurately from a calibration run with helium, which is very close to ideal at normal temperatures and for which P_{j-1}/P_j is remarkably linear with pressure (Fig 3-3), hence enabling the extrapolation to be performed with accuracy. However, there is the possibility of real changes in N between runs (Fig 3-12), particularly if the apparatus is subjected to temperature cycling.[24]

The major advantage of the graphical method is that unlike all analytical methods no equation of state need be assumed. On the other hand this method requires very precise measurements at low pressures where the graphical plot in Fig (3-1) is expected to be nearly linear. With an analytical method it is not necessary to have any low pressure points to obtain results.

3-2-2 The Analytical Method of Data Reduction

Any analytical method of P-V-T data reduction requires a supposition that the experimental data can be suitably represented by an equation of state,

$$P = f(T, \rho, a_1, a_2, \cdots a_k, \cdots a_m) \qquad (3\text{-}2\text{-}6)$$

For an individual isothermal Burnett run temperature, T, becomes a constant while pressure and density remain as variables. This can be regarded as special case of equation (3-2-6) and a simpler form of equation of state for each individual run can be described as

$$Z_j = Z(\rho_j, a_1, a_2, \cdots a_k, \cdots a_m), \text{ or}$$

$$Z_j = Z(P_j, a_1, a_2, \cdots a_k, \cdots a_m) \qquad (3\text{-}2\text{-}7)$$

In this work, as mentioned previously, the experimental data were treated as a whole using equation (3-2-6) as well as individually using Eq.(3-2-7). In both cases, however, the principle of the analytical data reduction is same, thus the description of the method will be based on the case of the individual Burnett run for the sake of simplicity.

In section (3-3-2) the data treatment by Eq.(3-2-6) will be discussed, in which case the equation of state is described as a function of temperature as well as density.

From the equation of state (3-2-7) the m parameters together with the apparatus constant, N, and sometimes the run constant, P_o/Z_o, are determined by means of a non-linear regression analysis which is based on the principle of least squares. The basic principle of the least-squares procedure is that the m parameters a_1, a_2, $\cdots a_m$ are best-fit to the equation of state when the objective function, S, which is defined as the sum of the weighted squares of the residuals, is a minimum with respect to the m least-squares parameters,

$$S = \sum_{j=1}^{n} \omega_j R_j^2 \qquad (3\text{-}2\text{-}8)$$

In Eq.(3-2-8) ω_j is a weighting factor which is defined as the reciprocal of the expected variance in the j'th residual, $1/\sigma_{R_j}^2$, R_j is the residual of j'th data point and n is the number of data points. The residual, R_j, is defined as the difference between an observed dependent variable, Y_j, and its adjusted value, Y_j'.

$$R_j = Y_j - Y_j' \qquad (3\text{-}2\text{-}9)$$

The adjusted value, Y_j', is calculated from the equation of condition with m least-squares parameters,

$$f'(Y_j', X_j, a_1, a_2, \cdots a_k, \cdots a_m) = 0 \qquad (3\text{-}2\text{-}10)$$

where X_j represents one or more independent variables. This is the general formulation of the least-squares problem as described by Deming.[32] Eq.(3-2-9) shows that by defining the residual as $(Y_j - Y_j')$ it is necessary that experimental error occurs only in the observed dependent variable, Y_j, and that these errors are randomly distributed.

In some previous work on Burnett apparatus[23,33,34] the objective function was chosen as,

$$S = \sum_{j=1}^{n} \omega_j \left(P_j - P_j' \right)^2 \qquad (3\text{-}2\text{-}11)$$

where P_j is the observed pressure and P_j' is the adjusted pressure which is calculated from the equations of condition, i.e. equations (3-2-4) and (3-2-7),

$$P_j' \cdot N^j = (P_o/Z_o) \cdot Z_j' \qquad (3\text{-}2\text{-}12)$$

and

$$Z_j = \frac{P_j}{RT\rho_j'} = Z\left(\rho_j', a_1, a_2, \ldots a_k, \ldots a_m\right) \qquad (3\text{-}2\text{-}13)$$

The adjusted pressure, P_j', is solved by an iterative method from equations (3-2-12) and (3-2-13). The M least-squares parameters are a_1, a_2, $\cdots$ a_k, $\cdots$ a_m, N and P_o/Z_o. This formulation of objective function requires an assumption that errors occur only in the observed pressure and that they are randomly distributed. In most cases, however, errors occur in the other variables, such as temperature, and there are normally present systematic errors in pressure measurement mainly due to the uncertainty in the piston area. For these reasons it is unlikely for any Burnett data to fulfill the supposition of Eq.(3-2-11).

Another form of objective function can be derived from Eq.(3-2-3),

$$\frac{P_{j-1}}{P_j} = N\frac{Z_{j-1}}{Z_j} \qquad (3\text{-}2\text{-}3)$$

$$S = \sum_{j=1}^{n} \omega_j \left(\frac{P_{j-1}}{P_j} - N\frac{Z_{j-1}}{Z_j}\right)^2 \qquad (3\text{-}2\text{-}14)$$

In this case the pressures, P_{j-1} and P_j are experimental values and not adjusted ones. The equation of condition is now the equation of state,

$$Z_j = \frac{P_j}{RT\rho_j} = Z\left(\rho_j, a_1, a_2, \ldots a_k, \ldots a_m\right) \qquad (3\text{-}2\text{-}15)$$

Here the M least-squares parameters are a_1, a_2, $\cdots$ a_m and N. This type of objective function has been criticised[35]

on the ground that it involves the sum of the squares of a function of pressure rather than a true pressure residual. The criticism is however based on an assumption that all systematic errors are absent.

In treatment of Burnett data the objective function of Eq.(3-2-14), which is expressed in terms of pressure ratio, is considered to be superior to that of Eq.(3-2-11) in two ways. Firstly since Eq.(3-2-14) involves a pressure ratio, P_{j-1}/P_j, any systematic error propotional to the pressure will be eliminated. Secondly by avoiding the iterative computation of the adjusted pressure, P_j', from Eq.(3-2-12) and (3-2-13), considerable computing time is saved, and this is especially so in the case of the "non-isothermal" Burnett apparatus.

For the reasons given above the objective function of Eq.(3-2-14) was chosen for use in the treatment of the experimental data of this work.

Another objective function can be derived from Eq.(3-2-3) by eliminating N between the expression for successive expansions, i.e.

$$\frac{P_{j-1}\,P_{j+1}}{P_j^2} = \frac{Z_{j-1}\,Z_{j+1}}{Z_j^2} \qquad (3\text{-}2\text{-}16)$$

Hence

$$S = \sum_{j=1}^{n} w_j \left(\frac{P_{j-1}\,P_{j+1}}{P_j^2} - \frac{Z_{j-1}\,Z_{j+1}}{Z_j^2} \right)^2 \qquad (3\text{-}2\text{-}17)$$

Now N is eliminated in Eq.(3-2-17) at the expense of one data point. A comparison between this and Eq.(3-2-14)[1]

showed little difference in the computed least-squares parameters.

After having chosen the objective function, the non-linear least-squares procedures from two different equations of state (i.e. the virial equation and the Bender equation) are described in sections (3-3-1) and (3-3-2) respectively.

3-3 The Non-Linear Least-Squares Procedure

All analytical methods of data treatment have one disadvantage; that is, no matter what form of objective function or least-squares procudure is employed, an adequate form of equation of state must be provided. It is desirable to have an equation of state which is able to represent the experimental compressibility factors with an accuracy greater than that inherent in the experimental pressure measurements. At low or moderate density ranges the equation chosen is usually the Leiden expansion,

$$Z = 1 + a_1\rho + a_2\rho^2 + \cdots a_k\rho^k + \cdots a_m\rho^m \qquad (3\text{-}3\text{-}1)$$

The coefficients of the m'th-order polynomial are not identical to the corresponding coefficients, B, C, · · etc. of the virial equaiton, which is infinite power series of density. The value of m that gives the 'best-fit', in a least-squares sense, to the data does not necessarily provide the best estimates of the second and third virial coefficients. Also, a least-squares fit to all the data points in <u>one</u> Burnett run will not necessarily provide the best estimates of all the compressibility factors.[1]

For the reason given above another form of equation of state is provided, namely Bender equation, in which the compressibility factor is expressed in terms of temperature as well as density,

$$P = \rho T \{ R + B\rho + C\rho^2 + D\rho^3 + E\rho^4 + F\rho^5 + (G + H\rho^2)\rho^2 \exp(-a_{20}\rho^2) \} \qquad (3\text{-}3\text{-}2)$$

where
$$B = a_1 - a_2/T - a_3/T^2 - a_4/T^3 - a_5/T^4$$
$$C = a_6 + a_7/T + a_8/T^2$$
$$D = a_9 + a_{10}/T$$
$$E = a_{11} + a_{12}/T$$
$$F = a_{13}/T$$
$$G = a_{14}/T^3 + a_{15}/T^4 + a_{16}/T^5$$
$$H = a_{17}/T^3 + a_{18}/T^4 + a_{19}/T^5$$

In the data treatment the basic difference between Eq.(3-3-1) and (3-3-2) is that, while the truncated virial equation (3-3-1) deals with the data points from each isothermal run once at a time, the Bender equation deals with <u>all</u> the different isothermal runs as a whole, since the density coefficients, B, C, etc., of Eq.(3-3-2) are expressed as a function of temperature. In the case of Eq.(3-3-1) actual manipulation beyond the third coefficient term was impractical because of the limited number of data point in <u>one</u> isothermal Burnett run. With Eq.(3-3-2) one can handle higher density terms, simply because more data points are available, thus giving more reliability in the calculated compressibility factors especially at high pressure region.

As will be discussed in section 3-6-3 not all 20 coefficients

of Eq.(3-3-2) are needed to represent the data points of this work. As a preliminary test the Bender equation was modified into a series of equations, each having different number of coefficients of 6, 9, 10 and 13. The exponential term, or correction term, of the equation was out of consideration in this investigation, since this term was considered to be unnecessary in the gas phase. As will be seen, the 10-coefficient equation was good enough to represent all data points of this work. In order to compare the results from the different equations, 6 and 10-coefficient equations were chosen and the experimental data were treated according to these two equations.

The final forms of the two equations are,

$$P = \rho T \{ R + (a_1 - a_2/T - a_3/T^2)\rho + (a_4 + a_5/T)\rho^2 + a_6\rho^3 \} \qquad (3\text{-}3\text{-}3)$$

and

$$P = \rho T \{ R + (a_1 - a_2/T - a_3/T^2 - a_4/T^3)\rho + (a_5 + a_6/T + a_7/T^2)\rho^2 + (a_8 + a_9/T)\rho^3 + a_{10}\rho^4 \} \qquad (3\text{-}3\text{-}4)$$

As is shown in section (3-4) the least-squares procedure requires the first approximation to the values of the M-least-squares parameters and the convergence of the least-squares procedure depends on the "goodness" of these first supplied values. In the case of the virial equation the first approximate values were taken from the published virial equation data for ethylene down to $-10^{\circ}C$[16,26,27] and the values at below $-10^{\circ}C$ were estimated by the extrapolation

from above values. For the mixtures the values were approximated from the equation,

$$B_{mix.} = x_1 B_1 + x_2 B_2 \qquad (3\text{-}3\text{-}5)$$

where x_1, x_2 = compositions of each component

B_1, B_2 = 2nd virial coefficients of each component.

These measures were proved to be adequate for supplying the approximate values of the least-squares parameter. In the case of the modified Bender equations, however, neither the orders of magnitude of the first few dominant coefficients nor their signs were known. Also, the least-squares computer programme would not converge with arbitrary values. We defer until section 3-5 the method used to obtain those first approximations.

3-3-1 The Non-Linear Least-Squares Procedure for Virial Equation

The virial equation deals with the data points from each isothermal run, one at a time, thus the data to be treated are temperature T and a series of pressures. The model equation of state for these data is

$$Z_j = \frac{P_j}{RT\rho_j} = 1 + a_1\rho_j + a_2\rho_j^2 + \cdots a_k\rho_j^k + \cdots a_m\rho_j^m \qquad (3\text{-}3\text{-}6)$$

where j goes from 1 to n which is the number of data points in a Burnett run at temperature T. First approximate values are assigned to the coefficients a_1, a_2, $\cdots a_k$, $\cdots a_m$, which are m least-squares parameter and the implicit function ρ_j, and hence Z_j, are solved by an iterative procedure from j = 1 to j = n.

The two volumes V_A and V_B were calculated from the measured dimensions of the vessels and having fixed the volume V_B, V_A was taken as the M'th least-squares parameter (M = m + 1). This is equivalent to taking $(V_A + V_B)/V_A$, or N, as the M'th parameter.

The object function to be minimized is

$$S = \sum_{j=1}^{n} \omega_j R_j^2 \qquad (3\text{-}3\text{-}7)$$

The residuals, R_j's, were already defined as functions of the observed dependent and independent variables as well as functions of the least-squares parameters,

$$R_j = f(Y_j, X_j, a_1, a_2, \cdots a_k, \cdots a_m) \qquad (3\text{-}3\text{-}8)$$

For the 'isothermal' Burnett apparatus, R_j was derived as,

$$R_j = \frac{P_{j-1}}{P_j} - N \frac{Z_{j-1}}{Z_i} \qquad (3\text{-}3\text{-}9)$$

In the case of the 'non-isothermal' Burnett apparatus the two vessels are at different temperatures and there normally are 'dead spaces' between the two vessels, hence the objective function cannot be expressed as equation (3-3-9). As will be shown in section (3-4) the objective function in this work was formulated in terms of the number of moles of the gas, in which the gas in the dead spaces was taken acount into the calculation of the residuals R_j's. This alteration of the 'form' of the residual R_j in Eq.(3-3-9), however, does not alter the definition of the residual in a physical sense, since the amount of material in each part of the apparatus was calculated from the observed dependent (P) and independent

variable (T) using the equation of condition (3-3-6) as described in section (3-2-2), Eq.(3-2-14).

The actual formulation of the residual for the non-isothermal apparatus will be shown in section (3-4).

Now the objective function, S, is to be minimized with respect to each of the M least-squares parameters,

$$\frac{\partial S}{\partial a_k} = 0 \qquad (3\text{-}3\text{-}10)$$

for k = 1, 2, · · k, · · m, M.

By substituting Eq.(3-3-7) into (3-3-10)

$$\frac{\partial}{\partial a_k}\left[\sum_{j=1}^{n} \omega_j R_j^2\right] = 2\sum_{j=1}^{n} \omega_j R_j \left(\frac{\partial R_j}{\partial a_k}\right) = 0 \qquad (3\text{-}3\text{-}11)$$

or

$$\sum_{j=1}^{n} \omega_j R_j \left(\frac{\partial R_j}{\partial a_k}\right) = 0 \qquad (3\text{-}3\text{-}12)$$

for k = 1, 2, · · · m, M.

This set of M equations are known as the normal equations and they are non-linear in the parameters. The non-linear normal equation (3-3-12) can be linearized by means of the Gauss-Newton method of linearization. In this method it is assumed that there exist the approximate values of the parameters, a_k', such that

$$a_k' = a_k + \Delta a_k \qquad (3\text{-}3\text{-}13)$$

The residual, R_j, may be expanded as a Taylor series about its value when S is a minimum,

$$R_j'(a_1', a_2' \cdots a_k' \cdots a_M') = R_j(a_1, a_2, \cdots a_k, \cdots a_M) + \left(\Delta a_1 \frac{\partial}{\partial a_1} + \Delta a_2 \frac{\partial}{\partial a_2} + \cdots \right.$$

$$\left. \Delta a_M \frac{\partial}{\partial a_M}\right) R_j + \frac{1}{2!}\left(\Delta a_1 \frac{\partial}{\partial a_1} + \Delta a_2 \frac{\partial}{\partial a_2} + \cdots \Delta a_M \frac{\partial}{\partial a_M}\right)^2 R_j + \cdots \qquad (3\text{-}3\text{-}14)$$

By assuming Δa_k be small enough so that the terms higher than the first derivatives in Eq.(3-3-14) may be neglected.

$$R_j'(a_1', a_2', \cdots a_k', \cdots a_M') = R_j(a_1, a_2, \cdots a_k, \cdots a_M) + \Delta a_1 \frac{\partial R_j}{\partial a_1} + \Delta a_2 \frac{\partial R_j}{\partial a_2} + \cdots \Delta a_M \frac{\partial R_j}{\partial a_M} \quad (3\text{-}3\text{-}15)$$

or by rearranging Eq.(3-3-15),

$$R_j(a_1, a_2, \cdots a_k, \cdots a_M) = R_j'(a_1', a_2', \cdots a_k', \cdots a_M') - \left\{ \Delta a_1 \left(\frac{\partial R_j}{\partial a_1}\right) + \Delta a_2 \left(\frac{\partial R_j}{\partial a_2}\right) + \cdots \Delta a_M \left(\frac{\partial R_j}{\partial a_M}\right) \right\} \quad (3\text{-}3\text{-}16)$$

This residual, which is now expressed in terms of the approximate values, a_k', is substituted into Eq.(3-3-12),

$$\sum_{j=1}^{n} w_j \left(\frac{\partial R_j}{\partial a_k}\right) \left\{ R_j'(a_1', a_2', \cdots a_k', \cdots a_M') - \left(\Delta a_1 \frac{\partial R_j}{\partial a_1} + \Delta a_2 \frac{\partial R_j}{\partial a_2} + \cdots \Delta a_M \frac{\partial R_j}{\partial a_M}\right) \right\} = 0 \quad (3\text{-}3\text{-}17)$$

Hence,

$$\Delta a_1 \sum_{j=1}^{n} w_j \left(\frac{\partial R_j}{\partial a_k}\right)\left(\frac{\partial R_j}{\partial a_1}\right) + \Delta a_2 \sum_{j=1}^{n} w_j \left(\frac{\partial R_j}{\partial a_k}\right)\left(\frac{\partial R_j}{\partial a_2}\right) + \cdots \Delta a_M \sum_{j=1}^{n} w_j \left(\frac{\partial R_j}{\partial a_k}\right)\left(\frac{\partial R_j}{\partial a_M}\right) = \sum_{j=1}^{n} w_j \left(\frac{\partial R_j}{\partial a_k}\right) R_j'(a_1', a_2', \cdots a_k', \cdots a_M') \quad (3\text{-}3\text{-}18)$$

for k = 1, 2, · · M.

These are the linearized normal equations. In order to solve the unknowns, $\Delta a_1, \Delta a_2, \cdots \Delta a_M$, from the M simultaneous equations (3-3-18) the following were calculated first:

(i) The approximated residual, R_j', was calculated basically from the Eq.(3-3-9) together with the equation of condition (3-3-6) using a_k' instead of a_k.

As was mentioned previously actual formulation of the residual for the non-isothermal apparatus will be deferred until section (3-4).

(ii) ω_j ; the weighting factors.

The weighting factor for each residual is given by the reciprocal of its expected variance,

$$\omega_j = \frac{1}{\sigma_{R_j}^2} \qquad (3\text{-}3\text{-}19)$$

$$\sigma_{R_j}^2 = \left(\frac{\partial R_j}{\partial P_{j-1}}\right)^2 \sigma_{P_{j-1}}^2 + \left(\frac{\partial R_j}{\partial P_j}\right)^2 \sigma_{P_j}^2 \qquad (3\text{-}3\text{-}20)$$

The expected variance in P_j is given by

$$\sigma_{P_j}^2 = \varepsilon^2 + \gamma^2 P_j^2 \qquad (3\text{-}3\text{-}21)$$

From the error analysis of experimental pressure in Chapter two eta and gamma in Eq.(3-3-21) were assigned as[5]

$\varepsilon = 0.69 \cdot 10^{-4}$ bar and $\gamma = 0.1 \cdot 10^{-4}$ respectively.

The partial derivatives $(\partial R_j / \partial P_{j-1})$ and $(\partial R_j / \partial P_j)$ were determined by straightforward partial differentiation.

(iii) $(\partial R_j / \partial a_k)$; The calculation of the partial derivatives in Eq.(3-3-18) is in principle impossible without knowing true residual R_j. Thus the derivatives $(\partial R_j' / \partial a_k')$ were calculated and used as approximations to $(\partial R_j / \partial a_k)$. This approximation, however, is exact at the convergence point, that is, when $\Delta a_k = 0$.

Having calculated all the elements in Eq.(3-3-18) the M unknowns are solved by following fashion.

In matrix notation, Eq.(3-3-18) are

$$\underline{X}\ \underline{\Delta a} = \underline{Y} \qquad (3\text{-}3\text{-}22)$$

where

$$\underline{X} = \begin{pmatrix} \sum_j w_j \left(\frac{\partial R_j}{\partial a_1}\right)\left(\frac{\partial R_j}{\partial a_1}\right), & \sum w_j \left(\frac{\partial R_j}{\partial a_1}\right)\left(\frac{\partial R_j}{\partial a_2}\right), & \cdots & \sum w_j \left(\frac{\partial R_j}{\partial a_1}\right)\left(\frac{\partial R_j}{\partial a_M}\right) \\ \sum w_j \left(\frac{\partial R_j}{\partial a_2}\right)\left(\frac{\partial R_j}{\partial a_1}\right), & \sum w_j \left(\frac{\partial R_j}{\partial a_2}\right)\left(\frac{\partial R_j}{\partial a_2}\right), & \cdots & \sum w_j \left(\frac{\partial R_j}{\partial a_2}\right)\left(\frac{\partial R_j}{\partial a_M}\right) \\ \cdot & \cdot & \cdot & \cdot \\ \sum w_j \left(\frac{\partial R_j}{\partial a_M}\right)\left(\frac{\partial R_j}{\partial a_1}\right), & \sum w_j \left(\frac{\partial R_j}{\partial a_M}\right)\left(\frac{\partial R_j}{\partial a_2}\right), & \cdots & \sum w_j \left(\frac{\partial R_j}{\partial a_M}\right)\left(\frac{\partial R_j}{\partial a_M}\right) \end{pmatrix}$$

thus $\underline{X}$ is a (M x M) square symmetric matrix,

$$\underline{Y} = \begin{pmatrix} \sum w_j \left(\frac{\partial R_j}{\partial a_1}\right) R_j'(a_1', a_2', \cdots a_M') \\ \sum w_j \left(\frac{\partial R_j}{\partial a_2}\right) R_j'(a_1', a_2', \cdots a_M') \\ \cdot \\ \sum w_j \left(\frac{\partial R_j}{\partial a_M}\right) R_j'(a_1', a_2', \cdots a_M') \end{pmatrix}$$

and

$$\underline{\Delta a} = \begin{pmatrix} \Delta a_1 \\ \Delta a_2 \\ \vdots \\ \Delta a_M \end{pmatrix}$$

By multiplying both sides of Eq.(3-3-22) by the inverse matrix of $\underline{X}$,

$$\underline{X}^{-1} \cdot \underline{X} \cdot \underline{\Delta a} = \underline{X}^{-1} \cdot \underline{Y} \qquad (3\text{-}3\text{-}23)$$

hence

$$\underline{\Delta a} = \underline{X}^{-1} \cdot \underline{Y} \qquad (3\text{-}3\text{-}24)$$

Eq.(3-3-24) is the solution to Eq.(3-3-22). After having calculated the solution of Eq.(3-3-24) the new approximation to a_k is given by,

$$a_k = a_k' - \Delta a_k \qquad (3\text{-}3\text{-}25)$$

These new values of a_k are used in the calculation of R_j'

in Eq.(3-3-14) and the solution of the normal equations (3-3-22). The iteration was continued until all the Δa_k have converged to predetermined accuracies of each parameters.

The variances and covariances of the parameters are given, approximately, by

$$\sigma_{k,l}^2 = \sigma^2 \cdot \chi_{k,l} \qquad (3\text{-}3\text{-}26)$$

where $x_{k,l}$ is the element of k'th row and l'th column of the inverse matrix $\underline{X}^{-1}$ and σ^2 is the variance of the data, an estimate of which is

$$\sigma^2 = \frac{\sum w_j R_j^2}{n-M} \qquad (3\text{-}3\text{-}27)$$

Thus the variance of the k'th parameter is

$$\sigma_k^2 = \frac{\sum w_j R_j^2}{n-M} \cdot \chi_{k,k} \qquad (3\text{-}3\text{-}28)$$

It has been shown by Barieau and Dalton[34] that, except for models with a high degree of non-linearity in the parameters, Eq.(3-3-28) is a very good approximation to the variance of the k'th parameter. However the presence of systematic error can lead to misleadingly small values of a_k.[1] For this reason the errors in a_k (in this case the a_k's are the 2nd and 3rd virial coefficients) were estimated from their relative values which were determined from different number of data point in one run (see section 3-5-3).

3-3-2 The Non-Linear Least-Squares Procedure for the Bender Equation

As was mentioned previously the basic difference between the virial equation and Bender equation is that in Bender equation the compressibility factor is expressed in terms of temperature and density, while in the virial equation the compressibility factor is expressed as a function of density only. Therefore in the case of Bender equation all data points from different isothermal Burnett runs can be treated as a whole.

The principle of least-squares procedure, however, is exactly same as in the case of the virial equation except for the mathematical notations, in pressure, P_{ij}, residuals, R_{ij}, and weighting factors, W_{ij}, etc. which now have double-subscripts; i stands for the different Burnett run and j, as in the case of virial equation, stands for individual data point in the i'th run.

In section (3-3) two modified Bender equations were given in Eq.(3-3-3) and (3-3-4) which have 6 and 10 coefficients respectively,

$$P_{ij} = \rho_{ij} T_i \left\{ R + (a_1 - a_2/T_i - a_3/T_i^2)\rho_{ij} + (a_4 + a_5/T_i)\rho_{ij}^2 + a_6 \rho_{ij}^3 \right\} \qquad (3\text{-}3\text{-}3)$$

$$P_{ij} = \rho_{ij} T_i \left\{ R + (a_1 - a_2/T_i - a_3/T_i^2 - a_4/T_i^3)\rho_{ij} + (a_5 + a_6/T_i + a_7/T_i^2)\rho_{ij}^2 + (a_8 + a_9/T_{ij})\rho_{ij}^3 + a_{10}\rho_{ij}^4 \right\} \qquad (3\text{-}3\text{-}4)$$

The objective function, S, to be minimized is,

$$S = \sum_{i}^{n} \sum_{j}^{n_i} w_{ij} R_{ij}^2 \qquad (3\text{-}3\text{-}29)$$

where n is the number of the isothermal Burnett run and n_i is the number of expansion in i'th run. The residuals, R_{ij}, are functions of the observed dependent and independent variables and m least-squares parameters.

$$R_{ij} = f\,(Y_{ij},\ X_{ij},\ a_1,\ a_2,\ \cdots\ a_m) \qquad (3\text{-}3\text{-}30)$$

For the 'isothermal apparatus', R_{ij} is

$$R_{ij} = \frac{P_{ij-1}}{P_{ij}} - N_i \frac{Z_{ij-1}}{Z_{ij}} \qquad (3\text{-}3\text{-}31)$$

Actual formulation of the residual, R_{ij}, for the 'non-isothermal apparatus' will be shown in section (3-4-2).

The equation of condition are the equation of state (3-3-3) for 6 coefficients and (3-3-4) for 10 coefficients. As shown in Eq.(3-3-31) the apparatus constant for i'th run N_i is independent of any data of non-i'th run. Thus M least-squares parameters for Bender equation are $a_1, a_2, \cdots a_m, N_1, N_2, \cdots N_n$ (M=m+n), where m is the number of parameters of the equations of state (either 6 or 10) and n is the number of isothermal Burnett runs.

Now the objective function, S, is to be minimized with respect to each of the M least-squares parameters,

$$\frac{\partial S}{\partial a_k} = 0 \qquad (3\text{-}3\text{-}32)$$

for k=1,2, $\cdots$ m,(m+1),(m+2), $\cdots$ M

$$\frac{\partial}{\partial a_k}\left[\sum_i^n \sum_j^{n_i} w_{ij} R_{ij}^2\right] = 2 \sum_i^n \sum_j^{n_i} w_{ij} R_{ij} \frac{\partial R_{ij}}{\partial a_k} = 0 \qquad (3\text{-}3\text{-}33)$$

or

$$\sum_{i}^{n}\sum_{j}^{M} w_{ij} R_{ij} \left(\frac{\partial R_{ij}}{\partial a_k}\right) = 0 \qquad (3\text{-}3\text{-}34)$$

for k=1,2, · · M

This set of M equations is equivalent to Eq.(3-3-12) and these too are non-linear in the parameters. Thus Eq.(3-3-34) was normalized by means of Gauss-Newton method and in matrix notation,

$$\underline{X} \cdot \underline{\Delta a} = \underline{Y} \qquad (3\text{-}3\text{-}35)$$

Eq.(3-3-35) is same as Eq.(3-3-22) except for the double summation in each element of $\underline{X}$ and $\underline{Y}$ instead of one as in the case of Eq.(3-3-22). Thus an element of k'th row and l'th column of matrix $\underline{X}$ is now,

$$(\chi_{kl}) = \sum_{i}\sum_{j} w_{ij} \left(\frac{\partial R_{ij}}{\partial a_k}\right)\left(\frac{\partial R_{ij}}{\partial a_l}\right) \qquad (3\text{-}3\text{-}36)$$

The calculation of R_{ij} and W_{ij} are exactly same as those in the previous section. In calculation of the derivatives, $\frac{\partial R_{ij}}{\partial a_k}$, however, they are divided into two groups, i.e. the derivatives with respect to the parameters of the eqation ($k \leq m$) and the derivatives with respect to the apparatus constants $N_1, N_2, \cdots N_n$ ($k > m$). In the latter case the derivatives, $\frac{\partial R_{ij}}{\partial a_k}$, were set to zero for $i \neq k - m$, since, as mentioned earlier in this section, the apparatus constant N_i is independent of non-i'th run.

Thus the (MxM) square symmetric matrix $\underline{X}$ in Eq.(3-3-35) is, in fact,

$$\underline{X} = \begin{pmatrix} x_{11} & \cdots & x_{1m} & \cdots & x_{1M} \\ \vdots & & \vdots & & \vdots \\ x_{m1} & \cdots & x_{mm} & \cdots & x_{mM} \\ \vdots & & \vdots & \diagdown\,0 & \\ x_{M1} & \cdots & x_{Mm} & 0\,\diagdown & x_{MM} \end{pmatrix}$$

where all the elements, $x_{k,l}$, in the two triangles are zeros.

3-4 Treatment of Experimental Data for the Non-Isothermal Burnett Apparatus

In the previous sections the objective function was set up on several assumptions, i.e.

(i) the Burnett apparatus was isothermal ($T_A = T_B$),

(ii) there were no dead-spaces between the two pressure vessels,

(iii) both volumes, V_A and V_B, were independent of pressure,

(iv) after expansion the pressures in both vessels were absolutely identical.

In the case of 'real' non-isothermal Burnett apparatus, however, following factors must be encountered in calculating the objective function, i.e.

(i) the expansion vessel is at temperature T^o (0^oC) with compressibility factor $Z(6)_j$,

(ii) the gas in the dead space,

(iii) pressure dependence of the volume of the vessel,

(iv) pressure differences in each part of the apparatus due to the hydraulic head of gas.

For these reasons the objective function was calculated in terms of the quantity of the gas by equating number of moles before and after the j'th expansion. This, however, does not change the physical meaning of the objective function, Eq.(3-2-14), since the calculation of the number of moles of the gas was based on the equation of conditions of the objective function. (see sections 3-3-1 and 3-3-2).

As was mentioned in Chapter Two, the apparatus was divided into 8 sections of volumes, V_1 to V_8, and shown in Fig 2-15. ($V_1=V_A$ and $V_6=V_B$ in previous notation). With reference to Fig 2-15 each subscripted number refers to the particular part of the apparatus. The final form of the residual at j'th expansion was chosen as,

$$R_j = \frac{PZMOL(j-1) - \{PZMOL(j) + EVMOL(j)\}}{EVMOL(j)} \qquad (3-4-1)$$

where PZMOL is number of moles in piezometer (V_1) and in the dead spaces upto the expansion valve and EVMOL is number of moles in the expansion vessel (V_6) and in the dead spaces upto the expansion valve. (j - 1) refers to the gas before j'th expansion and (j) refers to the gas after j'th expansion. Actual formulation of the residual (3-4-1) for the cases of virial equation and the modified Bender equations will be described in sections (3-4-1) and (3-4-2) respectively.

3-4-1 Calculation of the Residual from the Virial Equation

With reference to Fig 2-15 and Eq.(3-4-1) the residual, R_j, can be written as,

$$R_j = \frac{(n_1 + n_1')_{j-1} - (n_1 + n_1' + n_t + n_t')_j}{(n_t + n_t')_j} \qquad (3\text{-}4\text{-}2)$$

where n_1, n_6 = no. of moles in both vessels V_1 and V_6

$n_1' = n_2 + n_3 + n_7 + n_8$

$n_6' = n_4 + n_5$

The amount of gas in each part of the apparatus was calculated as following

(i) n_1

$$n_1(j) = \left(\frac{PV}{RTZ}\right)_{1,j} \qquad (3\text{-}4\text{-}3)$$

and

$$Z_{1,j} = \left(\frac{P}{RT\rho}\right)_{1,j} = 1 + a_1\rho_{1,j} + a_2\rho_{1,j}^2 + \cdots a_m\rho_{1,j}^m \qquad (3\text{-}4\text{-}4)$$

where $a_1, a_2, \cdots a_m$ are the m least-squares parameters.

(ii) n_6

$$n_6(j) = \left(\frac{PV}{RTZ}\right)_{6,j} \qquad (3\text{-}4\text{-}5)$$

and

$$Z_{6,j} = \left(\frac{P}{RT\rho}\right)_{6,j} = 1 + a_1\rho_{6j} + a_2\rho_{6j}^2 + \cdots a_m\rho_{6j}^m \qquad (3\text{-}4\text{-}6)$$

where T_{6j} = constant = 273.15

and a_1, a_2, etc. are the virial coefficients of the gas at 0°C. They are supplied in the computer programme and are

not subject to change in the least-squares procedure. Thus after treatment of all the 'isotherms', the virial coefficients were plotted against temperature so that the values at $0^{o}C$ could be readjusted. The data were then retreated using these new values at $0^{o}C$ until they were internally consistent.

(iii) n_3, n_4 and n_8

In the dead spaces V_3, V_4 and V_8 the temperatures were assumed to be constant and the no. of moles were calculated from the equations corresponding to Eq.(3-4-5) and (3-4-6).

(iv) n_5 and n_7

Although there were temperature gradients in V_5 and V_7 the volumes were very small and the temperature differences were not very wide. Thus the temperature gradients in these regions were assumed to be linear and their 'effective' temperatures, T_5 and T_7, were taken as the mean values of the temperatures at their extreme ends,

e.g. $T_5 = (T_4 + T_6)/2$ and $T_7 = (T_3 + T_8)/2$.

Using these temperatures the no. of moles were calculated in the same way as in (ii).

(v) n_2

As was mentioned in Chapter Two there existed a temperature gradient along the inlet tubing. 11 copper-constantan thermocouples at 3-cm interval were used to measure the e.m.f.'s which were converted to temperatures by means of a polynomial fitting to the relevant calibration curve. The no. of moles of the gas between k'th and (k+1)'th thermocouples was calculated by assuming linear gradients in temperature and compressibility factor between the thermocouples.

Consider two adjacent thermocouples k and (k+1), separated by a distance l (Fig 3-4). Then the number of moles of gas in dx at a distance x from thermocouple k is given by,

$$dn = \frac{P_k A\, dx}{R\, T_x Z_x} \qquad (3\text{-}4\text{-}7)$$

where A = cross-sectional area of the inlet tubing.

$$T_x = (T_{k+1} - T_k)\frac{x}{l} \qquad (3\text{-}4\text{-}8)$$

$$Z_x = (Z_{k+1} - Z_k)\frac{x}{l} \qquad (3\text{-}4\text{-}9)$$

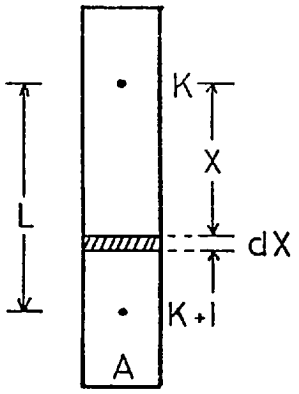


FIG 3-4

Integrating equation (3-4-7),

$$\int_0^{n_k} dn = \int_0^{l} \frac{P_k A\, dx}{R\{T_k + \frac{x}{l}(T_{k+1} - T_k)\}\{Z_k + \frac{x}{l}(Z_{k+1} - Z_k)\}} \qquad (3\text{-}4\text{-}10)$$

or

$$n_k = \frac{P_k A l}{R(Z_{k+1} \cdot T_k - T_{k+1} Z_k)} \ln \frac{T_k Z_{k+1}}{Z_k T_{k+1}} \qquad (3\text{-}4\text{-}11)$$

Thus

$$n_L = \sum_k n_k \qquad (3\text{-}4\text{-}12)$$

The pressure gradient between k and k+1 is given by,

$$\Delta P_k = \rho g l \qquad (3\text{-}4\text{-}13)$$

where

$$\rho = \frac{n_k M}{A l} \qquad (3\text{-}4\text{-}14)$$

Substituting Eq.(3-4-11) and (3-4-13) into (3-4-14),

$$\Delta P_k = \frac{P_k g M \ell}{R(Z_{k+1}T_k - T_{k+1}Z_k)} \ln \frac{T_k Z_{k+1}}{Z_k T_{k+1}} \qquad (3\text{-}4\text{-}15)$$

Eq.(3-4-15) was used to calculate the pressure gradient between a pair of thermocouples due to gravitational effect.

3-4-2 Calculation of the Residual from the Bender Equation

In this case the residuals, R_{ij}, can be written as,

$$R_{ij} = \frac{(n_1 + n_1')_{ij-1} - (n_1 + n_1' + n_6 + n_6')_{ij}}{(n_6 + n_6')_{ij}} \qquad (3\text{-}4\text{-}16)$$

Eq.(3-4-16) is equivalent to Eq.(3-4-2) and the notation used are same as in Eq.(3-4-2) except for the extra subscript i which stands for the i'th isotherm.

The basic difference between the two Eq.(3-4-2) and (3-4-16) is that n_1 and n_6 in Eq.(3-4-16) were evaluated from the same equation whose coefficients were the least-squares parameters, while n_6 in Eq.(3-4-2) was evaluated from the fixed coefficients of the equation of state.

Thus n_1 and n_6 in Eq.(3-4-16) were calculated from

$$n_1(i,j) = \rho_1(i,j) \cdot V_1(i,j) \qquad (3\text{-}4\text{-}17)$$

$$n_6(i,j) = \rho_6(i,j) \cdot V_6(i,j) \qquad (3\text{-}4\text{-}18)$$

The densities, ρ_1 and ρ_6, were calculated by an iterative method from the modified Bender equations, for example,

$$P = \rho T \{ R + (a_1 - a_2/T - a_3/T^2)\rho + (a_4 + a_5/T)\rho^2 + a_6\rho^3 \} \qquad (3\text{-}4\text{-}19)$$

The number of moles in the dead spaces between the

two vessels were calculated as in the previous section using equations corresponding to (3-4-5) and (3-4-6). The number of moles in the inlet-tubing were calculated from Eq.(3-4-11) and the pressure gradients from Eq.(3-4-15) (see section 3-4-1).

3-5 The Computation and the Results

3-5-1 Introduction

The computer programs were written in FORTRAN IV language for use on the Imperial College CDC 6400 and CYBER-73 computers. There were two separate main progrms (one for the virial equation and the other for the modified Bender equations), together with their relevant SUBROUTINE's. The main programs consisted of two parts, i.e. in the first part of the program all the necessary data for the least-squares procedure were calculated from the experimental measurements before iteration started, and in the second part of the program actual least-squares procedure was carried out. In this respect the two programs are the same in principle, and thus both programs are described in one flow-chart together with their SUBROUTINE's in Fig (3-5). As was mentioned in section (3-3) in both cases first approximated values of the least-squares parameters must be supplied before the iteration commences. In the case of the coefficients of the virial equation reasonably accurate values of the coefficients were calculated from the published P-V-T data (see section 3-3).

In the case of the modified Bender equations no information was available as to the values of these coefficients. Thus the first approximate values of the coefficients were determined

from the experimental pressures and temperatures together with the densities which had been determined previously from the virial equation by the least-squares procedures for all the Burnett isotherms. Thus from N points of data a set of N equations were established according to the equation chosen, for example,

$$P_k = \rho_k T_k \{ R + (a_1 - a_2/T_k - a_3/T_k^2) \rho_k + (a_4 + a_5/T_k) \rho_k^2 + a_6 \rho_k^3 \} \qquad (3\text{-}5\text{-}1)$$

for $k = 1, 2, \cdots N$ (for N is greater than 6)

or

$$\left(\frac{P_1}{\rho_1 T_1 R} - 1 \right) \frac{R}{\rho_1} = a_1 - \frac{a_2}{T_1} - \frac{a_3}{T_1^2} + a_4 \rho_1 + a_5 \frac{\rho_1}{T_1} + a_6 \rho_1^2 \qquad (3\text{-}5\text{-}2)$$

$$\vdots \qquad\qquad \vdots$$

$$\left(\frac{P_N}{\rho_N T_N R} - 1 \right) \frac{R}{\rho_N} = a_1 - \frac{a_2}{T_N} - \frac{a_3}{T_N^2} + a_4 \rho_N + a_5 \frac{\rho_N}{T_N} + a_6 \rho_N^2$$

Eq.(3-5-2) can be written in matrix notation,

$$\begin{vmatrix} 1 & -1/T_1 & -1/T_1^2 & \rho_1 & \rho_1/T_1 \\ 1 & -1/T_2 & -1/T_2^2 & \rho_2 & \rho_2/T_2 \\ & & \vdots & & \\ 1 & -1/T_N & -1/T_N^2 & \rho_N & \rho_N/T_N \end{vmatrix} \cdot \begin{vmatrix} a_1 \\ a_2 \\ \vdots \\ a_6 \end{vmatrix} = \begin{vmatrix} (Z_1 - 1) \frac{R}{\rho_1} \\ (Z_2 - 1) \frac{R}{\rho_2} \\ \vdots \\ (Z_N - 1) \frac{R}{\rho_N} \end{vmatrix} \qquad (3\text{-}5\text{-}3)$$

or

$$\underline{X} \cdot \underline{A} = \underline{Y} \qquad (3\text{-}5\text{-}4)$$

where $\underline{X}$ is a (N x 6) matrix and both $\underline{A}$ and $\underline{Y}$ are column matrices.

By assuming that all the P-ρ-T data in the matrices $\underline{X}$ and $\underline{Y}$ were 'exact', the least squares solution of $\underline{A}$ in Eq.(3-5-4) is straightforward;

$$\underline{X}^T \cdot \underline{X} \cdot \underline{A} = \underline{X}^T \cdot \underline{Y} \qquad (3\text{-}5\text{-}5)$$

where $\underline{X}^T$ = transpose of matrix $\underline{X}$, thus $(\underline{X}^T \cdot \underline{X})$ becomes a (6x6) square matrix.

From Eq.(3-5-5)

$$(\underline{X}^T \cdot \underline{X})^{-1} \cdot (\underline{X}^T \cdot \underline{X}) \cdot \underline{A} = (\underline{X}^T \cdot \underline{X})^{-1} \cdot \underline{X} \cdot \underline{Y} \qquad (3\text{-}5\text{-}6)$$

or

$$\underline{A} = (\underline{X}^T \cdot \underline{X})^{-1} \cdot \underline{X} \cdot \underline{Y} \qquad (3\text{-}5\text{-}7)$$

where $(\underline{X}^T \cdot \underline{X})^{-1}$ is an inverse matrix of $(\underline{X}^T \cdot \underline{X})$.

The column matrix $\underline{A}$ was solved (for which a computer program was written) and the a's were supplied as the first approximate values of the least-squares parameters.

For 9 and 10 coefficients same method was used for their first approximate values. In Fig 3-5 a flow chart for both main programs is shown in connection with their relevant SUBROUTINE's at various parts of the main programs. The routines are described in section (3-5-2). In section (3-5-3) the computed results are listed for both the virial equation and the modified Bender equations.

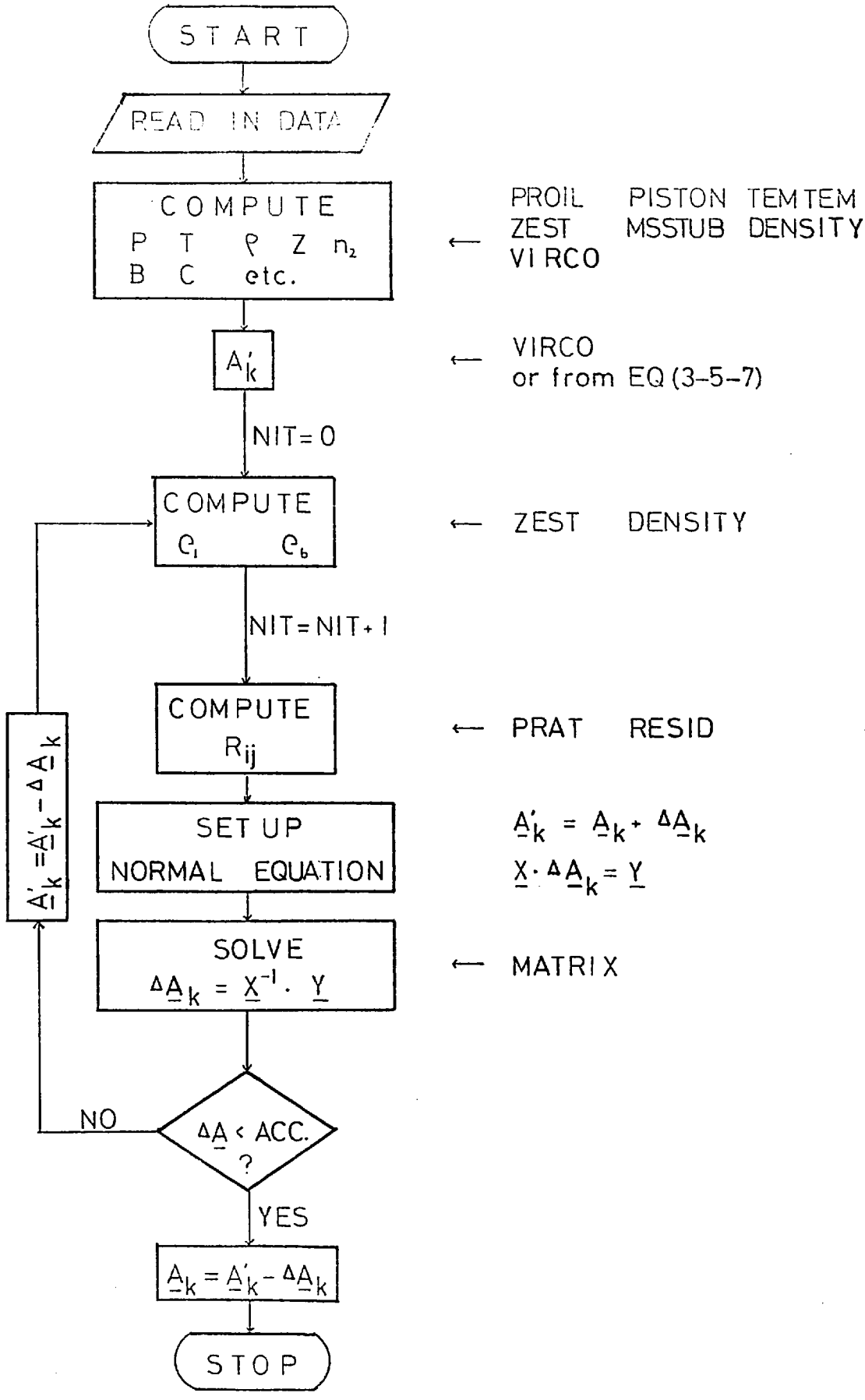
3-5-2 Description of Computer Program

As is shown in the flow-chart (Fig 3-5) the following subroutines were called in the main programs before the start of the actual least-squares procedure.

(i) PROIL

The experimental pressures were calculated as described in chapter two, the hydraulic heads of the gas between the D.P.C. (or the gas piston gauge) and the pressure vessels were

FIG 3-5 FLOW CHART & SUBROUTINES



taken account into the final values at both vessels. This subroutine was written for the calculations of the pressure sequence of each isotherm, P_j, thus the pressures were dimensioned in a single array.

(ii) PISTON

SUBROUTINE PROIL was modified such that by calling PISTON once this routine calculated the pressures, P_{ij}, for all i's and j's, thus dimensioned in a double array.

(iii) TEMTEM

In the main program the resistances across the platinum resistance thermometer was calculated from the voltages across the thermometer and the standard resistor measured by means of a potentiometer. By calling TEMTEM the resistance was converted to the temperature from a solution of the Callender-van-Dusen equation by means of a Newton-Raphson iteration method. This temperature was then converted to the IPTS68 scale as described in sections (2-7-2) and (2-7-3).

(iv) VIRCO

In the case of the virial equation this routine not only supplies the virial coefficients for the ice bath and dead spaces for use in calculation of $(Z2)_j - (Z8)_j$, but also provides the first trial values of the least-squares parameters at temperature T. In the case of the Bender equations, however, this routine was called only for the virial coefficients of the gas in the dead spaces.

(v) ZEST

The compressibility factor at temperature T and pressure P is calculated from the solution of

$$Z = \frac{P}{\rho R T} = 1 + a_1 \rho + a_2 \rho^2 + \cdots a_m \rho^m \qquad (3\text{-}5\text{-}8)$$

The iterative solution of this equation was obtained by Newton-Raphson method.

(vi) DENSITY

This routine is for the calculation of density from the modified Bender equation, (thus equivalent to SUBROUTINE ZEST) by means of Newton-Raphson method.

(vii) MSSTUB

This routine calculates the number of moles of gas in the inlet tube by means of Eq.(3-4-11) and at the same time it evaluates the pressure gradient along the inlet tube by means of Eq.(3-4-15). The compressibility, Z_k, at thermocouple k was calculated by first calling VIRCO for temperature T_k and calling ZEST for temperature T_k and pressure P_k.

Thus having all of the information assembled, the non-linear least-squares procedures, as described in sections (3-3) and (3-4), commenced.

As shown in the flow-chart the residuals were calculated by calling PRAT (For virial equation) or RESID (for Bender equation). These two routines are identical except for the equation of states used in the routines. For the first calling of PRAT (or RESID) only the weighting factors, W_j (or W_{ij}), were calculated according to equations (3-3-19), (3-3-20) and (3-3-21), setting $\gamma = 10^{-5}$ and $\varepsilon = 6.8 \cdot 10^{-4}$ bar. The derivatives, $\frac{\partial \rho_j}{\partial a_k}$, were determined numerically by changing each value of a_k by 0.001% in turn and recalling ZEST (or DENSITY) and PRAT (or RESID). The normal equations were then solved by calling MATRIX, which solves a set of simultaneous

linear equations (upto 100 equations) by means of a Gauss-Jordan double-pivotal elimination. The calculated Δa_k's by MATRIX were then compared with predetermined values of accuracies, for example $|\Delta a_1| < 10^{-5}$ for the virial equation and $|\Delta a_1| < 10^{-1}$ for Bender equation. When the Δa_k's were larger than the accuracies new approximate values were calculated according to equation (3-3-13) and SUBROUTINE's ZEST (or DENSITY) and PRAT (orRESID) were recalled again.

Thus the iteration continued until the Δa_k's were converged within the ranges of the accuracies required.

3-5-3 The Results

The computational results from the least-squares procedure are listed in this section in Table (3-1) to (3-5). In these tables (v) refers to the virial equation (6) and (10) refer to 6- and 10-coefficient modified Bender equations. Thus, for example, Z(V) is the compressibility factor evaluated from the virial equation. In each table the data are chosen and tabulated in following manner:

(i) Table 3-1

In this table the 6 and 10 coefficients of the modified Bender equations, (3-1-2) and (3-1-3), are listed together with the ranges of the experimental pressure and temperature, from which the coefficients were determined.

(ii) Table 3-2

This table contains the 2nd and 3rd virial coefficients which were evaluated from both methods. In the case of the virial equation the equation used in the least-squares procedure

was a truncated polynomial equation and not the true virial equation which is the infinite power series of density.

Although the problem of relating the coefficients of this truncated series to the corresponding virial coefficients had been considered by some workers,[33,36,37] the treatment was, in order to simplify the statistical analysis, normally based on the assumption that the experimental values of Z were subject to random errors but the values of the density, ρ, were known exactly. In practice, however, it is unlikely for any experimental P-ρ-T data to meet the above condition due

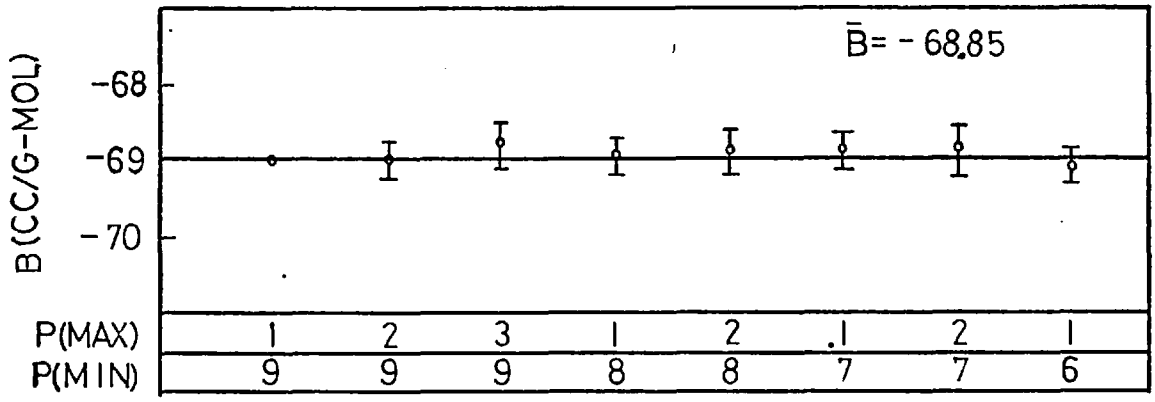


FIG 3-6 MIX.1 RUN 39 (288.8)

to the errors in the density and the presence of the systematic errors in pressure measurement and hence in the values of Z.

For this reason the second and third virial coefficients were chosen from several values which were determined simultaneously from different sets of pressure sequences. That is, in the computer program the non-linear least-squares procedure was in a 'DO' loop such that the least-squares parameters were determined from different sets of pressure sequences, i.e.

$(P_0, P_1, \cdots P_n)$, $(P_1, P_2, \cdots P_n)$ and $(P_1, P_2, \cdots P_{n+1})$ etc. with the equation of state

$$Z = \frac{P}{RT\rho} = 1 + B\rho + C\rho^2 \qquad (3\text{-}5\text{-}9)$$

This process gave several values of a_1 (=B) and a_2 (=C), and the mean values of these a_1 are presented in Table 3-2 as the second virial coefficients. Fig 3-6 shows a typical variation of B together with its calculated standard deviation according to Eq.(3-3-28), for mixture 1 at 288.8°K isotherm.

The evaluation of the virial coefficients from the Bender equation is quite straightforward. As will be discussed in section (3-6) the 10-coefficient Bender equation was chosen as the best equation of state and thus the second and third virial coefficients were evaluated from this Eq.(3-1-3) only.
Eq.(3-1-3) is of the form of

$$P = \rho T (R + C_1\rho + C_2\rho^2 + C_3\rho^3 + C_4\rho^4) \qquad (3\text{-}5\text{-}11)$$

where $C_1 = a_1 - a_2/T - a_3/T^2 - a_4/T^3$

$C_2 = a_5 + a_6/T + a_7/T^2$

$C_3 = a_8 + a_9/T$

$C_4 = a_{10}$

Re-arranging Eq.(3-5-11)

$$\frac{P}{\rho T R} = 1 + \frac{C_1}{R}\rho + \frac{C_2}{R}\rho^2 + \frac{C_3}{R}\rho^3 + \frac{C_4}{R}\rho^4 \qquad (3\text{-}5\text{-}12)$$

or

$$Z = 1 + B\rho + C\rho^2 + D\rho^3 + E\rho^4 \qquad (3\text{-}5\text{-}13)$$

where $B = (a_1 - a_2/T - a_3/T^2 - a_4/T^3) / R \qquad (3\text{-}5\text{-}14)$

$$C = (a_5 + a_6/T + a_7/T^2)/R$$

$$D = (a_8 + a_9/T)/R$$

$$E = a_{10}/T$$

Eq.(3-5-13) can be regarded as a truncated virial equation and thus B and C were calculated according to Eq.(3-5-14) and presented in Table 3-2.

(iii) Table 3-3

This table contains the densities determined from the least-squares procedure by using the virial equation, $f(V)$, and the modified Bender equations, $f(6)$, and $f(10)$.

In both cases the densities were solved by iterative methods.

(iv) Table 3-4

Compressibility factors at all the experimental points were calculated using

$$Z_j = \frac{P_j}{\rho_j T_j R} \qquad (3\text{-}5\text{-}15)$$

where P_j and T_j are the experimental values and ρ_j are the values solved in (iii).

(v) Table 3-5

The 10-coefficient Bender equation was used to calculate the compressibility factors of the experimental gases in the temperature range of 230°K - 295°K at an interval of 5°K and 5 bar - 55 bar at an interval of 2.5 bar. In this table the values inside the box represent the values within the experimental range and the values outside the box are therefore extrapolated ones.

However, as will be shown in section (3-6-8) the comparison between Michels' experimental Z at 298°K and the extrapolation from Eq.(3-1-3) shows that the values in Table 3-5 at 295°K for ethylene are believed to be accurate within 0.001.

3-5-4 The Interactional Second Virial Coefficients of Methane-Ethylene System

The 2nd virial coefficient of a mixture can be written as,(76)

$$B_{mix} = \sum_{i}^{c}\sum_{j}^{c} x_i x_j B_{ij} \qquad (3\text{-}5\text{-}16)$$

or for a binary mixture,

$$B_{mix} = x_1^2 B_{11} + 2x_1 x_2 B_{12} + x_2^2 B_{22} \qquad (3\text{-}5\text{-}17)$$

where x_1, x_2 = mole fractions of components 1 and 2 in the mixture, thus $x_2 = 1 - x_1$.

B_{11}, B_{22} = 2nd virial coefficients of components 1 and 2 at temperature T.

B_{12} = interactional 2nd virial coefficient of a hypothetical substance with intermolecular interactions equal to that of the unlike interactions between components 1 and 2 at temperature T.

As in the cases of B_{11} and B_{22} which are related to the intermolecular forces between like-molecules, B_{12} is related to the potential energy between unlike-molecules. Thus B_{12} is an important source for information on the potential energy between unlike molecules, and therefore, accurate 2nd virial coefficients for mixtures are important.

By rearranging Eq.(3-5-17), B_{12} can be expressed as

$$B_{12} = (B_{mix} - x_1^2 B_1 - x_2^2 B_2)/(2x_1x_2) \qquad (3\text{-}5\text{-}18)$$

In methane-ethylene system of this work, the subscript 1 refers to methane and 2 refers to ethylene. Since there are three mixtures in this work three values of B_{12} can be calculated at a given temperature T using Eq.(3-5-18). The calculated values of B_{12} at T from different mixtures differ from one another since the uncertainties in B_{12} depend on the uncertainties in the values of B_1, B_2, B_{mix} and x_1.

From Table 3-2 the maximum probable errors of 2nd virial coefficients are estimated as follows.

GAS	σ
ethylene	1.6 cc/mole
mixture 1 (0.6955 CH_4)	2.3 "
mixture 2 (0.4518 CH_4)	2.3 "
mixture 3 (0.2419 CH_4)	4.8 "

The uncertainties in B_{12} propagated from the errors in B_{mix} can be expressed as

$$\frac{\partial B_{12}}{\partial B_{mix}} = \frac{1}{2x_1x_2} \qquad \text{or} \qquad \Delta B_{12} \doteq \frac{\Delta B}{2x_1x_2}$$

Thus the maximum error, for example, of B_{12} calculated from mixture 1 is estimated as about 5.4 cc/mole.

B_{12} in Eq.(3.5.18) were calculated from 240 to 300°K with an interval of 5°K. B_{22} (ethylene) and B_{mix} were calculated from Eq.(3-5-14) using the coefficients given in Table (3-1). B_{11} (methane) were calculated from the 20-coefficient Bender equation using coefficients determined by Chapela.[57]

The expected variance of each B_{12} can be expressed as,

$$\sigma_{B_{12}}^2 = \left(\frac{\partial B_{12}}{\partial B_{mix}}\right)^2 \sigma_{B_{mix}}^2 + \left(\frac{\partial B_{12}}{\partial B_{22}}\right)^2 \sigma_{B_{22}}^2 + \left(\frac{\partial B_{12}}{\partial x_1}\right) \sigma_{x_1}^2 + \left(\frac{\partial B_{12}}{\partial B_{11}}\right) \sigma_{B_{11}}^2 \qquad (3\text{-}5\text{-}19)$$

where $\sigma_{B_{mix}}$, $\sigma_{B_{22}}$, and $\sigma_{x_1} >> \sigma_{B_{11}} \approx 0$

Maximum errors in x_1 are estimated as less than 0.1 mole % (see section 2-13), and hence $\sigma_{x_1} = x_1 \cdot 0.001$. The derivatives, $\frac{\partial B_{12}}{\partial B_{22}}$ and $\frac{\partial B_{12}}{\partial x_1}$ were determined analytically from Eq.(3-5-18). B_{12} at a given temperature was averaged from the three mixtures, i.e.,

$$\bar{B}_{12}^2 = \frac{\sum \omega B_{12}^2}{\sum \omega} \qquad (3\text{-}5\text{-}20)$$

where the weighting factor ω is given by

$$\omega = \frac{1}{\sigma_{B_{12}}^2} \qquad (3\text{-}5\text{-}21)$$

In Table 3-6 three values of B_{12} for three mixtures are listed together with $\bar{B}_{12}$ from Eq.(3-5-20). The results from mixture 3 differ substantially from those from the other two but since they are of lower precision they contribute little to the mean. The uncertainty in $\bar{B}_{12}$ is estimated at 5 - 10 cc/mole.

TABLE 3-1

BENDER COEFFICIENTS FOR EQUATIONS (3-6-2) AND (3-6-3)

ETHYLENE (FOR EXPERIMENTAL RANGE, SEE FIG 3-7)

	EQ(3-6-2)	EQ(3-6-3)
A(1)	-Ø.7281539658E+Ø4	Ø.9Ø39Ø785Ø2E+Ø5
A(2)	-Ø.4313535711E+Ø7	Ø.7123659771E+Ø8
A(3)	Ø.1672398620E+1Ø	-Ø.1764207277E+11
A(4)	-Ø.2668364218E+Ø5	Ø.1632640Ø65E+13
A(5)	Ø.1836241516E+Ø9	-Ø.7699390853E+Ø7
A(6)	Ø.1146379717E+Ø8	Ø.4539101816E+1Ø
A(7)		-Ø.6Ø74464549E+12
A(8)		-Ø.6888533651E+Ø8
A(9)		Ø.9471465598E+1Ø
A(1Ø)		Ø.6392976579E+1Ø

MIXTURE 1 (2Ø8 - 299 K UPTO 86 BAR)

	EQ(3-6-2)	EQ(3-6-3)
A(1)	Ø.4493157849E+Ø4	Ø.6127187487E+Ø4
A(2)	Ø.1916392311E+Ø7	Ø.3799400524E+Ø7
A(3)	Ø.2965566846E+Ø9	-Ø.3283690807E+Ø9
A(4)	-Ø.2190710419E+Ø6	Ø.6417539280E+11
A(5)	Ø.1465323020E+Ø9	Ø.2099486591E+Ø6
A(6)	Ø.1037515633E+Ø7	-Ø.5070847388E+Ø8
A(7)		Ø.2378169980E+11
A(8)		-Ø.8802393400E+Ø7
A(9)		Ø.6406964375E+Ø9
A(1Ø)		Ø.6953616228E+Ø9

TABLE 3-1 (CONTINUED)

BENDER COEFFTCIENTS FOR EQUATIONS (3-6-2) AND (3-6-3)

MIXTURE 2 (223 - 298 K UPTO 75 BAR)

	EQ(3-6-2)	EQ(3-6-3)
A(1)	Ø·6391514815E+Ø4	Ø·6658Ø9Ø9ØE+Ø4
A(2)	Ø·3121Ø513Ø2E+Ø7	Ø·4548Ø9537E+Ø7
A(3)	Ø·3Ø57796Ø75E+Ø9	-Ø·4574791637E+Ø9
A(4)	-Ø·2931662380E+Ø6	Ø·9947286392E+11
A(5)	Ø·2255934578E+Ø9	Ø·3610375066E+Ø6
A(6)	-Ø·76Ø0106Ø29E+Ø7	-Ø·1296384Ø9E+Ø9
A(7)		Ø·3660416957E+11
A(8)		-Ø·2132551187E+Ø8
A(9)		Ø·1Ø42Ø89782E+11
A(1Ø)		-Ø·1392842948E+1Ø

MIXTURE 3 (238 - 288 K UPTO 7Ø BAR)

	EQ(3-6-2)	EQ(3-6-3)
A(1)	-Ø·6939995923E+Ø3	Ø·3382251471E+Ø5
A(2)	-Ø·8834357568E+Ø6	Ø·27Ø18Ø0551E+Ø8
A(3)	Ø·1032899753E+1Ø	-Ø·6625648103E+1Ø
A(4)	-Ø·3928Ø7813E+Ø6	Ø·6992368626E+12
A(5)	Ø·2768136164E+Ø9	-Ø·59Ø7243180E+Ø6
A(6)	-Ø·5Ø24775240E+Ø7	Ø·2553447944E+Ø9
A(7)		-Ø·8320360283E+1Ø
A(8)		Ø·3221485193E+Ø8
A(9)		Ø·1131Ø04679E+11
A(1Ø)		-Ø·556Ø064826E+1Ø

TABLE 3-2

THE 2ND AND 3RD VIRIAL COEFFICIENTS

GAS	T (K)	B, CM^3MOLE^{-1} (EQ 3-6-1)	B, CM^3MOLE^{-1} (EQ 3-6-3)	C, CM^6MOLE^{-2} (EQ 3-6-3)
ETHYLENE				
	243·6	-211·16	-212·69	8389
	247·1	-205·67	-206·54	8677
	251·1	-199·59	-199·93	8940
	254·3	-194·98	-194·92	9101
	258·9	-187·60	-188·10	9266
	266·6	-176·25	-177·50	9381
	270·4	-171·36	-172·58	9372
	273·8	-167·49	-168·31	9331
	278·8	-161·30	-162·25	9220
	283·1	-151·60	-157·21	9078
	288·8	-149·70	-150·71	8836
	292·6	-146·40	-146·48	8641
MIXTURE 3				
	238·5	-177·29	-174·66	4013
	251·3	-159·10	-154·36	3531
	259·3	-150·00	-143·57	3250
	266·1	-141·80	-135·31	3023
	272·9	-134·90	-127·72	2805
	280·9	-126·40	-119·53	2560
	288·1	-119·50	-122·73	2349
MIXTURE 2				
	223·3	-159·70	-162·02	6189
	229·9	-151·00	-152·23	5890
	237·3	-143·10	-142·28	5590
	244·2	-133·60	-133·83	5340
	252·2	-126·60	-124·91	5081
	259·4	-119·50	-117·59	4874
	266·2	-113·10	-111·20	4698
	273·1	-106·97	-105·20	4536
	279·3	-101·04	-100·16	4403
	287·1	-95·68	-94·27	4252
	293·4	-91·39	-89·83	4142
	298·9	-87·58	-86·16	4053

TABLE 3-2 (CONTINUED)

THE 2ND AND 3RD VIRIAL COEFFICIENTS

GAS	T (K)	B, CM^3MOLE^{-1} (EQ 3-6-1)	B, CM^3MOLE^{-1} (EQ 3-6-3)	C, CM^6MOLE^{-2} (EQ 3-6-3)
MIXTURE 1				
	208.1	-138.10	-140.34	6199
	215.7	-128.50	-130.18	5845
	223.4	-120.10	-120.95	5526
	230.7	-112.90	-113.04	5255
	238.2	-105.52	-105.65	5005
	245.8	-98.42	-98.82	4777
	253.3	-92.40	-92.65	4575
	260.3	-87.22	-87.33	4403
	268.2	-80.78	-81.79	4227
	275.6	-77.27	-76.99	4077
	283.7	-71.71	-72.11	3920
	288.8	-68.85	-69.23	3842
	294.1	-66.39	-66.36	3758
	299.0	-63.50	-63.83	3684

TABLE 3-3

EXPERIMENTAL DATA, DENSITIES
(ETHYLENE)

RUN NUMBER	T (K)	PRESSURE (BAR)	RHO(V) EQ 3-6-1	RHO(6) EQ 3-6-2	RHO(10) EQ 3-6-3
19					
	273.80	35.116	.0023722	.0023694	.0023729
	273.79	27.363	.0015933	.0015913	.0015935
	273.79	20.236	.0010708	.0010697	.0010710
	273.79	14.481	.0007199	.0007193	.0007200
	273.79	10.149	.0004842	.0004839	.0004843
	273.79	7.014	.0003256	.0003255	.0003256
	273.79	4.807	.0002191	.0002191	.0002191
	273.79	3.270	.0001472	.0001472	.0001473
22					
	270.44	33.647	.0023026	.0023009	.0023040
	270.45	26.420	.0015610	.0015596	.0015616
	270.44	19.674	.0010564	.0010559	.0010571
	270.45	14.164	.0007143	.0007140	.0007146
	270.44	9.979	.0004828	.0004827	.0004830
	270.44	6.932	.0003262	.0003262	.0003263
	270.45	4.770	.0002204	.0002203	.0002204
	270.44	3.264	.0001489	.0001489	.0001489
23					
	266.60	33.610	.0024512	.0024514	.0024546
	266.60	27.122	.0016821	.0016828	.0016846
	266.60	20.596	.0011490	.0011492	.0011502
	266.60	15.036	.0007820	.0007821	.0007827
	266.59	10.723	.0005324	.0005324	.0005327
	266.60	7.518	.0003618	.0003618	.0003620
	266.58	5.214	.0002457	.0002457	.0002458
	266.59	3.592	.0001669	.0001669	.0001669

TABLE 3-3 (CONTINUED)

EXPERIMENTAL DATA, DENSITIES
(ETHYLENE)

RUN NUMBER	T (K)	PRESSURE (BAR)	RHO(V) EQ 3-6-1	RHO(6) EQ 3-6-2	RHO(10) EQ 3-6-3
28					
	251.15	20.096	.0012648	.0012645	.0012646
	251.14	15.377	.0008879	.0008880	.0008879
	251.14	11.383	.0006198	.0006199	.0006198
	251.14	8.243	.0004312	.0004312	.0004312
	251.13	5.881	.0002993	.0002993	.0002993
	251.13	4.154	.0002075	.0002075	.0002075
	251.13	2.915	.0001437	.0001437	.0001437
29					
	247.09	16.581	.0010081	.0010088	.0010086
	247.09	12.515	.0007101	.0007106	.0007104
	247.08	9.199	.0004978	.0004981	.0004979
	247.09	6.642	.0003479	.0003480	.0003479
	247.08	4.738	.0002426	.0002427	.0002426
	247.08	3.352	.0001690	.0001690	.0001690
	247.08	2.357	.0001176	.0001176	.0001176
30					
	243.66	15.426	.0009435	.0009442	.0009440
	243.66	11.664	.0006679	.0006685	.0006682
	243.66	8.598	.0004705	.0004708	.0004707
	243.66	6.230	.0003303	.0003305	.0003304
	243.67	4.461	.0002314	.0002315	.0002315
	243.65	3.169	.0001619	.0001620	.0001620

TABLE 3-3 (CONTINUED)

EXPERIMENTAL DATA, DENSITIES
(ETHYLENE)

RUN NUMBER	T (K)	PRESSURE (BAR)	RHO(V) EQ 3-6-1	RHO(6) EQ 3-6-2	RHO(10) EQ 3-6-3
31					
	254.35	21.831	.0013810	.0013805	.0013808
	254.35	16.735	.0009649	.0009647	.0009648
	254.35	12.382	.0006705	.0006704	.0006704
	254.33	8.950	.0004644	.0004643	.0004644
	254.34	6.369	.0003210	.0003209	.0003209
	254.33	4.484	.0002215	.0002215	.0002215
	254.34	3.135	.0001528	.0001528	.0001528
32					
	258.89	23.782	.0014960	.0014952	.0014964
	258.89	18.185	.0010369	.0010368	.0010372
	258.90	13.400	.0007153	.0007153	.0007155
	258.90	9.638	.0004921	.0004921	.0004922
	258.89	6.822	.0003380	.0003380	.0003381
	258.90	4.777	.0002319	.0002319	.0002319
	258.89	3.321	.0001590	.0001590	.0001590
33					
	278.86	34.219	.0021238	.0021215	.0021250
	278.85	25.774	.0014083	.0014072	.0014092
	278.84	18.608	.0009374	.0009369	.0009379
	278.85	13.079	.0006251	.0006248	.0006253
	278.83	9.037	.0004173	.0004171	.0004174
	238.84	6.175	.0002783	.0002386	.0002786
	278.83	4.189	.0001862	.0001862	.0001862
	278.84	2.829	.0001245	.0001245	.0001245

TABLE 3-3 (CONTINUED)

EXPERIMENTAL DATA, DENSITIES
(ETHYLENE)

RUN NUMBER	T (K)	PRESSURE (BAR)	RHO(V) EQ 3-6-1	RHO(6) EQ 3-6-2	RHO(10) EQ 3-6-3
34					
	283.15	37.899	.0023927	.0023898	.0023937
	283.15	28.556	.0015645	.0015627	.0015648
	283.15	20.575	.0010314	.0010304	.0010316
	283.14	14.414	.0006826	.0006821	.0006827
	283.15	9.918	.0004526	.0004524	.0004527
	283.14	6.746	.0003005	.0003003	.0003005
	283.14	4.554	.0001996	.0001996	.0001997
	283.13	3.059	.0001327	.0001327	.0001327
35					
	288.84	41.184	.0025670	.0025673	.0025708
	288.83	30.652	.0016463	.0016469	.0016485
	288.82	21.857	.0010723	.0010724	.0010733
	288.82	15.168	.0007027	.0007026	.0007031
	288.80	10.350	.0004622	.0004621	.0004624
	288.84	6.987	.0003046	.0003046	.0003047
	288.81	4.682	.0002009	.0002009	.0002010
	288.83	3.119	.0001325	.0001325	.0001325
36					
	292.59	41.282	.0024702	.0024673	.0024694
	292.56	30.165	.0015705	.0015688	.0015695
	292.57	21.233	.0010156	.0010146	.0010151
	292.58	14.593	.0006617	.0006613	.0006616
	292.58	9.872	.0004326	.0004323	.0004325
	292.59	6.616	.0002835	.0002834	.0002835
	292.58	4.404	.0001861	.0001860	.0001860
	292.58	2.923	.0001223	.0001223	.0001223

TABLE 3-3 (CONTINUED)

EXPERIMENTAL DATA, DENSITIES
(MIXTURE 1, .3045 ETHYLENE)

RUN NUMBER	T (K)	PRESSURE (BAR)	RHO(V) EQ 3-6-1	RHO(6) EQ 3-6-2	RHO(10) EQ 3-6-3
37					
	299.03	61.156	.0029126	.0029118	.0029146
	299.02	41.520	.0018695	.0018682	.0018699
	299.02	27.872	.0012078	.0012070	.0012078
	299.03	18.555	.0007837	.0007833	.0007837
	299.02	12.270	.0005096	.0005094	.0005096
	299.02	8.080	.0003318	.0003318	.0003319
	299.02	5.306	.0002163	.0002163	.0002164
	299.01	3.477	.0001411	.0001411	.0001411
38					
	294.10	62.059	.0030536	.0030521	.0030547
	294.08	42.656	.0019757	.0019740	.0019755
	294.09	28.935	.0012853	.0012844	.0012852
	294.09	19.428	.0008391	.0008386	.0008390
	294.08	12.954	.0005492	.0005490	.0005492
	294.08	8.588	.0003596	.0003595	.0003596
	294.08	5.676	.0002358	.0002357	.0002358
	294.08	3.743	.0001547	.0001546	.0001546
39					
	288.82	60.944	.0030877	.0030879	.0030902
	288.83	42.411	.0020165	.0020158	.0020171
	288.83	29.070	.0013226	.0013222	.0013229
	288.86	19.692	.0008697	.0008694	.0008698
	288.85	13.231	.0005729	.0005727	.0005729
	288.82	8.840	.0003777	.0003777	.0003778
	288.84	5.884	.0002492	.0002492	.0002492
	288.85	3.906	.0001645	.0001645	.0001645

TABLE 3-3 (CONTINUED)

EXPERIMENTAL DATA, DENSITIES
(MIXTURE 1, .3045 ETHYLENE)

RUN NUMBER	T (K)	PRESSURE (BAR)	RHO(V) EQ 3-6-1	RHO(6) EQ 3-6-2	RHO(10) EQ 3-6-3
40					
	283.72	85.897	.0049507	.0049536	.0049568
	283.72	61.733	.0032476	.0032470	.0032491
	283.70	43.580	.0021406	.0021396	.0021407
	283.70	30.229	.0014149	.0014144	.0014150
	283.71	20.689	.0009372	.0009369	.0009372
	283.69	14.027	.0006216	.0006214	.0006216
	283.71	9.449	.0004128	.0004125	.0004126
	283.68	6.331	.0002737	.0002737	.0002737
	283.70	4.234	.0001818	.0001818	.0001818
41					
	275.60	75.667	.0045079	.0045081	.0045110
	275.60	55.553	.0030172	.0030167	.0030177
	275.58	39.844	.0020205	.0020201	.0020206
	275.56	28.012	.0013542	.0013538	.0013542
	275.57	19.413	.0009077	.0009075	.0009077
	275.56	13.314	.0006086	.0006086	.0006087
	275.56	9.067	.0004083	.0004082	.0004083
	275.56	6.143	.0002738	.0002738	.0002738
	275.56	4.149	.0001836	.0001836	.0001836
42					
	268.23	75.050	.0047950	.0048003	.0048026
	268.23	56.632	.0032681	.0032723	.0032727
	268.22	41.570	.0022209	.0022231	.0022231
	268.22	29.800	.0015070	.0015079	.0015080
	268.22	20.986	.0010215	.0010219	.0010220
	268.21	14.589	.0006917	.0006919	.0006920
	268.21	10.073	.0004691	.0004692	.0004693
	268.20	6.903	.0003176	.0003176	.0003177
	268.19	4.710	.0002150	.0002150	.0002150

TABLE 3-3 (CONTINUED)

EXPERIMENTAL DATA, DENSITIES
(MIXTURE 1, .3045 ETHYLENE)

RUN NUMBER	T (K)	PRESSURE (BAR)	RHO(V) EQ 3-6-1	RHO(6) EQ 3-6-2	RHO(10) EQ 3-6-3
43					
	260.32	73.711	.0051171	.0051335	.0051346
	260.62	57.368	.0035611	.0035610	.0035606
	260.61	43.254	.0024610	.0024603	.0024598
	260.62	31.714	.0016929	.0016923	.0016921
	260.63	22.766	.0011616	.0011613	.0011613
	260.62	16.090	.0007957	.0007954	.0007954
	260.62	11.255	.0005446	.0005445	.0005445
	260.62	7.809	.0003722	.0003722	.0003722
	260.62	5.392	.0002544	.0002544	.0002544
	260.62	3.710	.0001739	.0001738	.0001738
45					
	253.32	67.686	.0049448	.0049477	.0049474
	253.30	53.688	.0035064	.0035099	.0035084
	253.30	41.416	.0024608	.0024626	.0024616
	253.30	30.880	.0017163	.0017171	.0017166
	253.31	22.492	.0011918	.0011921	.0011919
	253.30	16.110	.0008254	.0008256	.0008255
	253.29	11.402	.0005707	.0005708	.0005708
	253.30	8.004	.0003941	.0003941	.0003941
	253.30	5.585	.0002719	.0002720	.0002720
	253.31	3.882	.0001876	.0001876	.0001876
46					
	245.89	64.642	.0051495	.0051539	.0051517
	245.88	53.134	.0037347	.0037397	.0037375
	245.88	42.020	.0026711	.0026736	.0026720
	245.87	32.107	.0018922	.0018935	.0018927
	245.88	23.862	.0013321	.0013327	.0013324
	245.87	17.413	.0009340	.0009342	.0009341
	245.87	12.518	.0006531	.0006532	.0006531
	245.87	8.908	.0004557	.0004558	.0004558
	245.87	6.295	.0003177	.0003178	.0003178
	245.86	4.428	.0002214	.0002214	.0002214

TABLE 3-3 (CONTINUED)

EXPERIMENTAL DATA, DENSITIES
(MIXTURE 1, .3045 ETHYLENE)

RUN NUMBER	T (K)	PRESSURE (BAR)	RHO(V) EQ 3-6-1	RHO(6) EQ 3-6-2	RHO(10) EQ 3-6-3
47					
	238.18	60.979	.0053849	.0053912	.0053862
	238.18	51.940	.0040066	.0040110	.0040085
	238.17	42.458	.0029277	.0029297	.0029278
	238.17	33.397	.0021120	.0021126	.0021116
	238.17	25.462	.0015100	.0015102	.0015098
	238.16	18.959	.0010731	.0010731	.0010730
	238.17	13.877	.0007596	.0007596	.0007596
	238.17	10.032	.0005363	.0005363	.0005362
	238.16	7.190	.0003779	.0003779	.0003779
	238.16	5.120	.0002659	.0002659	.0002659
48					
	230.71	53.936	.0049923	.0050002	.0049981
	230.20	46.797	.0037771	.0037790	.0037778
	230.70	38.885	.0028031	.0028032	.0028022
	230.70	31.059	.0020509	.0020505	.0020500
	230.69	24.026	.0014855	.0014851	.0014849
	230.69	18.133	.0010682	.0010680	.0010679
	230.69	13.442	.0007646	.0007645	.0007645
	230.69	9.836	.0005456	.0005456	.0005456
	230.70	7.129	.0003884	.0003884	.0003884
	230.70	5.133	.0002761	.0002761	.0002761
50					
	223.38	36.036	.0027318	.0027332	.0027342
	223.39	29.282	.0020276	.0020288	.0020294
	223.38	23.015	.0014884	.0014892	.0014896
	223.39	17.631	.0010838	.0010843	.0010845
	223.39	13.251	.0007850	.0007853	.0007854
	223.39	9.820	.0005663	.0005665	.0005665
	223.38	7.204	.0004075	.0004075	.0004076
	223.38	5.246	.0002926	.0002927	.0002927

TABLE 3-3 (CONTINUED)

EXPERIMENTAL DATA, DENSITIES
(MIXTURE 1. .3045 ETHYLENE)

RUN NUMBER	T (K)	PRESSURE (BAR)	RHO(V) EQ 3-6-1	RHO(6) EQ 3-6-2	RHO(10) EQ 3-6-3
51					
	215.73	28.848	.0021530	.0021526	.0021557
	215.66	23.257	.0016076	.0016092	.0016108
	215.67	18.219	.0011889	.0011901	.0011909
	215.67	13.964	.0008732	.0008740	.0008744
	215.66	10.531	.0006382	.0006387	.0006389
	215.67	7.848	.0004648	.0004651	.0004652
	215.66	5.797	.0003377	.0003378	.0003379
	215.66	4.255	.0002449	.0002450	.0002450
52					
	208.13	20.010	.0014202	.0014199	.0014227
	208.14	15.772	.0010606	.0010608	.0010623
	208.13	12.179	.0007868	.0007870	.0007878
	208.13	9.263	.0005809	.0005811	.0005815
	208.13	6.964	.0004272	.0004273	.0004276
	208.14	5.193	.0003135	.0003136	.0003137
	208.13	3.849	.0002296	.0002296	.0002297

TABLE 3-3 (CONTINUED)

EXPERIMENTAL DATA, DENSITIES
(MIXTURE 2, .5482 ETHYLENE)

RUN NUMBER	T (K)	PRESSURE (BAR)	RHO(V) EQ 3-6-1	RHO(6) EQ 3-6-2	RHO(10) EQ 3-6-3
53					
	298.89	69.743	.0038187	.0038349	.0038139
	298.87	48.772	.0024028	.0024102	.0023984
	298.85	33.485	.0015376	.0015414	.0015353
	298.86	22.624	.0009922	.0009939	.0009910
	298.87	15.118	.0006435	.0006442	.0006429
	298.87	10.023	.0004184	.0004187	.0004181
	298.86	6.614	.0002726	.0002727	.0002725
	298.85	4.348	.0001777	.0001778	.0001777
54					
	293.46	68.783	.0039326	.0039525	.0039285
	293.44	49.025	.0025051	.0025151	.0025013
	293.45	34.159	.0016183	.0016232	.0016161
	293.44	23.361	.0010530	.0010553	.0010518
	293.45	15.770	.0006880	.0006890	.0006874
	293.46	10.552	.0004505	.0004510	.0004503
	293.43	7.015	.0002954	.0002956	.0002952
	293.43	4.645	.0001938	.0001939	.0001937
55					
	287.17	69.653	.0042686	.0042949	.0042657
	287.16	50.982	.0027559	.0027703	.0027530
	287.15	36.279	.0017997	.0018070	.0017978
	287.15	25.228	.0011818	.0011853	.0011807
	287.14	17.259	.0007784	.0007800	.0007778
	287.13	11.678	.0005136	.0005144	.0005134
	287.15	7.843	.0003393	.0003396	.0003392
	287.14	5.242	.0002243	.0002245	.0002243

TABLE 3-3 (CONTINUED)

EXPERIMENTAL DATA, DENSITIES
(MIXTURE 2, .5482 ETHYLENE)

RUN NUMBER	T (K)	PRESSURE (BAR)	RHO(V) EQ 3-6-1	RHO(6) EQ 3-6-2	RHO(10) EQ 3-6-3
56					
	279.37	74.059	.0051934	.0052385	.0051984
	279.37	56.750	.0034213	.0034443	.0034191
	279.38	41.961	.0022665	.0022790	.0022646
	279.37	30.072	.0015069	.0015132	.0015057
	279.36	21.067	.0010038	.0010068	.0010031
	279.35	14.529	.0006694	.0006708	.0006690
	279.35	9.921	.0004469	.0004475	.0004467
	279.35	6.724	.0002984	.0002987	.0002983
57					
	273.12	74.985	.0059175	.0059709	.0059212
	273.10	59.847	.0039916	.0040174	.0039850
	273.10	45.878	.0026860	.0027004	.0026810
	273.10	33.831	.0018068	.0018143	.0018037
	273.09	24.239	.0012159	.0012195	.0012141
	273.10	17.015	.0008180	.0008197	.0008170
	273.08	11.780	.0005503	.0005511	.0005498
	273.08	8.080	.0003703	.0003706	.0003700
	273.08	5.508	.0002491	.0002493	.0002490
58					
	266.24	74.217	.0067867	.0068701	.0068070
	266.23	62.187	.0047438	.0047789	.0047363
	266.22	50.026	.0032678	.0032882	.0032621
	266.22	38.399	.0022361	.0022474	.0022320
	266.22	28.383	.0015248	.0015306	.0015223
	266.21	20.416	.0010377	.0010406	.0010363
	266.20	14.417	.0007056	.0007071	.0007049
	266.22	10.048	.0004793	.0004799	.0004789
	266.21	6.942	.0003254	.0003257	.0003252

TABLE 3-3 (CONTINUED)

EXPERIMENTAL DATA, DENSITIES
(MIXTURE 2, .5482 ETHYLENE)

RUN NUMBER	T (K)	PRESSURE (BAR)	RHO(V) EQ 3-6-1	RHO(6) EQ 3-6-2	RHO(10) EQ 3-6-3
59					
	259.41	61.688	.0054343	.0054788	.0054238
	259.41	52.216	.0038598	.0038813	.0038496
	259.41	41.962	.0027006	.0027141	.0026940
	259.41	32.176	.0018719	.0018795	.0018678
	259.40	23.820	.0012911	.0012951	.0012887
	259.40	17.200	.0008876	.0008896	.0008863
	259.36	12.209	.0006092	.0006102	.0006086
	259.39	8.565	.0004175	.0004180	.0004172
	259.38	5.960	.0002860	.0002862	.0002859
60					
	252.24	48.831	.0038573	.0038794	.0038517
	252.25	40.327	.0027539	.0027698	.0027506
	252.24	31.663	.0019416	.0019515	.0019395
	252.23	24.915	.0014150	.0014338	.0014265
	252.22	17.566	.0009454	.0009482	.0009446
	252.22	12.655	.0006561	.0006575	.0006556
	252.22	8.995	.0004544	.0004551	.0004542
	252.23	6.334	.0003143	.0003147	.0003142
	252.23	4.433	.0002173	.0002174	.0002172
61					
	244.25	37.553	.0027246	.0027346	.0027197
	244.26	30.183	.0019537	.0019642	.0019536
	244.22	23.273	.0013884	.0013956	.0013891
	244.21	17.405	.0009801	.0009842	.0009806
	244.22	12.740	.0006889	.0006911	.0006892
	244.23	9.185	.0004828	.0004839	.0004829
	244.23	6.555	.0003378	.0003383	.0003378
	244.20	4.644	.0002361	.0002363	.0002361

TABLE 3-3 (CONTINUED)

EXPERIMENTAL DATA, DENSITIES
(MIXTURE 2, .5482 ETHYLENE)

RUN NUMBER	T (K)	PRESSURE (BAR)	RHO(V) EQ 3-6-1	RHO(6) EQ 3-6-2	RHO(10) EQ 3-6-3
62					
	237.37	29.056	.0019876	.0019932	.0019851
	237.39	22.843	.0014327	.0014366	.0014310
	237.36	17.378	.0010240	.0010265	.0010231
	237.36	12.912	.0007278	.0007291	.0007272
	237.32	9.436	.0005155	.0005162	.0005152
	237.33	6.815	.0003641	.0003645	.0003639
	237.36	4.882	.0002567	.0002569	.0002566
63					
	229.93	20.383	.0013145	.0013186	.0013152
	229.94	15.650	.0009503	.0009532	.0009509
	229.93	11.743	.0006830	.0006847	.0006834
	229.94	8.667	.0004889	.0004898	.0004890
	229.94	6.324	.0003490	.0003495	.0003491
	229.93	4.575	.0002486	.0002488	.0002486
64					
	223.27	18.585	.0012359	.0012378	.0012366
	223.27	14.408	.0009030	.0009050	.0009037
	223.27	10.916	.0006554	.0006567	.0006559
	223.27	8.135	.0004737	.0004745	.0004740
	223.27	5.992	.0003413	.0003417	.0003414
	223.26	4.376	.0002453	.0002456	.0002454

TABLE 3-3 (CONTINUED)

EXPERIMENTAL DATA, DENSITIES
(MIXTURE 3, .7581 ETHYLENE)

RUN NUMBER	T (K)	PRESSURE (BAR)	RHO(V) EQ 3-6-1	RHO(6) EQ 3-6-2	RHO(10) EQ 3-6-3
66					
	288.15	69.094	.0053578	.0053635	.0053038
	288.13	53.261	.0033014	.0033090	.0032768
	288.14	39.401	.0021237	.0021287	.0021100
	288.12	28.091	.0013852	.0013879	.0013776
	288.12	19.524	.0009090	.0009102	.0009050
	288.10	13.344	.0005985	.0005991	.0005966
	288.10	9.021	.0003948	.0003951	.0003939
	288.07	6.055	.0002608	.0002609	.0002604
	288.12	4.048	.0001725	.0001725	.0001723
68					
	280.96	49.370	.0031856	.0031898	.0031597
	280.93	37.387	.0020964	.0020999	.0020816
	280.93	27.140	.0013883	.0013902	.0013799
	280.95	19.146	.0009221	.0009231	.0009177
	280.92	13.257	.0006137	.0006142	.0006115
	280.95	9.067	.0004088	.0004091	.0004078
	280.94	6.152	.0002726	.0002727	.0002722
	280.96	4.154	.0001820	.0001820	.0001817
69					
	272.96	54.884	.0045817	.0045944	.0045387
	272.96	45.498	.0030844	.0030893	.0030660
	272.95	35.352	.0020780	.0020812	.0020628
	272.95	26.199	.0013998	.0014015	.0013909
	272.94	18.802	.0009426	.0009435	.0009378
	272.95	13.211	.0006347	.0006352	.0006323
	272.94	9.155	.0004275	.0004278	.0004264
	272.94	6.287	.0002881	.0002882	.0002875
	272.95	4.292	.0001942	.0001942	.0001939

TABLE 3-3 (CONTINUED)

EXPERIMENTAL DATA, DENSITIES
(MIXTURE 3, .7581 ETHYLENE)

RUN NUMBER	T (K)	PRESSURE (BAR)	RHO(V) EQ 3-6-1	RHO(6) EQ 3-6-2	RHO(10) EQ 3-6-3
70					
	266.13	44.585	.0033219	.0033291	.0032968
	266.11	36.029	.0022852	.0022917	.0022706
	266.11	27.516	.0015637	.0015674	.0015546
	266.11	20.216	.0010666	.0010685	.0010614
	266.10	14.468	.0007261	.0007276	.0007233
	266.10	10.180	.0004939	.0004943	.0004925
	266.10	7.081	.0003358	.0003360	.0003351
	266.11	4.889	.0002283	.0002284	.0002280
71					
	259.30	37.842	.0027174	.0027220	.0026970
	259.30	30.318	.0018965	.0019011	.0018843
	259.29	23.086	.0013133	.0013160	.0013062
	259.29	16.978	.0009052	.0009066	.0009012
	259.28	12.199	.0006223	.0006230	.0006202
	259.28	8.629	.0004271	.0004274	.0004261
	259.29	6.040	.0002929	.0002930	.0002924
	259.28	4.196	.0002006	.0002007	.0002003
72					
	251.34	28.689	.0018969	.0019054	.0018897
	251.34	22.346	.0013364	.0013420	.0013322
	251.33	16.755	.0009349	.0009380	.0009325
	251.36	12.239	.0006510	.0006525	.0006496
	251.35	8.785	.0004522	.0004530	.0004515
	251.35	6.231	.0003135	.0003139	.0003131
	251.36	4.384	.0002172	.0002174	.0002170

TABLE 3-3 (CONTINUED)

EXPERIMENTAL DATA, DENSITIES
(MIXTURE 3, .7581 ETHYLENE)

RUN NUMBER	T (K)	PRESSURE (BAR)	RHO(V) EQ 3-6-1	RHO(6) EQ 3-6-2	RHO(10) EQ 3-6-3
74					
	238.46	16.352	.0010242	.0010273	.0010222
	238.47	12.642	.0007295	.0007315	.0007285
	238.47	9.329	.0005170	.0005182	.0005165
	238.47	6.781	.0003654	.0003659	.0003651
	238.47	4.874	.0002575	.0002538	.0002573
	238.47	3.480	.0001813	.0001814	.0001812

TABLE 3-4

EXPERIMENTAL DATA, COMPRESSIBILITY FACTORS
(ETHYLENE)

RUN NUMBER	T (K)	PRESSURE (BAR)	Z(V) EQ 3-6-1	Z(6) EQ 3-6-2	Z(10) EQ 3-6-3
19					
	273.80	35.116	.6503	.6510	.6501
	273.79	27.363	.7544	.7554	.7543
	273.79	20.236	.8301	.8310	.8300
	273.79	14.481	.8836	.8844	.8835
	273.79	10.149	.9207	.9213	.9206
	273.79	7.014	.9463	.9467	.9462
	273.79	4.807	.9636	.9639	.9636
	273.79	3.270	.9755	.9757	.9754
22					
	270.44	33.647	.6498	.6503	.6494
	270.45	26.420	.7527	.7533	.7524
	270.44	19.674	.8282	.8286	.8277
	270.45	14.164	.8818	.8821	.8814
	270.44	9.979	.9192	.9194	.9188
	270.44	6.932	.9450	.9451	.9447
	270.45	4.770	.9626	.9628	.9624
	270.44	3.264	.9746	.9747	.9745
23					
	266.60	33.610	.6186	.6185	.6177
	266.60	27.122	.7274	.7271	.7263
	266.60	20.596	.8086	.8085	.8078
	266.60	15.036	.8673	.8673	.8667
	266.59	10.723	.9086	.9086	.9080
	266.60	7.518	.9373	.9374	.9370
	266.58	5.214	.9572	.9572	.9569
	266.59	3.592	.9708	.9709	.9706

TABLE 3-4 (CONTINUED)

EXPERIMENTAL DATA, COMPRESSIBILITY FACTORS
(ETHYLENE)

RUN NUMBER	T (K)	PRESSURE (BAR)	Z(V) EQ 3-6-1	Z(6) EQ 3-6-2	Z(10) EQ 3-6-3
28					
	251.15	20.096	.7609	.7611	.7610
	251.14	15.377	.8293	.8293	.8294
	251.14	11.383	.8795	.8794	.8795
	251.14	8.243	.9155	.9154	.9155
	251.13	5.881	.9410	.9409	.9410
	251.13	4.154	.9589	.9589	.9589
	251.13	2.915	.9715	.9714	.9715
29					
	247.09	16.581	.8006	.8000	.8002
	247.09	12.515	.8579	.8573	.8575
	247.08	9.199	.8995	.8990	.8992
	247.09	6.642	.9294	.9290	.9292
	247.08	4.738	.9505	.9503	.9504
	247.08	3.352	.9654	.9652	.9653
	247.08	2.357	.9759	.9758	.9758
30					
	243.66	15.426	.8070	.8064	.8066
	243.66	11.664	.8620	.8613	.8616
	243.66	8.598	.9021	.9015	.9018
	243.66	6.230	.9309	.9304	.9307
	243.67	4.461	.9514	.9511	.9512
	243.65	3.169	.9661	.9657	.9658

TABLE 3-4 (CONTINUED)

EXPERIMENTAL DATA, COMPRESSIBILITY FACTORS
(ETHYLENE)

RUN NUMBER	T (K)	PRESSURE (BAR)	Z(V) EQ 3-6-1	Z(6) EQ 3-6-2	Z(10) EQ 3-6-3
31					
	254.35	21.831	.7475	.7478	.7476
	254.35	16.735	.8201	.8202	.8202
	254.35	12.382	.8732	.8734	.8734
	254.33	8.950	.9114	.9115	.9114
	254.34	6.369	.9383	.9384	.9384
	254.33	4.484	.9573	.9573	.9573
	254.34	3.135	.9704	.9705	.9704
32					
	258.89	23.782	.7385	.7387	.7383
	258.89	16.185	.8147	.8148	.8145
	258.90	13.400	.8702	.8703	.8700
	258.90	9.638	.9098	.9098	.9096
	258.89	6.822	.9376	.9376	.9375
	258.90	4.777	.9570	.9570	.9569
	258.89	3.321	.9704	.9704	.9703
33					
	278.86	34.219	.6949	.6957	.6945
	278.85	25.774	.7894	.7900	.7889
	278.84	18.608	.8562	.8567	.8557
	278.85	13.079	.9024	.9029	.9021
	278.83	9.037	.9342	.9345	.9339
	278.84	6.175	.9557	.9560	.9555
	278.83	4.189	.9703	.9704	.9701
	278.84	2.829	.9801	.9802	.9799

TABLE 3-4 (CONTINUED)

EXPERIMENTAL DATA, COMPRESSIBILITY FACTORS
(ETHYLENE)

RUN NUMBER	T (K)	PRESSURE (BAR)	Z(V) EQ 3-6-1	Z(6) EQ 3-6-2	Z(10) EQ 3-6-3
34					
	283.15	37.899	.6728	.6736	.6725
	283.15	28.556	.7753	.7762	.7751
	283.15	20.575	.8473	.8481	.8472
	283.14	14.414	.8970	.8976	.8968
	283.15	9.918	.9308	.9313	.9307
	283.14	6.746	.9537	.9541	.9536
	283.14	4.554	.9691	.9693	.9690
	283.13	3.059	.9794	.9795	.9793
35					
	288.84	41.184	.6680	.6679	.6670
	288.83	30.652	.7753	.7750	.7742
	288.82	21.857	.8488	.8487	.8480
	288.82	15.168	.8989	.8989	.8983
	288.80	10.350	.9326	.9327	.9322
	288.84	6.987	.9552	.9553	.9549
	288.81	4.682	.9703	.9703	.9701
	288.83	3.119	.9803	.9804	.9802
36					
	292.59	41.282	.6869	.6878	.6872
	292.56	30.165	.7896	.7905	.7901
	292.57	21.233	.8594	.8602	.8598
	292.58	14.593	.9065	.9072	.9067
	292.58	9.872	.9381	.9386	.9382
	292.59	6.616	.9591	.9594	.9592
	292.58	4.404	.9730	.9732	.9730
	292.58	2.923	.9823	.9823	.9822

TABLE 3-4 (CONTINUED)

EXPERIMENTAL DATA, COMPRESSIBILITY FACTORS
(MIXTURE 1, .3045 ETHYLENE)

RUN NUMBER	T (K)	PRESSURE (BAR)	Z(V) EQ 3-6-1	Z(6) EQ 3-6-2	Z(10) EQ 3-6-3
37					
	299.03	61.156	.8445	.8447	.8439
	299.02	41.520	.8933	.8939	.8931
	299.02	27.872	.9282	.9288	.9282
	299.03	18.555	.9523	.9527	.9522
	299.02	12.270	.9665	.9688	.9684
	299.02	8.080	.9796	.9795	.9792
	299.02	5.306	.9864	.9865	.9864
	299.01	3.477	.9911	.9912	.9911
38					
	294.10	62.059	.8311	.8315	.8308
	294.08	42.656	.8830	.8837	.8831
	294.09	28.935	.9207	.9213	.9208
	294.09	19.428	.9469	.9474	.9469
	294.08	12.954	.9647	.9650	.9647
	294.08	8.588	.9766	.9769	.9766
	294.08	5.676	.9846	.9847	.9846
	294.08	3.743	.9898	.9899	.9898
39					
	288.82	60.944	.8219	.8218	.8212
	288.83	42.411	.8758	.8761	.8755
	288.83	29.070	.9152	.9155	.9150
	288.86	19.692	.9428	.9431	.9427
	288.85	13.231	.9617	.9619	.9616
	288.82	8.840	.9745	.9746	.9744
	288.84	5.884	.9830	.9831	.9830
	288.85	3.906	.9888	.9888	.9887

TABLE 3-4 (CONTINUED)

EXPERIMENTAL DATA, COMPRESSIBILITY FACTORS
(MIXTURE 1, .3045 ETHYLENE)

RUN NUMBER	T (K)	PRESSURE (BAR)	Z(V) EQ 3-6-1	Z(6) EQ 3-6-2	Z(10) EQ 3-6-3
40					
	283.72	85.897	.7355	.7351	.7346
	283.72	61.733	.8058	.8059	.8054
	283.70	43.580	.8631	.8635	.8630
	283.70	30.229	.9057	.9060	.9056
	283.71	20.689	.9358	.9361	.9358
	283.69	14.027	.9567	.9569	.9567
	283.71	9.449	.9704	.9711	.9709
	283.68	6.331	.9806	.9807	.9805
	283.70	4.234	.9870	.9871	.9870
41					
	275.60	75.667	.7325	.7325	.7320
	275.60	55.553	.8035	.8036	.8034
	275.58	39.844	.8606	.8608	.8606
	275.56	28.017	.9030	.9033	.9030
	275.57	19.413	.9334	.9336	.9334
	275.56	13.314	.9547	.9548	.9546
	275.56	9.067	.9693	.9694	.9692
	275.56	6.143	.9792	.9793	.9792
	275.56	4.149	.9861	.9861	.9860
42					
	268.23	75.050	.7018	.7010	.7007
	268.23	56.632	.7770	.7760	.7759
	268.22	41.570	.8393	.8385	.8384
	268.22	29.800	.8867	.8861	.8861
	268.22	20.986	.9212	.9209	.9208
	268.21	14.589	.9458	.9455	.9454
	268.21	10.073	.9628	.9626	.9625
	268.20	6.903	.9746	.9745	.9744
	268.19	4.710	.9827	.9827	.9826

TABLE 3-4 (CONTINUED)

EXPERIMENTAL DATA, COMPRESSIBILITY FACTORS
(MIXTURE 1, .3045 ETHYLENE)

RUN NUMBER	T (K)	PRESSURE (BAR)	Z(V) EQ 3-6-1	Z(6) EQ 3-6-2	Z(10) EQ 3-6-3
43					
	260.32	73.711	.6655	.6634	.6632
	260.62	57.368	.7434	.7434	.7435
	260.61	43.254	.8111	.8113	.8115
	260.62	31.714	.8645	.8648	.8649
	260.63	22.766	.9044	.9047	.9047
	260.62	16.090	.9332	.9335	.9335
	260.62	11.255	.9537	.9539	.9539
	260.62	7.809	.9681	.9682	.9682
	260.62	5.392	.9781	.9782	.9781
	260.62	3.710	.9849	.9850	.9850
45					
	253.32	67.686	.6499	.6495	.6496
	253.30	53.888	.7297	.7290	.7293
	253.30	41.416	.7991	.7985	.7989
	253.30	30.880	.8543	.8539	.8541
	253.31	22.492	.8961	.8959	.8960
	253.30	16.110	.9267	.9266	.9266
	253.29	11.402	.9487	.9486	.9486
	253.30	8.004	.9643	.9642	.9642
	253.30	5.585	.9752	.9752	.9751
	253.31	3.882	.9828	.9828	.9828
46					
	245.89	64.642	.6140	.6135	.6137
	245.88	53.134	.6959	.6950	.6954
	245.88	42.020	.7695	.7688	.7692
	245.87	32.107	.8300	.8295	.8298
	245.88	23.882	.8769	.8765	.8768
	245.87	17.413	.9120	.9118	.9119
	245.87	12.518	.9376	.9375	.9375
	245.87	8.908	.9561	.9560	.9560
	245.87	6.295	.9692	.9691	.9691
	245.86	4.428	.9784	.9784	.9784

TABLE 3-4 (CONTINUED)

EXPERIMENTAL DATA, COMPRESSIBILITY FACTORS
(MIXTURE 1, .3045 ETHYLENE)

RUN NUMBER	T (K)	PRESSURE (BAR)	Z(V) EQ 3-6-1	Z(6) EQ 3-6-2	Z(10) EQ 3-6-3
47					
	236.18	60.979	.5718	.5711	.5717
	236.18	51.940	.6546	.6539	.6543
	238.17	42.458	.7323	.7318	.7323
	238.17	33.397	.7985	.7983	.7986
	238.17	25.462	.8515	.8514	.8516
	238.16	18.959	.8922	.8922	.8923
	238.17	13.877	.9225	.9225	.9226
	238.17	10.032	.9447	.9447	.9448
	238.16	7.190	.9608	.9608	.9608
	238.16	5.120	.9722	.9723	.9722
48					
	230.71	53.936	.5632	.5623	.5625
	230.70	46.797	.6459	.6456	.6458
	230.70	38.685	.7232	.7232	.7234
	230.70	31.059	.7895	.7897	.7899
	230.69	24.026	.8432	.8434	.8435
	230.69	18.133	.8850	.8852	.8852
	230.69	13.442	.9165	.9166	.9166
	230.69	9.836	.9398	.9399	.9399
	230.70	7.129	.9568	.9569	.9569
	230.70	5.133	.9691	.9692	.9692
50					
	223.38	36.036	.7102	.7098	.7096
	223.39	29.282	.7775	.7770	.7768
	223.38	23.015	.8325	.8321	.8319
	223.39	17.631	.8758	.8754	.8752
	223.39	13.251	.9088	.9085	.9084
	223.39	9.820	.9336	.9334	.9332
	223.36	7.204	.9519	.9517	.9516
	223.38	5.246	.9653	.9652	.9651

TABLE 3-4 (CONTINUED)

EXPERIMENTAL DATA, COMPRESSIBILITY FACTORS
(MIXTURE 1, .3045 ETHYLENE)

RUN NUMBER	T (K)	PRESSURE (BAR)	Z(V) EQ 3-6-1	Z(6) EQ 3-6-2	Z(10) EQ 3-6-3
51					
	215.73	28.848	.7470	.7471	.7461
	215.66	23.257	.8067	.8060	.8052
	215.67	18.219	.8546	.8537	.8531
	215.67	13.964	.8918	.8910	.8906
	215.66	10.531	.9202	.9195	.9192
	215.67	7.848	.9415	.9410	.9407
	215.66	5.797	.9573	.9569	.9567
	215.66	4.255	.9689	.9686	.9684
52					
	208.13	20.010	.8142	.8144	.8128
	208.14	15.772	.8593	.8591	.8579
	208.13	12.179	.8945	.8942	.8933
	208.13	9.263	.9215	.9212	.9205
	208.13	6.964	.9419	.9416	.9411
	208.14	5.193	.9572	.9570	.9566
	208.13	3.849	.9685	.9684	.9681

TABLE 3-4 (CONTINUED)

EXPERIMENTAL DATA, COMPRESSIBILITY FACTORS
(MIXTURE 2, .5482 ETHYLENE)

RUN NUMBER	T (K)	PRESSURE (BAR)	Z(V) EQ 3-6-1	Z(6) EQ 3-6-2	Z(10) EQ 3-6-3
53					
	298.89	69.743	.7349	.7318	.7358
	298.87	48.772	.8168	.8143	.8183
	298.85	33.485	.8764	.8743	.8777
	298.86	22.624	.9176	.9160	.9187
	298.87	15.118	.9455	.9444	.9463
	298.87	10.023	.9641	.9633	.9647
	298.86	6.614	.9764	.9759	.9768
	298.85	4.348	.9845	.9842	.9848
54					
	293.46	68.783	.7168	.7132	.7176
	293.44	49.025	.8021	.7989	.8033
	293.45	34.159	.8651	.8625	.8663
	293.44	23.361	.9093	.9073	.9103
	293.45	15.770	.9395	.9381	.9403
	293.46	10.552	.9599	.9589	.9604
	293.43	7.015	.9735	.9728	.9739
	293.43	4.645	.9825	.9820	.9828
55					
	287.17	69.653	.6834	.6792	.6839
	287.16	50.982	.7748	.7708	.7756
	287.15	36.279	.8443	.8409	.8452
	287.15	25.228	.8941	.8915	.8949
	287.14	17.259	.9287	.9268	.9294
	287.13	11.678	.9523	.9509	.9528
	287.15	7.843	.9662	.9672	.9685
	287.14	5.242	.9788	.9782	.9791

TABLE 3-4 (CONTINUED)

EXPERIMENTAL DATA, COMPRESSIBILITY FACTORS
(MIXTURE 2, .5482 ETHYLENE)

RUN NUMBER	T (K)	PRESSURE (BAR)	Z(V) EQ 3-6-1	Z(6) EQ 3-6-2	Z(10) EQ 3-6-3
56					
	279.37	74.059	.6139	.6086	.6133
	279.37	56.750	.7141	.7093	.7146
	279.38	41.961	.7970	.7927	.3977
	279.37	30.072	.8591	.8556	.8598
	279.36	21.067	.9035	.9008	.9042
	279.35	14.529	.9345	.9326	.9350
	279.35	9.921	.9552	.9544	.9562
	279.35	6.724	.9702	.9693	.9705
57					
	273.12	74.985	.5580	.5530	.5576
	273.10	59.847	.6603	.6560	.6614
	273.10	45.878	.7522	.7482	.7536
	273.10	33.831	.8246	.8212	.8260
	273.09	24.239	.8780	.8753	.8793
	273.10	17.015	.9160	.9142	.9172
	273.08	11.780	.9428	.9414	.9436
	273.08	8.080	.9611	.9601	.9617
	273.08	5.508	.9737	.9730	.9741
58					
	266.24	34.217	.4940	.4880	.4925
	266.23	62.187	.5922	.5878	.5931
	266.22	50.026	.6916	.6873	.6928
	266.22	38.399	.7758	.7719	.7772
	266.22	28.383	.8409	.8377	.8423
	266.21	20.416	.8889	.8864	.8900
	266.20	14.417	.9231	.9213	.9240
	266.22	10.048	.9471	.9458	.9479
	266.21	6.942	.9638	.9629	.9643

TABLE 3-4 (CONTINUED)

EXPERIMENTAL DATA, COMPRESSIBILITY FACTORS
(MIXTURE 2, .5482 ETHYLENE)

RUN NUMBER	T (K)	PRESSURE (BAR)	Z(V) EQ 3-6-1	Z(6) EQ 3-6-2	Z(10) EQ 3-6-3
59					
	259.41	61.688	.5263	.5220	.5273
	259.41	52.216	.6272	.6237	.6289
	259.41	41.962	.7204	.7168	.7222
	259.41	32.176	.7969	.7937	.7987
	259.40	23.820	.8554	.8528	.8570
	259.40	17.200	.8985	.8965	.8998
	259.36	12.209	.9293	.9278	.9303
	259.39	8.565	.9511	.9500	.9518
	259.38	5.960	.9662	.9655	.9668
60					
	252.24	48.831	.6036	.6002	.6045
	252.25	40.327	.6982	.6942	.6990
	252.24	31.663	.7776	.7737	.7784
	252.23	24.915	.8396	.8286	.8328
	252.22	17.566	.8860	.8834	.8868
	252.22	12.655	.9197	.9178	.9204
	252.22	8.995	.9438	.9424	.9443
	252.23	6.334	.9609	.9599	.9613
	252.23	4.433	.9728	.9721	.9731
61					
	244.25	37.553	.6787	.6762	.6799
	244.26	30.183	.7607	.7566	.7607
	244.22	23.273	.8255	.8212	.8250
	244.21	17.405	.8746	.8710	.8741
	244.22	12.740	.9107	.9079	.9104
	244.23	9.185	.9369	.9348	.9367
	244.23	6.555	.9555	.9540	.9554
	244.20	4.644	.9688	.9677	.9687

TABLE 3-4 (CONTINUED)

EXPERIMENTAL DATA, COMPRESSIBILITY FACTORS
(MIXTURE 2, .5482 ETHYLENE)

RUN NUMBER	T (K)	PRESSURE (BAR)	Z(V) EQ 3-6-1	Z(6) EQ 3-6-2	Z(10) EQ 3-6-3
62					
	237.37	29.056	.7407	.7386	.7416
	237.39	22.843	.8078	.8056	.8087
	237.36	17.378	.8599	.8578	.8606
	237.36	12.912	.8990	.8973	.8996
	237.32	9.436	.9277	.9264	.9282
	237.33	6.815	.9486	.9476	.9490
	237.36	4.882	.9636	.9629	.9639
63					
	229.93	20.383	.8111	.8085	.8106
	229.94	15.650	.8614	.8588	.8608
	229.93	11.743	.8993	.8971	.8988
	229.94	8.667	.9273	.9256	.9270
	229.94	6.324	.9478	.9465	.9476
	229.93	4.575	.9627	.9617	.9625
64					
	223.27	18.585	.8100	.8088	.8096
	223.27	14.408	.8595	.8577	.8588
	223.27	10.916	.8971	.8953	.8964
	223.27	8.135	.9252	.9236	.9246
	223.27	5.992	.9458	.9446	.9454
	223.26	4.376	.9609	.9600	.9606

TABLE 3-4 (CONTINUED)

EXPERIMENTAL DATA, COMPRESSIBILITY FACTORS
(MIXTURE 3, .7581 ETHYLENE)

RUN NUMBER	T (K)	PRESSURE (BAR)	Z(V) EQ 3-6-1	Z(6) EQ 3-6-2	Z(10) EQ 3-6-3
66					
	288.15	69.094	.5382	.5377	.5437
	288.13	53.261	.6734	.6719	.6785
	288.14	39.401	.7744	.7726	.7794
	288.12	28.091	.8465	.8449	.8512
	288.12	19.524	.8966	.8954	.9005
	288.10	13.344	.9308	.9299	.9338
	288.10	9.021	.9538	.9532	.9560
	288.07	6.055	.9693	.9689	.9708
	288.12	4.048	.9796	.9793	.9807
68					
	280.96	49.370	.6634	.6626	.6689
	280.93	37.387	.7635	.7622	.7689
	280.93	27.140	.8369	.8358	.8420
	280.95	19.146	.8888	.8880	.8931
	280.92	13.257	.9248	.9241	.9281
	280.95	9.067	.9493	.9489	.9518
	280.94	6.152	.9660	.9656	.9677
	280.96	4.154	.9772	.9770	.9784
69					
	272.96	54.884	.5278	.5263	.5328
	272.96	45.498	.6500	.6489	.6551
	272.95	35.352	.7496	.7484	.7552
	272.95	26.199	.8247	.8237	.8300
	272.94	18.802	.8790	.8781	.8834
	272.95	13.211	.9171	.9165	.9206
	272.94	9.155	.9436	.9431	.9461
	272.94	6.287	.9617	.9614	.9635
	272.95	4.292	.9741	.9738	.9754

TABLE 3-4 (CONTINUED)

EXPERIMENTAL DATA, COMPRESSIBILITY FACTORS
(MIXTURE 3, .7581 ETHYLENE)

RUN NUMBER	T (K)	PRESSURE (BAR)	Z(V) EQ 3-6-1	Z(6) EQ 3-6-2	Z(10) EQ 3-6-3
70					
	266.13	44.585	.6065	.6052	.6112
	266.11	36.029	.7125	.7105	.7171
	266.11	27.516	.7953	.7934	.8000
	266.11	20.216	.8566	.8551	.8608
	266.10	14.468	.9006	.8995	.9040
	266.10	10.180	.9316	.9308	.9342
	266.10	7.081	.9531	.9525	.9550
	266.11	4.889	.9680	.9676	.9693
71					
	259.30	37.842	.6459	.6448	.6508
	259.30	30.318	.7415	.7397	.7463
	259.29	23.086	.8154	.8137	.8198
	259.29	16.978	.8700	.8687	.8739
	259.28	12.199	.9094	.9083	.9124
	259.28	8.629	.9372	.9364	.9395
	259.29	6.040	.9566	.9561	.9583
	259.28	4.196	.9702	.9698	.9714
72					
	251.34	28.689	.7237	.7205	.7264
	251.34	22.346	.8002	.7968	.8027
	251.33	16.755	.8576	.8548	.8599
	251.36	12.239	.8996	.8975	.9015
	251.35	8.785	.9296	.9280	.9311
	251.35	6.231	.9509	.9498	.9521
	251.36	4.384	.9659	.9650	.9667

TABLE 3-4 (CONTINUED)

EXPERIMENTAL DATA, COMPRESSIBILITY FACTORS
(MIXTURE 3, .7581 ETHYLENE)

RUN NUMBER	T (K)	PRESSURE (BAR)	Z(V) EQ 3-6-1	Z(6) EQ 3-6-2	Z(10) EQ 3-6-3
74					
	238.46	16.752	.8249	.8225	.8265
	238.47	12.642	.8740	.8716	.8752
	238.47	9.329	.9100	.9080	.9110
	238.47	6.781	.9361	.9345	.9368
	238.47	4.874	.9548	.9536	.9553
	238.47	3.480	.9681	.9672	.9685

TABLE 3-5

CALCULATED COMPRESSIBILITY FACTORS
FROM EQ 3-6-3

T (K)	P (BAR)	COMPRESSIBILITY FACTORS MIXTURE 1	MIXTURE 2	MIXTURE 3	ETHYLENE
230.0					
	5.0	.9697	.9590	.9477	.9330
	7.5	.9541	.9374	.9195	.8958
	10.0	.9382	.9151	.8895	.8552
	12.5	.9220	.8918	.8575	.8098
	15.0	.9054	.8675	.8228	.7575
	17.5	.8883	.8420	.7848	.6932
	20.0	.8709	.8151	.7422	.5985
	22.5	.8530	.7865	.6926	.0978
	25.0	.8345	.7559	.6305	.1083
	27.5	.8155	.7227	.5308	.1188
	30.0	.7958	.6859	-.1176	.1293
	32.5	.7755	.6442	-.1273	.1397
	35.0	.7543	.5944	-.1370	.1500
	37.5	.7323	.5277	-.1467	.1603
	40.0	.7092	.1733	-.1563	.1706
	42.5	.6849	.1727	-.1659	.1808
	45.0	.6593	.1404	-.1755	.1910
	47.5	.6321	.1534	-.1851	.2011
	50.0	.6031	-.1166	-.1947	.2112
	52.5	.5721	-.1224	-.2043	.2213
	55.0	.5392	-.1282	-.2139	.2313
235.0					
	5.0	.9717	.9618	.9516	.9379
	7.5	.9572	.9418	.9257	.9038
	10.0	.9425	.9211	.8984	.8670
	12.5	.9274	.8997	.8694	.8267
	15.0	.9121	.8774	.8384	.7814
	17.5	.8964	.8542	.8050	.7285
	20.0	.8804	.8300	.7683	.6619
	22.5	.8640	.8044	.7272	.5508
	25.0	.8473	.7774	.6795	.1131
	27.5	.8301	.7486	.6200	.1240
	30.0	.8124	.7175	.5267	.1347
	32.5	.7942	.6836	-.1262	.1454
	35.0	.7755	.6456	-.1357	.1561
	37.5	.7561	.6017	-.1453	.1667
	40.0	.7361	.5473	-.1549	.1772
	42.5	.7153	.4654	-.1644	.1877
	45.0	.6937	-.1036	-.1739	.1981
	47.5	.6713	.1459	-.1834	.2084
	50.0	.6478	.1567	-.1929	.2187
	52.5	.6233	.1696	-.2024	.2290
	55.0	.5979	-.1264	-.2119	.2392

NOTE: THOSE VALUES INSIDE THE BOX ARE WITHIN THE EXPERIMENTAL RANGE OF THIS WORK.

TABLE 3-5 (CONTINUED)

CALCULATED COMPRESSIBILITY FACTORS
FROM EQ 3-6-3

T (K)	P (BAR)	COMPRESSIBILITY FACTORS MIXTURE 1	MIXTURE 2	MIXTURE 3	ETHYLENE
240.0					
	5.0	.9736	.9643	.9552	.9422
	7.5	.9601	.9457	.9313	.9108
	10.0	.9463	.9265	.9062	.8772
	12.5	.9324	.9068	.8798	.8409
	15.0	.9182	.8863	.8519	.8009
	17.5	.9037	.8651	.8220	.7558
	20.0	.8890	.8431	.7898	.7026
	22.5	.8740	.8201	.7546	.6339
	25.0	.8586	.7959	.7153	.1186
	27.5	.8430	.7705	.6699	.1297
	30.0	.8270	.7436	.6141	.1408
	32.5	.8106	.7147	.5314	.1518
	35.0	.7938	.6835	-.1345	.1627
	37.5	.7766	.6493	-.1440	.1735
	40.0	.7590	.6108	-.1534	.1843
	42.5	.7408	.5658	-.1629	.1950
	45.0	.7221	.5093	-.1723	.2056
	47.5	.7029	.4219	-.1817	.2161
	50.0	.6831	.2787	-.1911	.2266
	52.5	.6627	.1609	-.2005	.2370
	55.0	.6418	.2401	-.2099	.2474
245.0					
	5.0	.9753	.9666	.9583	.9460
	7.5	.9626	.9493	.9362	.9170
	10.0	.9498	.9315	.9132	.8861
	12.5	.9369	.9132	.8890	.8531
	15.0	.9237	.8943	.8636	.8173
	17.5	.9103	.8748	.8367	.7779
	20.0	.8967	.8547	.8081	.7332
	22.5	.8829	.8338	.7772	.6800
	25.0	.8688	.8121	.7436	.6097
	27.5	.8545	.7894	.7063	.1366
	30.0	.8400	.7656	.6637	.1479
	32.5	.8251	.7405	.6123	.1591
	35.0	.8100	.7139	.5413	.1702
	37.5	.7945	.6855	-.1426	.1812
	40.0	.7788	.6547	-.1520	.1921
	42.5	.7627	.6210	-.1613	
	45.0	.7462	.5833	-.1707	
	47.5	.7294	.5398	-.1800	
	50.0	.7122	.4870	-.1893	
	52.5	.6947	.4187	-.1986	
	55.0	.6768	.3438	-.2078	

NOTE: THOSE VALUES INSIDE THE BOX ARE WITHIN THE EXPERIMENTAL RANGE OF THIS WORK.

TABLE 3-5 (CONTINUED)

CALCULATED COMPRESSIBILITY FACTORS
FROM EQ 3-6-3

T (K)	P (BAR)	COMPRESSIBILITY FACTORS MIXTURE 1	MIXTURE 2	MIXTURE 3	ETHYLENE
250.0					
	5.0	.9768	.9687	.9611	.9495
	7.5	.9650	.9525	.9407	.9224
	10.0	.9531	.9360	.9194	.8940
	12.5	.9410	.9190	.8972	.8638
	15.0	.9287	.9015	.8739	.8314
	17.5	.9163	.8836	.8495	.7963
	20.0	.9037	.8651	.8238	.7576
	22.5	.8910	.8461	.7964	.7135
	25.0	.8780	.8263	.7670	.6609
	27.5	.8649	.8059	.7352	.5902
	30.0	.8516	.7846	.7001	.1567
	32.5	.8380	.7625	.6605	.1680
	35.0	.8243	.7393	.6138	.1791
	37.5	.8103	.7148	.5535	.1901
	40.0	.7961	.6890	-.1505	.2010
	42.5	.7817	.6615	-.1598	.2118
	45.0	.7670	.6320	-.1690	.2226
	47.5	.7521	.5999	-.1782	.2333
	50.0	.7370	.5647	-.1875	.2439
	52.5	.7216	.5254	-.1966	.2544
	55.0	.7060	.4813	-.2058	.2648
255.0					
	5.0	.9782	.9707	.9637	.9526
	7.5	.9672	.9555	.9446	.9274
	10.0	.9560	.9401	.9249	.9010
	12.5	.9448	.9243	.9044	.8732
	15.0	.9334	.9081	.8831	.8437
	17.5	.9218	.8915	.8608	.8121
	20.0	.9101	.8745	.8374	.7778
	22.5	.8983	.8570	.8128	.7400
	25.0	.8864	.8390	.7868	.6969
	27.5	.8743	.8205	.7590	.6455
	30.0	.8620	.8013	.7290	.5761
	32.5	.8496	.7815	.6962	.1800
	35.0	.8371	.7609	.6597	.1906
	37.5	.8244	.7395	.6178	.2012
	40.0	.8115	.7172	.5667	.2118
	42.5	.7984	.6938	.4936	.2224
	45.0	.7852	.6692	-.1674	.2329
	47.5	.7719	.6432	-.1765	.2434
	50.0	.7584	.6157	-.1856	.2538
	52.5	.7447	.5864	-.1947	.2642
	55.0	.7309	.5551	-.2038	.2745

NOTE: THOSE VALUES INSIDE THE BOX ARE WITHIN THE EXPERIMENTAL RANGE OF THIS WORK.

TABLE 3-5 (CONTINUED)

CALCULATED COMPRESSIBILITY FACTORS
FROM EQ 3-6-3

T (K)	P (BAR)	COMPRESSIBILITY FACTORS MIXTURE 1	MIXTURE 2	MIXTURE 3	ETHYLENE
260.0					
	5.0	.9796	.9724	.9660	.9554
	7.5	.9692	.9583	.9483	.9318
	10.0	.9588	.9439	.9299	.9073
	12.5	.9482	.9291	.9110	.8816
	15.0	.9376	.9141	.8913	.8545
	17.5	.9269	.8987	.8708	.8258
	20.0	.9160	.8830	.8495	.7951
	22.5	.9050	.8669	.8272	.7618
	25.0	.8940	.8504	.8038	.7251
	27.5	.8828	.8334	.7791	.6834
	30.0	.8715	.8160	.7529	.6338
	32.5	.8601	.7981	.7248	.5679
	35.0	.8486	.7797	.6944	.2086
	37.5	.8370	.7607	.6611	.2172
	40.0	.8252	.7410	.6237	.2264
	42.5	.8134	.7206	.5801	.2359
	45.0	.8014	.6995	.5257	.2457
	47.5	.7893	.6775	.4381	.2555
	50.0	.7771	.6546	-.1838	.2654
	52.5	.7649	.6307	-.1928	.2753
	55.0	.7526	.6058	-.2018	.2853
265.0					
	5.0	.9808	.9741	.9682	.9580
	7.5	.9711	.9608	.9516	.9359
	10.0	.9613	.9473	.9345	.9130
	12.5	.9514	.9336	.9169	.8891
	15.0	.9415	.9195	.8986	.8641
	17.5	.9315	.9053	.8798	.8379
	20.0	.9214	.8907	.8603	.8100
	22.5	.9112	.8758	.8399	.7803
	25.0	.9009	.8606	.8187	.7482
	27.5	.8906	.8451	.7965	.7128
	30.0	.8801	.8292	.7732	.6729
	32.5	.8696	.8129	.7486	.6259
	35.0	.8590	.7962	.7225	.5650
	37.5	.8483	.7791	.6945	.4306
	40.0	.8376	.7616	.6642	.2508
	42.5	.8267	.7435	.6309	.2560
	45.0	.8158	.7250	.5935	.2631
	47.5	.8048	.7058	.5502	.2712
	50.0	.7938	.6862	.4962	.2798
	52.5	.7827	.6659	.4102	.2887
	55.0	.7716	.6450	-.1998	.2977

NOTE: THOSE VALUES INSIDE THE BOX ARE WITHIN THE EXPERIMENTAL RANGE OF THIS WORK.

TABLE 3-5 (CONTINUED)

CALCULATED COMPRESSIBILITY FACTORS
FROM EQ 3-6-3

T (K)	P (BAR)	COMPRESSIBILITY FACTORS MIXTURE 1	MIXTURE 2	MIXTURE 3	ETHYLENE
270.0					
	5.0	.9819	.9756	.9701	.9604
	7.5	.9728	.9632	.9546	.9396
	10.0	.9636	.9505	.9386	.9182
	12.5	.9544	.9376	.9222	.8960
	15.0	.9451	.9245	.9053	.8728
	17.5	.9357	.9112	.8879	.8487
	20.0	.9263	.8977	.8699	.8233
	22.5	.9168	.8839	.8512	.7964
	25.0	.9073	.8699	.8319	.7678
	27.5	.8977	.8556	.8118	.7369
	30.0	.8880	.8410	.7909	.7031
	32.5	.8783	.8261	.7690	.6653
	35.0	.8685	.8109	.7460	.6214
	37.5	.8586	.7955	.7217	.5666
	40.0	.8487	.7796	.6960	.4825
	42.5	.8388	.7634	.6686	.3019
	45.0	.8289	.7469	.6390	.2929
	47.5	.8189	.7300	.6067	.2945
	50.0	.8087	.7127	.5709	.2993
	52.5	.7986	.6951	.5303	.3058
	55.0	.7885	.6771	.4820	.3131
275.0					
	5.0	.9830	.9770	.9719	.9626
	7.5	.9744	.9653	.9574	.9431
	10.0	.9658	.9534	.9424	.9230
	12.5	.9571	.9414	.9271	.9022
	15.0	.9484	.9291	.9114	.8808
	17.5	.9397	.9167	.8952	.8584
	20.0	.9309	.9041	.8786	.8351
	22.5	.9220	.8913	.8614	.8106
	25.0	.9131	.8783	.8437	.7848
	27.5	.9042	.8651	.8254	.7574
	30.0	.8952	.8517	.8064	.7279
	32.5	.8862	.8380	.7867	.6959
	35.0	.8771	.8241	.7662	.6604
	37.5	.8680	.8100	.7448	.6198
	40.0	.8589	.7956	.7224	.5713
	42.5	.8497	.7810	.6988	.5069
	45.0	.8405	.7661	.6740	.4015
	47.5	.8313	.7510	.6477	.3418
	50.0	.8221	.7356	.6196	.3312
	52.5	.8129	.7200	.5894	.3305
	55.0	.8037	.7041	.5567	.3336

NOTE: THOSE VALUES INSIDE THE BOX ARE WITHIN THE EXPERIMENTAL RANGE OF THIS WORK.

TABLE 3-5 (CONTINUED)

CALCULATED COMPRESSIBILITY FACTORS
FROM EQ 3-6-3

T (K)	P (BAR)	COMPRESSIBILITY FACTORS MIXTURE 1	MIXTURE 2	MIXTURE 3	ETHYLENE
280.0					
	5.0	.9840	.9783	.9736	.9646
	7.5	.9759	.9673	.9599	.9463
	10.0	.9678	.9562	.9459	.9274
	12.5	.9597	.9448	.9316	.9080
	15.0	.9515	.9334	.9169	.8880
	17.5	.9433	.9218	.9019	.8673
	20.0	.9351	.9100	.8865	.8458
	22.5	.9268	.8981	.8706	.8233
	25.0	.9185	.8860	.8543	.7999
	27.5	.9102	.8738	.8375	.7752
	30.0	.9018	.8614	.8202	.7490
	32.5	.8934	.8488	.8023	.7211
	35.0	.8850	.8360	.7838	.6909
	37.5	.8766	.8230	.7647	.6578
	40.0	.8681	.8099	.7448	.6208
	42.5	.8597	.7966	.7242	.5781
	45.0	.8512	.7831	.7027	.5263
	47.5	.8427	.7695	.6802	.4612
	50.0	.8343	.7556	.6568	.3996
	52.5	.8258	.7416	.6322	.3728
	55.0	.8173	.7275	.6063	.3643
285.0					
	5.0	.9849	.9796	.9751	.9666
	7.5	.9773	.9692	.9623	.9493
	10.0	.9697	.9587	.9492	.9316
	12.5	.9620	.9480	.9358	.9134
	15.0	.9544	.9373	.9221	.8947
	17.5	.9467	.9264	.9080	.8754
	20.0	.9390	.9154	.8937	.8555
	22.5	.9312	.9043	.8790	.8348
	25.0	.9235	.8931	.8639	.8134
	27.5	.9157	.8817	.8484	.7909
	30.0	.9079	.8702	.8325	.7674
	32.5	.9001	.8585	.8162	.7426
	35.0	.8923	.8468	.7994	.7163
	37.5	.8845	.8348	.7821	.6880
	40.0	.8766	.8228	.7643	.6574
	42.5	.8688	.8106	.7459	.6238
	45.0	.8610	.7983	.7270	.5862
	47.5	.8531	.7859	.7074	.5434
	50.0	.8453	.7733	.6871	.4950
	52.5	.8375	.7607	.6661	.4472
	55.0	.8297	.7479	.6444	.4148

NOTE: THOSE VALUES INSIDE THE BOX ARE WITHIN THE EXPERIMENTAL RANGE OF THIS WORK.

TABLE 3-5 (CONTINUED)

CALCULATED COMPRESSIBILITY FACTORS
FROM EQ 3-6-3

T (K)	P (BAR)	COMPRESSIBILITY FACTORS MIXTURE 1	MIXTURE 2	MIXTURE 3	ETHYLENE
290.0					
	5.0	.9857	.9807	.9765	.9684
	7.5	.9786	.9709	.9645	.9521
	10.0	.9714	.9610	.9522	.9355
	12.5	.9642	.9510	.9396	.9184
	15.0	.9570	.9409	.9268	.9009
	17.5	.9498	.9307	.9137	.8829
	20.0	.9426	.9205	.9003	.8644
	22.5	.9353	.9101	.8866	.8453
	25.0	.9281	.8996	.8726	.8256
	27.5	.9208	.8890	.8584	.8051
	30.0	.9135	.8783	.8437	.7838
	32.5	.9063	.8675	.8287	.7614
	35.0	.8990	.8566	.8134	.7380
	37.5	.8917	.8455	.7977	.7133
	40.0	.8844	.8344	.7815	.6870
	42.5	.8772	.8232	.7650	.6588
	45.0	.8699	.8120	.7480	.6284
	47.5	.8626	.8006	.7306	.5952
	50.0	.8554	.7891	.7128	.5590
	52.5	.8482	.7776	.6944	.5203
	55.0	.8410	.7661	.6757	.4823
295.0					
	5.0	.9865	.9818	.9779	.9701
	7.5	.9798	.9725	.9665	.9548
	10.0	.9730	.9632	.9549	.9391
	12.5	.9663	.9538	.9431	.9231
	15.0	.9595	.9443	.9311	.9067
	17.5	.9527	.9347	.9189	.8900
	20.0	.9459	.9251	.9064	.8727
	22.5	.9391	.9154	.8937	.8550
	25.0	.9324	.9055	.8807	.8368
	27.5	.9256	.8957	.8674	.8179
	30.0	.9188	.8857	.8539	.7984
	32.5	.9120	.8756	.8401	.7782
	35.0	.9052	.8655	.8260	.7571
	37.5	.8984	.8553	.8116	.7351
	40.0	.8916	.8451	.7969	.7119
	42.5	.8849	.8347	.7819	.6875
	45.0	.8781	.8243	.7666	.6617
	47.5	.8714	.8139	.7510	.6341
	50.0	.8647	.8034	.7350	.6048
	52.5	.8580	.7929	.7187	.5736
	55.0	.8514	.7823	.7021	.5413

NOTE: THOSE VALUES INSIDE THE BOX ARE WITHIN THE EXPERIMENTAL RANGE OF THIS WORK.

TABLE 3-6

THE INTERACTIONAL SECOND VIRIAL COEFFICIENTS OF
THE METHANE – ETHYLENE SYSTEM

T (K)	B12 MIXTURE 1	B12 MIXTURE 2	B12 MIXTURE 3	B12(MEAN) EQ 3-5-20
240	-118·1	-118·6	-114·2	-118·1
245	-113·2	-113·4	-106·7	-112·8
250	-108·5	-108·5	-99·8	-107·8
255	-104·0	-103·7	-93·4	-103·1
260	-99·7	-99·2	-87·5	-98·6
265	-95·7	-94·9	-82·1	-94·4
270	-91·9	-90·9	-77·2	-90·4
275	-88·3	-87·1	-72·7	-86·7
280	-84·9	-83·6	-68·6	-83·2
285	-81·6	-80·3	-64·9	-79·9
290	-78·5	-77·2	-61·5	-76·8
295	-75·6	-74·4	-58·6	-74·0
300	-72·9	-71·8	-55·9	-71·3

3-6 Discussion

3-6-1 Introduction

In the previous section the compressibility factors, densities and 2nd and 3rd virial coefficients of pure ethylene and three methane-ethylene mixtures were presented. As described in sections (3-3) and (3-4) different methods or different equations of state in the non-linear least-squares procedure produced different results (see Table 3-4).

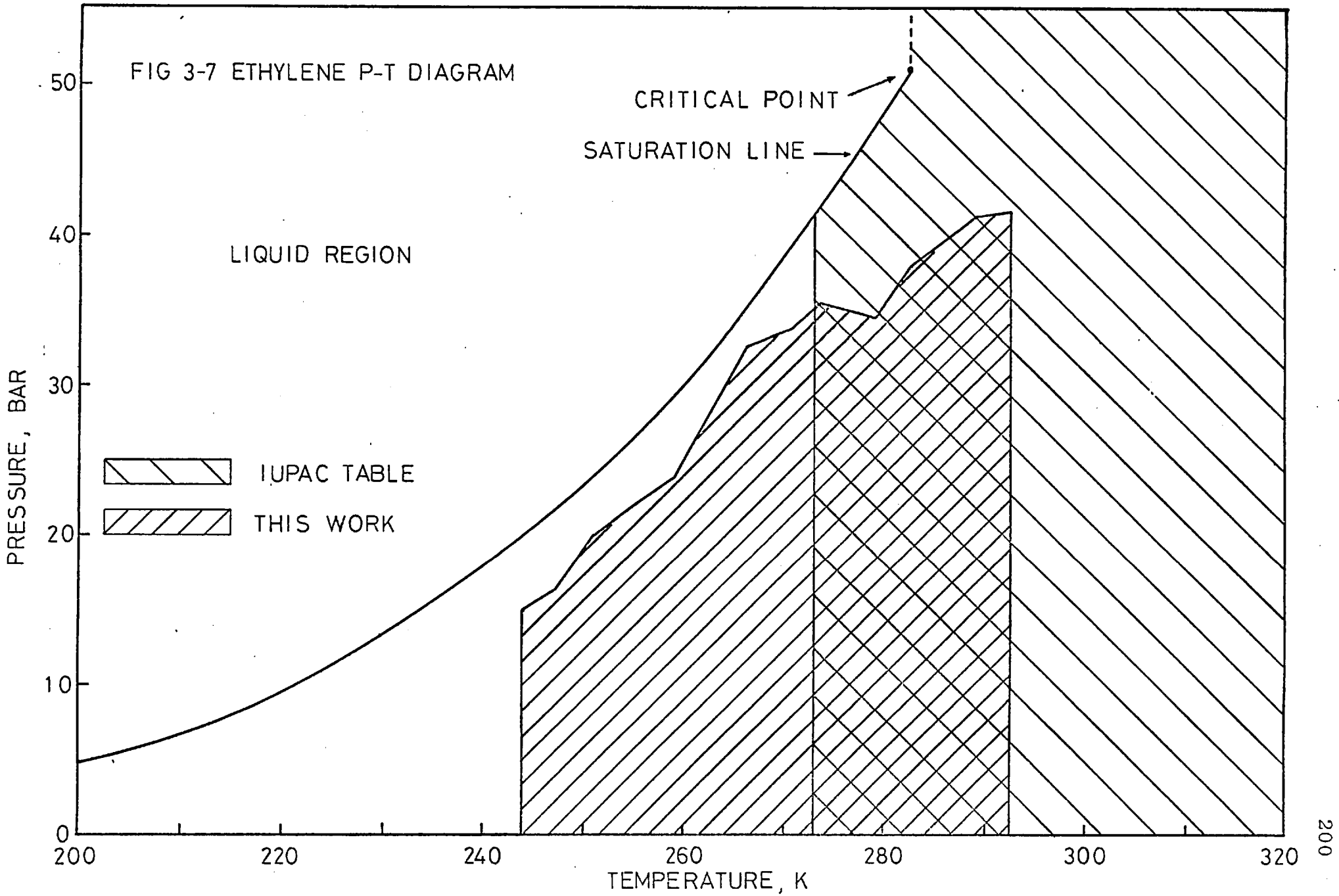
Thus in this section the compressibility factors in Table 3-4 are systematically compared each other (i.e. Z(V), Z(6) and Z(10)) and this comparison will be followed by a discussion on the way to choose valid values (and hence how to choose valid equation).

In the experimental range of this work few other worker's data are available for making comparisons. Although Michels' original data for ethylene[14,15,16] are still regarded as the most acceptable values, the experimental temperature range was from $0^{o}C$ upwards with an interval of $25^{o}C$, between which the critical point ($9.5^{o}C$) lies.

For this reason in the IUPAC Table 'ETHYLENE, 1972', compiled by Angus,[17] the region below $0^{o}C$ for the gas phase is left blank.

Thus Fig 3-7 shows that this work covers a region between 245 - $293^{o}K$ under saturation line and hence duplicates to that of IUPAC ethylene table in the range of 273 - $293^{o}K$ between which only 8 Michels' experimental data points exist, on the $0^{o}C$ isotherm.

In the case of methane-ethylene system McMath and Edmister published vapor-phase compressibility factors at -7, 4.5 and


FIG 3-7 ETHYLENE P-T DIAGRAM
CRITICAL POINT
SATURATION LINE
LIQUID REGION
IUPAC TABLE
THIS WORK
PRESSURE, BAR
TEMPERATURE, K
0
10
20
30
40
50
200
220
240
260
280
300
320

15°C and pressures from 17 bar to 151 bar.[18] Lee and Edmister reported on the same mixture at 25, 50 and 75°C upto about 800 bar.[19]

3-6-2 Comparison of the Compressibility Factors

Table 3-4 shows three sets of compressibility factors for all data point from three different equations of state,

$$Z = \frac{PV}{RT} = 1 + B\rho + C\rho^2 \qquad (3\text{-}6\text{-}1)$$

$$P = \rho T (R + B\rho + C\rho^2 + D\rho^3) \qquad (3\text{-}6\text{-}2)$$

where $B = a_1 - a_2/T - a_3/T^2$

$C = a_4 + a_5/T$

$C = a_6$

$$P = \rho T (R + B\rho + C\rho^2 + D\rho^3 + E\rho^4) \qquad (3\text{-}6\text{-}3)$$

where $B = a_1 - a_2/T - a_3/T^2 - a_4/T^3$

$C = a_5 + a_6/T + a_7/T^2$

$D = a_8 + a_9/T$

$E = a_{10}$

(The a's in Eq. 3-6-2 and 3-6-3 are in Table 3-1)

From the Table (3-4) one can see considerable differences in the compressibility factors (i.e. Z(V), Z(6) and Z(10)) for mixture 3 (nominal 75% ethylene) especially at high pressures. Also it is seen that the magnitudes of the deviations for mixture 2 (nominal 50% ethylene) are smaller than those in the case of mixture 3, and in the case of mixture 1 (nominal 25% ethylene) they are much smaller again than those of the other two mixtures, i.e.

$$|\Delta(\text{mixture 3})| > |\Delta(\text{mixture 2})| > |\Delta(\text{mixture1})|$$

where $\Delta = Z(V) - Z(10)$

or $\Delta = Z(V) - Z(6)$

This systematic trend in the differences of the computed Z from different equations of state, (3-6-1), (3-6-2) and (3-6-3), suggests that the capabilities of the equations to represent the P-ρ-T data are different especially in the highly non-ideal region ($Z \doteqdot 0.5 \sim 0.6$).

Thus in order to choose the best equation among the three (hence choosing the best values of Z) modified Bender equations will be compared with each other and these will be then compared with the virial equation. The discussion is based on the principle of least-squares and as a starting point the results of mixture 3 for the 6-coefficient Bender equation will be considered first.

The compressibility factors of ethylene in Table 3-4 are not considered in this discussion, since the maximum experimental pressure of the gas (41 bar, 292°K, $Z \doteqdot 0.6872$) is much lower than those of the mixtures (70 bar, 288°K, $Z \doteqdot 0.54$ for mixture 3). Thus the comparison between the results of ethylene and the other mixtures is considered to be unrealistic.

3-6-3 The Compressibility Factors of Mixture 3

Using the 6-coefficient Bender equation (3-6-2) the computation of the least-squares procedure converged after 14 iterations from the first approximate values of the least-squares parameters which were determined as described in section (3-5-1).

The values of the objective function, S, decreased rapidly

in each iteration and the final value was,

$$S_6 = \sum_{i}^{n} \sum_{j}^{n'} W_{ij} \cdot R_{ij}^{\,2} = 0.23044 \cdot 10^{-5} \qquad (3\text{-}6\text{-}4)$$

where n = number of isotherms

n'= number of expansion at i'th isotherm.

W_{ij} = weighting factor defined in Eq.(3-3-19)

R_{ij} = residuals defined in Eq.(3-4-16)

After the 6 coefficients were determined for mixture 3 the residuals, R_{ij}, for all i's and all j'th, were again computed by means of Eq.(3-4-16). Here two matters need to be considered,

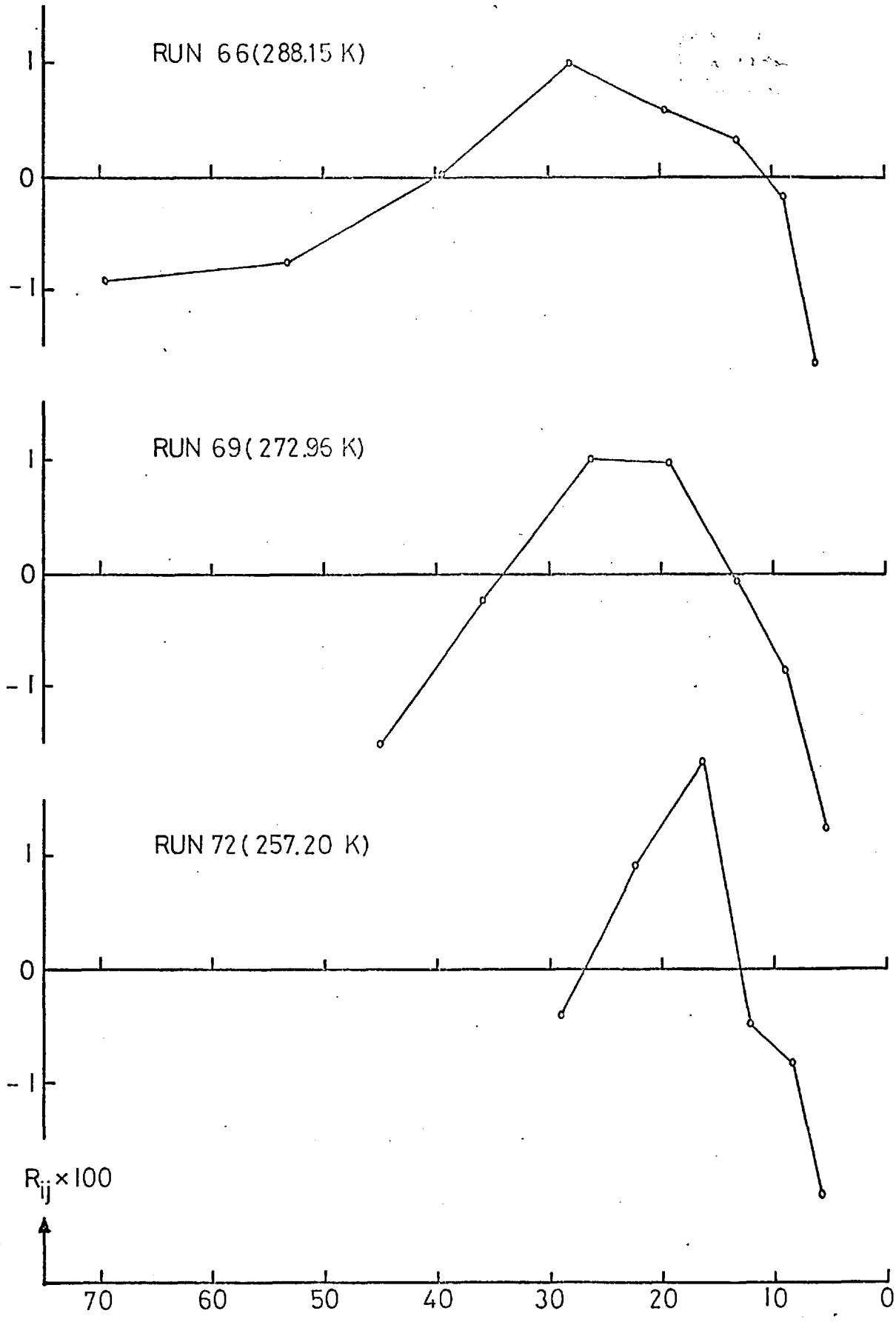
(i) the order of magnitude of the objective function,

(ii) the random (or systematic) variation of the residuals with the pressures and temperatures.

From the point of view of the least-squares principle the better equation is considered to be the one which gives a smaller value of objective function, no matter what form of equation of state is used, provided that the definition of the residual, i.e. Eq.(3-4-16), remains unchanged.

A more important matter to be considered here is the change of residuals as functions of pressure and temperature. Thus when the residuals, R_{ij}, were plotted against the experimental pressure (before expansion) a distinctive systematic 'pattern' was found in all seven runs for mixture 3 ($238^{o}K$ - $288^{o}K$).

In Fig 3-8, by way of example, the residuals were plotted against the experimental pressure (before expansion) for three isotherms.



EQ. 3-6-2

FIG 3-8 RESIDUAL V. PRESSURE

The figure shows that

(i) the pattern of the residual change with pressure is a downward parabola with positive values in the middle pressure range and negative values at both ends,

(ii) the values of R_{ij} at the low pressure range are more or less the same at pressures below 10 bar, e.g. at about 5 bar $R_{ij} \doteqdot 2.0 \cdot 10^{-2} \doteqdot$ constant,

(iii) at pressures higher than 10 bar the magnitudes of R_{ij} increase with pressure,

(iv) at lower temperatures the parabola becomes sharper and shifts to the right hand side.

These facts suggest that the equation of state (3-6-2) is unable to represent the experimental P-V-T data in two senses.

(i) Firstly, from the parabolic shape in Fig 3-8, the systematic behaviour of the residuals with respect to pressure indicates that the equation of state used in the least-squares procedure was not able to handle adequately all the experimental pressures. Thus the equation is considered to need more density terms.

(ii) Secondly, the increase in magnitude of R_{ij} at lower temperature suggests that more temperature terms are needed in order to present all the experimental data points in one equation.

In these regards the 6-coefficient equation was altered to 10-coefficient equation, i.e.

from

$$P = \rho T \{ R + (a_1 - a_2/T - a_3/T^2 \square) \rho + (a_4 + a_5/T \square) \rho^2 + (a_6 \square) \rho^3 \square \} \qquad (3\text{-}6\text{-}2)$$

to

$$P = \rho T \{ R + (a_1 - a_2/T - a_3/T^2 - \boxed{a_4/T^3}) \rho + (a_5 + a_6/T + \boxed{a_7/T^2}) \rho^2 + (a_8 + \boxed{a_9/T}) \rho^3 + \boxed{a_{10} \rho^4} \} \qquad (3\text{-}6\text{-}3)$$

Before evaluating the 10 coefficients in Eq.(3-6-3) the first approximate values to these coefficients were determined by using all experimental data points as explained in section (3-5-1).

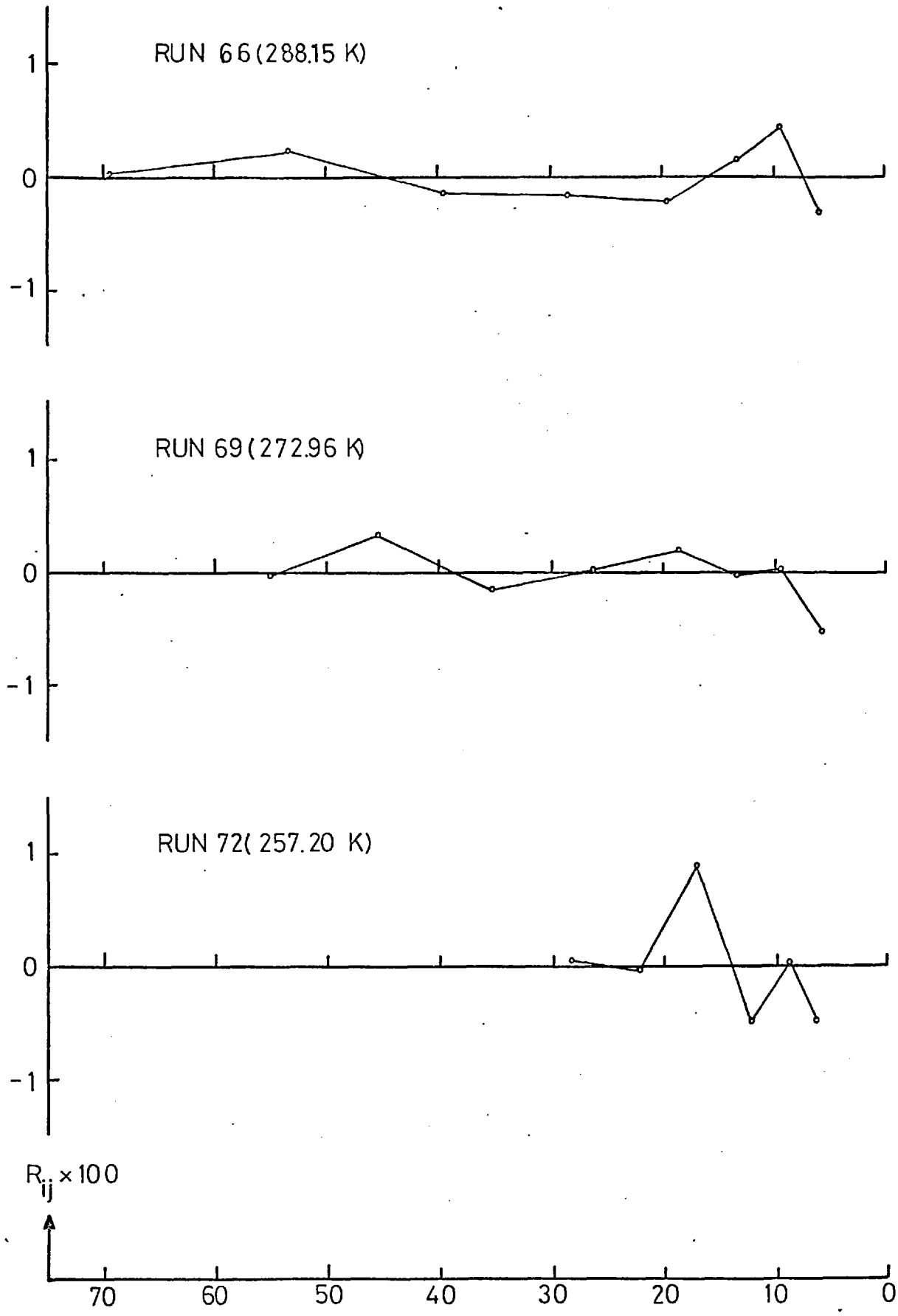
Determination of 17 least-squares parameters, i.e. $a_1, a_2, \cdots a_{10}, N_1, N_2, \cdots N_7$, took, as expected, more computing time and more iterations. After having converged ($\Delta a_1 < 0.1$), the objective function, S, and the residuals, R_{ij}, were evaluated for every i'th run and every j'th expansion.

The value of S from Eq.(3-6-3) is now

$$S_{10} = \sum_{i}^{n} \sum_{j}^{n'} W_{ij} \cdot R_{ij}^{\,2} = 0.22770 \cdot 10^{-6} \qquad (3\text{-}6\text{-}5)$$

Compared to the value from the 6-coefficient equation this value, S_{10}, is about 10 times less than S_6 ($0.230 \cdot 10^{-5}$). Thus it has been proved that Eq.(3-6-3) is 'better' equation than Eq.(3-6-2).

However this fact alone does not tell whether equation (3-6-3) is 'adequate' to represent all the experimental data points, until the magnitudes and the behaviour of the residuals in each run have been examined.



EQ. 3-6-3

FIG 3-9 PRESSURE V RESIDUAL

Thus the residuals, R_{ij}, were again plotted against the experimental pressures and Fig 3-9 shows three of them, which are the same isotherms as those in Fig 3-8. Comparison between these two figures shows that the magnitudes of the residuals for Eq.(3-6-3) decreased sharply and also the systematic pattern (the parabola in Fig 3-7) had disappeared and shows a random behaviour. Thus, from the facts considered so far, it can be concluded that;

"In the case of mixture 3 (nominal 75% ethylene) the 10-coefficient Bender equation (3-6-3) is not only 'better' than Eq.(3-6-2) but also 'adequate' to represent all the experimental data points of this work."

Finally the compressibility factors from the virial equation, Z(V), in Table (3-4) are compared with Z(6) and Z(10). As the table shows the deviations of Z(6) and Z(V) from Z(10) are similar and somewhat systematic with pressure changes. A typical example is shown in Table (3-6') for RUN 66 (288.1°K).

TABLE 3-6'

P(bar)	Z(10)	$\Delta Z(6)^*$	$\Delta Z(V)^{**}$
69.09	.5437	.0060	.0055
53.26	.6785	.0066	.0051
39.40	.7794	.0068	.0050
28.09	.8512	.0063	.0047
19.52	.9005	.0051	.0039
13.34	.9338	.0039	.oo30
9.02	.9538	.0028	.0022
6.06	.9708	.0019	.0015
4.05	.9807	.0014	.0011

* $\Delta Z(6) = Z(10) - Z(6)$

** $\Delta Z(v) = Z(10) - Z(V)$

As Table (3-6) clearly shows, the deviations are ranging from about 1% at 70 bar (Z=0.5437, ΔZ=0.0055) to 0.1% at 4 bar (Z=0.9807, ΔZ=0.0011), which means that the changes of deviations, $\Delta Z(6)$ and $\Delta Z(V)$, are systematic with pressure changes. In Fig 3-10 the deviations, $\Delta Z(6)$ and $\Delta Z(V)$, are plotted against the experimental temperature for RUN 66. From the graph one can notice that at pressures below 40 bar both $\Delta Z(6)$ and $\Delta Z(V)$ decrease with pressure systematically. The regularity however disappears at pressures above 40 bar which is regarded too close to the vapour pressure of this mixture at the expansion vessel at $0^{o}C$.[20]

In order to examine the characteristics of the virial equation (3-6-1) and to compare this with Eq.(3-6-3) the compressibility factors at first pressure of each run were considered rather than the pressures themselves, because the temperatures as well as the pressures were taken account into the estimation of the compressibility factors. Thus RUNs 70, 72 and 74 (Table 3-7) were chosen and the deviations, $\Delta Z(V)$, were plotted against the experimental pressure in Fig 3-11.

TABLE 3-7

RUN	T(K)	$P_{max.}$(bar)	Z(10)
70	266.1	44.59	.6112
72	251.3	28.69	.7264
74	238.4	16.75	.8265

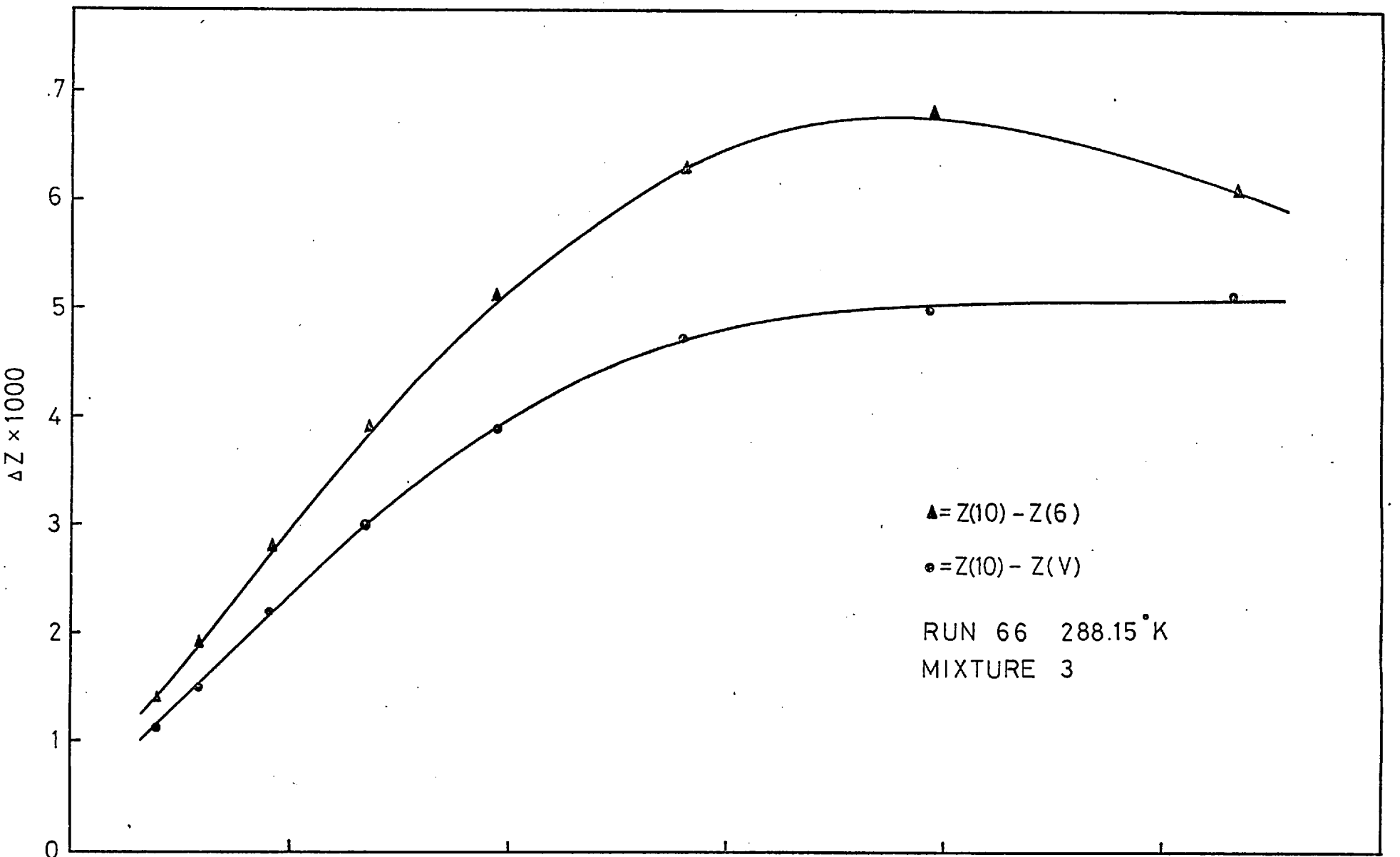


FIG 3-10 ΔZ V EXP. PRESSURE

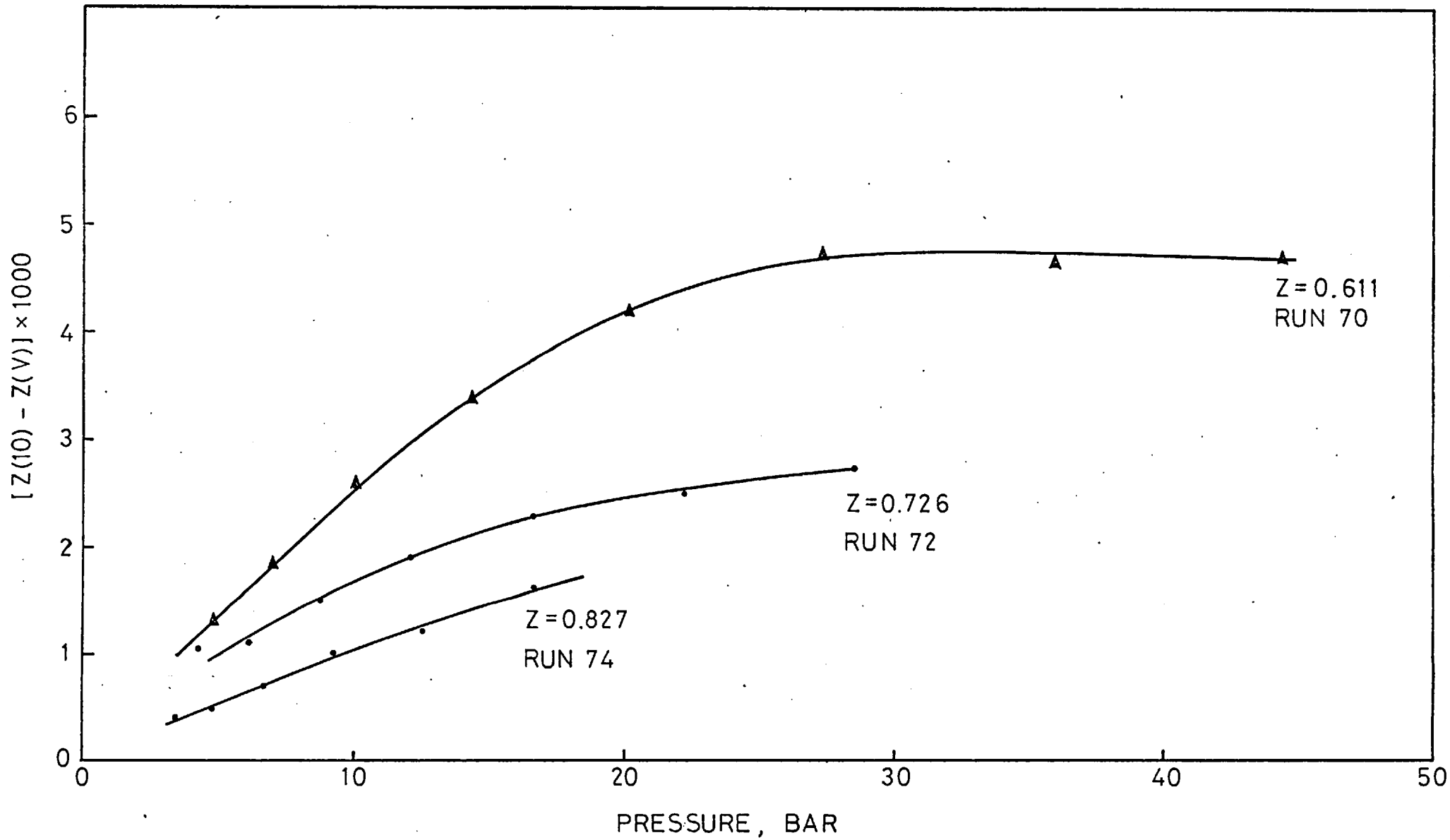


FIG 3-11 Δ Z V PRESSURE

It can be seen in Fig 3-11 that the magnitude of the deviation, $\Delta Z(V)$, depends on the compressibility factor at maximum pressure of Burnett run, i.e. the further from the ideality at first pressure (RUN 70, Z=0.6) the larger the deviation $\Delta Z(V)$. This fact suggests that the virial equation with only 2nd and 3rd virial coefficients was not good enough to calculate the compressibility factors and thus needed higher density terms especially at high pressure region, since the contribution of higher terms become significant at high pressure region where the non-ideality is great. For example, the contributions of the third coefficient term ($C\rho^2$) to Z were estimated at two extreme pressures for RUN 66 ($288^{o}K$).

TABLE 3-8*

P(bar)	ρ	Z	$C\rho^2$
69.10	$0.5304 \cdot 10^{-2}$	.5437	0.0661
4.04	$0.1723 \cdot 10^{-3}$	.9807	$0.6976 \cdot 10^{-4}$

* The density is in gm-mole/cc

Table 3-8 shows the contributions of $C\rho^2$ term to Z at 69 bar is almost 12%, while the contribution at 4 bar is negligible (0.007%).

For this reason the deviations in Fig 3-11 can be regarded as the intrinsic error due to the inadequacy of the virial equation (3-6-1), i.e. too few density terms.

Nevertheless the equation was not altered throughout this work, since the number of data point in one run was

normally no more than 8 and the least-squares procedure for more than four parameters (i.e., B,C,D and N) from this limited number of data was considered to be unrealiable.[21]

The superiority of 10-coefficient equation (3-6-3) over the 6-coefficient equation (3-6-2) has already been discussed and from comparison between equations (3-6-1) and (3-6-3) it can be concluded that the compressibility factors estimated from equation (3-6-3), Z(10), are the most acceptable values among the values in Table 3-4.

3-6-4 The Compressibility factors of Other Mixtures.

So far the discussion has been concentrated on the results of mixture 3 which contains the largest amount of ethylene among the mixtures and hence showed distinctive disagreements between Z(V), Z(6) and Z(10). In the previous section the disagreements were discussed from the point of view of the non-ideality which was large due to the presence of a large proportion of ethylene gas. Thus smaller values of ΔZ for mixtures 1 and 2 than those of mixture 3 can be expected. Table 3-4 shows that the deviations of Z(V) from Z(10) of both mixtures are not only smaller than those of mixture 3 but they show more or less random behaviour.

Hence it is believed that the characteristics of the two equations (3-6-1) and (3-6-3) can no more show such apparent differences in compressibility factors as in the case of mixture 3.

In order to compare Eq.(3-6-2) with (3-6-3) the objective functions were evaluated from the two equations and they are listed in Table 3-9 together with those from mixture 3.

TABLE 3-9**

	S_6*	S_{10}*	S_6/S_{10}
mixture 1	$0.4249 \cdot 10^{-5}$	$0.3769 \cdot 10^{-5}$	1.1
mixture 2	$0.3191 \cdot 10^{-5}$	$0.6001 \cdot 10^{-6}$	5.3
mixture 3	$0.2304 \cdot 10^{-5}$	$0.2277 \cdot 10^{-6}$	10.1

* $S = \sum_{i}^{n} \sum_{j}^{ni} W_{ij} \cdot R_{ij}^{2}$

S_6: estimated from 6-coefficient equation (3-6-2)

S_{10}: estimated from 10-coefficient equation (3-6-3)

** The objective functions for one mixture in this table cannot be compared with that for another, since they were determined from different number of data points and least-squares parameters.

It can be seen that the objective functions, S_6 and S_{10} are not as different for mixtures 1 and 2 as in the case of mixture 3.

3-6-5 The Compressibility Factors of Ethylene

In the case of ethylene the first experimental pressures were much lower than those of the mixtures because of its high critical temperature (9.5°C) and hence most of the experimental isotherms were below this critical temperature. Although the inlet tubes were heated by two heaters (section 2-2-4) there were always possibilities of condensation of the gas especially during expansion at high pressures.

Thus the maximum experimental pressures used were less than 85% of the vapour pressure of the gas at the experimental temperature. (see Fig 3-7). Consequently the first compressibility factor, Z_o, in each run was nearer to 1 than those of the mixtures.

The objective functions in this case were,

$S_6 = 0.1223 \cdot 10^{-5}$

$S_{10} = 0.1151 \cdot 10^{-5}$

This small difference in the objective functions suggests that the two equations are comparable within the experimental pressure and temperature ranges investigated.

The residuals too showed no sign of any systematic pattern as was shown in the case of mixture 3. Table 3-4 shows that the compressibility factors from Eq.(3-6-1), Z(V), differ from Z(10) no more than the uncertainties in Z themselves except for runs 23 and 30.

In these particular two RUNs the deviations, Z(10) - Z(V), were more than twice the values which might be expected from the other runs, although the maximum differences in both cases were less than 0.001.

These large deviations were due to following reasons.

(i) RUN 23.

From the fact that the 3rd and 4th residuals from both Eq.(3-6-1) and (3-6-3), were exceptionally larger than the other residuals in this run (Table 3-10), it is believed that there is a large error in 4th pressure measurement.

TABLE 3-10

	R_{ij}(Eq. 3-6-1)	R_{ij}(Eq. 3-6-3)
	$0.1437 \cdot 10^{-3}$	$-0.1700 \cdot 10^{-3}$
	$-0.9972 \cdot 10^{-3}$	$-0.1852 \cdot 10^{-3}$
*	$0.2478 \cdot 10^{-2}$	$0.2812 \cdot 10^{-2}$
**	$-0.2599 \cdot 10^{-2}$	$-0.2692 \cdot 10^{-2}$
	$0.4313 \cdot 10^{-3}$	$0.1690 \cdot 10^{-3}$
	$0.1067 \cdot 10^{-3}$	$0.6422 \cdot 10^{-3}$
	$0.4226 \cdot 10^{-3}$	$0.9017 \cdot 10^{-3}$

(ii) RUN 30

The first pressure of this run was only 15.4 bar due to its low temperature (244^{o}K) and the number of experimental data points was only six. Therefore the estimation of three least-squares parameters (B,C and N) out of six data points is regarded as unreliable.

Thus we consider that in both runs the experimental errors are more likely to be reflected in the virial coefficients than the Bender coefficients, and the differences, Z(10) - Z(V), in runs 23 and 30 are regarded as errors from the virial equation and not from the modified Bender Equation.

3-6-6 Errors in the Compressibility Factors

The basic differences in determining the compressibility factors between the virial equation and the Bender equation are:

(i) In the case of the virial equation the compressibility factor of the gas in the ice bath (0^{o}C) was estimated from the prefixed virial coefficients at 0^{o}C and unchanged throughout the least-squares procedure of each run. Thus after having completed the experiment with one gas the virial coefficients were readjusted graphically by plotting the virial coefficients against the temperature. Then the entire runs were retreated with these new virial coefficients at 0^{o}C. This process was repeated until the values were consistent.

(ii) Since the compressibility factor from Bender equation is expressed in terms of temperature as well as density,

'same coefficients' were used to determine the number of moles of the gas in the ice bath as well as in the pressure vessel.

Thus the largest error in case (i) could be induced from the uncertainties in the virial coefficients at $0^{\circ}C$. Other sources of errors in both cases were uncertainties in ice bath temperature ($0.02^{\circ}K$), dead space volumes, dead space temperature and the uncertainties in the number of moles in the inlet tube. It can be seen in Table 3-4 that apart from mixture 3 (see section 3-6-3) the compressibility factors are very consistent with each other in both cases, despite the different approaches used in determinating the compressibility factors. Therefore the differences between Z(10) and Z(V) are considered to be within the experimental errors due to various sources mentioned above. The errors in the compressibility factors from Eq.(3-6-3) are thus estimated as less than ± 0.0005 for all mixtures. In the case of ethylene the errors are estimated as less than ± 0.0003 for all values of Z with a probable maximum error of ± 0.0005 in some cases at high pressures.

Runs 30 and 23 were excluded in estimating the errors for reasons given in section (3-6-5).

It is well known that gas adsorption can lead a significant error in P-V-T measurements,[2] especially when the experimental pressure approaches the vapour pressure at experimental temperature. The magnitude of the error due to the gas adsorption depends on several factors i.e. the polarity of the molecule, the size of the molecule and most important of all

the condition of the surface of the vessel with which the experimental gas comes into contact.

Previous work in this laboratory on Ar and Kr has shown that although there is a small amount of adsorption on an unpolished copper vessel wall when the pressure approaches that at saturation, this can be virtually eliminated, as far as P-V-T measurements are concerned, by polishing to a mirror finish.[23,24]

Since neither methane nor ethylene is a polar substance and both pressure and expansion vessels were polished (chapter 2) it is assumed that there was no adsorption of the gases on the wall throughout this work.

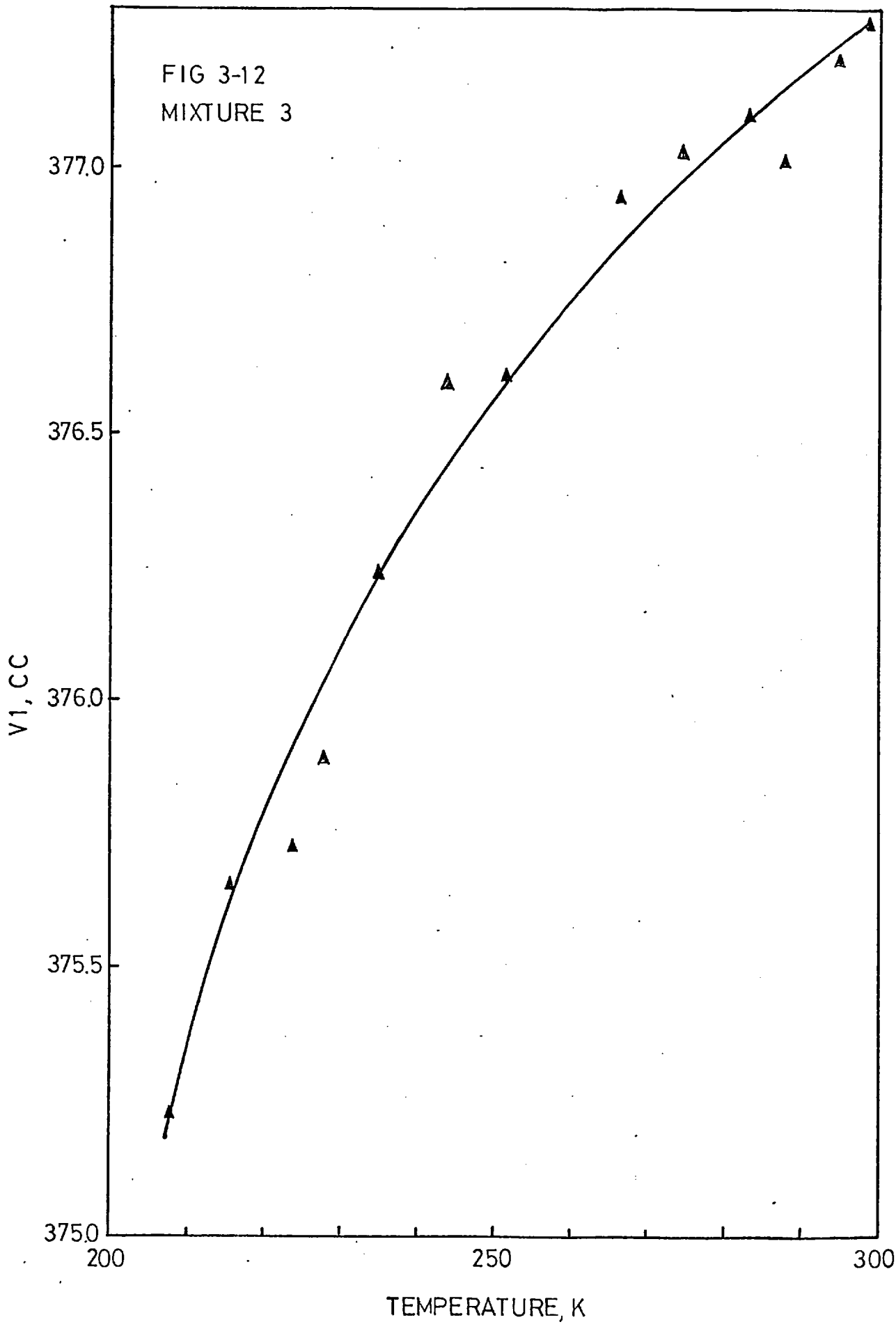
3-6-7 The volume of the Pressure Vessel

In the course of the least-squares procedure for the Bender equation each volume of the pressure vessel was determined as well as the coefficients of the equation (section 3-4). This measure corresponds to the determination of the volume ratio, N, or run constant. Since the least-squares procedure for Bender equation treated all data points for all Burnett runs, in the case of ethylene, for example, 12 volumes were determined for each of 12 isothermal runs.

The magnitude of the vessel volume for a particular run, however, was independent of data points for all other runs.

For this reason the derivatives $\frac{\partial R_{ij}}{\partial V_R}$ was determined such that only when the run number (i) in R_{ij} and the volume number (k) in V_k were equal, the derivatives were calculated and other wise, i.e. $i \neq k$, the derivatives were set to zero.

For 3-12 shows, as an example, the variation of the


FIG 3-12
MIXTURE 3
377.0
376.5
376.0
375.5
375.0
V1, CC
200
250
300
TEMPERATURE, K

pressure vessel volumes (least-squares curve-fit) with respect to the experimental temperature.

3-6-8 Compressibility Factors of Other Workers

(i) Ethylene

As was mentioned earlier in this chapter few P-V-T data below 0°C of this gas have been published. Above 0°C the principal data, which have been available for many years, are due to Michels and his co-workers of the van der Waals Laboratory. The data produced by the laboratory, however, are limited in temperature range from 0°C to 150°C, although ranging widely in pressure, from 16 to 3042 bar. Michels, de Bruyter and Niesen published in 1936 density measurements along isotherms from 0°C to 150°C at 25°C intervals measured at pressures from 16 to 274 bar.[14] In 1942 Michels and Geldermans[15] corrected the previous data due to inaccuracy of the thermometer used in their experiment. There is a group of 16 points from the Kammerlingh Onnes Laboratory in the range of 272 - 293°K and 22 - 38 bar.[25] However Angus[17] criticised the accuracy of the data due to lack of self-consistency. Butcher and Dadson reported the experimental virial coefficient of ethylene by using a Burnett type apparatus in the range of 263 - 473°K.[26] In this paper the authors dealt only with the virial coefficients and did not present actual experimental P-V-T data. Besides, the second virial coefficient at 0°C (-161.4 cc/gm-mole) differs from of Michels (-167.84)[27] and of this work (-169.11).

Thus the comparison was made between this work and that of Michels and co-workers[15] at two temperatures, 0°C and

$25^{o}C$.

The density of Amagat unit and pressure of atm. unit of Michels data were converted into gm-mole/cc and bar respectively using following conversion factors, i.e.

1 atm = 1.01325 bar (3-6-7)

1 Amagat = 538.73 cal/mole = 22245.719 atm·cc (3-6-8)

At each experimental pressure and temperature the density was calculated according to the Bender equation by Newton-Raphson iteration method.

The results are listed in Tables (3-11) and (3-12), and the differences in compressibility factors at both temperatures are shown in Fig 3-13.

TABLE 3-11*

Comparisons of ρ and Z at $0^{o}C$

P_m	ρ_m	ρ_b	Z_m	Z_b	Z_b-Z_m
16.7623	$.85596\cdot10^{-3}$	$.85641\cdot10^{-3}$	.8623	.8618	-.0005
20.1766	$.10714\cdot10^{-2}$	$.10715\cdot10^{-2}$	.8295	.8291	-.0004
23.2977	$.12864\cdot10^{-2}$	$.12868\cdot10^{-2}$	.7974	.7972	-.0002
26.0739	$.14968\cdot10^{-2}$	$.14973\cdot10^{-2}$	.7669	.7667	-.0002
28.7094	$.17184\cdot10^{-2}$	$.17186\cdot10^{-2}$	.7358	.7355	-.0003
31.0450	$.19373\cdot10^{-2}$	$.19376\cdot10^{-2}$	.7056	.7055	-.0001
33.0846	$.21521\cdot10^{-2}$	$.21523\cdot10^{-2}$	.6769	.6768	-.0001
34.9196	$.23711\cdot10^{-2}$	$.23709\cdot10^{-2}$	.6484	.6485	+.0001

* The subscripts m stands for Michels data and b stands for the Bender equation (3-6-3).

ρ = density, gm-mole/cc

P = pressure, bar.

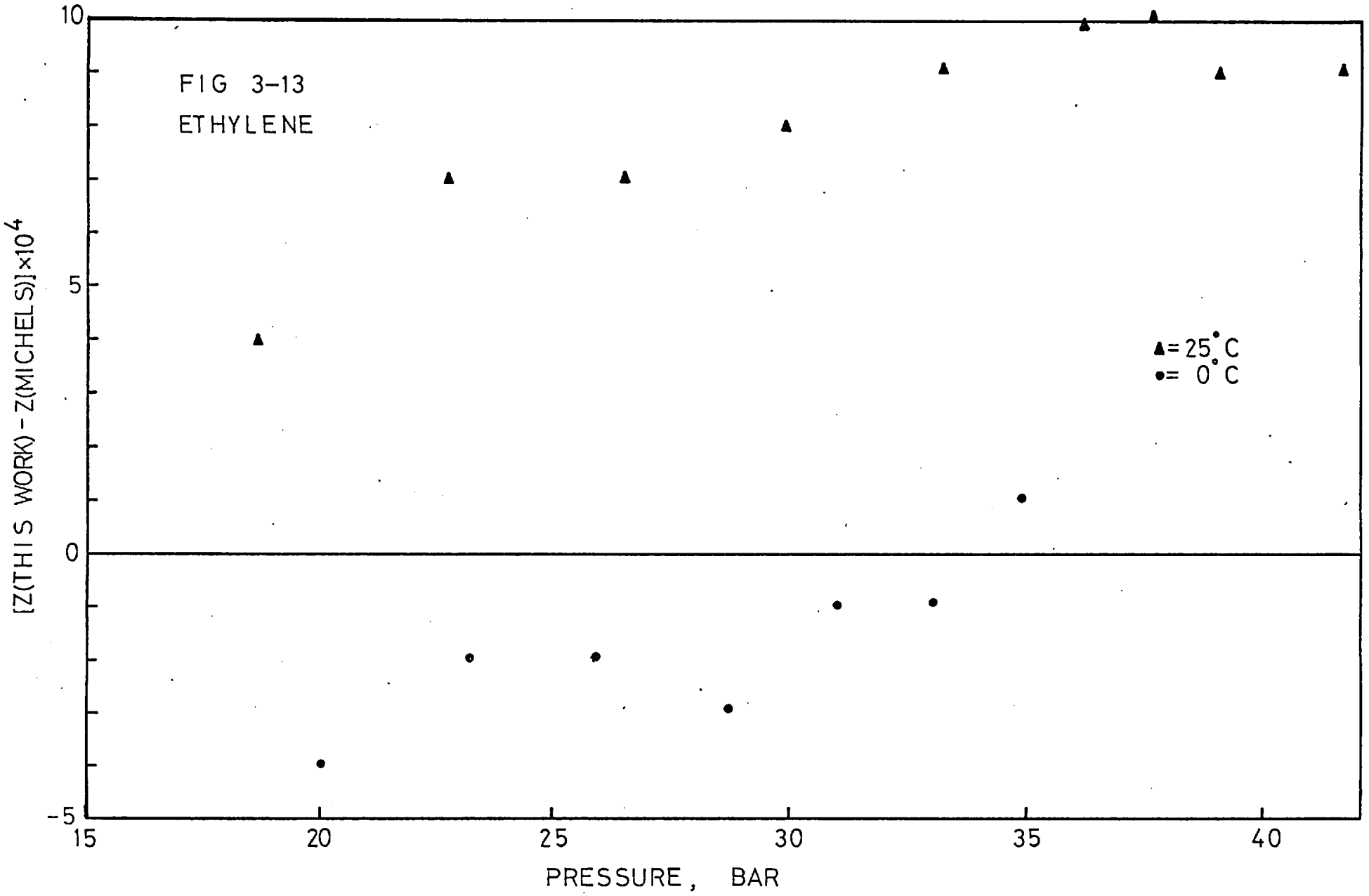

FIG 3-13
ETHYLENE
10
5
0
-5
15
20
25
30
35
40
[Z(THIS WORK) - Z(MICHELS)] ×10^4
PRESSURE, BAR
▲= 25° C
●= 0° C

TABLE 3-12**

The comparison of ρ and Z at 25°C

P_m	ρ_m	ρ_b	Z_m	Z_b	$Z_b - Z_m$
18.785	$.85593 \cdot 10^{-3}$	$.85552 \cdot 10^{-2}$	.8853	.8857	.0004
22.785	$.10711 \cdot 10^{-2}$	$.10702 \cdot 10^{-2}$	.8581	.8588	.0007
26.525	$.12864 \cdot 10^{-2}$	$.12852 \cdot 10^{-2}$	.8318	.8325	.0007
29.933	$.14968 \cdot 10^{-2}$	$.14953 \cdot 10^{-2}$	.8067	.8075	.0008
33.270	$.17180 \cdot 10^{-2}$	$.17160 \cdot 10^{-2}$	.7810	.7819	.0009
36.323	$.19373 \cdot 10^{-2}$	$.19348 \cdot 10^{-2}$	.7563	.7573	.0010
37.816	$.20509 \cdot 10^{-2}$	$.20481 \cdot 10^{-2}$	.7438	.7448	.0010
39.102	$.21512 \cdot 10^{-2}$	$.21496 \cdot 10^{-2}$	.7329	.7338	.0009
41.716	$.23711 \cdot 10^{-2}$	$.23681 \cdot 10^{-2}$	.7097	.7106	.0009

** The values ρ_b and Z_b in Table 3-12 were evaluated from the Bender equation (3-6-3) by extrapolation.

Table 3-11 (0°C) shows that the differences in compressibility factors are within the range of the expected error in this work (max. probable error of ± 0.0005). The discrepencies at 25°C (Table 3-10) are somewhat larger than those of 0°C (maximum of 0.001). However, as shown in Fig. 3-7, the maximum experimental temperature of this work was 293°K so that the values in Table 3-12 were, in effect, evaluated by extrapolation using the Bender equation (3-6-3).

(ii) Ethylene-Methane Mixtures.

P-V-T results for this system have been reported in two paper by other workers. McMath and Edmister[18] published isochoric measurements of P-V-T properties at 20, 40, 60 and 77°F with pressures in the range 260 to 2220 psia for four different mixtures (78.8%, 57.2%, 38.4% and 18.4% methane).

The method used was to confine the gas mixtures in a constant volume vessel (calibrated at the reference temperature 77°F) and to measure the pressure and temperature. After taking the measurements the vessel was heated/cooled to another temperature and the P and T were measured again.

Lee and Edmister[19] reported data on the same mixture (same compositions as those of the above work) at 25, 50 and 75°C with pressures upto 12,000 psi using a Burnett type apparatus.

Although the temperature range of McMath and Edmister's work overlaps this work in part, its pressure range ($P_{min.}$=18 bar, c.f. 2.5 bar of this work) and its interval (⟩ 30 bar) differ greatly. In the case of Lee and Edmister's report, only one isotherm at 25°C can be compared with this work.

In Fig. (3-14) to (3-17) compressibility factors for all four isotherms (McMath and Edmister) are plotted against the pressure with compositions as parameters. Similarly in Fig (3-18) the compressibility factors at 25°C isotherm (Lee and Edmister) are compared with those of this work. In these graphs Z of this work were calculated from Eq.(3-6-3) using the coefficients given in Table 3-1.

Due to the different compositions used in this work and in Edmister et al, direct comparison of Z cannot be made, that is, the figures (3-14) to (3-18) show only qualitative behaviour of Z with respect to the compositions of the mixture.

Nevertheless they can be compared quantitatively by examining the compressibility factors of the mixture as a function of composition at given temperature and pressure. The pressure chosen for each isotherm was either 40 bar (298.15°K)

or 30 bar (288.7, 277.6 and 266.5^{o}K) according to the experimental ranges.

It can be seen from Fig (3-20) that at 288.7^{o}K (McMath and Edmister[18]) the deviations are positive and increasing with methane content, and thus giving an extrapolated value of pure methane about 0.95 which is about 0.01 (or abour 1%) larger than the calculated value from the 20-coefficient Bender equation using Chapela's coefficients.[57]

Fig (3-21) shows that at 277.59^{o}K the values of Z are randomly scattered about the smooth line drawn through the values from this work, whereas only one point (18.4% CH_4) at 266.6^{o}K is below the smoothed curve by about 0.015 (about 2%).

Except for the points mentioned above, which are believed to be the errors in the isochoric measurements, the agreement is good to within the uncertainties in the graphical interpolation of Z from figures (3-14) to (3-18).

Lee and Edmister[19] used same mixtures (exactly same compositions) as in the previous work but using a Burnett apparatus. The agreement is good and is as seen in Fig (3-23) within 0.2% deviation from the smooth curve.

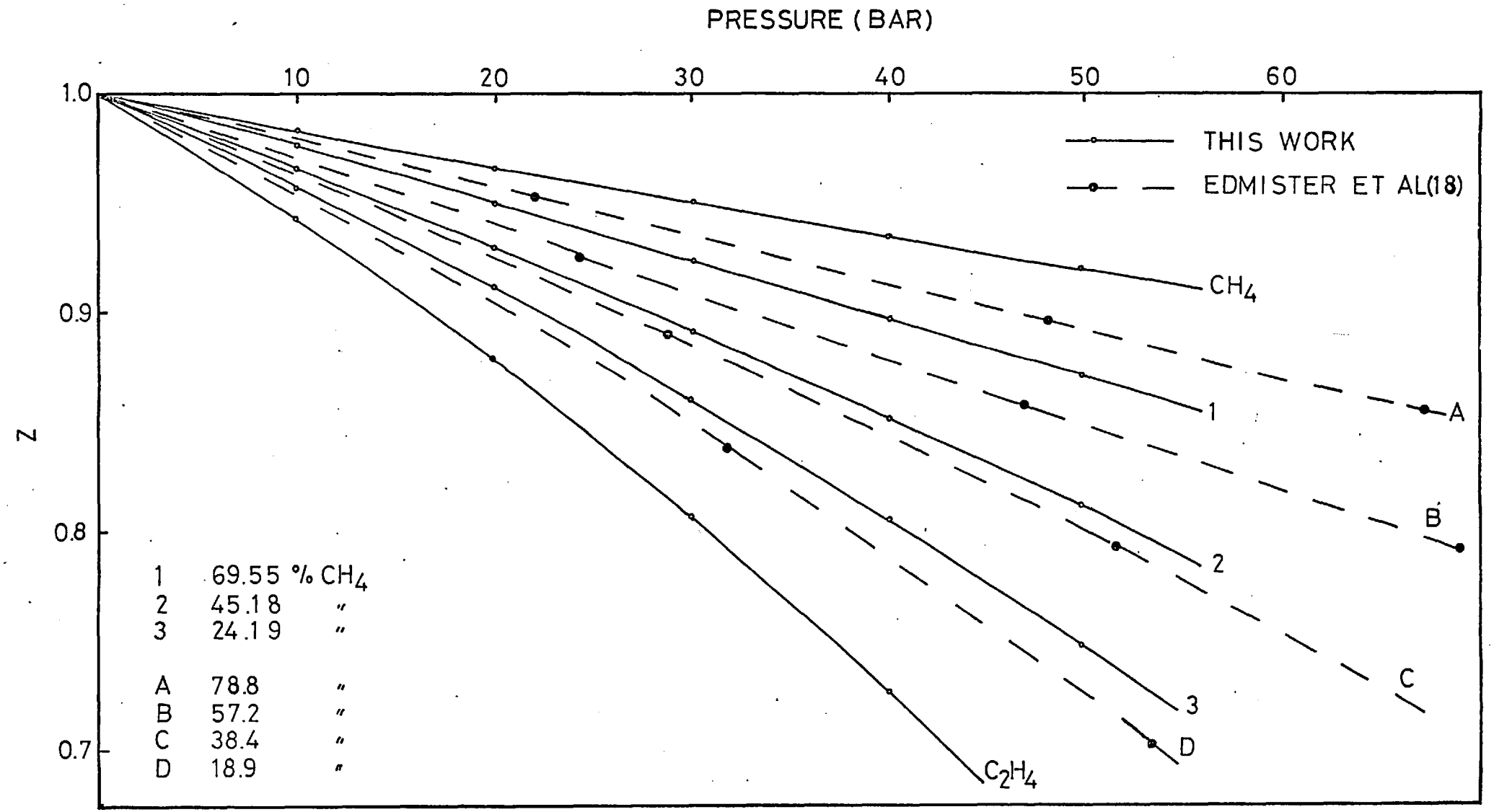


FIG 3-14 $Z_{mix.}$ V. PRESSURE AT 298.1°K

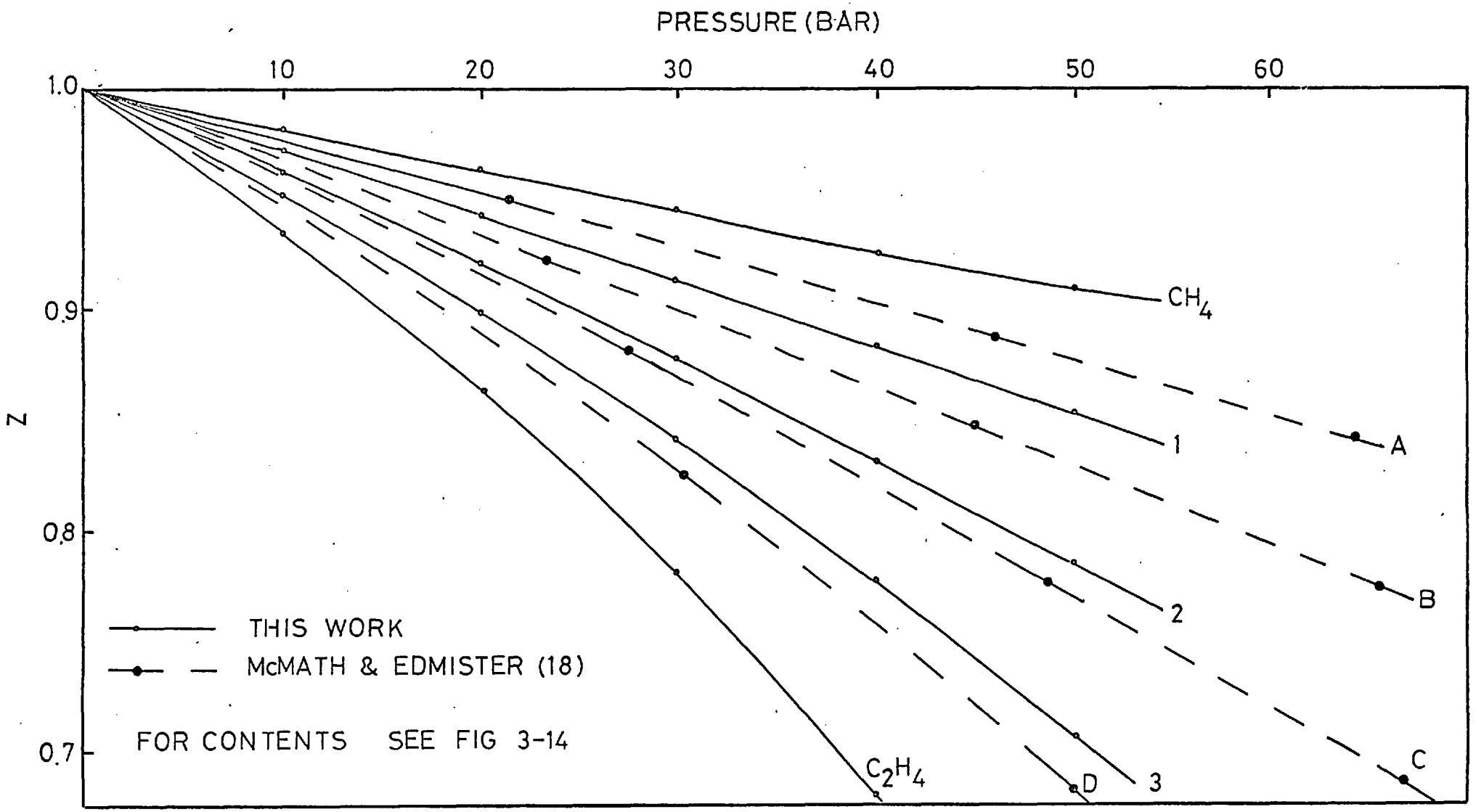


FIG 3-15 $Z_{mix.}$ V. PRESSURE AT 288.7°K

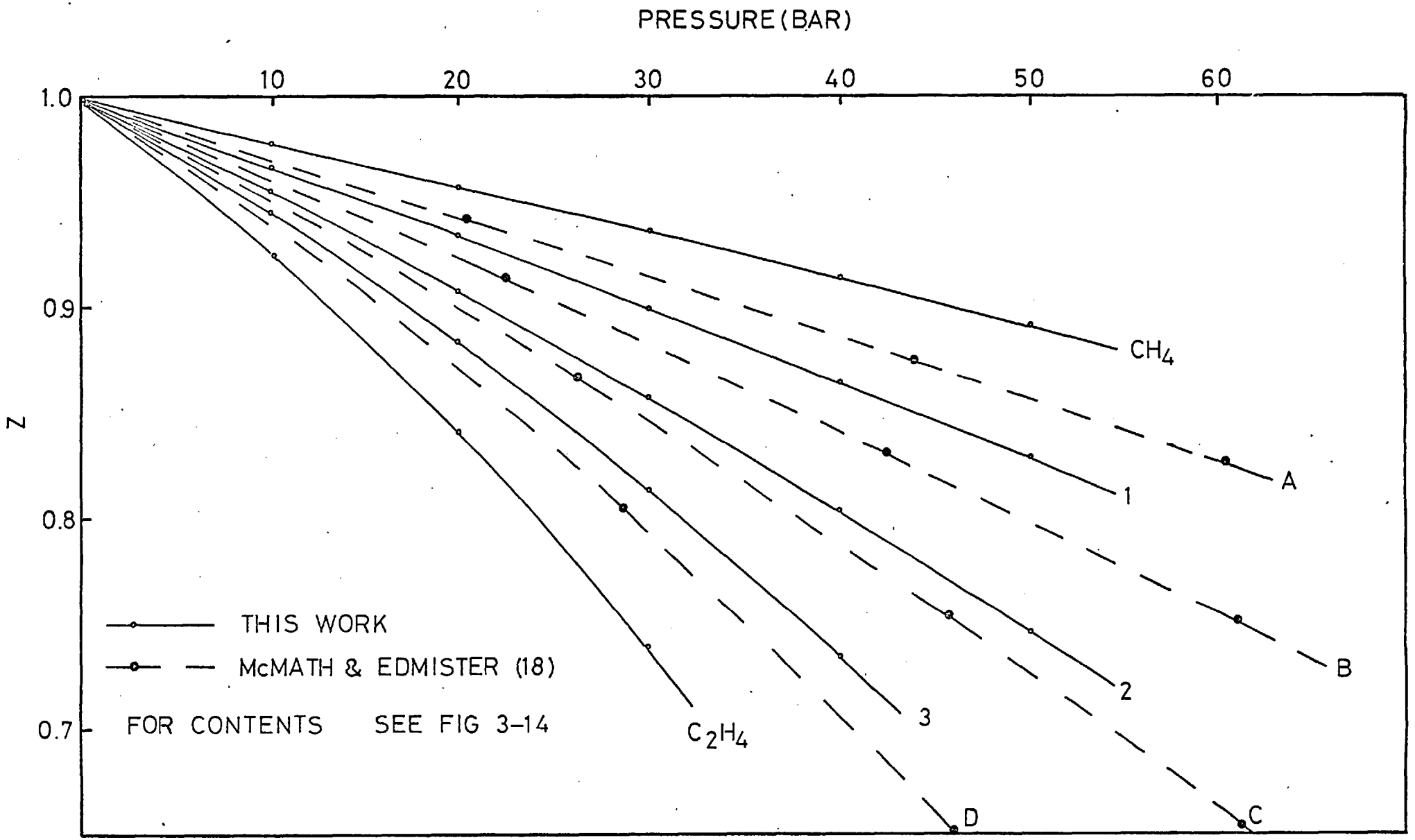


FIG 3–16 $Z_{mix.}$ V. PRESSURE AT 277.6°K

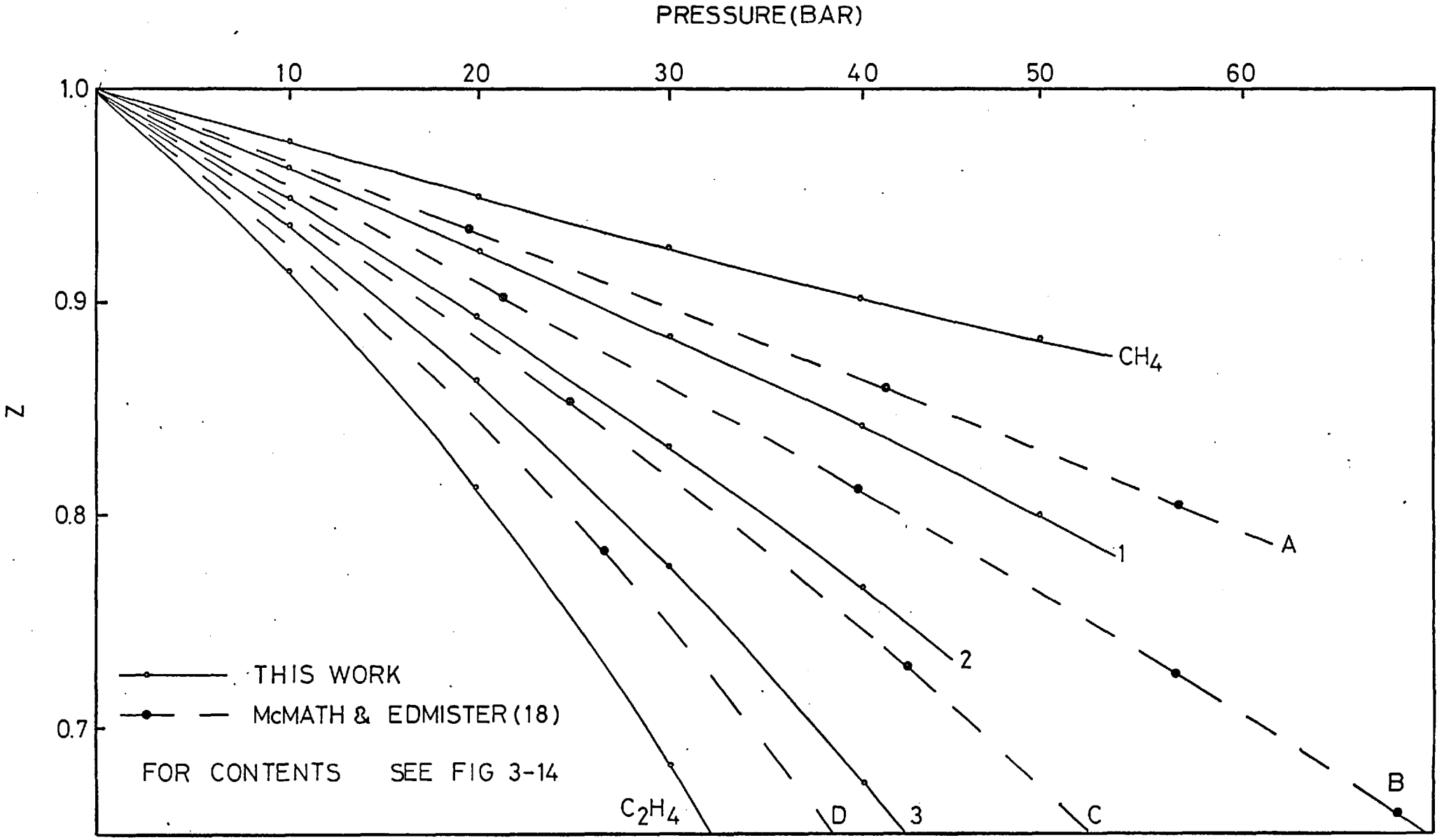


FIG 3-17 $Z_{mix.}$ V. PRESSURE AT 266.5°K

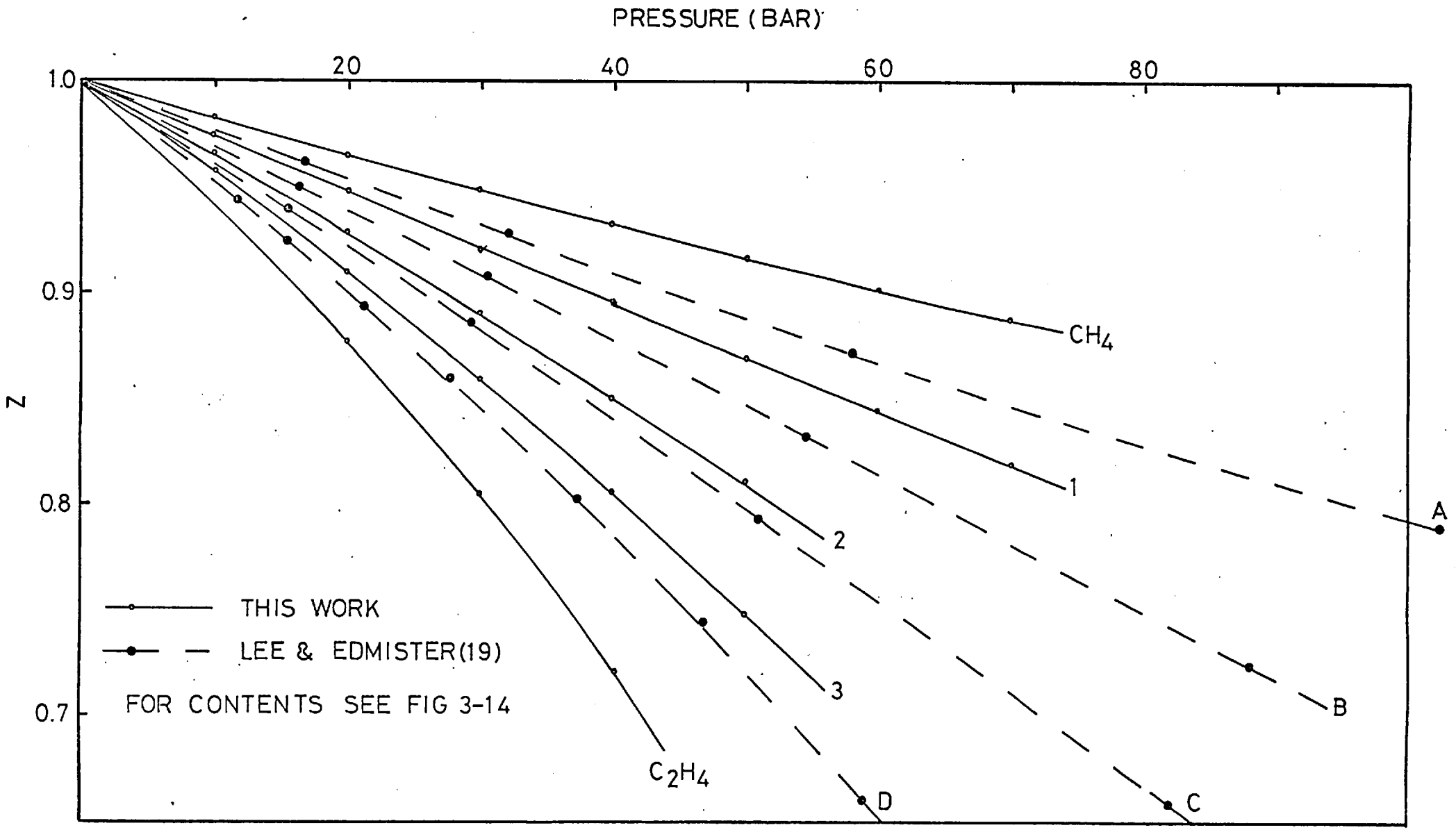


FIG 3—18 $Z_{mix.}$ V. PRESSURE AT 298.15°K

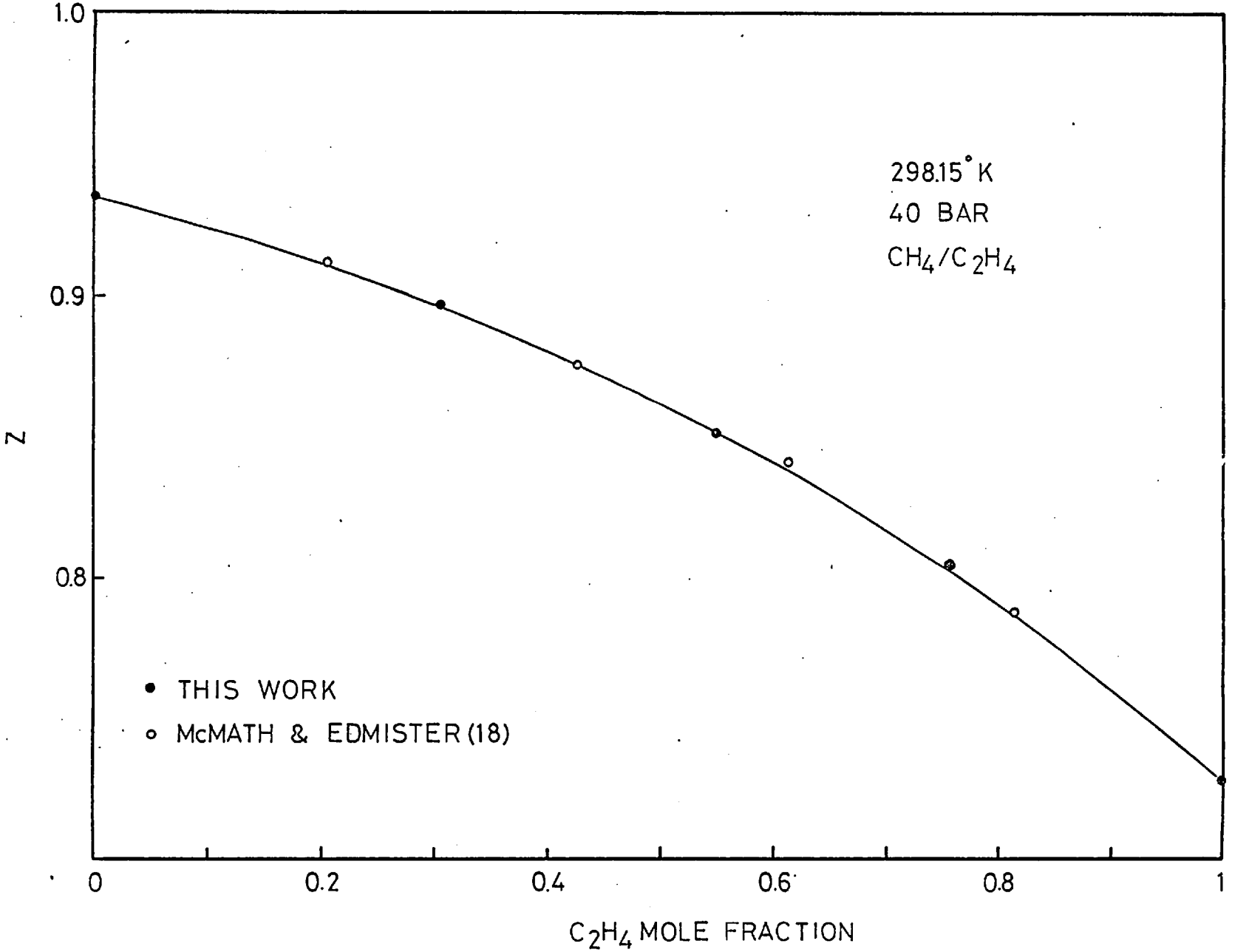


FIG 3-19 Z V. COMPOSITION

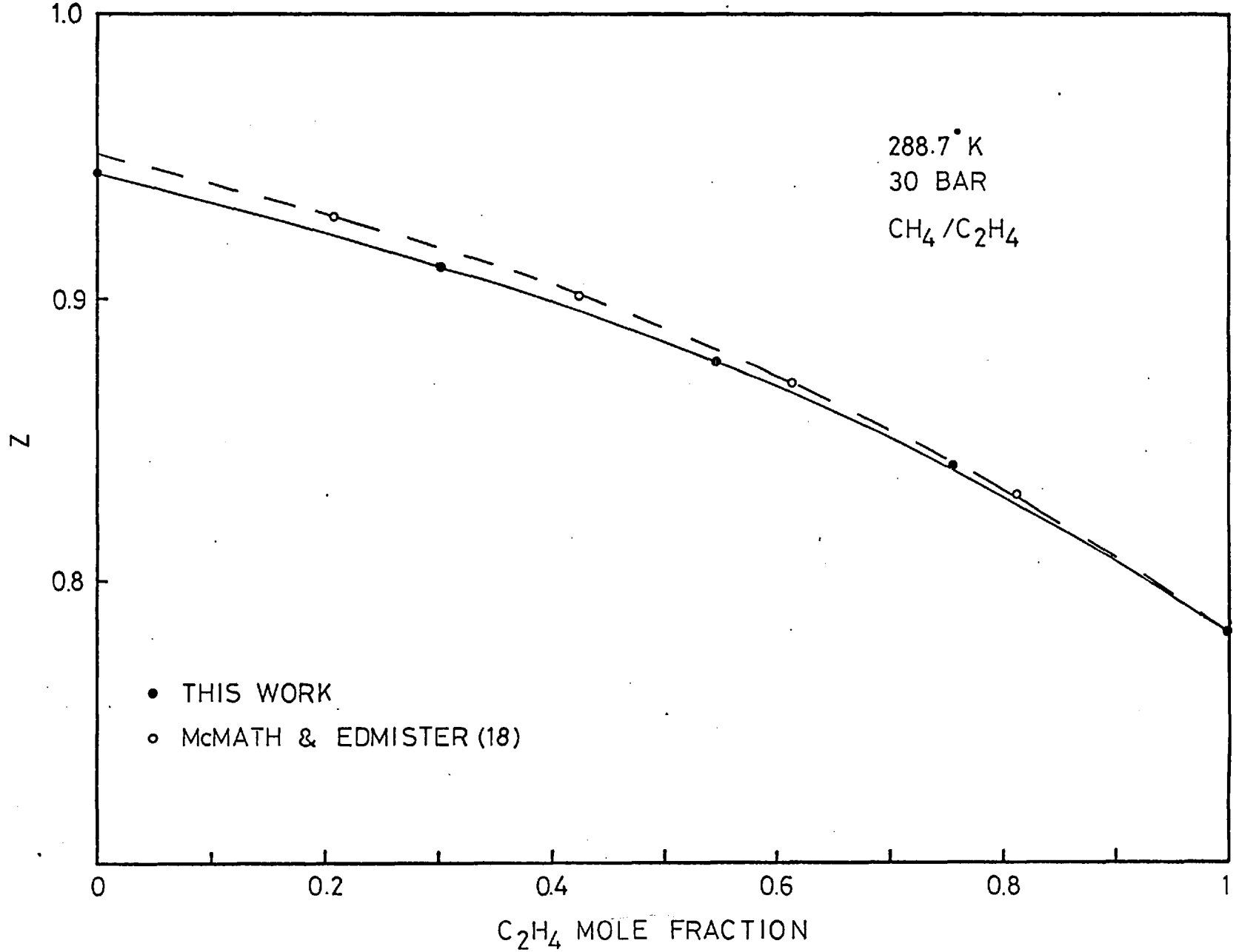


FIG 3-20 Z V. COMPOSITION

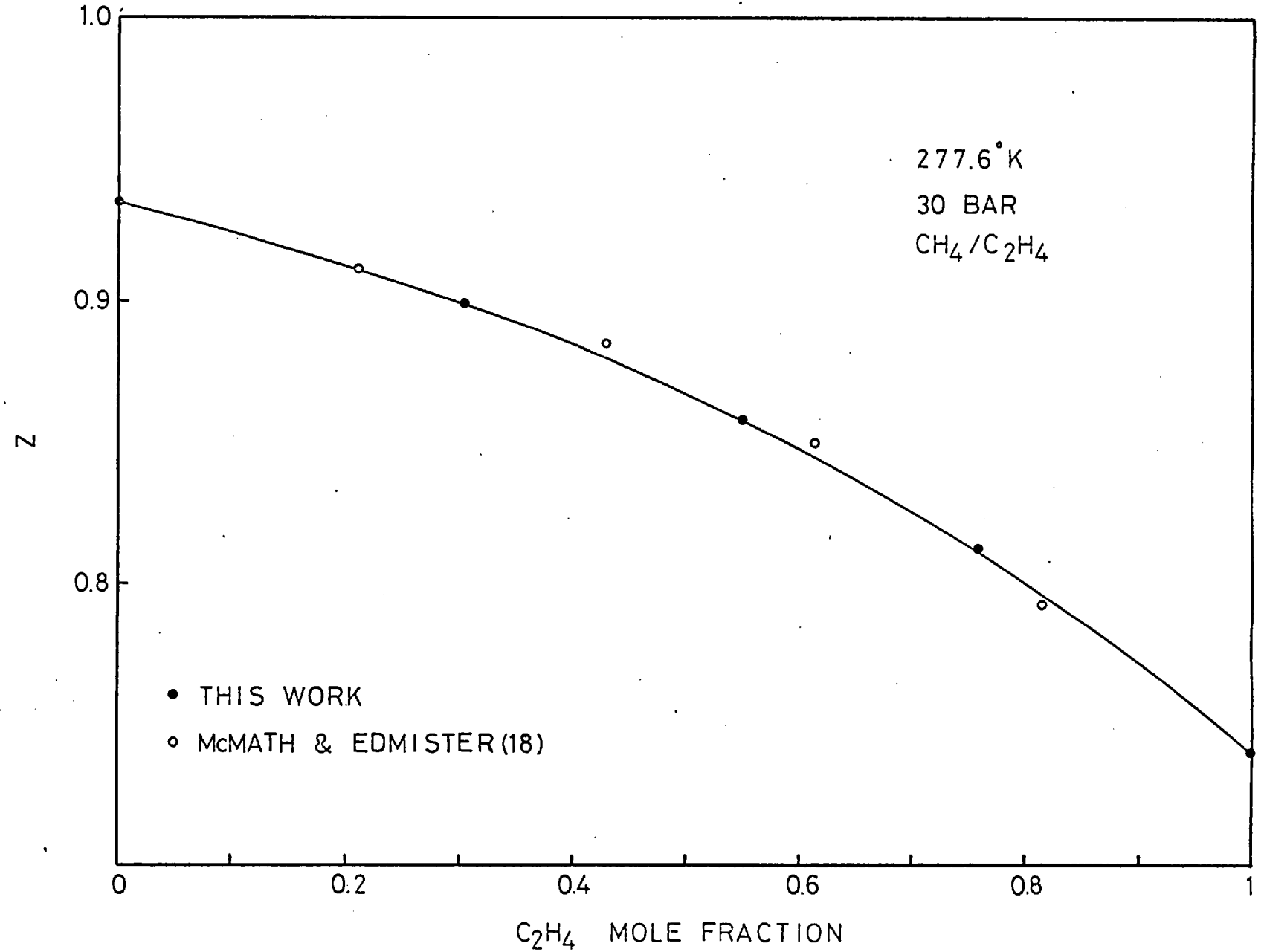


FIG. 3-21 Z V.. COMPOSITION

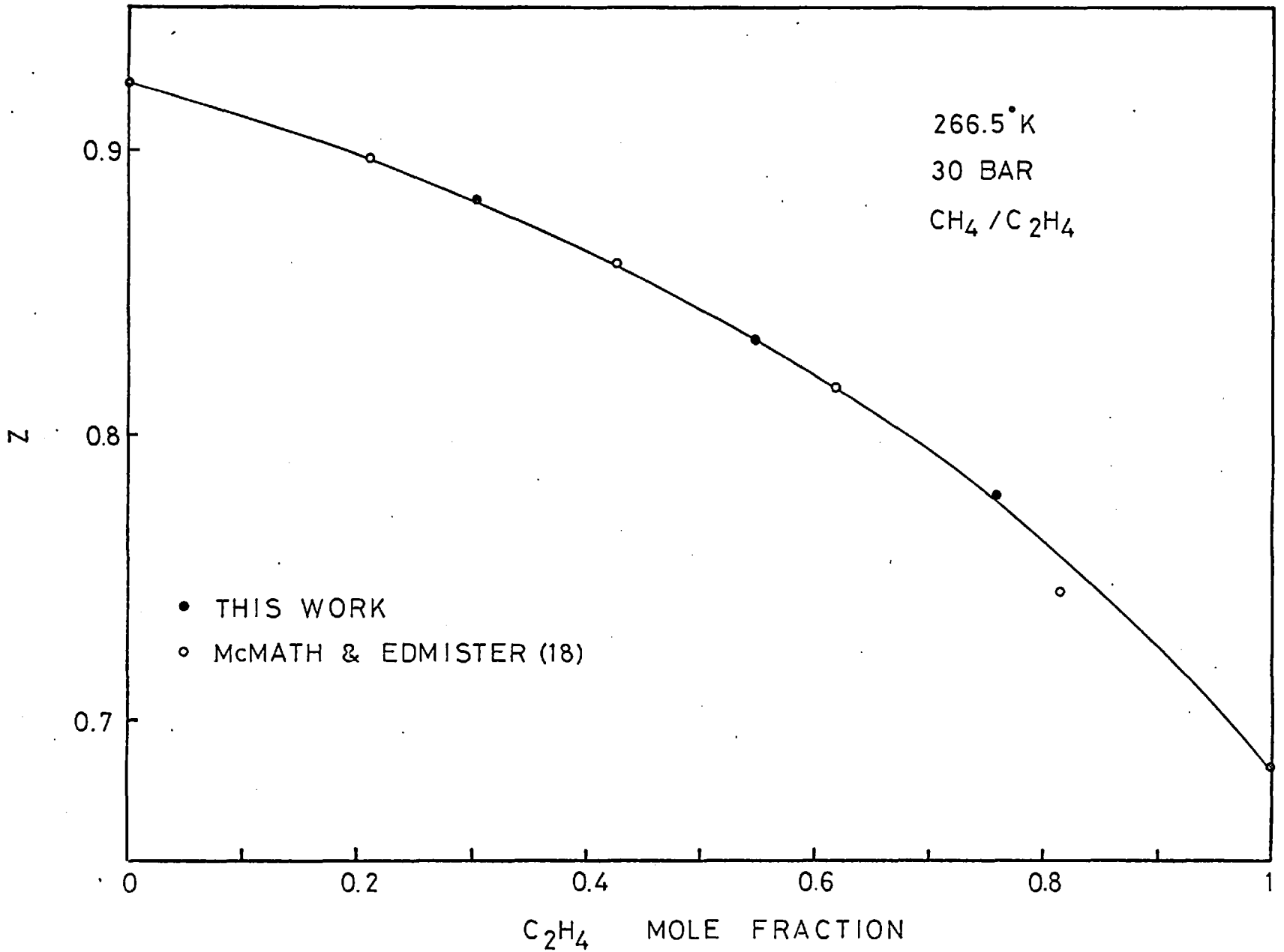


FIG 3-22 Z V. COMPOSITION

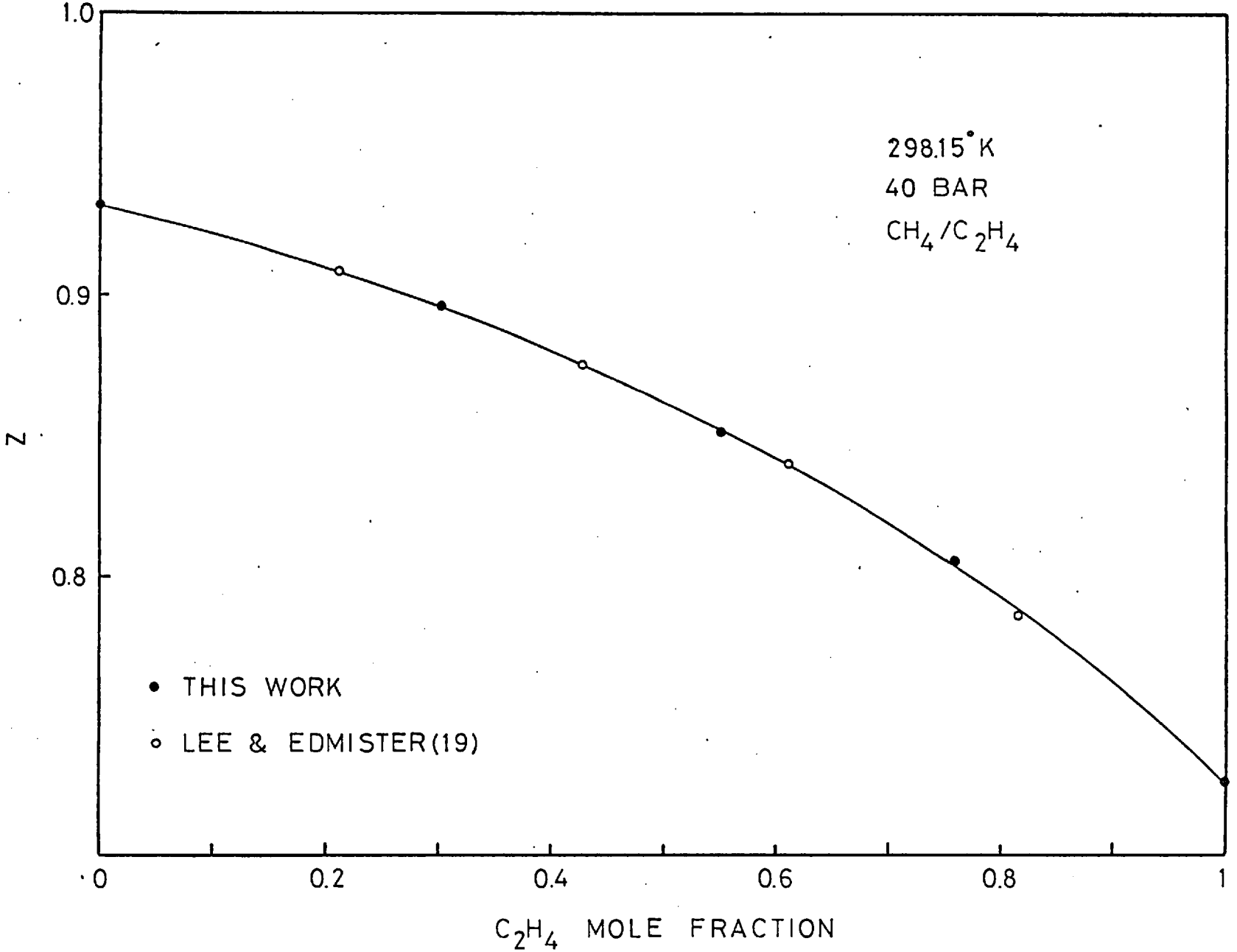


FIG 3-23 Z V. COMPOSITION

CHAPTER FOUR

PREDICTION OF COMPRESSIBILITY FACTORS

4-1 Introduction

There have been numerous methods proposed in the literature for calculation of accurate compressibility factors and other thermodynamic properties of pure gases as well as multicomponent mixtures.

Methods for the prediction of unmeasured properties fall into three main categories.

Firstly we have the method using corresponding states principle and its extension which is the basis of the compressibility factor charts and tabulations in use today.[38,39] The method has been extended to include mixtures by including the hypothesis of a 'one fluid model' as put forward to Leland et al,[40] and Rowlinson and co-workers.[68,69]

Secondly there are methods which employ an empirical equation of state whose coefficients are determined empirically for each gas under investigation. This is no more than a convenient method of interpolation if it is applied to a pure substance, but becomes a method of prediction for mixtures once empirical rules are established for describing the dependence of the coefficients on composition.[29] It can, however, become dangerously inaccurate when used in unfamiliar situation.[41]

The best known equations of this class are those of Redlich and Kwong[42] and Benedict, Webb and Rubin (or simply B-W-R equation).[43]

The Redlich-Kwong equation is based on the van der Waals

equation but gives greater numerical accuracy. However, since it contains only two arbitrary constants, it cannot reproduce the P-V-T behaviour of widely different types of fluids over extensive ranges of density with an accuracy approaching that of experimental measurement. Its utility stems from its simplicity, and the fact that, like the van der Waals equation, it is a well-behaved function which can be used to represent vapour phase properties over a wide range of pressure with moderate accuracy.[44] However this equation is no better than the van der Waals equation in the region of the critical point.

The B-W-R equation has 8 parameters and gives a satisfactory representation of the fluid properties, except immediate vicinity of the critical point, within an average accuracy of 0.5% at densities up to 1.8 times the critical value. The accuracy of the equation at higher than 1.8 times the critical point has been improved by adding more temperature dependent parameters such as was done by Strobridge (16 coefficients);[45] Bender (20 coefficients),[29,30] and as recently as 1973 Stewart and Jacobsen used a 33-coefficient equation for oxygen and nitrogen.[46] McCarty[47] used the same equation and determined the 33 parameters for methane by a least-squares curve fit of published experimental P-V-T data.

Thirdly we have a mixed method which uses the principle of corresponding state and the empirical equation for different parts of the problem. This method mitigates some of disadvantages of the first and second methods.[48,49]

The first method is used in this work to correlate the measured compressibility factors of ethylene and ethylene-methane

mixtures, since, as is shown in next section, its theoretical basis on statistical thermodynamics gives one the hope that it can then be used to predict other thermodynamic properties of this system with high accuracy and wide application.(41)

4-2 The Theoretical Basis of the Principle of Corresponding States

Statistical thermodynamics provides us the linkage between the microscopic molecular information and the macroscopic thermodynamic properties.

The starting equation is the relationship between the Helmholtz free energy and the canonical ensemble partition function,

$$A = -kT\ln(Z) \qquad (4\text{-}2\text{-}1)$$

where A = Helmholtz free energy

k = Boltzmann's constant, $1.38044\cdot10^{-16}$ erg·K^{-1}

$$Z = \sum_{\alpha} e^{-E_\alpha/kT} \qquad (4\text{-}2\text{-}2)$$

Z is called the 'phase integral' or the 'partition function'. Once the free energy A is known all other thermodynamic properties can be derived from the relationships of the four 'fundamental equations' of U, A, H and G.

The pressure and the internal energy, for example, can be expressed as

$$P = -\left(\frac{\partial A}{\partial V}\right)_T = -kT\left(\frac{\partial \ln Z}{\partial V}\right)_T \qquad (4\text{-}2\text{-}3)$$

$$U = A - T\left(\frac{\partial A}{\partial T}\right)_V = kT^2\left(\frac{\partial \ln Z}{\partial T}\right)_V \qquad (4\text{-}2\text{-}4)$$

Thus the problem is to calculate the system energy, E_α, (Eq.4-2-2),

and in turn the partition function, Z.

In the case of perfect gas each molecule can be treated independently in calculating the energy, since, by definition, no intermolecular force exists between molecules. The total energy of each molecule is the sum of the translational, rotational, vibrational and electronic energy. For example a monatomic molecule has only translational energy states (electronic states are normally its ground state provided the temperature is not too high) and is given by

$$\varepsilon_{p,q,r} = \frac{h^2}{8m}\left(\frac{p^2}{a^2} + \frac{q^2}{b^2} + \frac{r^2}{c^2}\right) \qquad (4\text{-}2\text{-}5)$$

where $h = 6.62517 \cdot 10^{-27}$ erg·sec., Plank's constant

m = mass of the molecules

p,q,r = quantum numbers $p \geq 1$, $q \geq 1$, $r \geq 1$

a,b,c = dimensions of sides of a rectangular container.

From Eq.(4-2-1) and (4-2-5) one can derive thermodynamic properties of N identical molecules, such as,

$$A = -NkT \ln\left[\frac{eV}{N}\left(\frac{2\pi m k T}{h^2}\right)^{3/2}\right] \qquad (4\text{-}2\text{-}6)$$

$$P = NkT/V \qquad (4\text{-}2\text{-}7)$$

where e is the base of natural lograithm.

In the case of a real gas, however, apart from the molecular energy described above there exists an additional force between molecules, namely 'the potential energy of the intermolecular forces'. When molecules are closely packed together their mutual forces of attraction can lower the energy by amounts large compared with NkT. The clearest menifestation of this

energy is the latent heat of evaporation which is the enthalpy needed to separate the molecules of a liquid and disperse them as a gas of much lower density. This potential energy is a smooth function of the mutual separations of all N molecules.

Thus the energy involved in calculating the partition function is now,

$$E = E_{mol} + U(r) \tag{4-2-8}$$

where E_{mol} is the molecular part energy such as translational, rotational and vibrational energy of N molecules and U(r) is the potential energy or also called the 'configurational energy'. In U(r) r represents all the vectors $r_1, \cdots r_N$, needed to specify the positions of N molecules in a volume V.

Eq.(4-2-8) suggests that the partition function can be divided into two parts, (i) a molecular part and (ii) a configurational part. Thus, for example, the partition function of a monatomic gas can be expressed as,

$$Z = \left(\frac{2\pi m kT}{h^2}\right)^{3N/2} \cdot Q = Z_{mol} \cdot Q \tag{4-2-9}$$

where

$$Q = \frac{1}{N!} \int_V \cdots \int \exp\left[-U(r)/kT\right] dr_1\, dr_2 \cdots dr_N \tag{4-2-10}$$

In order to calculate the partition function, Eq.(4-2-2), the configurational integral Eq.(4-2-10) must be solved, and two difficult problems arise here. That is,

(i) The potential energy U(r) is not known accurately as a function of r,

(ii) even if U(r) is known, the evaluation of the integral in Eq.(4-2-10) is, in practice, not possible because it is a 3N-fold integral where N is the order of 10^{23}.

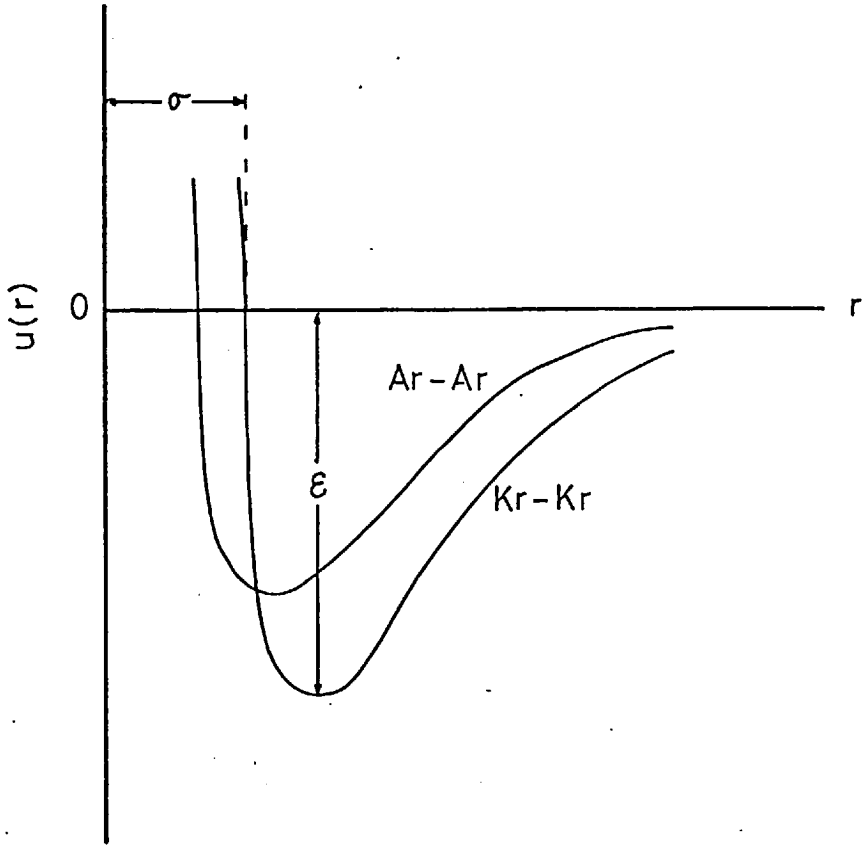


FIG 4-1 POTENTIAL ENERGY CURVES (SCHEMATIC)

It is, however, a reasonable approximation that U(r) is a sum of the independent interaction of molecules in all possible pairs, that is, for example, the potential energy between three molecules is assumed to be $U_{123} = U_{12} + U_{23} + U_{13}$ and thus for N molecules,

$$U(r) = \sum_{l<m}^{N-1} \sum^{N} u(r_{lm}) \qquad (4\text{-}2\text{-}11)$$

where $u(r_{lm})$ = potential energy between a pair of molecules l and m which are separated by a distance r_{lm}

Fig 4-1 shows the functions for a pair of argon atoms and for a pair of krypton atoms. Other molecules behave

qualitatively in a similar way, that is u is large and positive at short separations (repulsive force), it then becomes negative with a depth comparable with kT^c, and finally goes rapidly to zero, being proportional to r^{-6} as it does so.(44)

Thus by substituting Eq.(4-2-11) into Eq.(4-2-10),

$$Q = \frac{1}{N!}\int \cdots \int \prod_{l<m}^{N-1} \prod^{N} \left[\exp\left(-u_{lm}/kT\right)\right] d\tau_1 \cdots d\tau_N \qquad (4\text{-}2\text{-}12)$$

Although it is still impossible to evaluate Eq.(4-2-12), by defining a new function, f_{lm}, such that

$$f_{lm} = \exp(-u_{lm}/kT) - 1 \qquad (4\text{-}2\text{-}13)$$

the partition function can, at least, be broken down into parts and the infinite series virial equation can be derived by differentiating the Helmholtz free energy with respect to volume,

$$(PV/NkT) = 1 + B(N/V) + C(N/V)^2 + \cdots \qquad (4\text{-}2\text{-}14)$$

where

$$B = -\frac{1}{2}\int_0^{\infty} f_{12}\, 4\pi r_{12}^2\, dr_{12} \qquad (4\text{-}2\text{-}15)$$

$$C = -\frac{1}{3}\int\int\int f_{12}\, f_{13}\, f_{23}\, 8\pi^2 r_{12}\, r_{13}\, r_{23}\, dr_{12}\, dr_{13}\, dr_{23} \qquad (4\text{-}2\text{-}16)$$

Eq.(4-2-14) is the virial equation which is expressed in molecular unit and equivalent to Eq.(3-6-1) which was expressed in molar unit.

As is shown in Eq.(4-2-15) and (4-2-16) the virial equation is theoretically important, since the virial coefficients, B, C, etc. are directly related to the intermolecular forces. However, its use is, in practice, restricted to a moderately dense gas. Another disadvantage of the virial equation is that the virial

expansion cannot be used beyond the 3rd coefficient term because it is practically impossible to evaluate the 4th, 5th coefficients etc. with any accuracy.

Thus we examine an alternative way of evaluating the configurational integral, namely the principle of corresponding states, in which the configurational integral of one system (or gas) is related to that of another by correlating with the intermolecular potentials of the two systems involved.

4-3 The Principle of Corresponding States

Fig 4-1 shows that the intermolecular potentials of Ar-Ar and Kr-Kr are different but of the same form. This suggests that by simple change in scale of one potential the two curves can duplicate one another. The scaling factors can then be the collision diameter σ and the well depth of the potential energy, ε . A set of substances which have same functional form of potential energy but only differ in the values of σ and ε are called 'conformal'. That is, if substances 0 and 1 are mutually conformal, then the potential energy of substance 1 can be obtained from the potential energy of substance 0 by multiplying by the appropriate scaling factors as defined by

$$u_1(r) = f_{1,0} u_0(r/h_{1,0}^{1/3}) \qquad (4\text{-}3\text{-}1)$$

where u_1 = potential energy between species 1

u_0 = potential energy between species 0

$$f_{1,0} = \varepsilon_1^*/\varepsilon_0^* \qquad (4\text{-}3\text{-}2)$$

$$h_{1,0} = \left(\sigma_1^*/\sigma_0^*\right)^3 \qquad (4\text{-}3\text{-}3)$$

Eq.(4-3-1) shows that potential energy between two molecules

of species 1, u_1, can be obtained from that of species 0 by using the two scaling factors, $f_{1,0}$ and $h_{1,0}$ which are defined in Eq.(4-3-2) and (4-3-3). (Substance 0 will hereafter called a reference substance, since its potential is assumed to be known.)

If N molecules of reference substance, 0, are confined in a volume V and at a temperature T and N molecules of substance 1 are confined in a geometrically same but different volume of $V \cdot h_{1,0}$ and at a temperature $T \cdot h_{1,0}$, then for each configuration of the molecules of reference substance there is a corresponding configuration of those of substance 1, i.e., from Eq.(4-3-1),

$$\frac{U_1[r_1 h_{1,0}^{1/3}, \cdots r_N h_{1,0}^{1/3}]}{k(T \cdot f_{1,0})} = \frac{U_0[r_1, \cdots r_N]}{kT} \qquad (4\text{-}3\text{-}4)$$

Eq.(4-3-4) enables us to calculate the configurational integral of substance 1 from the configurational integral of reference substance and, therefore, the fundamental theoretical basis of the principle of corresponding states lies here.

From Eq.(4-2-10)

$$Q_0[V, T] = \frac{1}{N!} \int_V \cdots \int \exp[-U_0(r_1, \cdots r_N)/kT] \, dr_1, \cdots dr_N \qquad (4\text{-}3\text{-}5)$$

$$\begin{aligned} & Q_1[V h_{1,0}, T f_{1,0}] \\ &= \frac{1}{N!} \int_V \cdots \int \exp[-U_1(r_1 h_{1,0}^{1/3}, \cdots r_N h_{1,0}^{1/3})/kT \cdot f_{1,0}] \, dr_1 \cdot h_{1,0} \cdots dr_N h_{1,0} \\ &= \frac{h_{1,0}^N}{N!} \int_V \cdots \int \exp[-U_1(r_1 h_{1,0}^{1/3}, \cdots r_N h_{1,0}^{1/3})/k \cdot T f_{1,0}] \, dr_1 \cdots dr_N \end{aligned} \qquad (4\text{-}3\text{-}6)$$

Hence

$$Q_1[h_{1,0}V,\ f_{1,0}T] = h_{1,0}^{N}\ Q_0[V, T] \qquad (4\text{-}3\text{-}7)$$

or by replacing V and T by $V(h_{1,0})^{-1}$ and $T(f_{1,0})^{-1}$

$$Q_1[V, T] = h_{1,0}^{N}\ Q_0[V h_{1,0}^{-1},\ T f_{1,0}^{-1}] \qquad (4\text{-}3\text{-}8)$$

Thus using Eq.(4-3-7) or (4-3-8) the configurational part of the free energy of substance 1 can be determined from that of substance 0, i.e.

$$A = A_{mol} + A_{config} \qquad (4\text{-}3\text{-}9)$$

where A_{mol} arises from the molecular part of Z in Eq.(4-2-9) and A_{config} from the configurational integral Q. Hence from Eq.(4-2-1) and (4-3-8)

$$(A_{config})_1 (V, T) = -kT \ln [Q_1 (V, T)] \qquad (4\text{-}3\text{-}10)$$

$$(A_{config})_0 (V h_{1,0}^{-1},\ T f_{1,0}^{-1})$$

$$= -k (T \cdot f_{1,0}^{-1}) \ln [Q_0 (V h_{1,0}^{-1},\ T f_{1,0}^{-1})] \qquad (4\text{-}3\text{-}11)$$

and hence

$$(A_{config})_1 (V, T)$$

$$= f_{1,0}\ (A_{config})_0 (V h_{1,0}^{-1},\ T f_{1,0}^{-1}) - NkT \ln h_{1,0} \qquad (4\text{-}3\text{-}12)$$

Since $P = -\left(\frac{\partial A}{\partial V}\right)_T$

$$P_1 (V, T) = (f_{1,0} \cdot h_{1,0}^{-1}) \cdot P_0 (V h_{1,0}^{-1},\ T f_{1,0}^{-1}) \qquad (4\text{-}3\text{-}13)$$

Eq.(4-3-12) and (4-3-13) enable us to calculate the presumed unknown properties of substance 1 from the presumed known

properties of a conformal reference, 0. Moreover Eq.(4-3-13) shows that the P-V-T surface of one substance is related to that of another conformal substance macroscopically by means of the two scale factors, h and f, which were defined microscopically from their potential curve. That is, Eq.(4-3-13) clearly shows that a P-V-T surface of substance 1, in a three dimensional space, can be reconstructed from substance 0 by multiplying the volume scale by h^{-1}, the temperature scale by f^{-1} and the pressure scale by $f \cdot h^{-1}$. Thus if an equation of state of a reference substance is expressed as

$$F_o(P,V,T) = 0 \qquad (4\text{-}3\text{-}14)$$

then that of substance 1 can be expressed as

$$F_1(P \cdot f_{1,o} h_{1,o}^{-1},\ V h_{1,o},\ T f_{1,o}) = 0 \qquad (4\text{-}3\text{-}15)$$

Thus

$$F_o(P, V, T) = F_1(P f_{1,o} h_{1,o}^{-1},\ V h_{1,o},\ T f_{1,o}) \qquad (4\text{-}3\text{-}16)$$

or more frequently

$$F_1(P, V, T) = F_o(P h_{1,o} f_{1,o}^{-1},\ V h_{1,o}^{-1},\ T f_{1,o}^{-1}) \qquad (4\text{-}3\text{-}17)$$

Eq.(4-3-17) implies that all singular points on the P-V-T surface, for example, the triple point, and the critical point, have the values of P,V,T in the same ratios of those scaling factors. If we choose the critical point as a characteristic parameter, then their ratios of P, V, T also have same values of scaling factors, i.e.

$$f_{1,0} = T_1^c/T_o^c \qquad \text{or} \qquad T_1^c = T_o^c \cdot f_{1,0} \qquad (4\text{-}3\text{-}18\text{-}a)$$

$$h_{1,o} = V_1^c/V_o^c \qquad \text{or} \qquad V_1^c = V_o^c \cdot h_{1,o} \tag{4-3-18-b}$$

$$f_{1,o}/h_{1,o} = P_1^c/P_o^c \qquad \text{or} \qquad P_1^c = P_o^c \cdot f_{1,o}/h_{1,o} \tag{4-3-18-c}$$

By combining Eq.(4-3-17) and (4-3-18),

$$F_o(P/P_o^c\ ,\ V/V_o^c\ ,\ T/T_o^c) = F_1(P/P_1^c\ ,\ V/V_1^c\ ,\ T/T_1^c) \tag{4-3-19}$$

Similarly the compressibility factors can be related as

$$Z_o(V,T) = Z_1(Vh_{1,o}\ ,\ Tf_{1,o}) \tag{4-3-20}$$

or by choosing P and T as parameters instead of V and T

$$Z_o(P,T) = Z_1(P\cdot f_{1,o}/h_{1,o}\ ,\ Tf_{1,o}) \tag{4-3-21}$$

or

$$Z_1(P,T) = Z_o(P\cdot h_{1,0}/f_{1,0}\ ,\ Tf_{1,0}^{-1}) \tag{4-3-22}$$

Hence the compressibility factor of substance 1 can be calculated from that of reference substance by using either Eq.(4-3-20) or Eq.(4-3-22) according to the parameters chosen.

There are, however, two restrictions on this simple form of the principle, that is,

(i) Eq.(4-3-19) holds only over restricted sets of substances such as Ar, Kr, Xe or, with less accuracy, for example, to the set of isomers of hexane.

(ii) The principle applies only for pure substances.

The first restriction in effect limits its use to spherically symmetrical and non-polar molecules. If we exclude polar molecules, the departure from the principle of corresponding states is due to the shape of molecules since the potential

energy between molecules are functions not only of their distance apart but of their orientation. Therefore the potential energy given by Eq.(4-2-11) does not hold for non-spherical molecules. However this departure is not random and can be characterised by adding a third parameter such as Pitzer's acentric factor ω .[39,51]

Since this work dealt with ethylene (non-spherical) and its mixtures with methane, direct application of Eq.(4-3-22) was not possible. Hence in section (4-4) the departure from the corresponding states principle for pure gas will be discussed in connection with the acentric factor and Leland's shape factors.[53] The predicted values of compressibility factors for ethylene will be compared with experimental values. In section (4-5) the extension of the principle for the mixtures will be described for one fluid model and the predicted results will be compared with experimental values of mixture 1, 2, and 3 of this work.

4-4 Departure from the Principle of Corresponding States: The Compressibility Factors of Ethylene

If the molecules are not spherically symmetrical, the pair potential energy is a function not only of the scalar distance, r, but also of the relative orientations of the two molecules. Hence the parameters h and f are also functions of orientations. Thus the non-spherical molecules need the third parameter to characterise the potential energy in Eq.(4-2-8).

A convenient but empirical method for distinguishing quantitatively between simple fluids such as Ar, Kr, Xe and

non-simple fluids is by comparison of the reduced vapour pressure at a common reduced temperature. Pitzer therefore introduced as the third parameter the 'acentric factor', based on the observation that the reduced vapour pressure curves of non-spherical molecules depart from that of simple fluids such as Ar, Kr, Xe, in such a way that the more non-spherical the molecule, the further is the departure. The acentric factor is defined as,

$$\omega = -\log \frac{P_\sigma}{P_c} - 1.0 \qquad (4\text{-}4\text{-}1)$$

where P_σ = vapour pressure at $T_r = 0.7$.

$T_r = 0.7$ was chosen purely for convenience since the reduced vapour pressure of the simple fluid at this temperature is almost exactly 0.1, thus $\omega = 0.0$ for the simple fluids. The values for other materials can be found from the list by Reid and Sherwood.[54]

If the acentric factor is less than about 0.2 then the departure from corresponding states is approximately linear in ω hence the compressibility factor can be written

$$Z = Z(P_r, T_r, \omega) \qquad (4\text{-}4\text{-}2)$$

or more conveniently

$$Z(P_r, T_r) = Z_o(P_r, T_r) + \omega Z_1(P_r, T_r) \qquad (4\text{-}4\text{-}3)$$

where Z_o is the compressibility factor of a simple fluid as a function of pressure and temperature,

$$P_r = P/P_c \quad \text{and} \quad T_r = T/T_c \qquad (4\text{-}4\text{-}4)$$

and Z_1 is an auxiliary function which must be found empirically.

Both tabulations and graphs of Z_o and Z_1 can be found in the literature.(55,56)

As an alternative to determining the auxiliary function Z_1, 'shape factors' can be used.(53) If substance 0 and 1 have similar but non-identical reduced equations of state (Eq.4-3-19) then the parameters, h and f are slowly varying functions of V and T, but which are always close to the ratio of critical values. The departure of h and f from the critical constants can thus be incorporated into slowly varying functions, θ and Φ which Leland et al(40) called 'shape factors'. That is,

$$f_{1,o}(v_1, T_1) = \left(\frac{T_1^c}{T_o^c}\right) \theta_{1,o}(v_1^R, T_1^R) \qquad (4\text{-}4\text{-}5)$$

$$h_{1,o}(v_1, T_1) = \left(\frac{v_1^c}{v_o^c}\right) \Phi_{1,o}(v_1^R, T_1^R) \qquad (4\text{-}4\text{-}6)$$

The functions $\theta_{1,o}$ and $\Phi_{1,o}$ can be combined to produce a factor $\Psi_{1,o}$ which modifies the critical pressure P_1^c, thus

$$g_{1,o}(P_1, T_1) = \left(\frac{P_1^c}{P_o^c}\right) \Psi_{1,o}(P_1^R, T_1^R) \qquad (4\text{-}4\text{-}7)$$

The shape factors θ and Φ are functions of temperature and volume, and the dependence of these factors on T_1^r and V_1^r might be thought to be specific to the pair of substances 1 and 0 under consideration. However, from the fact that departures from the principle of corresponding states are not random, the shape factors in Eq.(4-4-5) and (4-4-6) can be characterized by one additional parameter, such as Pitzer's acentric factor, ω, and Leland and Leach(40) have shown that

$\theta_{1,0}$ and $\Phi_{1,0}$ can be written, at least for non-polar substances, as unique functions of V_1^r, T_1^r and the difference $(\omega_1 - \omega_0)$. They found that when methane is the reference substance, the two shape factors are given as follows,

$$\theta_{1,0} = 1 + (\omega_1 - \omega_0)\left[0.0892 - 0.8493 \ln T_1^R + (0.3063 - 0.4506/T_1^R)(V_1^R - 0.5)\right] \tag{4-4-8}$$

$$\Phi_{1,0} = \left\{1 + (\omega_1 - \omega_0)\left[0.3903\,(V_1^R - 1.0177) - 0.9462\,(V_1^R - 0.7663)\ln T_1^R\right]\right\}\left(\frac{Z_0^c}{Z_1^c}\right) \tag{4-4-9}$$

In order to calculate the shape factors from Eq.(4-4-8) and (4-4-9) the reduced volume, V_1^r, and temperature, T_1^r, must be known. In general, pressure and temperature are measured rather than volume and temperature and hence an iterative method is involved in solving for these factors.

Thus the sequence for predicting the compressibility factor of substance 1 (in this case ethylene) at a given pressure and temperature, from the equation of state of substance 0, can be summerized as follows.

(i) Problem to be solved is the equation of state of the reference substance, i.e. from Eq.(4-3-17),

$$F_0\left(P\frac{h_{1,0}}{f_{1,0}},\ Vh_{1,0}^{-1},\ Tf_{1,0}^{-1}\right) = 0 \tag{4-4-10}$$

for a given P and T.

(ii) The scaling factors, $f_{1,0}$ and $h_{1,0}$ are given in Eq.(4-4-5) and (4-4-6) for non-spherical molecule.

(iii) The shape factors in Eq.(4-4-5) and (4-4-6) are given in

Eq.(4-4-8) and (4-4-9) as functions of volume and temperature.

(iv) Since volume is not known the shape factors (and therefore the volume) are solved by an iterative method.

In this work methane was chosen as a reference substance and the Bender equation (3-3-2) was used as the equation of state, whose 20 coefficients for methane were determined by Chapela[57] by means of least-squares procedure using recently published experimental data.[1,58-63]

In predicting the compressibility factor of ethylene from the equation of state of methane, the actual computational procedure was as follows.

(i) Before iteration starts both shape factors are set to unity, i.e.

$$\theta_{1,0} = 1.0, \qquad \Phi_{1,0} = 1.0 \tag{4-4-11}$$

(ii) The scaling factors, $f_{1.0}$ and $h_{1,0}$, are then calculated according to Eq.(4-4-5) and (4-4-6).

(iii) With known values of P and T and the scaling factors, $h_{1,0}$ and $f_{1,0}$ which are determined in (ii), the equation of state (4-4-10) is solved. In this case the reference pressure, P_o, is $P \cdot h_{1,0}/f_{1,0}$ and the reference temperature, T_o, is $T/f_{1,0}$. Thus the solution of Eq.(4-4-10) gives V_o or $V/h_{1,0}$. The Bender equation used in this work is an implicit function of density (and hence volume), therefore the reference volume, V_o $(=V/h_{1,0})$ too is solved by an iterative method.

(iv) The reference volume, $V/h_{1,0}$, is multiplied by $h_{1,0}$

to give the predicted volume V.

(v) The shape factors, $\theta_{1,0}$ and $\Phi_{1,0}$, are now calculated using V evaluated in (iv) according to Eq.(4-4-8) and (4-4-9).

(vi) The shape factors are compared with those of previously assumed values. If the differences are greater than pre-set accuracies, new values of $\theta_{1,0}$ and $\Phi_{1,0}$ are determined by means of Newton-Raphson method using previously calculated volume V.

(vii) These new values are supplied to (ii) above and thus the interation continues until the conditions in (vi) satisfied.

The computer program of the iteration method involved the above procedure was provided by Saville,[64] who modified the Newton-Raphson method in such a way that the iteration starts with the Newton method until it converges to a certain accuracy, then the computation is switched to secant method in order to 'speed up' the computation at the last stage of the computation.

As was mentioned in section (4-4) the acentric factor, ω, was introduced in order to correct the departure from the principle of corresponding state for non-spherical molecules and was defined in terms of reduced vapour pressure at $0.7 \cdot T^c$. However, it does not necessarily follow that the value of ω determined in this way is the value most appropriate for the whole fluid region. We therefore decided to examine empirically the suitability of the value of ω determined in the traditional way.

From the vapour pressure data[17] using Eq.(4-4-1) the

acentric factor ω was calculated as about 0.085, whereas Reid and Sherwood determined ω from the normal boiling point as 0.073.[65] Thus ω was varied from 0.073 to 0.13 with an interval of about 0.005. The compressibility factor and other thermodynamic functions (e.g. S and f^*/P) were calculated using different values of ω, and the deviations of these calculated values were compared each other by means of the root-mean-square deviation which is of the form of,

$$(RMS)_x = \sqrt{\frac{\sum[(x-x_{cal})/x]^2}{N}} \qquad (4\text{-}4\text{-}12)$$

The aim was to choose the best value of ω such that the root-mean-square (or simply rms) deviations were as small as possible for Z and for the other thermodynamic functions both inside and outside the experimental range of this work. Considering first values within the pressure and temperature range investigated experimentally in this work, the rms values of Z were calculated for <u>all</u> experimental data points and entropy, S, and the fugacity-pressure ratio, f^*/P, for three isotherms (273.15, 278.15 and 283.15^{o}K) each at 10, 20 and 30 bar pressure. The rms values of S and f^*/P were calculated from the values of IUPAC Table according to Eq.(4-4-12).

It was found that as the value of ω increases the $(rms)_Z$ decreases while $(rms)_S$ and $(rms)_{f/P}$ increase, i.e.

ω	$(rms)_Z$	$(rms)_S$	$(rms)_{f/P}$
0.073	$0.286\cdot10^{-2}$	$0.110\cdot10^{-2}$	$0.320\cdot10^{-2}$
0.085	$0.239\cdot10^{-2}$	$0.123\cdot10^{-2}$	$0.330\cdot10^{-2}$
0.130	$0.127\cdot10^{-2}$	$0.444\cdot10^{-2}$	$0.340\cdot10^{-2}$

When ω was 0.073 the calculated Z were systematically larger than those of the experimental values and thus resulted the largest $(rms)_Z$. Although $(rms)_{f/P}$ was minimum at ω=0.073 the differences were small compared with $(rms)_Z$ and $(rms)_S$. For these reasons ω=0.073 was discarded in choosing the optimum value of acentric factor and the values between 0.085 and 0.13 were compared further with values outside of our own experimental range taken from the IUPAC tables.

The entropy and fugacity-pressure ratio were calculated at four isotherms (293.15, 323.15, 373.15 and 423.15°K) with 12 pressures ranging 40 to 3000 bar. The $(rms)_s$ and $(rms)_{f/P}$ for 48 points were;

ω	$(rms)_S$	$(rms)_{f/P}$
0.085	$0.415 \cdot 10^{-2}$	$0.839 \cdot 10^{-2}$
0.130	$1.098 \cdot 10^{-2}$	$1.749 \cdot 10^{-2}$

Finally vapour-liquid equilibrium temperatures (T_σ) were calculated for pressures from 0.1 to 40 bar and the $(rms)_{T_\sigma}$ for different values of acentric factors were as follows,

ω	$(rms)_{T_\sigma}$
0.073	$0.378 \cdot 10^{-2}$
0.085	$0.190 \cdot 10^{-2}$
0.130	$1.032 \cdot 10^{-2}$

The results above show that although a value of ω nearer 0.13 gives a better fit with our P-V-T measurements than does

0.085, the errors are in any case quite small for both values. However, the larger values of ω leads to substantially larger errors at values of P and T well outside our range. Thus we consider 0.085 to be close to the optimum and we shall continue to use this value in what follows.

In table 4-1 the 'calculated' (or predicted) values of the compressibility factors for all our experimental P and T are presented together with the experimental compressibility factors (that is, determined from the 10-coefficient Bender equation 3-6-3) and individual per cent deviation of each predicted Z from the experimental value.

The root-mean-square deviation of predicted Z was, as mentioned earlier, $0.239 \cdot 10^{-2}$ or less than 0.24% on average.

TABLE 4-1

COMPARISON OF EXPERIMENTAL AND PREDICTED COMPRESSIBILITY FACTORS (ETHYLENE)

RUN NUMBER	T (K)	PRESSURE (BAR)	Z EQ 3-6-3	Z PREDICTION	DEVIATIONS (PER CENT)
19					
	273.80	35.116	.6501	.6509	-.1338
	273.79	27.363	.7543	.7568	-.3357
	273.79	20.236	.8300	.8328	-.3307
	273.79	14.481	.8835	.8859	-.2681
	273.79	10.149	.9206	.9225	-.2004
	273.79	7.014	.9462	.9475	-.1436
	273.79	4.807	.9636	.9645	-.1006
	273.79	3.270	.9754	.9761	-.0693
22					
	270.44	33.647	.6494	.6510	-.2394
	270.45	26.420	.7524	.7550	-.3543
	270.44	19.674	.8277	.8305	-.3320
	270.45	14.164	.8814	.8837	-.2663
	270.44	9.979	.9188	.9206	-.1987
	270.44	6.932	.9447	.9460	-.1426
	270.45	4.770	.9624	.9634	-.1001
	270.44	3.264	.9745	.9752	-.0693
23					
	266.60	33.610	.6177	.6201	-.3910
	266.60	27.122	.7263	.7291	-.3859
	266.60	20.596	.8078	.8106	-.3510
	266.60	15.036	.8667	.8691	-.2828
	266.59	10.723	.9080	.9100	-.2130
	266.60	7.518	.9370	.9384	-.1541
	266.58	5.214	.9569	.9580	-.1089
	266.59	3.592	.9706	.9714	-.0759

TABLE 4-1 (CONTINUED)

COMPARISON OF EXPERIMENTAL AND PREDICTED COMPRESSIBILITY FACTORS
(ETHYLENE)

RUN NUMBER	T (K)	PRESSURE (BAR)	Z EQ 3-6-3	Z PREDICTION	DEVIATIONS (PER CENT)
28					
	251.15	20.096	.7610	.7654	-.5775
	251.14	15.377	.8294	.8325	-.3799
	251.14	11.383	.8795	.8818	-.2642
	251.14	8.243	.9155	.9172	-.1857
	251.13	5.881	.9410	.9422	-.1304
	251.13	4.154	.9589	.9598	-.0913
	251.13	2.915	.9715	.9721	-.0637
29					
	247.09	16.581	.8002	.8043	-.5171
	247.09	12.515	.8575	.8604	-.3382
	247.08	9.199	.8992	.9013	-.2310
	247.09	6.642	.9292	.9307	-.1599
	247.08	4.738	.9504	.9514	-.1113
	247.08	3.352	.9653	.9661	-.0775
	247.08	2.357	.9758	.9764	-.0539
30					
	243.66	15.426	.8066	.8111	-.5581
	243.66	11.664	.8616	.8647	-.3566
	243.66	8.598	.9018	.9039	-.2391
	243.66	6.230	.9307	.9322	-.1637
	243.67	4.461	.9512	.9523	-.1131
	243.66	3.169	.9656	.9665	-.0785

TABLE 4-1 (CONTINUED)

COMPARISON OF EXPERIMENTAL AND PREDICTED COMPRESSIBILITY FACTORS
(ETHYLENE)

RUN NUMBER	T (K)	PRESSURE (BAR)	Z EQ 3-6-3	Z PREDICTION	DEVIATIONS (PER CENT)
31					
	254.35	21.831	.7476	.7517	-.5529
	254.35	16.735	.8202	.8233	-.3775
	254.35	12.382	.8734	.8757	-.2698
	254.33	8.950	.9114	.9132	-.1928
	254.34	6.369	.9384	.9397	-.1365
	254.33	4.484	.9573	.9582	-.0959
	254.34	3.135	.9704	.9711	-.0670
32					
	258.89	23.782	.7383	.7419	-.4888
	258.89	18.185	.8145	.8175	-.3638
	258.90	13.400	.8700	.8724	-.2720
	258.90	9.638	.9096	.9114	-.1987
	258.89	6.822	.9375	.9388	-.1422
	258.90	4.777	.9569	.9578	-.1003
	258.89	3.321	.9703	.9710	-.0701
33					
	278.86	34.219	.6945	.6958	-.1812
	278.85	25.774	.7889	.7915	-.3345
	278.84	18.608	.8557	.8583	-.3090
	278.85	13.079	.9021	.9043	-.2426
	278.83	9.037	.9339	.9355	-.1776
	278.84	6.175	.9555	.9567	-.1255
	278.83	4.189	.9701	.9709	-.0868
	278.84	2.829	.9799	.9805	-.0594

TABLE 4-1 (CONTINUED)

COMPARISON OF EXPERIMENTAL AND PREDICTED COMPRESSIBILITY FACTORS (ETHYLENE)

RUN NUMBER	T (K)	PRESSURE (BAR)	Z EQ 3-6-3	Z PREDICTION	DEVIATIONS (PER CENT)
34					
	283.15	37.899	.6725	.6727	-.0242
	283.15	28.556	.7751	.7775	-.3091
	283.15	20.575	.8472	.8498	-.3139
	283.14	14.414	.8968	.8991	-.2531
	283.15	9.918	.9307	.9324	-.1870
	283.14	6.746	.9536	.9548	-.1324
	283.14	4.554	.9690	.9699	-.0916
	283.13	3.059	.9793	.9799	-.0624
35					
	288.84	41.184	.6670	.6663	.1067
	288.83	30.652	.7742	.7764	-.2723
	288.82	21.857	.8480	.8505	-.2987
	288.82	15.168	.8983	.9005	-.2447
	288.80	10.350	.9322	.9339	-.1815
	288.84	6.987	.9549	.9561	-.1282
	288.81	4.682	.9701	.9709	-.0884
	288.83	3.119	.9802	.9808	-.0599
36					
	292.59	41.282	.6872	.6869	.0477
	292.56	30.165	.7901	.7921	-.2606
	292.57	21.233	.8598	.8622	-.2746
	292.58	14.593	.9067	.9088	-.2220
	292.58	9.872	.9382	.9398	-.1631
	292.59	6.616	.9592	.9602	-.1145
	292.58	4.404	.9730	.9738	-.0784
	292.58	2.923	.9822	.9827	-.0529

4-5 The Extension of the Principle of Corresponding States; The Compressibility Factors of Methane-Ethylene mixtures

The prediction of thermodynamic properties of mixtures is one of the most important fields in the application of thermodynamics to chemical engineering, since, practically, it is impossible to measure the P-V-T properties of every pure substance and every multi-component system of interest to the chemical engineers.

As described in section (4-3) the theoretical foundation of the principle of corresponding states is a simple relation between the configurational integrals of two substances, one of whose properties are known, and the other one whose properties are to be calculated from the known properties of the other substance.

Thus in the case of mixtures the problem is now to relate the configurational integral of a mixture to those of C individual components from which the mixture is composed, so that, from the knowledge of the properties of the individual component, the properties of the mixture can be estimated.

From Eq.(4-2-10) the configurational integral of a mixture can be written,

$$Q = \frac{1}{\prod_{\alpha} N_\alpha!} \int \cdots \int_V \exp[-U(r)/kT]\, dr_1\, dr_2 \cdots dr_N \qquad (4\text{-}5\text{-}1)$$

where

$$\sum_{\alpha=1}^{C} N_\alpha = N \qquad (4\text{-}5\text{-}2)$$

The potential energy U(r) in Eq.(4-5-1) now depends not

only on the comfigurations of N molecules but also on the assignment by species to these configurations. In a pure fluid U(r) is a function only of the positions and not of the assignment of the 'indistinguishable' molecules to these positions. (For the sake of simplicity the N molecules are assumed to be spherical as in Eq. 4-2-10).

In a mixture of m components there are ${}_mC_2$ or $\frac{1}{2}$ m(m+1) different pair potentials of the kind of $u_{ij}(r)$. That is, in a pure component, i, only a single potential $u_{ii}(r)$ exists whereas in a binary with components, i and j, there are three different pair potentials, i.e. $u_{ii}(r)$, $u_{jj}(r)$ and $u_{ij}(r)$. These cross-terms, $u_{ij}(r)$, etc. cannot be known from the knowledge of the potential of pure i and pure j alone, and even if all the potentials are known, the dependence of U(r) in Eq.(4-5-1) on assignment-by-species precludes the use of the simple dimensional arguments in section (4-3).

Thus two problems arise here, i.e.

(i) the calculation of $u_{ij}(r)$

(ii) the calculation of Q of the mixture.

In the case of an isotopic mixture, that is, U is independent of the assignment to the configurations of N molecules, and the pair potentials u(r) are the same for every species, then, the difference between Helmholtz free evergy of the mixture, $A_{mix}(V,T)$ and that of any one of the same number of molecules of one of the pure components, $A_o(V,T)$ can be written,[44]

$$A_{mix}(V,T) - A_o(V,T) = -kT \ln \frac{Q}{Q_o} = kT \ln \frac{\pi N_i!}{N!} \qquad (4\text{-}5\text{-}3)$$

By applying Stirling's rule, i.e. for large N,

$$\ln(N!) = N\ln(N) - N \qquad (4\text{-}5\text{-}4)$$

Eq.(4-5-3) can be rearranged as

$$A_{mix}(V,T) - A_o(V,T) = NkT \sum \chi_\alpha \ln \chi_\alpha \qquad (4\text{-}5\text{-}5)$$

where χ_α is the mole fraction of component α.

Eq.(4-5-5) was derived for an 'isotopic mixture', whose potentials depend only on the configuration and not on the assignment. In the case of a real gas mixture, Eq.(4-5-5) is hardly applicable, since any difference in u(r) arising from differences in molecular size, shape, polarity etc. leads to deviations from ideality in Eq.(4-5-5).

Nevertheless Eq.(4-5-5) suggests that by manipulating U(r) in Eq.(4-5-1) appropriately, $A_o(V,T)$ can be replaced by an 'equivalent free energy term' for the mixture. One way of doing this is to take an average value of U for over all possible assignments for each configuration so that the potential energy U is again a function only of the configurations of N molecules. By substituting this average potential into Eq.(4-5-1),

$$A_{mix}(V,T) - A_{av.}(V,T) = NkT \sum \chi_\alpha \ln \chi_\alpha \qquad (4\text{-}5\text{-}6)$$

$A_{av}(V,T)$ in Eq.(4-5-6) is the free-energy from the configurational integral which is, in turn, related to the average potential energy.

Thus by comparing Eq. (4-5-5) and (4-5-6) it can be said that the configurational free energy of the mixture, after subtraction of the ideal mixing term, can be replaced by that of a single equivalent substance. This hypothetical 'single fluid' will be different for each mixture and is denoted by the single subscript x.

Thus,

$$(A_{conf.})_{mix} = (A_{conf})_x + NkT \sum x_i \ln x_i \qquad (4\text{-}5\text{-}7)$$

where

$$(A_{conf})_x = -kT\ln Q_x = \frac{1}{N!} \int_v \cdots \int \exp[-U_x(r)/kT]\, dr_1 \cdots dr_N \qquad (4\text{-}5\text{-}8)$$

and

$$U_x(r) = \sum_{l<m}^{N-1} \sum^{N} u_x(r_{lm}) \qquad (4\text{-}5\text{-}9)$$

A set of equations (4-5-7) to (4-5-9) is called an 'one fluid approximation', since $(A_{conf})_{mix}$ is calculated from a configurational free energy of a hypothetical single component.

The principle of corresponding states is now introduced, so that if the potential u_x in Eq.(4-5-9) is conformal with those of the pure components from which mixture is made, u_{ii}, u_{jj} etc., then Q_x in Eq.(4-5-8) can be related to Q_o (o refers to a reference substance) in a similar manner as in Eq.(4-3-7) and (4-3-8).

$$Q_x = h_x^N\, Q_o[V h_x^{-1},\ T f_x^{-1}] \qquad (4\text{-}5\text{-}10)$$

and hence

$$(A_{conf})_x(V, T) = f_x (A_{conf})_o (V h_x^{-1},\ T f_x^{-1}) - NkT \ln h_x \qquad (4\text{-}5\text{-}11)$$

where

$$f_x = T_x^c / T_o^c \qquad h_x = V_x^c / V_o^c \qquad (4\text{-}5\text{-}12)$$

$$u_x(r) = f_x \cdot u_o(r \cdot h_x^{-1/3}) \qquad (4\text{-}5\text{-}13)$$

Thus f_x and h_x are the parameters of the equivalent substance

x with respect to the reference substance o. T_x^c and V_x^c are the pseudo-critical temperature and volume of the hypothetical fluld, and therefore this model is also called the pseudo-critical approximation.

A similar but alternative method is the so called 'two-fluid model' in which each real substance is replaced by an 'equivalent component' and each of these equivalent components are assumed to mix ideally to form the mixture.(41)

Thus in this case the equations (4-5-7) and (4-5-11) are replaced by

$$(A_{conf})_{mix} = \sum_{\alpha} x_\alpha \{ (A_{conf})_\alpha + RT \ln x_\alpha \} \qquad (4\text{-}5\text{-}14)$$

and

$$(A_{conf})_\alpha = f_{\alpha,o} (A_{conf})_o (v h_{\alpha,o}^{-1}, T f_{\alpha,o}^{-1}) - RT \ln h_{\alpha,o} \qquad (4\text{-}5\text{-}15)$$

Watson and Rowlinson(66) compared the two models in predicting the bubble-point temperature and vapour compositions of Ar-N_2-O_2 system and found only small differences between the two methods but with a small preference for the one fluid model. In this work, therefore, the one-fluid model was adopted for predicting the compressibility factors of methane-ethylene system using Eq.(4-5-7) and (4-5-11) with methane as a reference substance.

Thus in order to calculate $(A_{conf})_x$ in Eq.(4-5-11) f_x and h_x, or, from Eq.(4-5-12), T_x^c and V_x^c must be known. One of the crude estimation of T_x^c and V_x^c, which is widely used in chemical engineering calculation, is the kind which was introduced by Kay(67) as

$$T_x^c = \sum_i x_i T_i^c \qquad P_x^c = \sum_i x_i P_i^c \tag{4-5-16}$$

or from Eq.(4-3-18) and (4-5-16)

$$f_x = \sum_i x_i f_{ii} \qquad h_x = \frac{\sum_i x_i f_{ii}}{\sum_i x_i f_{ii} h_{ii}^{-1}} \tag{4-5-17}$$

Although this kind of approximation is widely used mainly due to its simplicity, it is a crude approximation, since f_x and h_x in Eq.(4-5-17) are calculated only from f_{ii} and h_{ii} and hence the dependence of f_x and h_x on the forces between unlike molecules, that is f_{ij} and h_{ij} $(i \neq j)$ is ignored.

Among others the so called van der Waals recipe is considered to be the best approximation[68,69] and this is expressed as,

$$f_x = \frac{\sum_i^c \sum_j^c x_i x_j f_{ij} h_{ij}}{\sum_i^c \sum_j^c x_i x_j h_{ij}} \tag{4-5-18}$$

$$h_x = \sum_i^c \sum_j^c x_i x_j h_{ij} \tag{4-5-19}$$

where c is the number of components in the mixture. Those for the like-interactions f_{ii}, h_{ii} etc. are calculated from the critical constants by Eq.(4-3-18). However, in the case of the unlike terms f_{ij}, h_{ij} $(i \neq j)$, it is assumed that f_{ij} and h_{ij} can be expressed as some kind of average of the like-terms, i.e.

$$f_{ij} = \xi_{ij} (f_{ii} \cdot f_{jj})^{1/2} \tag{4-5-20}$$

$$h_{ij} = \eta_{ij} \left(\tfrac{1}{2} h_{ii}^{1/3} + \tfrac{1}{2} h_{jj}^{1/3} \right)^3 \tag{4-5-21}$$

The use of geometric mean (Eq. 4-5-20) and arithmetic

mean (Eq.4-5-21) is purely empirical and the correction factors ξ_{ij} and η_{ij} are to be determined from experiment. In the absence of direct information it is recommended that one puts $\eta_{ij} = 1.0$ but takes ξ_{ij} as slightly less than unity.(44) Some typical values of ξ_{ij} for binary systems are given in the literature.(70-73)

Thus having all necessary information (except for ξ_{ij} and η_{ij} which are to be determined empirically) the calculation of the compressibility factors of methane-ethylene mixture can be summarised as follows.

(i) By differentiation of Eq.(4-5-11) with respect to volume, the pressure can be written as

$$P_x(v,T) = (f_x h_x^{-1})\, P_o(v h_x^{-1},\ T f_x^{-1}) \qquad (4\text{-}5\text{-}22)$$

Thus equation of state to be solved in the mixture is now

$$F_x(P,v,T) = F_o(P h_x f_x^{-1},\ v h_x^{-1},\ T f_x^{-1}) \qquad (4\text{-}5\text{-}23)$$

Here P and T are given.

(ii) In Eq.(4-5-20) and (4-5-21) subscript i refers to methane which is the reference substance of this work and j refers to ethylene. Thus both j_{ii} and h_{ii} are unity and f_{jj} and h_{jj} (or equivalently $f_{1,0}$ and $h_{1,0}$ in the previous section) are calculated in exactly same way as described in section (4-4) for given T, P and ω (=0.085). Thus the cross-terms f_{ij} and h_{ij} are calculated by means of Eq.(4-5-20) and (4-5-21). The choice of optimum values of the correction terms, ξ_{ij} and η_{ij}, will be discussed separately, thus for the time being, they are

fixed, e.g. $\xi_{ij} = \eta_{ij} = 1.0$

(iii) f_x and h_x are now calculated by means of Eq.(4-5-18) and (4-5-19).

(iv) Given P, T, f_x and h_x, the equation of state of the reference substance is solved, i.e.

$$F_o(Ph_x f_x^{-1}, Vh_x^{-1}, Tf_x^{-1}) = 0 \qquad (4\text{-}5\text{-}24)$$

As was mentioned in section (4-4) the equation of state (Bender equation) is an implicit function of density, hence Eq.(4-5-24) is solved by the iterative method.

(v) The solution is Vh_x^{-1}, thus the 'predicted' volume of the mixture at P and T is $(Vh_x^{-1})\cdot h_x$, and the calculation of the 'predicted' compressibility factor is straightforward, i.e. Z = PV/RT.

For simplicity, the above account ignores the shape factors introduced in section (4-4) to allow for the non-spherical nature of the molecules involved, particularly ethylene. In practice however all calculation on mixtures were made with shape factors included. This in no way affects the general procedure. It only increases the numerical complexity.

The above procedure was repeated with different values of ξ_{ij} and η_{ij} in order to find out the optimum values of the correction factors which could give the minimum value of root-mean-square deviations defined in Eq.(4-4-12).

In Fig 4-2 the root-mean-square deviations are plotted against ξ_{ij} ranging from 1.02 to 0.92 with a fixed value of $\eta_{ij} = 1.0$. The graph shows that the three minima occur at different

values of ζ_{ij} , i.e.

gas	ζ_{ij}	rms
0.6955 CH_4	0.965	$0.32 \cdot 10^{-2}$
0.4518 "	0.976	$0.46 \cdot 10^{-2}$
0.2419 "	0.985	$0.29 \cdot 10^{-2}$

and thus there appears to be a small composition dependence of ζ_{ij}.

Although the maximum difference of ζ_{ij} from the mean value ($\mp$ 0.975) is less than the probable uncertainties in the ζ_{ij} of most other systems[44] it is nevertheless desirable to try to bring all those minima closer together by varying η_{ij} . The same procedure was therefore repeated with different values of η_{ij} and the rms's are plotted against ζ_{ij} in Fig 4-3 with a fixed value of η_{ij} =0.99 and in Fig 4-4 with η_{ij} =1.01. These graphs show the same trend for the variation of optimum ζ_{ij} with composition the only difference being a small shift in the abscissa of the minimum of 0.005 per 0.001 of η_{ij} .

Thus, for this system at least, ζ_{ij} and η_{ij} appear to be correlated such that both cannot be treated as independently adjustable. We therefore take η_{ij} = 1.0 and for the moment at least, accept the slight composition dependence of ζ_{ij}.

One way of further examining the dependence of ζ_{ij} on composition is to check the behaviour of ζ_{ij} for the phase equilibrium in the methane-ethylene system. There are, however, few other workers' equilibrium data available, for this binary system,[74,75] and our investigations lead us to believe that errors in the data are larger than the sensitivity

of the principle of corresponding states as used in this work. For example Tully and Edmister[75] have published vapour-liquid equilibrium data with an accuracy of 0.2% in the temperature measurement. We found that the predicted bubble point temperature for 0.408 (molar fraction) methane mixture (226.8°K determined experimentally) varies from 226.34°K ($\zeta_{ij} = 1.0$, $\eta_{ij} = 1.0$) to 226.07°K ($\eta_{ij} = 1.0$, $\zeta_{ij} = 0.99$), and hence the change in the predicted temperature by changing ζ_{ij} by 0.01 is about 0.12% which is much smaller than the experimental error.

Therefore whether ζ_{ij} shows an apparent variation with composition is considered to be subject for further investigation.

For reason given above the optimum value of ζ_{ij} in this work was taken as the minimum value of the average rms of the three mixtures, i.e.

$$\zeta_{ij} = 0.975 \qquad \pm 0.01$$

and

$$\eta_{ij} = 1.0$$

Using these factors the predicted compressibility factors for all experimental data points were calculated and they are listed in Table 4-2 together with experimental Z and the individual deviations in %.

The root-mean-square deviations are

mixture 1	rms = $0.52 \cdot 10^{-2}$
mixture 2	rms = $0.47 \cdot 10^{-2}$
mixture 3	rms = $0.45 \cdot 10^{-2}$

The over-all average deviation was estimated as about $0.48 \cdot 10^{-2}$.

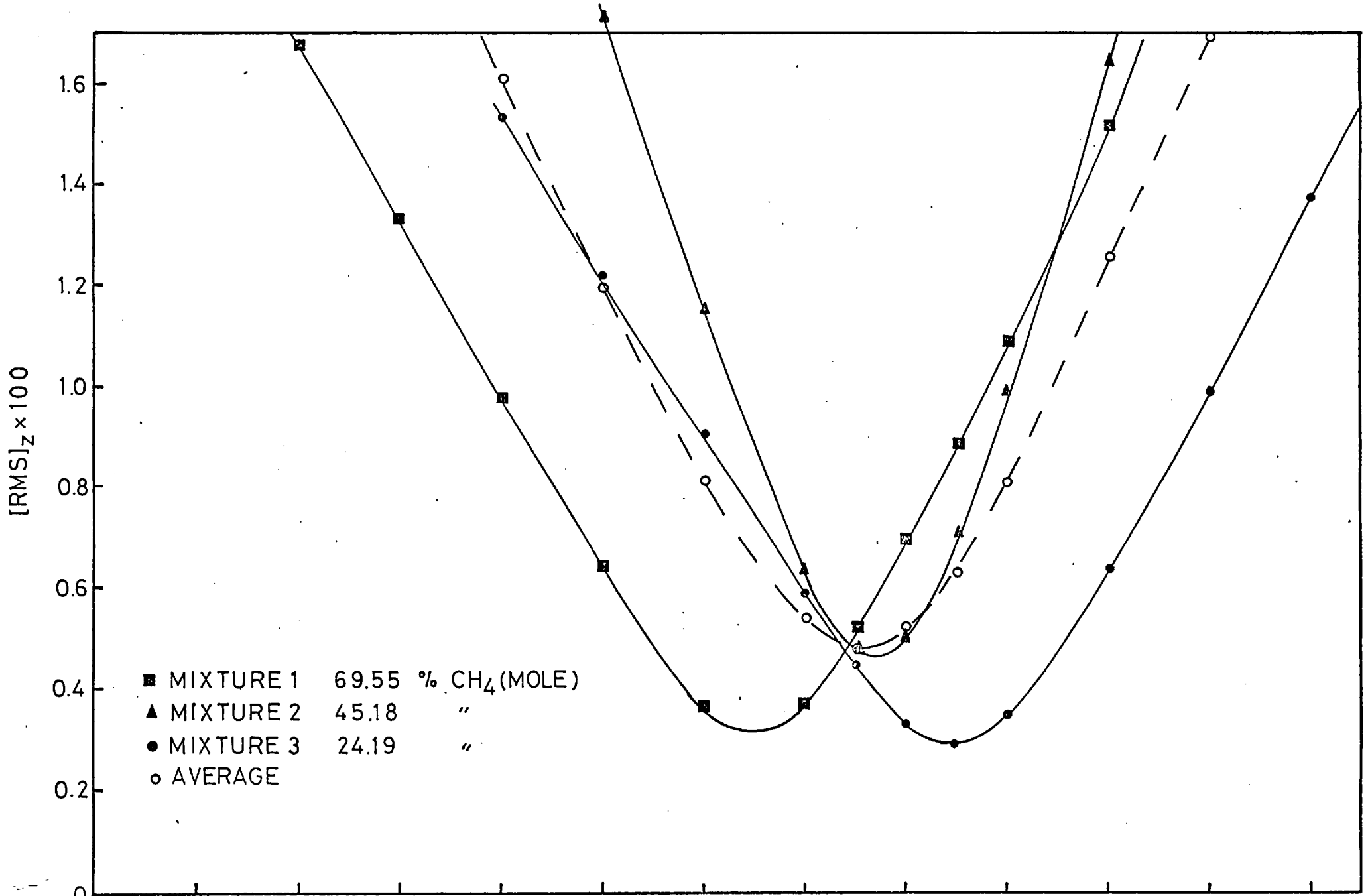


FIG 4-2 $[RMS]_z$ V. ξ_{ij} WHEN $\gamma_{ij} = 1.0$

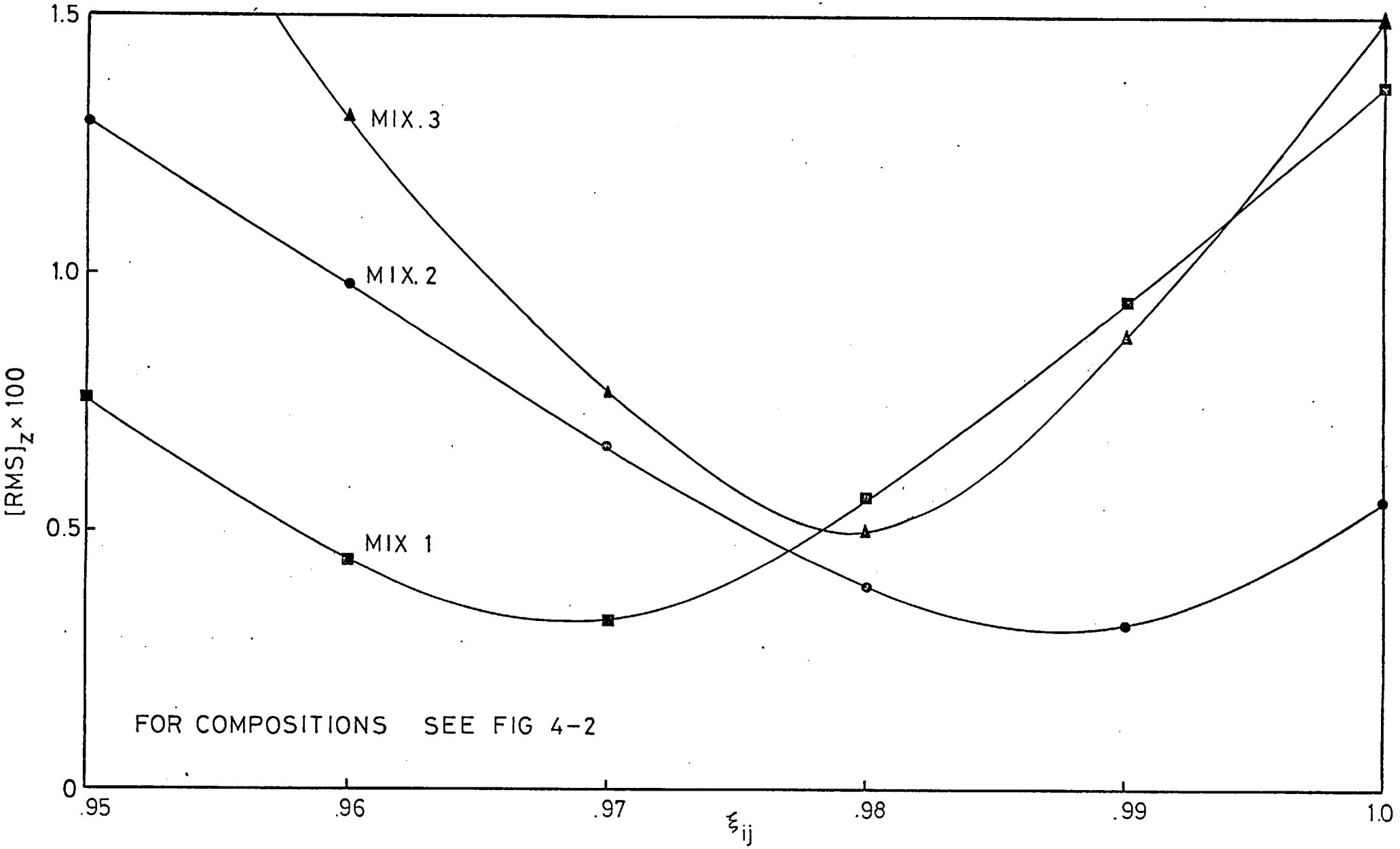


FIG 4-3 $[RMS]_z$ V. ξ_{ij} WHEN $\eta_{ij} = 0.99$

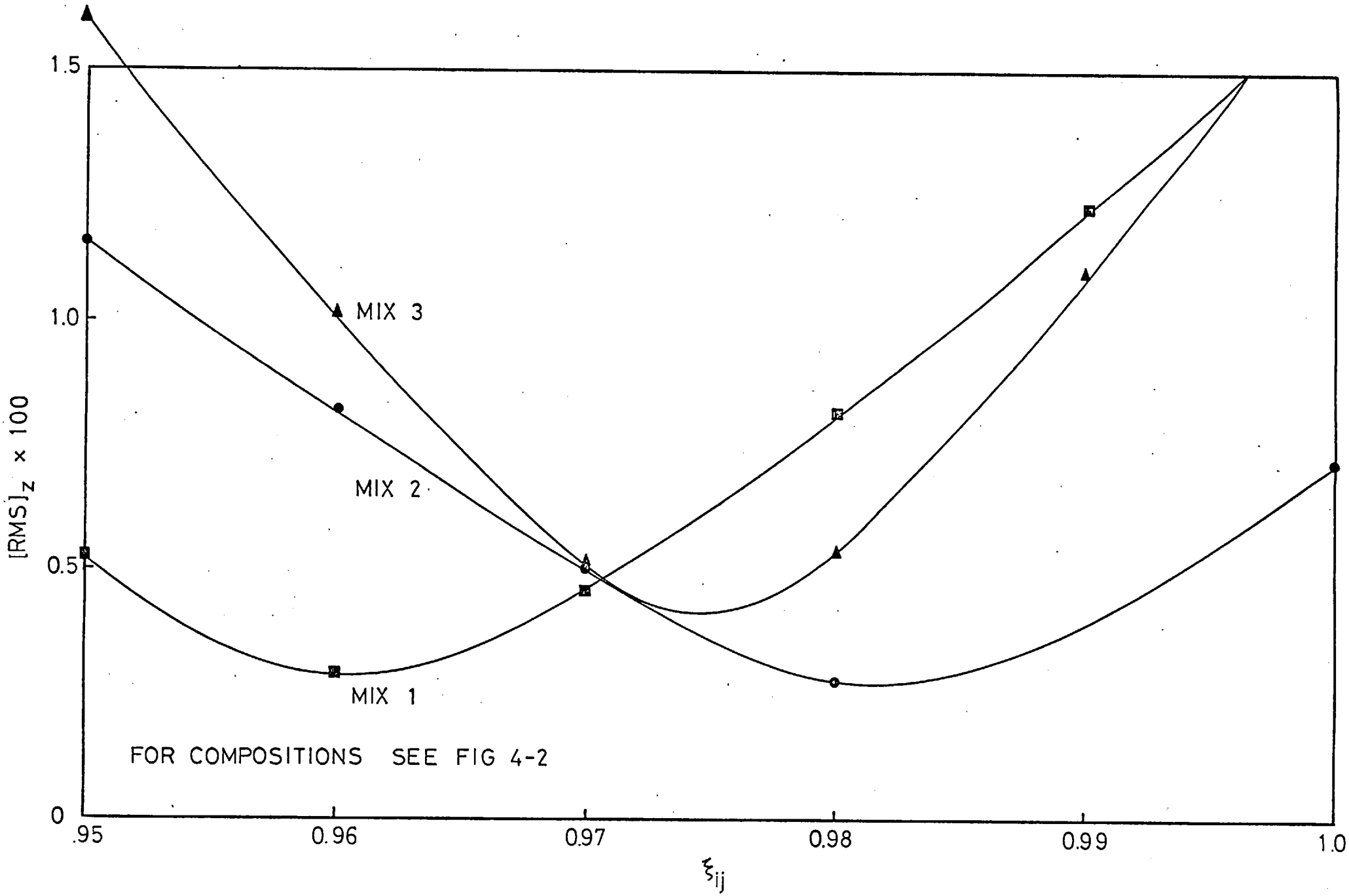


FIG 4-4 $[RMS]_z$ V. ξ_{ij} WHEN $\eta_{ij} = 1.01$

TABLE 4-2

COMPARISON OF EXPERIMENTAL AND PREDICTED COMPRESSIBILITY FACTORS
(MIXTURE 1, 0.3045 ETHYLENE)

RUN NUMBER	T (K)	PRESSURE (BAR)	Z EQ 3-6-3	Z PREDICTION	DEVIATIONS (PER CENT)
37					
	299.01	89.274	.7802	.7760	.5396
	299.03	61.156	.8439	.8434	.0554
	299.02	41.520	.8931	.8941	-.1129
	299.02	27.872	.9282	.9295	-.1409
	299.03	18.555	.9522	.9534	-.1212
	299.02	12.270	.9684	.9693	-.0917
	299.02	8.080	.9792	.9799	-.0652
	299.02	5.306	.9864	.9868	-.0449
	299.01	3.477	.9911	.9914	-.0303
38					
	294.09	89.252	.7645	.7594	.6584
	294.10	62.059	.8308	.8300	.1003
	294.08	42.656	.8831	.8840	-.1023
	294.09	28.935	.9208	.9221	-.1436
	294.09	19.428	.9469	.9481	-.1278
	294.08	12.954	.9647	.9656	-.0985
	294.08	8.588	.9766	.9773	-.0709
	294.08	5.676	.9846	.9850	-.0493
	294.08	3.743	.9898	.9902	-.0335
39					
	288.79	86.269	.7529	.7474	.7308
	288.82	60.944	.8212	.8202	.1255
	288.83	42.411	.8755	.8764	-.0967
	288.83	29.070	.9150	.9163	-.1458
	288.86	19.692	.9427	.9439	-.1325
	288.85	13.231	.9616	.9626	-.1034
	288.82	8.840	.9744	.9751	-.0752
	288.84	5.884	.9830	.9835	-.0527
	288.85	3.906	.9887	.9891	-.0361

TABLE 4-2 (CONTINUED)

COMPARISON OF EXPERIMENTAL AND PREDICTED COMPRESSIBILITY FACTORS
(MIXTURE 1, 0.3045 ETHYLENE)

RUN NUMBER	T (K)	PRESSURE (BAR)	Z EQ 3-6-3	Z PREDICTION	DEVIATIONS (PER CENT)
40					
	283.72	85.897	.7346	.7280	.8944
	283.72	61.733	.8054	.8039	.1925
	283.70	43.580	.8630	.8637	-.0775
	283.70	30.229	.9056	.9070	-.1462
	283.71	20.689	.9358	.9371	-.1394
	283.69	14.027	.9567	.9577	-.1113
	283.71	9.449	.9709	.9717	-.0822
	283.68	6.331	.9805	.9811	-.0582
	283.70	4.234	.9870	.9874	-.0403
41					
	275.60	75.667	.7320	.7261	.8063
	275.60	55.553	.8034	.8022	.1496
	275.58	39.844	.8606	.8614	-.0933
	275.56	28.017	.9030	.9044	-.1518
	275.57	19.413	.9334	.9347	-.1420
	275.56	13.314	.9546	.9557	-.1133
	275.56	9.067	.9692	.9700	-.0841
	275.56	6.143	.9792	.9798	-.0600
	275.56	4.149	.9860	.9864	-.0419
42					
	268.23	75.050	.7007	.6929	1.1163
	268.23	56.632	.7759	.7738	.2786
	268.22	41.570	.8384	.8389	-.0537
	268.22	29.800	.8861	.8874	-.1498
	268.22	20.986	.9208	.9222	-.1532
	268.21	14.589	.9454	.9466	-.1271
	268.21	10.073	.9625	.9635	-.0968
	268.20	6.903	.9744	.9751	-.0704
	268.19	4.710	.9826	.9831	-.0498

TABLE 4-2 (CONTINUED)

COMPARISON OF EXPERIMENTAL AND PREDICTED COMPRESSIBILITY FACTORS
(MIXTURE 1, Ø.3Ø45 ETHYLENE)

RUN NUMBER	T (K)	PRESSURE (BAR)	Z EQ 3-6-3	Z PREDICTION	DEVIATIONS (PER CENT)
43					
	26Ø.32	73.711	.6632	.6528	1.5665
	26Ø.62	57.368	.7435	.74ØØ	.4689
	26Ø.61	43.254	.8115	.8114	.ØØ18
	26Ø.62	31.714	.8649	.8661	-.1397
	26Ø.63	22.766	.9Ø47	.9Ø62	-.1639
	26Ø.62	16.Ø9Ø	.9335	.9348	-.1435
	26Ø.62	11.255	.9539	.9549	-.1125
	26Ø.62	7.8Ø9	.9682	.969Ø	-.Ø835
	26Ø.62	5.392	.9781	.9787	-.Ø6Ø1
	26Ø.62	3.71Ø	.985Ø	.9854	-.Ø425
45					
	253.32	67.686	.6496	.639Ø	1.6243
	253.3Ø	53.888	.7293	.7256	.5Ø15
	253.3Ø	41.416	.7989	.7987	.Ø199
	253.3Ø	3Ø.88Ø	.8541	.8554	-.1436
	253.31	22.492	.896Ø	.8975	-.1729
	253.3Ø	16.11Ø	.9266	.928Ø	-.1536
	253.29	11.4Ø2	.9486	.9497	-.122Ø
	253.3Ø	8.ØØ4	.9642	.9651	-.Ø916
	253.3Ø	5.585	.9751	.9758	-.Ø666
	253.31	3.882	.9828	.9833	-.Ø476
46					
	245.89	64.642	.6137	.6ØØ7	2.1169
	245.88	53.134	.6954	.69Ø3	.7311
	245.88	42.Ø2Ø	.7692	.7684	.1Ø4Ø
	245.87	32.1Ø7	.8298	.83Ø9	-.1275
	245.88	23.882	.8768	.8784	-.1842
	245.87	17.413	.9119	.9134	-.1735
	245.87	12.518	.9375	.9388	-.1421
	245.87	8.9Ø8	.956Ø	.957Ø	-.1Ø9Ø
	245.87	6.295	.9691	.9699	-.ØØC7
	245.86	4.428	.9784	.9789	-.Ø585

TABLE 4-2 (CONTINUED)

COMPARISON OF EXPERIMENTAL AND PREDICTED COMPRESSIBILITY FACTORS
(MIXTURE 1, 0.3045 ETHYLENE)

RUN NUMBER	T (K)	PRESSURE (BAR)	Z EQ 3-6-3	Z PREDICTION	DEVIATIONS (PER CENT)
47					
	238.18	60.979	.5717	.5554	2.8513
	238.18	51.940	.6543	.6472	1.0785
	238.17	42.458	.7323	.7306	.2382
	238.17	33.397	.7986	.7994	-.0952
	236.17	25.462	.8516	.8533	-.1952
	238.16	18.959	.8923	.8941	-.1990
	238.17	13.877	.9226	.9242	-.1695
	238.17	10.032	.9448	.9460	-.1334
	238.16	7.190	.9608	.9617	-.1006
	238.16	5.120	.9722	.9730	-.0740
48					
	230.71	53.936	.5625	.5475	2.6719
	230.70	46.797	.6458	.6396	.9497
	230.70	38.885	.7234	.7222	.1670
	230.70	31.059	.7899	.7910	-.1383
	230.69	24.026	.8435	.8454	-.2253
	230.69	18.133	.8852	.8872	-.2222
	230.69	13.442	.9166	.9183	-.1881
	230.69	9.836	.9399	.9413	-.1483
	230.70	7.129	.9569	.9580	-.1124
	230.70	5.133	.9692	.9700	-.0833
50					
	223.38	36.036	.7096	.7089	.0998
	223.39	29.282	.7768	.7783	-.1885
	223.36	23.215	.8319	.8341	-.2661
	223.39	17.631	.8752	.8775	-.2560
	223.39	13.251	.9084	.9103	-.2158
	223.39	9.820	.9332	.9348	-.1707
	223.38	7.204	.9516	.9528	-.1303
	223.38	5.246	.9651	.9660	-.0973

TABLE 4-2 (CONTINUED)

COMPARISON OF EXPERIMENTAL AND PREDICTED COMPRESSIBILITY FACTORS
(MIXTURE 1, 0.3045 ETHYLENE)

RUN NUMBER	T (K)	PRESSURE (BAR)	Z EQ 3-6-3	Z PREDICTION	DEVIATIONS (PER CENT)
51					
	215.73	28.848	.7461	.7478	-.2313
	215.66	23.257	.8052	.8078	-.3260
	215.67	18.219	.8531	.8558	-.3169
	215.67	13.964	.8906	.8930	-.2704
	215.66	10.531	.9192	.9212	-.2165
	215.67	7.848	.9407	.9423	-.1671
	215.66	5.797	.9567	.9579	-.1262
	215.66	4.255	.9684	.9694	-.0940
52					
	208.13	20.010	.8128	.8162	-.4180
	208.14	15.772	.8579	.8610	-.3681
	208.13	12.179	.8933	.8960	-.3015
	208.13	9.263	.9205	.9227	-.2371
	208.13	6.964	.9411	.9428	-.1818
	208.14	5.193	.9566	.9579	-.1372
	208.13	3.849	.9681	.9691	-.1025

TABLE 4-2 (CONTINUED)

COMPARISON OF EXPERIMENTAL AND PREDICTED COMPRESSIBILITY FACTORS
(MIXTURE 2, 0.5482 ETHYLENE)

RUN NUMBER	T (K)	PRESSURE (BAR)	Z EQ 3-6-3	Z PREDICTION	DEVIATIONS (PER CENT)
53					
	298.89	69.743	.7358	.7377	-.2534
	298.87	48.772	.8183	.8219	-.4355
	298.85	33.485	.8777	.8811	-.3801
	298.86	22.624	.9187	.9213	-.2786
	298.87	15.118	.9463	.9481	-.1920
	298.87	10.023	.9647	.9659	-.1288
	298.86	6.614	.9768	.9777	-.0854
	298.85	4.348	.9848	.9854	-.0563
54					
	293.46	68.783	.7176	.7193	-.2431
	293.44	49.025	.8033	.8070	-.4598
	293.45	34.159	.8663	.8699	-.4095
	293.44	23.361	.9103	.9131	-.3034
	293.45	15.770	.9403	.9423	-.2106
	293.46	10.552	.9604	.9618	-.1423
	293.43	7.015	.9739	.9748	-.0949
	293.43	4.645	.9828	.9834	-.0629
55					
	287.17	69.653	.6839	.6851	-.1756
	287.16	50.982	.7756	.7794	-.4843
	287.15	36.279	.8452	.8491	-.4597
	287.15	25.228	.8949	.8980	-.3490
	287.14	17.259	.9294	.9316	-.2455
	287.13	11.678	.9528	.9544	-.1673
	287.15	7.843	.9685	.9696	-.1125
	287.14	5.242	.9791	.9798	-.0751

TABLE 4-2 (CONTINUED)

COMPARISON OF EXPERIMENTAL AND PREDICTED COMPRESSIBILITY FACTORS
(MIXTURE 2, Ø.5482 ETHYLENE)

RUN NUMBER	T (K)	PRESSURE (BAR)	Z EQ 3-6-3	Z PREDICTION	DEVIATIONS (PER CENT)
56					
	279.37	74.Ø59	.6133	.6129	.Ø618
	279.37	56.75Ø	.7146	.7178	-.4516
	279.38	41.961	.7977	.8Ø2Ø	-.5478
	279.37	3Ø.Ø72	.8598	.8637	-.4488
	279.36	21.Ø67	.9Ø42	.9Ø71	-.3265
	279.35	14.529	.935Ø	.9372	-.2268
	279.35	9.921	.9562	.9576	-.1546
	279.35	6.724	.97Ø5	.9715	-.1Ø43
57					
	273.12	74.985	.5576	.5562	.2624
	273.1Ø	59.847	.6614	.6638	-.3693
	273.1Ø	45.878	.7536	.7582	-.611Ø
	273.1Ø	33.831	.826Ø	.83Ø5	-.5421
	273.Ø9	24.239	.8793	.8829	-.4Ø76
	273.1Ø	17.Ø15	.9172	.9198	-.2881
	273.Ø8	11.78Ø	.9436	.9454	-.1984
	273.Ø8	8.Ø8Ø	.9617	.963Ø	-.135Ø
	273.Ø8	5.5Ø8	.9741	.975Ø	-.Ø914
58					
	266.24	74.217	.4925	.49Ø1	.4886
	266.23	62.187	.5931	.5944	-.21ØØ
	266.22	5Ø.Ø26	.6928	.6974	-.66Ø2
	266.22	38.399	.7772	.7824	-.669Ø
	266.22	28.383	.8423	.8468	-.5295
	266.21	2Ø.416	.89ØØ	.8935	-.384Ø
	266.2Ø	14.417	.924Ø	.9265	-.2686
	266.22	1Ø.Ø48	.9479	.9496	-.1848
	266.21	6.942	.9643	.9656	-.1262

TABLE 4-2 (CONTINUED)

COMPARISON OF EXPERIMENTAL AND PREDICTED COMPRESSIBILITY FACTORS
(MIXTURE 2, 0.5482 ETHYLENE)

RUN NUMBER	T (K)	PRESSURE (BAR)	Z EQ 3-6-3	Z PREDICTION	DEVIATIONS (PER CENT)
59					
	259.44	70.259	.4363	.4328	.8098
	259.41	61.688	.5273	.5279	-.1096
	259.41	52.216	.6289	.6333	-.7110
	259.41	41.962	.7222	.7281	-.8162
	259.41	32.176	.7987	.8041	-.6813
	259.40	23.820	.8570	.8613	-.5079
	259.40	17.200	.8998	.9030	-.3608
	259.36	12.209	.9303	.9326	-.2512
	259.39	8.565	.9518	.9534	-.1731
	259.38	5.960	.9668	.9679	-.1188
60					
	252.24	48.831	.6045	.6106	-1.0190
	252.25	40.327	.6990	.7060	-.9927
	252.24	31.663	.7784	.7847	-.8008
	252.23	24.915	.8328	.8380	-.6205
	252.22	17.566	.8868	.8905	-.4227
	252.22	12.655	.9204	.9231	-.2956
	252.22	8.995	.9443	.9463	-.2051
	252.23	6.334	.9613	.9626	-.1417
	252.23	4.433	.9731	.9741	-.0978
61					
	244.25	37.553	.6799	.6885	-1.2606
	244.26	30.183	.7607	.7680	-.9586
	244.22	23.273	.8250	.8308	-.6998
	244.21	17.405	.8741	.8785	-.4977
	244.22	12.740	.9104	.9136	-.3494
	244.23	9.185	.9367	.9389	-.2438
	244.23	6.555	.9554	.9570	-.1698
	244.20	4.644	.9687	.9699	-.1182

TABLE 4-2 (CONTINUED)

COMPARISON OF EXPERIMENTAL AND PREDICTED COMPRESSIBILITY FACTORS
(MIXTURE 2, 0.5482 ETHYLENE)

RUN NUMBER	T (K)	PRESSURE (BAR)	Z EQ 3-6-3	Z PREDICTION	DEVIATIONS (PER CENT)
62					
	237.37	29.056	.7416	.7502	-1.1561
	237.39	22.843	.8087	.8154	-.8290
	237.36	17.378	.8606	.8657	-.5886
	237.36	12.912	.8996	.9034	-.4144
	237.32	9.436	.9282	.9309	-.2910
	237.33	6.815	.9490	.9509	-.2040
	237.36	4.882	.9639	.9653	-.1428
63					
	229.93	20.383	.8106	.8179	-.8986
	229.94	15.650	.8608	.8663	-.6341
	229.93	11.743	.8988	.9029	-.4474
	229.94	8.667	.9270	.9299	-.3155
	229.94	6.324	.9476	.9497	-.2226
	229.93	4.575	.9625	.9640	-.1573
64					
	223.27	18.585	.8096	.8176	-.9878
	223.27	14.408	.8588	.8648	-.6965
	223.27	10.916	.8964	.9009	-.4927
	223.27	8.135	.9246	.9278	-.3493
	223.27	5.992	.9454	.9477	-.2482
	223.26	4.376	.9606	.9623	-.1765

TABLE 4-2 (CONTINUED)

COMPARISON OF EXPERIMENTAL AND PREDICTED COMPRESSIBILITY FACTORS
(MIXTURE 3, Ø.7581 ETHYLENE)

RUN NUMBER	T (K)	PRESSURE (BAR)	Z EQ 3-6-3	Z PREDICTION	DEVIATIONS (PER CENT)
66					
	288.15	69.Ø94	.5437	.5445	-.1428
	288.13	53.261	.6785	.6797	-.1848
	288.14	39.4Ø1	.7794	.78Ø6	-.1535
	288.12	28.Ø91	.8512	.8516	-.Ø533
	288.12	19.524	.9Ø05	.9Ø05	.ØØ36
	288.1Ø	13.344	.9338	.9335	.Ø24Ø
	288.1Ø	9.Ø21	.9560	.9558	.Ø268
	288.Ø7	6.Ø55	.9708	.9706	.Ø228
	288.12	4.Ø48	.9807	.9805	.Ø175
68					
	28Ø.96	49.37Ø	.6689	.6714	-.3850
	28Ø.93	37.387	.7689	.77Ø9	-.2511
	28Ø.93	27.14Ø	.842Ø	.843Ø	-.1125
	28Ø.95	19.146	.8931	.8934	-.Ø343
	28Ø.92	13.257	.9281	.9281	-.ØØØ1
	28Ø.95	9.Ø67	.9518	.9516	.Ø116
	28Ø.94	6.152	.9677	.9676	.Ø133
	28Ø.96	4.154	.9784	.9783	.Ø115
69					
	272.96	54.884	.5328	.5397	-1.3Ø14
	272.96	45.498	.6551	.6597	-.6971
	272.95	35.352	.7552	.7582	-.3979
	272.95	26.199	.83ØØ	.8316	-.1991
	272.94	18.8Ø2	.8834	.8842	-.Ø89Ø
	272.95	13.211	.92Ø6	.92Ø9	-.Ø348
	272.94	9.155	.9461	.9462	-.Ø107
	272.94	6.287	.9635	.9636	-.ØØØ9
	272.95	4.292	.9754	.9753	.ØØ24

TABLE 4-2 (CONTINUED)

COMPARISON OF EXPERIMENTAL AND PREDICTED COMPRESSIBILITY FACTORS
(MIXTURE 3, Ø.7581 ETHYLENE)

RUN NUMBER	T (K)	PRESSURE (BAR)	Z EQ 3-6-3	Z PREDICTION	DEVIATIONS (PER CENT)
7Ø					
	266.13	44.585	.6112	.6192	-1.3205
	266.11	36.Ø29	.7171	.7221	-.6899
	266.11	27.516	.8ØØØ	.8Ø29	-.3633
	266.11	2Ø.216	.86Ø8	.8624	-.1856
	266.1Ø	14.468	.9Ø4Ø	.9Ø49	-.Ø925
	266.1Ø	1Ø.18Ø	.9342	.9346	-.Ø455
	266.1Ø	7.Ø81	.955Ø	.9552	-.Ø222
	266.11	4.889	.9693	.9694	-.Ø1Ø9
71					
	259.3Ø	37.842	.65Ø8	.66Ø2	-1.4467
	259.3Ø	3Ø.318	.7463	.7518	-.7412
	259.29	23.Ø86	.8198	.8231	-.3977
	259.29	16.978	.8739	.8758	-.216Ø
	259.28	12.199	.9124	.9135	-.1192
	259.28	8.629	.9395	.94Ø1	-.Ø671
	259.29	6.Ø4Ø	.9583	.9587	-.Ø387
	259.28	4.196	.9714	.9716	-.Ø231
72					
	251.34	28.689	.7264	.735Ø	-1.1789
	251.34	22.346	.8Ø27	.8Ø78	-.6429
	251.33	16.755	.8599	.863Ø	-.3667
	251.36	12.239	.9Ø15	.9Ø35	-.2151
	251.35	8.785	.9311	.9324	-.13Ø1
	251.35	6.231	.9521	.9528	-.Ø8Ø7
	251.36	4.384	.9667	.9672	-.Ø512

TABLE 4-2 (CONTINUED)

COMPARISON OF EXPERIMENTAL AND PREDICTED COMPRESSIBILITY FACTORS
(MIXTURE 3, Ø.7581 ETHYLENE)

RUN NUMBER	T (K)	PRESSURE (BAR)	Z EQ 3-6-3	Z PREDICTION	DEVIATIONS (PER CENT)
74					
	238.46	16.752	.8265	.8337	-.8663
	238.47	12.642	.8752	.8799	-.5317
	238.47	9.329	.911Ø	.914Ø	-.3374
	238.47	6.781	.9368	.9389	-.2194
	238.47	4.874	.9553	.9567	-.1454
	238.47	3.48Ø	.9685	.9694	-.Ø979

4-6 The Application of the Principle of Corresponding States to the Second Virial Coefficients

It has been shown in section (4-3) that the principle of corresponding states provides us with a way to correlate the macroscopic properties between conformal substances with microscopic molecular information such as the collision diameter, σ^*, and the potential-well depth, ε^*. It follows that, at a given P, V and T, the reduced equations of state are all identical for conformal substances, or, analogously, the reduced potential energy curves all over-lap one another (in fact, this is the definition of the principle), that is,

$$\frac{\varepsilon_1}{\varepsilon_1^*} = u\left(\frac{r_1}{r_1^*}\right) \tag{4-6-1}$$

$$\frac{\varepsilon_2}{\varepsilon_2^*} = u\left(\frac{r_2}{r_2^*}\right) \tag{4-6-2}$$

where u is the same function for all conformal substances. Thus from Eq.(4-3-17) and (4-3-19) the characteristic quantities can be related as

$$\frac{T_1^c}{\varepsilon_1^*} = \frac{T_2^c}{\varepsilon_2^*} \tag{4-6-3}$$

$$\frac{V_1^c}{(r_1^*)^3} = \frac{V_2^c}{(r_2^*)^3} \tag{4-6-4}$$

A different approach to the principle of corresponding states from that of the previous sections is to examine the second virial coefficient, since, as seen in Eq.(4-2-5), B is related to the pair potential and is a function of temperature only. Following Guggenheim and McGlashan,[77] we define the 'reduced second virial coefficient', B^r, as

$$B^r = B/V^c \qquad (4\text{-}6\text{-}5)$$

Then according to the principle of corresponding states, that is, Eq.(4-6-1) and (4-6-2), the dependence of B on the temperature is of the form

$$B/V^c = \phi\,(T/T^c) \qquad (4\text{-}6\text{-}6)$$

where ϕ denotes the same function for all conformal substances. Thus for conformal substances 1 and 2

$$B_1/V_1^c = \phi(T/T_1^c) \qquad \text{and} \qquad B_2^c = \phi(T/T_2^c) \qquad (4\text{-}6\text{-}7)$$

Eq.(4-6-7) clearly shows that if the function ϕ is known either empirically or theoretically from B_1 as a function of temperature, then B_2 can be determined by the same function ϕ and this is analogous to the reduced equation of state (4-3-19) which is expressed in terms of reduced P, V and T.

In the case of a mixture of 1 and 2 the principle can be extended by assuming that the interaction energy ε_{12} between two molecules of different kinds depends on their distance apart r_{12} by the relation

$$\frac{\varepsilon_{12}}{\varepsilon_{12}^*} = u\left(\frac{r_{12}}{r_{12}^*}\right) \qquad (4\text{-}6\text{-}8)$$

where r_{12}^* and ε_{12}^* are the collision diameter and the well-depth of the potential energy curve between unlike-molecules. Since u in Eq.(4-6-8) is the same function in Eq.(4-6-1) and (4-6-2), Eq.(4-6-8) implies that the potential energy between 1 and 2 is conformal to those of pure substances 1 and 2 respectively and hence it follows that the critical temperature and volume of the mixture can be related to ε_{12}^* and r_{12}^*

as in Eq.(4-6-3) and (4-6-4), i.e.

$$T^c_{12}/\varepsilon^*_{12} = T^c_1/\varepsilon^*_1 = T^c_2/\varepsilon^*_2 \qquad (4\text{-}6\text{-}9)$$

$$V^c_{12}/(r^*_{12})^3 = V^c_1/(r^*_1)^3 = V^c_2/(r^*_2)^3 \qquad (4\text{-}6\text{-}10)$$

It then follows by an immediate extension of the argument for single substances that

$$B_{12}/V^c_{12} = \phi(T/T^c_{12}) \qquad (4\text{-}6\text{-}11)$$

where B_{12} is the interactional second virial coefficient of a mixture of 1 and 2, which arises from the interaction between unlike molecules, 1 and 2 (see section 3-5-4).

Eq.(4-6-11) shows that the cross second virial coefficient B_{12} can be obtained from the 2nd virial coefficient of the conformal substance 1 or 2 provided V^c_{12} and T^c_{12} are known. Thus problem is now reduced to that of predicting the values of the characteristic quantities T^c_{12} and V^c_{12} as in the case of the previous section.

Guggenheim and McGlashan used the so-called 'Lorentz-Berthelot mixing rule' for r^*_{12} and ε^*_{12}, that is,

$$r^*_{12} = (r^*_1 + r^*_2)/2 \qquad (4\text{-}6\text{-}12)$$

$$\varepsilon^*_{12} = (\varepsilon^*_1 \cdot \varepsilon^*_2)^{\frac{1}{2}} \qquad (4\text{-}6\text{-}13)$$

These are identical to Eq.(4-5-20) and (4-5-21) except for the presence of the correction factors, ξ_{ij} and η_{ij}, in estimating f_{ij} and h_{ij} in the previous section, or analogously, the above equations (4-6-12) and (4-6-13) are regarded as special cases with $\xi_{ij} = \eta_{ij} = 1.0$.

Combining Eq.(4-6-9) and (4-6-13)

$$T_{12}^{c} = (T_1^{c} \cdot T_2^{c})^{\frac{1}{2}} \qquad (4\text{-}6\text{-}14)$$

and similarly from Eq.(4-6-10) and (4-6-12)

$$(V_{12}^{c})^{1/3} = \tfrac{1}{2}(V_1^{c})^{1/3} + \tfrac{1}{2}(V_2^{c})^{1/3} \qquad (4\text{-}6\text{-}15)$$

The arithmetic mean in Eq.(4-5-21) and (4-6-15) would be true if the two kinds of molecules are regarded as rigid spheres. The geometric mean in Eq.(4-5-20) and (4-6-13) is mainly regarded as an empirical rule. However, when the potential energy of the mixture is dominated by the 'London dispersion forces'[79] Mason and Spurling[76] have shown that ε_{12} in the mixture can be expressed as,

$$\varepsilon_{12}^{*} = (\varepsilon_1^{*} \cdot \varepsilon_2^{*})^{\frac{1}{2}}(r_1^{*} \cdot r_2^{*}/r_{12}^{*2})^{3} \cdot \left[2(E_1E_2)^{2}/(E_1 + E_2)\right] \qquad (4\text{-}6\text{-}16)$$

where E_1 and E_2 are mean characteristic energies of atoms 1 and 2 in calculating the first coefficient of the London force,

$$U(\text{dispersion}) = -\, c'/r^{6} - c''/r^{8} - \cdots \qquad (4\text{-}6\text{-}17)$$

From Eq.(4-6-16) it follows that, if the arithmetic mean rule for r_{12}^{*} holds, then from the fact that the arithmetic mean is always larger than geometric mean,

(i) $\quad r_1^{*} \cdot r_2^{*}/r_{12}^{*2} \leq 1$

(ii) similarly $\quad 2(E_1E_2)^{2}/(E_1+E_2) \leq 1$

hence

$$\varepsilon_{12}^{*} \leq (\varepsilon_1^{*} \cdot \varepsilon_2^{*})^{2} \qquad (4\text{-}6\text{-}18)$$

Thus in this case too the geometric mean ε_{12}^* and hence T_{12}^* in Eq.(4-6-14) are corrected and the correction factor is subject to be found empirically, that is, Eq.(4-6-13) and (4-6-14) are now

$$\varepsilon_{12}^* = \xi_{12} (\varepsilon_1^* \cdot \varepsilon_2^*)^{1/2} \qquad (4\text{-}6\text{-}19)$$

$$T_{12}^* = \xi_{12} (T_1^c \cdot T_2^c)^{1/2} \qquad (4\text{-}6\text{-}20)$$

The correction factor ξ_{ij} is, in principle, same as in Eq.(4-5-20), but we now propose to determine it from the interactional 2nd virial coefficient B_{12}.

In this case the subscripts 1 and 2 correspond to methane and ethylene respectively and their 2nd virical coefficients at temperatures ranging 240 to 300^{o}K are listed in Table 3-6. The interactional 2nd virial coefficients at same temperature range were calculated from the three mixtures using Eq.(3-5-20) and also listed in Table 3-6.

In Fig (4-5) B/V^c is plotted against T/T^c for methane and ethylene and for methane-ethylene mixture, that is, B_{12}/V_{12}^c v. T/T_{12}^c for three values of ξ_{ij} (1.0, 0.975 and 0.95).

It can be seen from Fig (4-5) that the functions ϕ defined in Eq.(4-6-6) for methane and ethylene are not identical. However this discrepancy is not unexpected since the principle as introduced in this section (i.e. same ϕ) holds only for the conformal substances. Fortunately the differences are not too large, and it is possible to examine the variation of B_{12}^r with respect to the correction factor ξ_{ij}. Although we are prevented from obtaining highly accurate values of ξ_{ij} due to the disagreement of ϕ_{CH_4} and $\phi_{C_2H_4}$ it can be seen, however,

that, when ζ_{ij} is either 1.0 or 0.95, B_{12}^r is far from either $B_{CH_4}^r$ or $B_{C_2H_4}^r$ whereas $\zeta_{ij} = 0.975$ gives the values of B_{12}^r which are reasonably close to both $B_{CH_4}^r$ and $B_{C_2H_4}^r$.

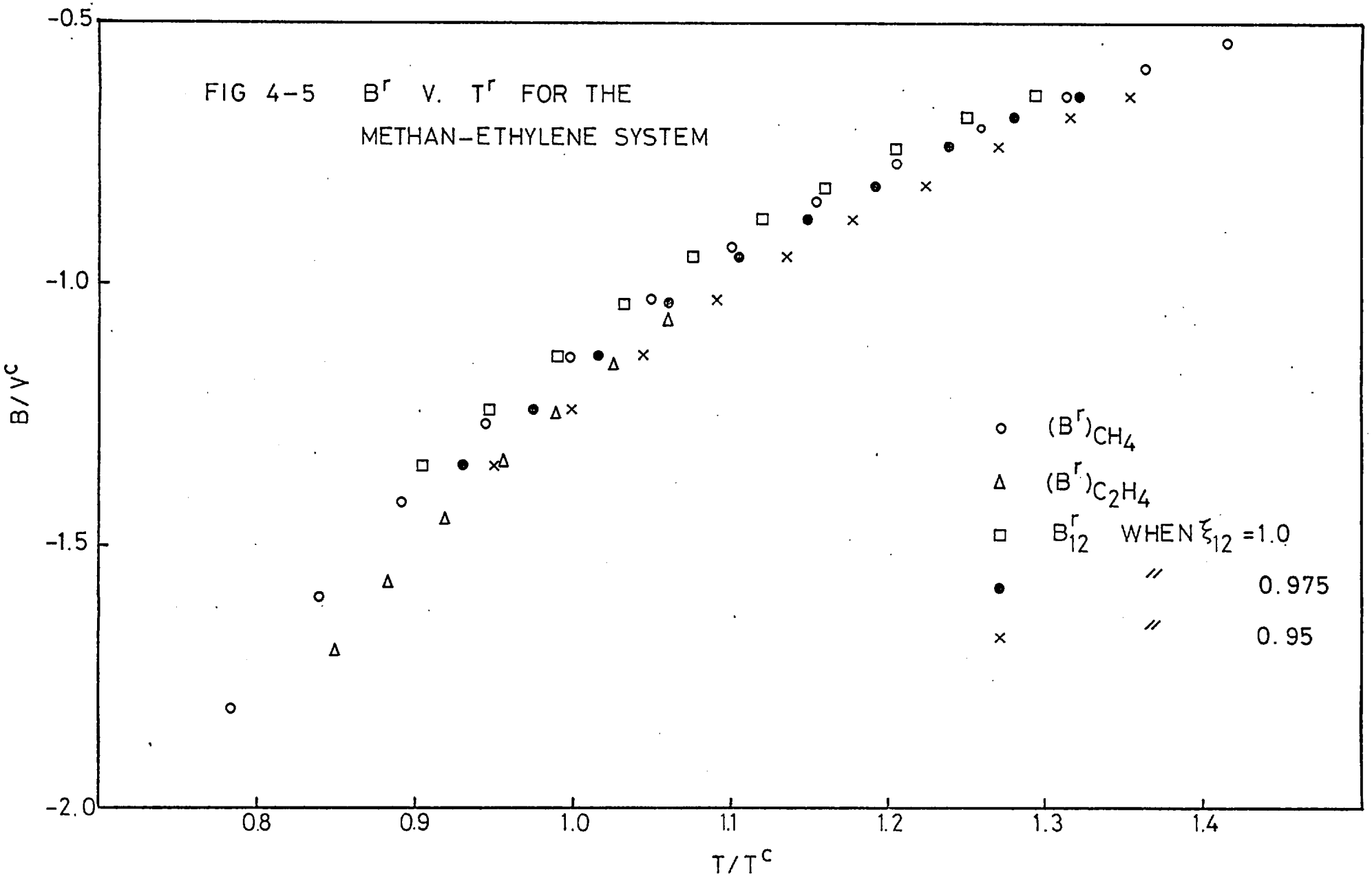
Moreover from the facts that

(i) the disagreement between ϕ_{CH_4} and $\phi_{C_2H_4}$ is mainly due to the non-spherical shape of ethylene molecule, and

(ii) Pitzer and Curl[80] have shown that the second virial coefficients can be expressed as a function of the acentric factor, ω, defined by Eq.(4-4-1) in section(4-4), (the change in B^r in Fig 4-5 is approximately same order of magnitude which can be expected from the Pitzer's correlation between B and ω),

one can expect the reduced second virial coefficient of the hypothetical fluid, B_{12}^r, or ϕ_{12} in Fig (4-5) may have the values in between ϕ_1 (or ϕ_{CH_4}) and ϕ_2 ($\phi_{C_2H_4}$), and this was the case when the correction factor ζ_{12} was 0.975 as seen in Fig (4-5).

This qualitative result of $\zeta_{12} = 0.975$ agrees well with that obtained in the previous section and hence can be considered as confirmation of the correctness of this value for the methane-ethylene system.


FIG 4-5 B^r V. T^r FOR THE METHAN-ETHYLENE SYSTEM
-0.5
-1.0
-1.5
-2.0
B/V^c
0.8
0.9
1.0
1.1
1.2
1.3
1.4
T/T^c
$(B^r)_{CH_4}$
$(B^r)_{C_2H_4}$
B^r_{12} WHEN ξ_{12} =1.0
// 0.975
// 0.95

REFERENCES

(1) Roe, D.R., Ph.D. Thesis, University of London, (1972).

(2) Saville, G., 'Measurement of P-V-T Properties of gases and Gas Mixtures at Low Pressure', Experimental Thermodynamics (IUPAC), Chap.6, (1975).

(3) Weast, R.C., 'Handbook of Chemistry and Physics', 51st Ed., CRC Press (1970).

(4) Roe, D.R., loc. cit., Chapter 3-4(g).

(5) Weir, R., Ph.D. Thesis, University of London, (1966).

(6) Hust, J.G., Cryogenics, 9, 443 (1969).

(7) Bett, K., Ph.D. Thesis, University of London, (1959).

(8) Cook, A.H., and Hammond, J.A., Metrologia, 5 141 (1969).

(9) Kaye, G.W.C. and Laby, T.H., 'Tables of Physical and Chemical constants', 13'th Ed., Longmans (1966).

(10) Hayward, A.T.J., J. Inst. Petrol., 56 12 (1970).

(11) Bigg, P.H., Brit. J. Appl. Phys., 15 1111 (1970).

(12) Gould, F.A. and Vickers, T., J. Sci. Inst., 29 85 (1952).

(13) Bett, K.E. and Newitt. D.M., 'Chemical Engineering Practice', Vol. 5, Butterworths, (1958).

(14) Michels, A., De Gruyter, J. and Neisen, F., Physica, 's Grav., 3 346 (1936).

(15) Michels, A. and Geldermans, M., Physica, 's Grav., 9 967 (1942).

(16) Michels, A., Geldermans, M. and De Groot, S.R., Physica, 's Grav., 12 105 (1949).

(17) Angus, S., 'International Thermodynamic Tables of Fluid State, ETHYLENE,1972', Butterworths, (1974).

(18) McMath, H.G. and Edmister, W.C., A.I.Ch.E.J., 15 370 (1969).

(19) Lee, R.C. and Edmister, W.C., A.I.Ch.E.J., 16 1047 (1970).

(20) Saville, G., Private Communication.

(21) Saville, G., Private Communication.

(22) Burnett, E.S., J. App. Mech., 58 A-136 (1936).

(23) Weir, R.D., Jones, W., Rowlinson, J.S. and G. Saville, Trans. Faraday Soc. 63 1320 (1967).

(24) Pollard, C.A., Ph.D. Thesis, University of London, (1971).

(25) Crommelin, C.A. and Watts, H.G., 'Communs. Phys. Lab. Univ. Leiden', 189c (1927).

(26) Butcher, E.G. and Dadson, R.S., Proc. Roy. Soc., A277 448 (1964).

(27) Dymond, J.H. and Smith, E.B., 'The virial Coefficients of Gases', Clarendon Press, (1969).

(28) Rowlinson, J.S., 'Liquids and Liquid Mixtures', 2nd Ed, Butterworths, (1969).

(29) Bender, E., Ph.D. Thesis, Ruhr University, Translated by Angus, S., (IUPAC), (1972).

(30) Bender, E., Proc. Fifth Symposium of Thermophysical Properties, Amer. Soc. Mech. Eng., N.Y., 1970, s. pp 227/235.

(31) Canfield, F.B., Leland, T.W. and Kobayashi, R., Adv. Cryog. Eng., 8 146 (1963).

(32) Deming, W.E., Phil. Mag., 11 146 (1936).

(33) Hall, K.R. and Canfield, F.B., Physica, 47 99 (1970).

(34) Barieau, R.E. and Dalton, B.J., U.S. Bur. Mines, 'Report of Investigation No. 6900', (1967).

(35) Barieau, R.E. and Dalton, B.J., U.S. Bur. Mines, 'Report of Investigation No. 7020', (1967).

(36) Michels, A., Abels, J.C., ten Seldan, C.A. and de Graaff, W., Physica, 26 381 (1960).

(37) Van Doren, K.R., U.S. Bur. Mines, 'Information Circular No. 8437 (1969).

(38) American Gas Association Research Project, NX-19, 'Manual for the Determination of Super-Compressibility Factors for Natural Gas', American gas Association, (1962).

(39) Pitzer, K.S., Lippmann, D.Z., Curl, R.F., Huggins, C.M. and Peterson, D.E., J.Amer. Chem. Soc. 77 3433 (1955).

(40) Leach, J.W., Chappelear, P.S. and Leland, T.W., A.I.Ch.E.J., 14 No.4, 568 (1968).

(41) Rowlinson, J.S. and Watson, I.D., Chem. Eng. Sci., 24 1565 (1969).

(42) Redlich, O. and Kwong, J.N.S., Chem. Rev., 44 233 (1949).

(43) Benedict, M., Webb, G.B. and Rubin, L.C., J. Chem. Phys., 8 334 (1940).

(44) Bett, K.E., Rowlinson, J.S. and Saville, G. 'Thermodynamics for Chemical Engineers', Chapter 9, The Athlone Press, (1975).

(45) Strobridge, T.R., NBS Technical Note, 129A, (Feb., 1963).

(46) Stewart, R.B. and Jacobsen, R.T., Crygenics, September, (1973).

(47) McCarty, R.D., Cryogenics, May, (1974).

(48) Prausnitz, J.M., Eckert, C.A., Orye, R.V. and O'Connell, J.P., 'Computer Calculations for Vapour-Liquid Equilibria', Prentice-Hall, (1967).

(49) Prausnitz, J.M. and Chueh, P.L., 'Computer calculations for High-Pressure Vapor-Liquid Equilibria', Prentice Hall, (1968).

(50) Hill, T.L., 'Introduction to Statistical Thermodynamics', Addison-Wesley Publishing Co., (1960).

(51) Curl, R.F. and Pitzer, K.S., Ind. Engng. Chem., 60 265 (1958).

(52) Reid, R.C. and Sherwood, T.K., 'The Properties of Gases and Liquids', 2nd Ed., Chapter 7, McGraw-Hill, (1966).

(53) Leland, T.W., Chappelear, P.S. and Gamson, B.W., A.I.Ch.E.J., 8 482 (1962).

(54) Reid, R.C. and Sherwood, T.K., loc. cit., Appendix A.

(55) Edmister, W.C., Petrol. REfiner, 37(4), 173 (1958).

(56) Americal Petroleum Institute, Technical Data Book, Jan., (1972).

(57) Chapela, G.A., Ph.D. Thesis, University of London, (1975).

(58) Douslin, R.D., Harrison, R.H., Moore, R.T. and McCullough, J.P., J. Chem. Eng. Data, 9 358 (1964).

(59) Michels, A. and Neder, G., Physica, s' Grav., 2 1000 (1935), and 3 569 (1936).

(60) Schamp, H.W., Richardson, A.C.B. and Altman, A., Physics of Fluids, 1 329 (1958).

(61) Goodwin, R.D. and Prydz, R., J. Res. NBS(U.S.), 76A; 81 (1972).

(62) van Itterbeck, A., Verbecke, O. and States, K., Physica, 29 742 (1963).

(63) Jasoone, V., Gielsen, H., de Doelpaep, J. and Verveke, O.B., Physica, 46 213 (1970).

(64) Saville, G., Private Communication.

(65) Reid, R.C. and Sherwood, T.K., loc. cit., Chapter 3 and Appendix A.

(66) Watson, I.D. and Rowlinson, J.S., Chem. Eng. Sci., 24 1575 (1969).

(67) Kay, W.B., Ind. Eng. Chem., 28 1014 (1936).

(68) Leland, T.W., Rowlinson, J.S. and Sather, G.A., Trans. Faraday Soc., 64 1447 (1968)

(69) Rowlinson, J.S., 'Liquids and Liquid Mixtures', Chapter 9, Butterworths, (1971).

(70) Rowlinson, J.S., ibid., pp. 326-332.

(71) Gunning, A.J. and Rowlinson, J.S., Chem. Eng. Sci., 28 521 (1973).

(72) Teja, A.S. and Rowlinson, J.S., Chem. Eng. Sci., 28 529 (1973).

(73) Hiza, M.J. and Duncan, A.G., A.I.Ch.E.J., 16 733 (1970).

(74) Guter, M., Newitt, D.M. and Ruhemann, M., Pro. R. Soc., A176 140 (1940).

(75) Tully, P.C. and Edmister, W.C., A.I.Ch.E.J., 13 155 (1967).

(76) Mason, E.A. and Spurling, T.H., 'The virial Equation of State', Chapter 2, Pergamon Press (1969).

(77) Guggenheim, E.A. and McGlashan, M.L., Proc. Roy. Soc., A206 448 (1951).

(78) Rowlinson, J.S., loc. cit., Chapter 7.

(79) Miller, S.A. 'Ethylene and Its Industrial Derivatives', Ernest Benn Ltd., (1969).

(80) Pitzer, K.S. and Curl, R.F., J. Amer. Chem. Soc., 79 2369 (1957).

(81) Rowlinson, J.S., Nature, 244 414 (1973).

(82) Mason, E.A. and Spurling, T.H., loc. cit., Chapter 1.

(83) Mason, E.A. and Spurling, T.H., ibid., Chapter 2.